

JOURNAL OF FACADE DESIGN & ENGINEERING

VOLUME 10 / NUMBER 2 / 2022

SPECIAL ISSUE POWERSKIN 2022

EDITORS IN CHIEF

ULRICH KNAACK & THALEIA KONSTANTINO

GUEST EDITORS

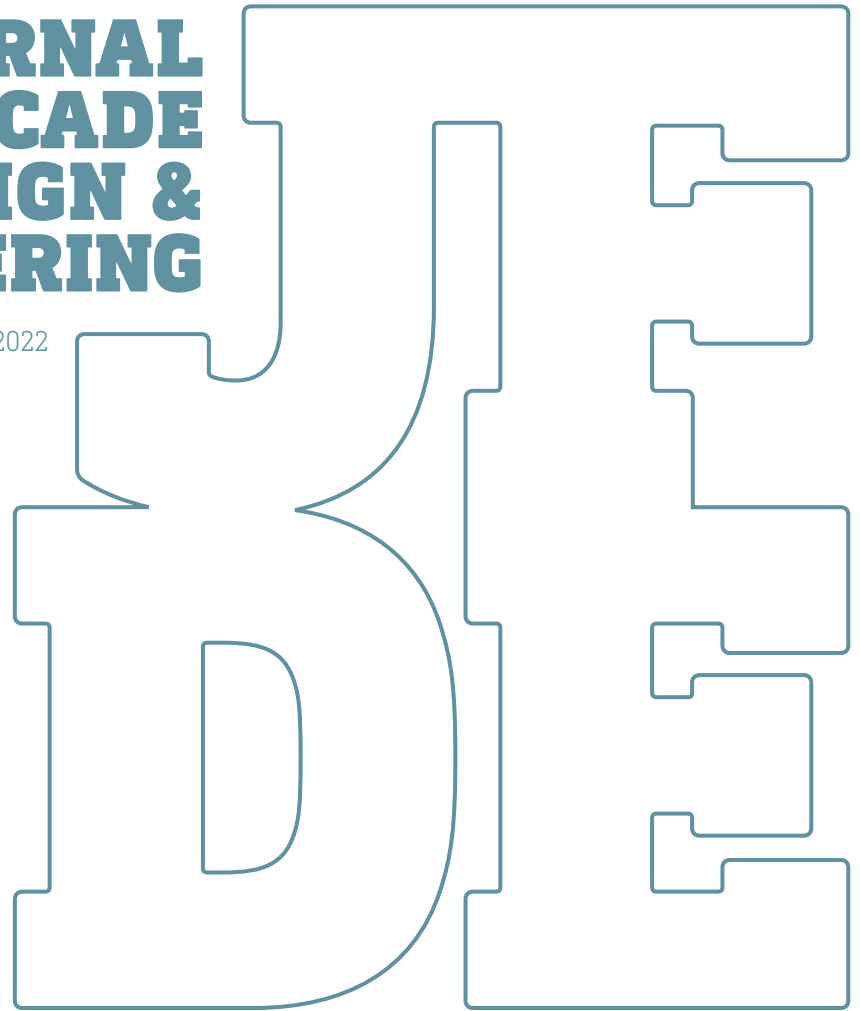
THOMAS AUER, JENS SCHNEIDER,

LINDA HILDEBRAND & DANIELE SANTUCCI

SUPPORTED BY THE EUROPEAN FACADE NETWORK

**JOURNAL
OF FACADE
DESIGN &
ENGINEERING**

VOLUME 10 / NUMBER 2 / 2022



EDITORS IN CHIEF

ULRICH KNAACK AND THALEIA KONSTANTINO

GUEST EDITORS

THOMAS AUER, JENS SCHNEIDER,

LINDA HILDEBRAND AND DANIELE SANTUCCI

SUPPORTED BY THE EUROPEAN FACADE NETWORK

SPECIAL ISSUE

POWERSKIN

2022

JFDE Journal of Facade Design and Engineering

JFDE presents new research results and new proven practice of the field of facade design and engineering. The goal is to improve building technologies, as well as process management and architectural design. JFDE is a valuable resource for professionals and academics involved in the design and engineering of building envelopes, including the following disciplines:

- Architecture
- Building Engineering
- Structural design
- Climate design
- Building Services Engineering
- Building Physics
- Design Management
- Facility Management

JFDE is directed at the scientific community, but it will also feature papers that focus on the dissemination of science into practice and industrial innovations. In this way, readers explore the interaction between scientific developments, technical considerations and management issues.

Publisher

TU Delft / Faculty of Architecture and the Built Environment
Julianalaan 134, 2628 BL Delft, The Netherlands

Contact

Alessandra Luna Navarro
editors@jfde.eu
<https://jfde.eu/>

Policies

Peer Review Process – The papers published in JFDE are double-blind peer reviewed.

Open Access – JFDE provides immediate Open Access (OA) to its content on the principle that making research freely available to the public supports a greater global exchange of knowledge.

Licensed under a Creative Commons Attribution 4.0 International License (CC BY 4.0).

Indexation – JFDE is indexed in the Directory of Open Access Journals (DOAJ), Google Scholar, Inspec IET and Scopus.

Publication Ethics – Editors, authors and publisher adopt the guidelines, codes of conduct and best practices developed by the Committee on Publication Ethics (COPE).

Copyright Notice – Author(s) hold their copyright without restrictions.

Design & layout

Design – Sirene Ontwerpers, Amsterdam

Layout – Stichting OpenAccess, Rotterdam

Open access

Website, indexing, DOIs – Stichting OpenAccess, Rotterdam

ISSN 2213-302X (Print)
ISSN 2213-3038 (Online)
ISBN 978-90-832713-2-3

Editorial board

Editors in Chief

Ulrich Knaack
Thaleia Konstantinou
Delft University of Technology, The Netherlands

Editors

Alessandra Luna Navarro
Tatiana Armijos Moya
Delft University of Technology, The Netherlands

Editorial Board

Tillmann Klein, *Delft University of Technology, Architecture and the Built Environment, Netherlands* // Alejandro Prieto Hoces, *Universidad Diego Portales, Escuela de Arquitectura, Chile* // Daniel Aelenei, *Universidade Nova de Lisboa, Lisbon, Portugal* // Enrico de Angelis, *Polytechnico Milano, Milan, Italy* // Julen Astudillo, *TECNALIA Research & Innovation, San Sebastian, Spain* // Carlo Battisti, *IDM Südtirol - Alto Adige, Italy* // Anne Beim, *Royal Danish Academy of Fine Arts, Copenhagen, Denmark, Denmark* // Jan Belis, *Ghent University, Belgium* // Jan Cremers, *Hochschule für Technik Stuttgart (HFT), Germany* // Andy van den Dobbelaere, *Delft University of Technology, Delft, the Netherlands* // Paul Donnelly, *Washington University, St. Louis, USA* // Chris Geurts, *TNO, Delft, Netherlands* // Mikkel K. Kragh, *University of Southern Denmark, Odense, Denmark* // Klaus Kreher, *Lucerne University of Applied Sciences and Art, Lucerne, Switzerland* // Bert Lieverse, *Association of the Dutch Façade Industry, Nieuwegein, The Netherlands* // Steve Lo, *University of Bath, Bath, United Kingdom* // Andreas Luible, *Lucerne University of Applied Sciences and Art, Lucerne, Switzerland* // Enrico Sergio Mazzucchelli, *Politecnico di Milano ABC Department, Italy* // David Metcalfe, *Centre for Window and Cladding Technology, United Kingdom* // Mauro Overend, *University of Cambridge, Cambridge, United Kingdom* // Uta Pottgiesser, *Delft University of Technology, Architecture and the Built Environment, Netherlands* // Josemi Rico-Martinez, *University of the Basque Country, Donostia- San Sebastian, Spain* // Paolo Rigone, *UNICMI, Milan, Italy* // Holger Strauss, *Innobuild GmbH, Berlin, Germany* // Jens Schneider, *University of Darmstadt, Darmstadt, Germany* // Holger Techen, *University of Applied Sciences Frankfurt, Frankfurt, Germany* // Nil Turkeri, *Istanbul Technical University, Istanbul, Turkey* // Claudio Vásquez Zaldívar, *Pontificia Universidad Católica de Chile, Santiago, Chile* // Aslihan Ünlü Tavil, *Istanbul Technical University, Istanbul, Turkey* // Stephen Wittkopf, *Lucerne University of Applied Sciences and Art, Lucerne, Switzerland*

Submissions

All manuscripts and any supplementary material should be submitted to the Editorial Office (editors@jfde.eu), through the Open Journal System (OJS) at the following link: <https://jfde.eu/>

Author Guidelines

Detailed guidelines concerning the preparation and submission of manuscripts can be found at the following link:
<https://journals.open.tudelft.nl/index.php/jfde/about/submissions>

Contents

- v **Editorial**
Ulrich Knaack
- 001 **Active, Passive and Cyber-Physical Adaptive Façade Strategies: a Comparative Analysis Through Case Studies**
Jens Böke, Paul-Rouven Denz, Natchai Suwannapruk, Puttakhun Vongsingha
- 019 **Influence of Automated Façades on Occupants: A Review**
Pedro de la Barra, Alessandra Luna-Navarro, Alejandro Prieto, Claudio Vásquez, Ulrich Knaack
- 039 **CoolSkin**
Andreas Greiner, Olaf Böckmann, Simon Weber, Martin Ostermann, Micha Schaefer
- 057 **Renovating Modern Heritage – The Upgraded Façade of Commerzbank Düsseldorf**
Rouven S. Grom, Andreas W. Putz
- 071 **Timber-based Façades with Different Connections and Claddings: Assessing Materials' Reusability, Water Use and Global Warming Potential**
Miren Juaristi, Ilaria Sebastiani, Stefano Avesani
- 087 **The Potential of Static and Thermochromic Window Films for Energy Efficient Building Renovations**
A.J.J. Kragt, E.R. van den Ham, H. Sentjens, A.P.H.J. Schenning, T. Klein
- 105 **Additively Manufactured Urban Multispecies Façades for Building Renovation**
Iuliia Larikova, Julia Fleckenstein, Ata Chokhachian, Thomas Auer, Wolfgang Weisser, Kathrin Dörfler
- 127 **Retrofitting Potential of Building envelopes Based on Semantic Surface Models Derived From Point Clouds**
Edina Selimovic, Florian Noichl, Kasimir Forth, André Borrmann
- 141 **Suntex: Weaving Solar Energy Into Building Skin**
Pauline van Dongen, Ellen Britton, Anna Wetzels, Rogier Houtman, Ahmed Mohamed Ahmed, Stephanie Ramos

Editorial

The PowerSkin conference series is a biennial event organised cooperatively between TU München, TU Darmstadt, and TU Delft, which is already in its fourth edition, having started in 2017. This coming edition of PowerSkin has also been supported and organised with the support of RWTH Aachen. The conference addresses the role of building skins in accomplishing a carbon-neutral building stock. Therefore, integrating the environmental dimension of material and construction into the design phase is increasingly essential. This is done primarily by considering the energy and emissions linked to the building fabric's fabrication and its ability for reuse and recycling.

For this reason, the focus of the PowerSKIN Conference 2022 is the building fabric with its environmental potential to unlock. Therefore the theme is: **"Build in stock – renovation strategies: inorganic, circular materials vs organic, compostable materials"**.

This theme is discussed through the following sub-themes:

- 1 Envelope: the building envelope as an interface for interacting between indoor and outdoor environments, new functionalities, technical developments and material properties.
- 2 Energy: new concepts, accomplished projects, and visions for the interaction between building structure, envelope and energy technologies.
- 3 Environment: Façades or elements of façades which aim to provide highly comfortable surroundings where environmental control strategies, energy generation and/or storage are an integrated part of an active skin.

This special issue of the Journal of Façade Design and Engineering dedicated to PowerSKIN 2022 showcases the conference's most prominent and relevant papers, aiming to enhance their visibility for a larger audience.

Ulrich Knaack - Editor in Chief

DOI

<http://doi.org/10.47982/jfde.2022.powerskin.00>

Active, Passive and Cyber-Physical Adaptive Façade Strategies: a Comparative Analysis Through Case Studies

Jens Böke¹, Paul-Rouven Denz¹, Natchai Suwannapruk¹, Puttakhun Vongsingha¹

* Corresponding author, Jens.Boeke@priedemann.net

¹ Priedemann Fassadenberatung GmbH, Germany

Abstract

In view of the required energy savings in the building sector, there is an urgent need for innovative and sustainable solutions to increase the performance of building envelopes. Adaptive façades can make an important contribution, whereby passive low-tech strategies and active high-tech solutions are apparently incompatible. In current digitalization, new technologies and methods for the implementation of adaptive façades emerge in the framework of Cyber-Physical Systems. The investigation follows the research question: How can active and passive approaches of adaptive façades be mediated and what potential do Cyber-Physical Systems have for the implementation of hybrid solution approaches in the future? The article presents a comparative case study of the two research projects ADAPTEX and PRÄKLIMA as examples of passive and active adaptation strategies in the façade industry. In this context, the potential for further research of Cyber-Physical Systems in the application domain of adaptive façades as a catalyst for high-performance and multifunctional solutions, and as a mediator between both strategies, is highlighted. The main findings are the potential application of cyber-physical system technologies to the design and monitoring of passive adaptive façade solutions, as well as the possible integration of passively conceptualized components into active overall systems.

Keywords

adaptive façade, smart material, intrinsic adaptation, extrinsic control, artificial intelligence, prototyping, monitoring, ADAPTEX, PRÄKLIMA

DOI

<http://doi.org/10.47982/jfde.2022.powerskin.01>

1 INTRODUCTION

As part of the digital transformation of our society and economy, a wide range of new automation technologies emerges with associated strategies for their application (Gupta & Bose, 2019; Nambisan et al., 2019). Example disciplines are autonomous driving or the decentrally organized “smart factories” of Industry 4.0 (Pisching et al., 2016). The combination of mature cloud infrastructure and growing Artificial Intelligence (AI) capabilities is leading to a new generation of digital tools and methods that are showing their potential in many application fields through the deployment of Cyber-Physical Systems (Rajkumar et al., 2010). They promise greater efficiencies and more flexibility for architects, engineers, and developers. There is an ongoing debate as to whether they also contribute to a more sustainable built environment or promote “business as usual”.

In view of ongoing climate change with global effects on our environment, the United Nations formulated the increasing need for action with regard to sustainable development in their goal definitions (United Nations Department of Economic and Social Affairs, 2021). In the European Union, the building sector accounts for about 40 % of primary energy consumption and 36 % of greenhouse emissions (In Focus: Energy Efficiency in Buildings, 2020). In line with global ambitions as formulated by IEA (2021) to become climate neutral by 2050, European measures include revising current policies by amending the Energy Performance of Buildings Directive (EPBD) and Energy Efficiency Directive (EED), which focus on nearly net-zero buildings, energy performance certificates, long term renovation strategies for EU countries, also taking smart and innovative technologies for new buildings into account (EUR-Lex - 52020DC0098 - EN, 2020).

In line with the formulated energy-saving targets, sustainability is a key issue in the construction industry and is pursued by various building strategies, like improved insulation of the buildings, building-integrated energy generation, and application of reversible construction methods. In addition, smart technologies are discovered as a possible contributor to improved sustainability in the building sector. The existing building stock accounts for a large share of the energy demand, with approximately 75 % of the total building stock being energy inefficient. (EUR-Lex - 52020DC0098 - EN, 2020)

With the building envelope acting as a barrier between the indoor and outdoor environment it plays a crucial role in regulating the indoor environment which directly affects the energy performance of a building. Therefore, the design of an energy-efficient façade presents itself as one of the potential solutions to tackle the imminent issue as various researches have shown that adaptive façades have the potential to reduce the energy consumption of a building by up to 29 % (Bui et al., 2020; Shi & Pouramini, 2022). In addition to its role as a barrier between the indoor and outdoor environment, a high-performance sustainable façade should also serve as a building system that actively responds to the ambient environment and contributes to reducing the building energy consumption while providing optimal comfort to the users. (Aksamija, 2013)

2 ADAPTIVE FAÇADE STRATEGIES

In its role, as defined by Herzog et al. (2004), of an interface between the external climatic conditions and the desired indoor environmental quality of a building, the façade significantly affects the energy performance of a building, as well as the provided interior comfort. Adaptive façade systems offer considerable potential for optimization in this context, as they are able to adapt

independently and dynamically to changing circumstances and requirements in order to provide the most efficient configuration of the construction for the respective boundary conditions (Kasinalis et al., 2014). In practice and according to the current state of the art, adaptive façades are mainly project-dependent, with only selective individual adaptive features like sun shading or ventilation. The overarching objective of holistic multifunctional adaptive building envelopes remains uncommon as commercially available products (Böke et al., 2019; Loonen et al., 2013).

There are two basic approaches to establishing adaptability: First, via a low-tech approach that makes use of physical effects and material behaviour. Loonen et al. (2013) classify this passive strategy as intrinsic adaptation due to its integrated actuation feature and the autonomy of its control. The second approach, as a high-tech solution, relies on the extensive use of automation technologies and digital control. Following Loonen et al. (2013), such systems can, due to the required external impulse to trigger adaptations, be accordingly defined as extrinsic.

2.1 PASSIVE ADAPTATION STRATEGIES

To tackle the immediate challenges of reducing carbon emissions and stalling global warming, it is generally acknowledged that passive strategies should be implemented as the first strategy in designing an energy-efficient building (Prieto et al., 2018). Due to their simplicity and low-threshold approach, passive strategies have been commonly practiced in vernacular architecture, designed to accommodate the immediate environment. Prominent examples of passive solutions include the use of wind towers for passive air conditioning in hot and dry climates and the use of trombe walls as a passive solar heating strategy in temperate climates (Maleki, 2011; Wang et al., 2021). Nevertheless, due to the changes in lifestyle, technological advancement, and higher requirements for high-performance buildings, passive features are also adapting to conform to architectural trends and modern lifestyles (Konis & Selkowitz, 2017). This is reflected in the recent façade developments which are multifunctional and highly adaptive systems, allowing the façade to change its functions to adapt to the immediate environment (Loonen et al., 2015).

In today's implementation of passive adaptation strategies, the application of smart materials plays an important role, as they enable the initiation of self-sufficient adaptation processes via material-immanent capabilities. Commercially introduced in the early 20th century, smart materials such as Nitinol are gaining acceptance as an alternative solution to meet the technological demands of today. Defined by Addington et al. (2007) as "highly engineered materials that respond intelligently to their environment", smart materials broaden the design possibilities and introduce new design options in various sectors including the building industry. In recent years there has been increasing investigation into how "smart materials" respond to various environmental stimuli. Hensel (2013) defines materials with such capacities as "material systems" based on their respective ability to react to their environment. In a similar understanding, Menges et al. (2014) explore the exploitation of intrinsic material properties to perform adaptations through the application of digital design methods. One example is the "HYGROSKIN – METEOROSENSITIVE PAVILION" project, in which wood composites allow for opening and closing the structure purely in response to changes in humidity (Menges & Reichert, 2015).

Due to the intrinsic characteristics, different research projects offer an alternative approach in place of mechanical shading and ventilation systems. Examples are the vertically moving screen system developed by Decker & Zarzycki (2014), an operable modular shading panel that incorporates two sets of counteracting SMA by Payne & Johnson (2013), and the project "Bloom", incorporating a

thermal bi-metal shell structure which curls when heated to ventilate a specific area under the shell (Fox, 2016). The innovative solutions allow immediate response to the environment while presenting the potential to minimize energy consumption during operation. Nevertheless, despite operational simplicity and intrinsic characteristic, the automatic response to the environment can also create dissatisfaction for the users, as it limits personal control and often fails to accommodate the demands of different users, especially in a shared space (Luna-Navarro et al., 2020).

2.2 ACTIVE ADAPTATION STRATEGIES

Adaptive façades are today mainly implemented as part of building automation systems (BAS) on the basis of automation technologies (Böke et al., 2020a). Their operation is based on a set of electrical and mechanical devices that perform automated tasks assigned through a control network. According to the current state of the art, BAS are structured as hierarchically organized control concepts following the idea of automation pyramids as shown in FIG 1. (Cerf, 2010; Soucek & Loy, 2007). In a simplified understanding, they consist of a bottom assembly level with sensors and actuators of the system architecture, the digital direct controllers (DDC) and terminal strips for control and regulation in the middle levels, and the central control management at the top (Merz et al., 2009). Different product standards and platforms exist, such as ZigBee, KNX, BACnet, Modbus and LonWorks. Building automation systems themselves represent a potential solution to reduce energy consumption by controlling the HVAC system during building operation, enabling monitoring and maintenance, and thereby also providing user comfort. The development of building automation technologies is vendor-driven, which in practice often leads to integration problems due to inconsistent product standards and protocols (Domingues et al., 2016).

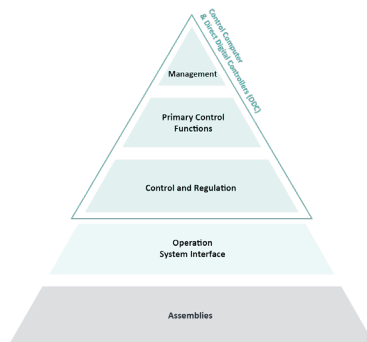


FIG. 1 Concept of the automation pyramid adopted from (Merz et al., 2009)

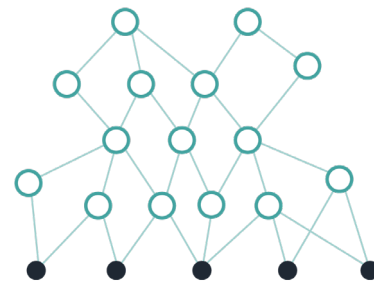


FIG. 2 Decentralized nature of Cyber-Physical Systems adopted from (Monostori et al., 2016)

According to the findings of Loonen et al. (2015), the main characteristic of active façade controls is the incorporation of feedback loops which allow for the current configuration or action to be evaluated by the desired state or a benchmark. Despite the wide range of operational characteristics and categorization of adaptive façades, active operations are based on three main stages: data collection or input, processing of the acquired data and finally executing physical actions as the output. Accordingly, automated adaptive façades comprise of a sensor system that collects relevant information as input data, a processing system that translates them into control parameters that are received by the actuators, and actuators that execute the control decisions as adaptation measures of the façade configuration.

One of the most common applications of active façade adaptations is dynamic shading devices. The dynamic aspect of the façade grants a higher level of design freedom for the designer to plan with a higher level of transparency without compromising to the limitation in thermal performances and window-to-wall ratio aspects. Therefore, they are usually implemented as machinal louvres, shutters, screens, or blinds, as a means to control solar gains and utilize passive solar energy (Loonen et al., 2015). These examples are evident in projects such as Q1 Thyssen Krupp Headquarter by JSWD architects, the Oval Offices by Sauerbruch Hutton, or a more sophisticated application at the Al Bahr tower by Aedas architects. In recent years, chromogenic façades gained increased attention and are becoming more commercially available. Due to its operational approach which relies on electrochemical reactions in the layers of semiconducting materials, mechanical parts are eliminated, and the system can run with low operating costs (Sandak et al., 2019). Active ventilation systems represent another example for extrinsic implementations of adaptive façades. They are usually integrated as automated operating windows to regulate natural ventilation or within closed cavity façades to control airflow and provide heat dissipation (Attia et al., 2020).

Automated adaptive façades occur as in the given examples with selective implemented automated functions and their integration into the BAS, while limitations still exist in the availability of holistically coordinated multifunctional adaptive façades. At this point, Cyber-Physical Systems, as explained in Section 1.3, can make a major contribution by allowing for highly flexible and decentralized control concepts.

Actively automated and controlled systems offer a high degree of flexibility and intervention possibilities in digital control. At the same time, they also entail a number of disadvantages due to the fact that they are high-tech solutions with a limited lifetime of the electrotechnical components and their susceptibility to malfunctions. This can lead to a high maintenance effort in the operation of actively automated façades. In addition, while offering the possibility of reducing the building's overall energy consumption by offsetting HVAC expenses, they are also primarily dependent on the additionally invested electrical power supply (Loonen et al., 2013).

2.3 CYBER-PHYSICAL FAÇADE SYSTEMS (CPFS)

Cyber-Physical Systems (CPS) are the main driver of the current digital transformation of our society and environment. They are based on the close interaction of physical products, plants, and systems with their digital control (Broy, 2010). The technical requirement for this integration is the possible embedding of physical devices with independent processing capabilities, which is possible today due to both miniaturization and the increase in the performance of computer technologies (Wolf, 2012). An important aspect of CPS is its shift from the former hierarchical automation pyramid organization (FIG 1) to cloud-based networking and decentralized control as shown in FIG 2 (Monostori, 2014).

In addition to their appearance in the form of the Internet of Things (IoT), Cyber-Physical Systems find their application in many different sectors today, such as medicine, transportation, power grids, and industrial production (Jamaludin & Rohani, 2018). In building industry, Cyber-Physical Systems are already being researched and deployed, as described by Bonci et al. (2019) for building efficiency monitoring, in fabrication and computer-aided manufacturing processes as presented by Menges (2015), and smart building automation (Karbasi & Farhadi, 2021; Reena et al., 2015). A prominent application field is smart factories of Industry 4.0, where such systems are defined as intelligent technical systems (Dumitrescu et al., 2013). Their implementation is closely related to the development of digital twins (Biesinger et al., 2019; Negri et al., 2017). According to the basic concept

of CPS, individual plants of production lines are equipped with individual control and networked to form decentrally organized production systems (Herwan et al., 2018). The aim is to increase both the productivity and flexibility of the production processes (Monostori, 2014). The utilization of the Cyber-Physical System concept is evident in various industrial sectors ranging from equipment manufacturers, and operators, as well as service organizations such as airport facility management (Herterich et al., 2015).

Under the similar objective of increasing flexibility and energy performance, Cyber-Physical Systems can also be applied to automated adaptive building envelopes. The corresponding implementation of a cyber-physical façade system (CPFS) was investigated by Authors in the development of a prototype which, in addition to its physical components with deployed sensors, actuators, embedded control, and realized communication system, also includes a representation as a digital twin for monitoring the system behaviour. Automated individual façade functions such as solar shading, ventilation, and heating and cooling were part of the consideration. Based on the environmental information provided by the integrated sensors, the instances of the automated façade functions make independent adaptation decisions via feedback loops on the installed microcontrollers and coordinate these via the communication system to coordinate measures of the overall system (Böke et al., 2020b). The result is a flexible and independently operating organism of individually automated and cooperating façade functions.

In comparison to other industrial sectors, the innovative automation strategy of Cyber-Physical Systems had just been introduced in the Architectural, Engineering, and Construction (AEC) fields, therefore, their application is still premature (Böke et al., 2019). Many open questions remain regarding relevant façade construction and automation technologies, advanced control concepts, and current implementation strategies. This can be further specified to the following core topics still to be investigated: In addition to the structural implementation of cyber-physical façades, one main aspect is to increase the efficiency of decision-making processes at the higher control level by using AI strategies. Another open question is on the provision of project-specific tailored datasets, which requires both the selection and component integration of appropriate sensor technology. From an accessibility point of view, the interaction between users and the façade is an interesting aspect that has not yet been thoroughly explored in the field of CPFS. In this context, similar to the inability to obtain full control over the system, relates to passive solutions described in section 1.2.1, the effects of adaptation processes on user comfort as well as the user's possibilities to interact with the cyber-physically automated façade are relevant open questions. Nevertheless, in view of the technological capabilities existing today, the research on CPFS already shows great potential for automated system application, especially in adaptive façades. This is due to the integrated nature of physical construction and its embedded digital control, which enables further digital optimization strategies like the application of AI and machine learning. AI is increasingly recognized for use in architecture and façade engineering (Chaillou, 2022; Kraus & Drass, 2020). In this sense, cyber-physical façades represent a door opener, especially for performance-enhancing innovations on the cyber level.

3 PROBLEM STATEMENT

While the adaptability of façades has been already recognized and intensively researched as a strategy for improving the energy performance of buildings, solutions to date are mostly fragmented and project-dependent implementations of individual adaptive functions (Aelenei et al., 2016; Loonen et al., 2013). The goal of holistically conceived implementations of multifunctional and well-

coordinated overall systems remains largely unachieved in the implementation of adaptive façades to date. In particular, a disconnect exists in the two contrasting mindsets of either a passive low-tech solution, for example via the use of material-inherent smart properties formulated by Hensel (2013), and an alternative high-tech approach via extensively equipped automation technologies and digital control.

4 OBJECTIVE

In response to the posted problem statement, the objective of this paper is to review previous theories behind active, passive and cyber-physical systems and compare these concepts in a physical case study. It therefore elaborates the ongoing investigation of two exemplary Research and Development projects, ADAPTEX and PRÄKLIMA, which represent the described passive and active approach to adaptivity and already implemented aspects of Cyber-Physical Façade Systems (CPFS) in their design framework. Insights from the research by design process and the utilization of the Cyber-Physical system framework is described to establish a base for discussion in examining the possibility of a hybrid adaptive façade system.

One goal of the study is to question both ways of thinking and to explore possible interfaces. Cyber-Physical Systems represent a new stage of development in automation in many fields of application (Rajkumar et al., 2010). In this context, it questions how correspondingly available technologies and application methods can play a mediating role and contribute to future comprehensively adaptable façade systems. Accordingly, the paper follows the research question: How can active and passive approaches of adaptive façades be mediated and what potential do Cyber-Physical Systems have for the implementation of hybrid solution approaches in the future?

5 CASE STUDIES: ADAPTEX AND PRÄKLIMA

5.1 METHODOLOGY

The study discloses the experiences from the prototypical implementation of both projects and draws a comparative balance of the two solution approaches between passive implemented adaptivity and active control. Two research projects, ADAPTEX and PRÄKLIMA, demonstrate the application of smart materials, digital technologies, and respective methods in order to reach desired façade performance objectives. Therefore, they have been selected as case studies to examine the implementation of the Cyber-Physical system through its roles as either a facilitator or a mediator, in a passive or active implementation potential of adaptative measures in the building envelope. In both cases, the test operation on the 1:1 scale prototype and the related assessment of the actual contribution of the respective concept to the energy performance of the façade are presented and discussed.

ADAPTEX is an autarkic and adaptive textile sun shading solution which implemented the smart material, Shape Memory Alloy (SMA) as an actuator. The system operations and the employment of the Cyber-Physical system framework as a facilitator through the series of sensors system which enables an effective selection of 'smart materials' that is tailored to a site-specific context and monitoring the behaviour of the passive operation of the system is discussed in the result section.

On the other hand, PRÄKLIMA is a self-sufficient modular, unitized façade system which incorporates an air-conditioning system and solar control with a predictive, self-learning control system. It represents an active system that enables automated and multi-functional adaptations. Hence, the role of Cyber-Physical system as a mediator between design variables to enhance the decision-making process of a machine learning integrated decentralized façade system will be examined.

The potential of both approaches is reflected with regard to further investigation from the viewpoint of a cyber-physical realization of a hybrid façade system as illustrated in the methodology diagram in FIG 3. Furthermore, an outlook toward a more comprehensive implementation of CPFS in the building industry is presented in the Discussion chapter.

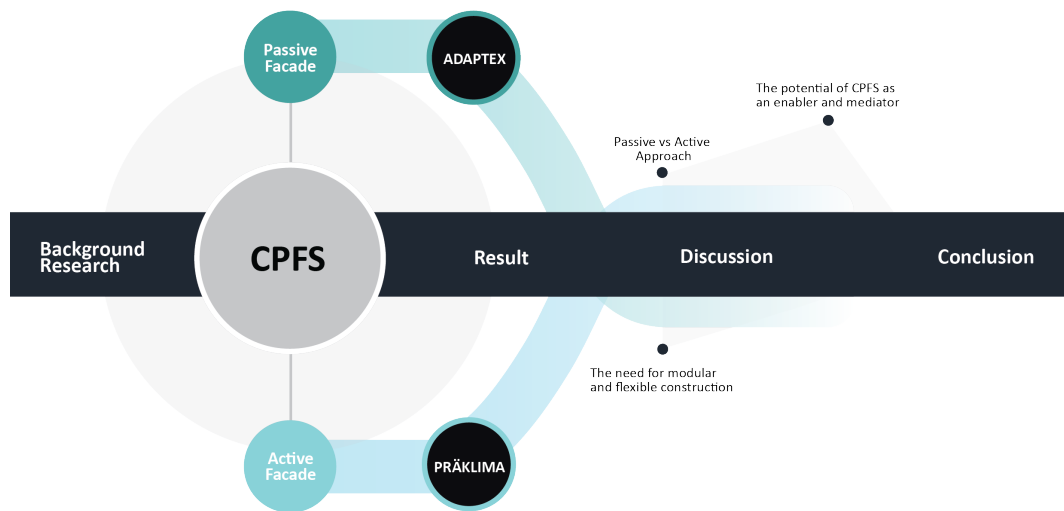


FIG. 3 Methodology diagram

The following two sections document the implementation of the research projects ADAPTEX, an autarkic and adaptive textile sun shading solution, as an exemplary application of a passive adaptation strategy, and PRÄKLIMA, a self-sufficient modular, unitized façade system which incorporates an air-conditioning system and solar control with a predictive, self-learning control system, in terms of an automated and active control of adaptation measures.

5.2 RESEARCH PROJECT ADAPTEX AS PASSIVE APPROACH TO ADAPTIVITY

The ADAPTEX research project focuses on the investigation and development of integrating Shape Memory Alloy (SMA) as an actuator in textile, adaptive sun shading solutions to achieve an autarkic operation that passively adapts themselves to the changes in ambient temperature. (Denz et al., 2021) Shape memory alloys (SMA) are among the so-called smart materials. They react to temperature changes through deformation and/or shrinkage, depending on their geometry and the predefinition of their material configuration. The ADAPTEX project takes advantage of this effect by integrating SMAs as wires into the textile structure and using them as actuators inducing high forces relative to its size to operate the system.

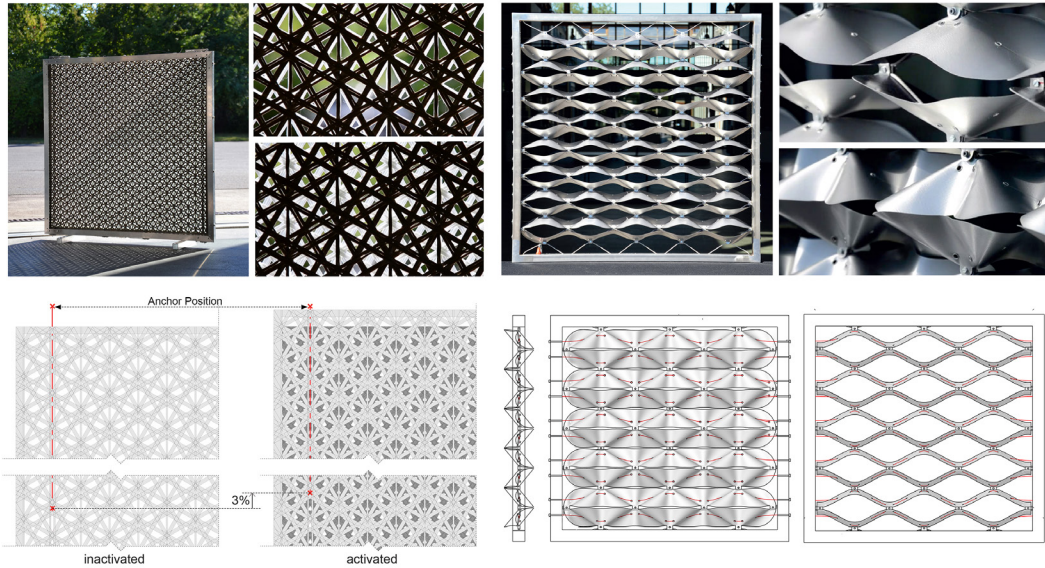


FIG. 4 ADAPTEX textile adaptive sun shading concepts: Mesh on the left - Wave on the right.

Two concepts have been developed following the principle of the SMA behaviour. The concepts, ADAPTEX Mesh and ADAPTEX Wave differ both in their textile structure and kinetic mechanism. ADAPTEX Mesh consists of two identical non-woven textile layers. The operation relies on the SMA which is integrated into the layer behind. In the inactivated state, as the identical perforation aligns, maximum permeability is achieved. When activated, the deformation of the SMA causes the panel behind to slide up creating an overlapping pattern that reduces the overall permeability. The operation provides an openness factor which ranges between 63% (inactivated) to 39% (activated) (Schneider, et al., 2021).

ADAPTEX Wave, on the other hand, is based on a geometrical deformation of wave-shaped textile bands. The deformation is induced by the SMA wire that is interwoven along the length of the textile bands. As the SMA shrinks, it forces the tape to buckle, enabling an open and closed state comparable to eyelids. The operation states allow the openness factor to be configured within the range of 70% during inactivation and 5% when activated. (Schneider, et al., 2020)

The operating principle of both concepts was investigated by the development of a 1.35 x 2.80 m demonstrator at a 1:1 scale. After implementation and proof of general functionality, they were subjected to various measurements and investigations of their physical performance. In this initial phase of the project, the SMA was activated by the external introduction of an electrical current to manipulate the required temperature change in order to initiate the adaptation mechanism where the SMA length becomes shorter when activated. (Denz et al., 2021). This allowed for both automation and manual control by the user. Later, as in the recent development of the ADAPTEX KLIMA+ project, both solar shading concepts were designed to be completely self-sufficient, without dependency on introduced electrical power, and solely activated by the changes of ambient temperature and irradiation exposure on the textile surfaces.

This passive approach simplifies the system and eliminates previously required technical infrastructure to control and activate the SMA. At the same time, it imposes additional requirements for pre-planning and selecting the suitable SMA for the prevailing temperature range. Since the properties and activation ranges of the SMAs are defined during their production process, ADAPTEX

KLIMA+ sun shading only operates in accordance with the pre-programmed configuration with only minor manipulations allowed. These small manipulations are possible by the adjustment of secondary variables like changing the weight or the strength of the textile, as well as by increasing or reducing the length of the applied SMA. The consideration of the individual needs of different users is neglected in the current development stage ADAPTEX KLIMA+ because the focus is on understanding the behaviour of the SMA and the textile materials. Therefore, the design of the concepts focused on an application of the self-sufficient sunshade for use in public areas, where the need for individual manual control was not part of the requirements.

Operation as a passive solar shading system requires a deep understanding of the textile and SMA material properties. The subtropical and dry climate in Muscat, Oman, provides an ideal environment for the investigation of material behaviours under the extreme alternation of prevailing hot daytime temperatures and relatively cooler night-time temperatures. After initial tests under controlled conditions at the Priedemann Façade-Lab in Berlin shown in FIG 5. , the shading system will be further investigated under real conditions of the outdoor climate in Oman. For this purpose, one ADAPTEX Wave solar shading screen, consisting of three individual elements, and one Mesh screen, consisting of five smaller individual elements were produced to be installed at the Eco House of the German University of Technology in Oman (GUtech) in Muscat as illustrated in FIG 6.



FIG. 5 Testing of the SMA-behavior under maintained and supervised temperature conditions



FIG. 6 Application of the passive ADAPTEX sun shading to the EcoHouse at GUtech in Muscat, Oman

An important aspect of the ADAPTEX application in Oman is the monitoring of the system. The Cyber-Physical system framework has been employed as a mediator to collect comprehensive data on the environmental conditions and on the behaviour of the system in response to occurring changes of the climate. Automation technologies and IoT concepts come into play in this context. Installed as a decentral organized sensor network, the monitoring system takes solar radiation, ambient temperature, as well as wind conditions into account. At the same time, the surface temperatures of the SMA are recorded via thermal coupling sensors at different locations. The reaction of the system is documented via displacement measurements and video recordings. All sensors are connected to different Arduino MKR1010 Wifi microcontrollers, which share their data with the central Raspberry PI 4 broker via wireless network using an MQTT communication protocol. FIG 7. shows the technical setup of the monitoring system.

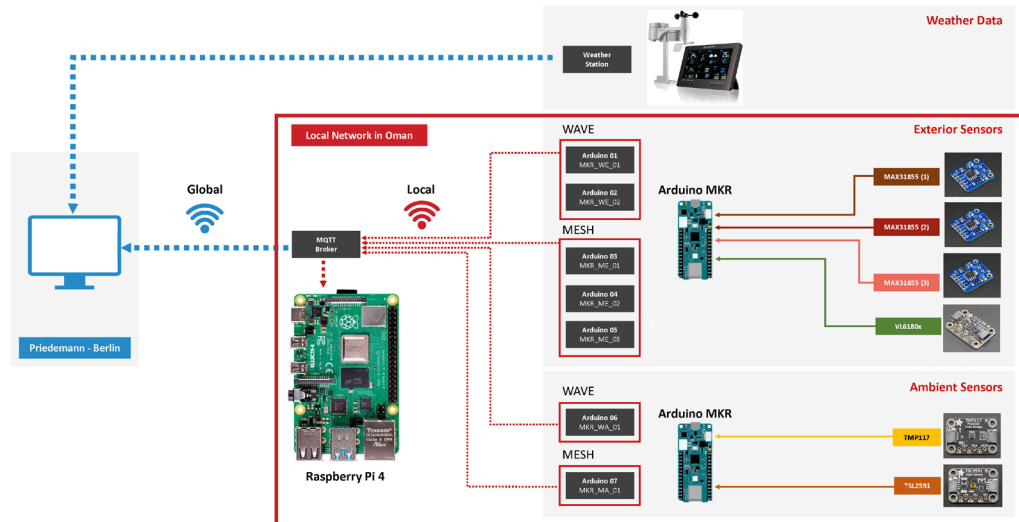


FIG. 7 Decentrally organized sensor network for monitoring the adaptex sunshading in Oman

The Raspberry Pi acts as a broker and connects to the Internet. It enables cloud-based data logging and access to real-time monitoring data remotely. This is crucial to the success of the project, as the prototypes are left unattended most of the time. The monitoring system runs autonomously with external control for maintenance and diagnostics, allowing the collected data to be accessed over the cloud in real time.

5.3 PRÄKLIMA AS ACTIVE APPROACH TO ADAPTIVITY

PRÄKLIMA is a research project, developed to meet the sustainability goals to achieve a near climate neutral building stock by 2050. Together with various partners from both academic and industrial sectors, the formulated objective of the PRÄKLIMA project from the beginning was to develop a modular, multifunctional, adaptive and at the same time, self-sufficient façade system with a predictive-self learning algorithm to control the façade integrated actuators.

PRÄKLIMA is developed as a double skin, unitized façade system with two main elements: an opaque, technical module and a transparent module. To achieve the desired multifunctionality and self-sufficiency, the technical module is incorporated with photovoltaic (PV), LUNOS Next ventilation unit with mechanical ventilation and heat recovery system, as well as a battery for electricity storage. The decentralized LUNOS Next ventilation unit in the opaque element provides air conditioning for heating and cooling. It is positioned behind the photovoltaic (PV) element and takes in the supply air from the cavity space provided for the PV module – thus creating a hybrid air collector. Moreover, a solenoid operated flap has been integrated to control air flow direction into the ventilation system. This allows differentiated control of the ventilation behaviour, depending on seasonal requirements. To efficiently utilize the pre-heated air in winter, it is taken from bottom of the PV panel, and to avoid overheating during summer, the air is taken in from a shorter route from the top of the panel. On the other hand, the transparent module consists of a mechanically operated window that provides natural ventilation, lighting, views to the outside and the use of passive solar gains, which can be controlled by the additional integrated automated venetian blinds. The façade is currently installed according to FIG 8. as a prototype in front of a 2.00 x 3.00 x 3.00 m insulated chamber, which serves as a test stand at SOMMER Fassadensysteme in Hof, Germany. The functionality and performance of the system are investigated using this setup in the ongoing test operation.



FIG. 8 PRÄKLIMA façade in front of the insulated chamber serving as a testbed for ongoing monitoring, the opaque element on the right, the transparent one left side.

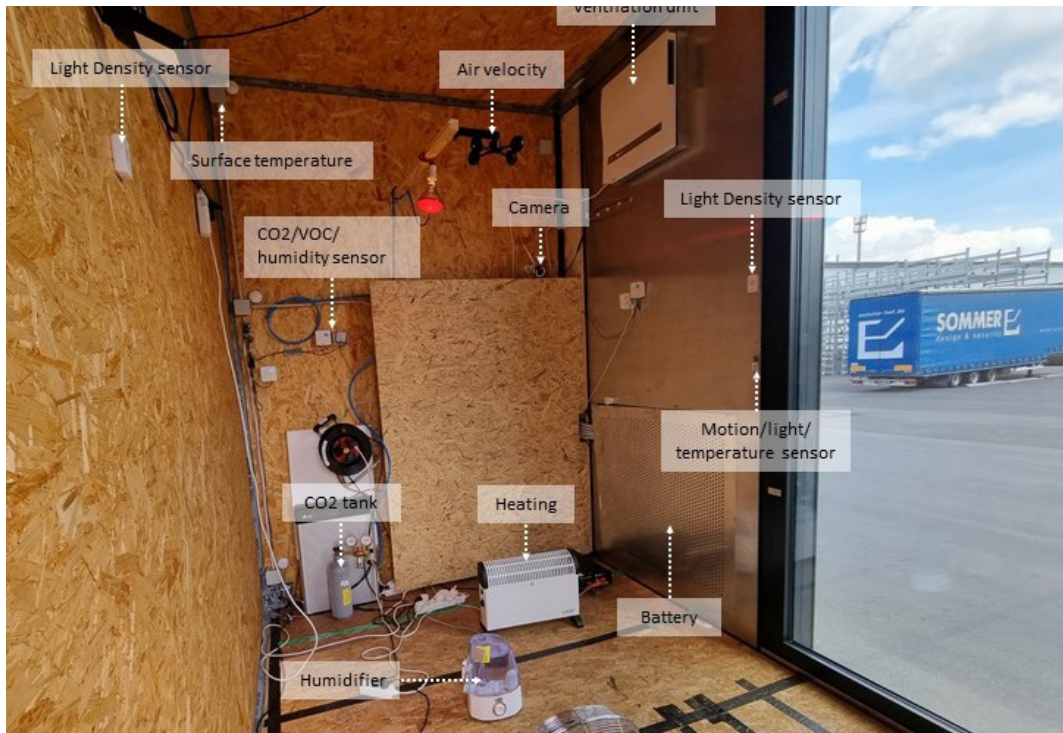


FIG. 9 Interior view of the PRÄKLIMA Testbed highlighting main sensor and actuator devices

Under the Cyber-Physical system framework, the PRÄKLIMA façade incorporates an extensive sensor technology serving as mediators to enable different automated functions, providing for the technical implementation of adaptation strategies. The sensor technology is installed in various locations including inside the test chamber as visible in FIG 9., within the façade element between the cavity, and at the exterior of the façade element in areas that are exposed to environmental influences. The setup considers, among many others, the measurement of wind speed, precipitation, illuminance in the outdoor environment, while for example CO₂, air temperature, motion, and illuminance sensors are deployed inside to provide a meaningful information base on the conditions of the indoor environment.

The name of the PRÄKLIMA project derives from its predictive and adaptive control strategy. An installed Raspberry Pi microcomputer and a small field-programmable gate array (FPGA) form the control unit of the façade and utilize the gathered information from the sensor system by means of a self-learning algorithm that also takes global information like weather forecasts and user behaviour into account. The control concept is illustrated in FIG 10. Based on the information provided, the self-learning algorithm makes independent decisions about the control of the automated façade functions. Because it takes into account previous responses and data, the decision-making regarding the optimal configuration improves during its operational lifetime.

Control flow

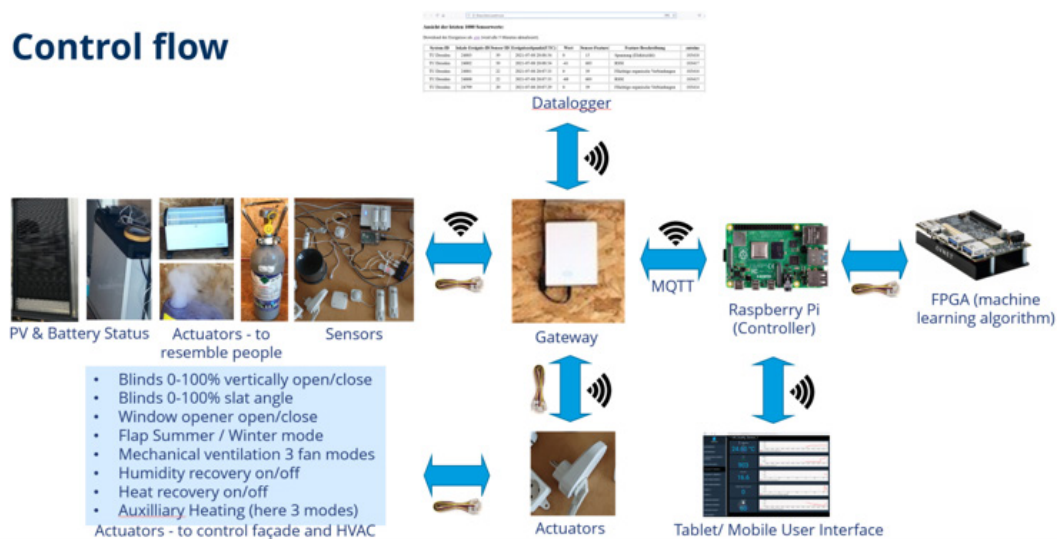


FIG. 10 Control concept of the self-learning PRÄKLIMA façade

Under the objective of a self-sufficient and autarkic operation of the PRÄKLIMA façade, the integrated PV module is a crucial component, as it makes the electrical operation of the technical equipment, such as sensors and automated façade functions, independent of additionally invested energy from the power grid. This ideal complete autarkic operation is not yet fully achieved, as in the preliminary configuration of the prototype the energy consumption of the Lunos Next device exceeds the provided power supply.

6 RESULTS AND DISCUSSION

The ADAPTEX concepts Wave and Mesh, as described in Section 5.2, demonstrate a passive approach to autonomous opening and closing of textile sun shading via integrated shape memory alloys. In the PRÄKLIMA project, extensive automation technologies and a self-learning algorithm were applied in order to enable the adaptivity of the façade. The two case studies exemplarily contrast the passive approach of using smart materials with the active solution through the use of automation technologies and digital control. Both approaches led to functional and effective concepts within the framework of their respective project goals.

6.1 PASSIVE VS. ACTIVE APPROACH

Due to their operational simplicity with minimal components and the absence of high-tech electronic components, passive solutions offer an advantage over active, automated adaptive concepts, which essentially consists of their reduced vulnerability to technical errors as well as their independence of an additional energy supply. Compared to an active control system however passive systems conversely lack control options and overriding possibilities of the adjustment processes during operation. As learned from the ADAPTEX project, the preconfigured material properties are permanent and cannot be adapted to possibly changed requirements. However, the monitoring system in the project, implemented via a decentralized sensor network, has shown promising application possibilities of automation technologies in passive systems with regard to their pre-configuration and for the purpose of their function monitoring during operation. Furthermore, the question arises whether there are possible interfaces between active and passive solutions, after the passive ADAPTEX sun shading concept was initially activated by the supply of electrical energy. Thus, an override of passive adjustment processes by a digital control appears as possible as the inclusion of the SMA as a part of the sensor system of an automated concept. Vice-versa, it also seems possible that the integration of passive adaptation strategies can also be designed as a component of active control systems, as long as their properties and states can be detected during operation and taken into account in the overall control of the façade. In this way of thinking, the passively acting components as resilient actuators with their material-integrated intelligence contribute to the simplicity and resilience of active automated, multifunctional adaptive façades. Thus, the passively operating sun shading solution ADAPTEX could also be integrated into the automation concept of PRÄKLIMA, utilizing the intrinsic capacities of SMA. In this yet hypothetical application, the performance of the shading system can be detected by sensors and coordinated with other actively controlled components such as the ventilation system. If necessary, the non-activated state of the sun shading could be overridden by supplying electrical energy as a secondary mechanism. In this way of thinking, smart materials can become part of actively controlled systems, leading also into desirable further research about the programmability of non-electric systems which is already being pursued in various projects (*Everything under Control*, 2013).

6.2 THE POTENTIAL OF CPFS AS AN ENABLER AND MEDIATOR

The potential of the CPFS system as both an enabler and a mediator has been presented through the development of ADAPTEX and PRÄKLIMA. While in ADAPTEX, the Cyber-Physical system framework has been applied only as a mediator for data collection, the automation concept of the PRÄKLIMA façade project already features broader aspects of a cyber-physical system. This includes comprehensive data collection via extensive sensor technology, wireless communication of data

within the system, and the application of a self-learning algorithm in the control of the system. As described in Section 1.3, one of the main aspects of CPS is the flexibility of the system, since the structure no longer follows the hierarchical concept of an automation pyramid, but is based on the decentralized interaction of individual, independently intelligent system components. This opens up a new way of looking at the intelligence of the components itself, where it no longer matters whether it is based on material intelligence or on digital control. On the different levels of the cyber-physical system concept, new interfaces for the interlocking of active and passive components are emerging in the data acquisition of sensor technology, in cyber-control of the system, as well as in the execution of decisive adaptation processes. This approach dissolves the boundaries between previous purely passive or active adaptation concepts by expanding the pool of technologies that can be integrated into the system, thus enabling new design freedom in the configuration of coordinated adaptations. This paves the way for a new generation of universal multifunctional adaptive façade systems.

6.3 THE NEED FOR MODULAR AND FLEXIBLE CONSTRUCTION

Ensuring that shorter-lived components can be reconfigured and replaced contributes to the sustainability of the façade as an overall system, since it is possible to react flexibly to changing requirements without having to replace the entire façade. This is particularly evident in view of the increasing integration of computer and automation technologies with short life spans. Therefore, as defined by Kaelbling (1987), modularity and adaptivity are important aspects of intelligent reactive systems. Therefore, a particular requirement for component exchangeability exists, for which the research into multifunctional plug & play façades provides a possible answer to ensure modularity and reversibility of façade construction (Mach et al., 2015). Cyber-physically automated façades meet this requirement for modularity due to their decentrally organized structure, in which individual components such as sensors or actuators can be removed or modified without compromising the overall operation of the system. The cyber-physical structure of the façade automation also makes an important contribution to the long-lasting usability of the automated façade construction. It enables software updates to be made to adapt the configuration of the structure to changing requirements over the course of its service life, which makes the physical replacement of components obsolete to a certain extent.

7 CONCLUSIONS

In shedding light on the ADAPTEX passive-adaptive concept and the extensive automation in the PRÄKLIMA project, the study concludes possible interfaces that suggest both the use of automation technologies for configuring and monitoring passive adaptation processes and the integration of supposedly passive technologies such as smart materials in active automation concepts. Through the Cyber-Physical system, necessary data points such as ambient conditions, or indoor conditions can be systematically collected. These data can be further analysed, interpreted, and utilized as the control signal. Due to their decentralized character and control concept, Cyber-Physical Systems can play an important mediating role in the design of corresponding hybrid solutions in the sense of holistically considered, multifunctional adaptive façades, as they allow a high degree of flexibility in the configuration and interaction of the active and passive system components.

Acknowledgements

The projects presented in this scientific paper are the result of close cooperation between various research partners. Acknowledgements belong to the Technische Universität Dresden Institut für Baukonstruktion und Institut für Technische Informatik, SOMMER Fassadensysteme – Stahlbau – Sicherheitstechnik GmbH & Co. KG, and Die Netz-Werker AG for their contributions and cooperation in the project PRÄKLIMA. The project PRÄKLIMA is funded by the BMWK - Zentrales Innovationsprogramm Mittelstand (ZIM). For the project ADAPTEX, the research partners weißensee kunsthochschule berlin, Fraunhofer-Institut für Werkzeugmaschinen und Umformtechnik IWU, Carl Stahl ARC GmbH, VERSEIDAG-INDUTEX GmbH, i-Mesh, ITP GmbH and SGS Ingenieurdienstleistungen im Bauwesen GmbH are acknowledged. ADAPTEX is funded by the German Federal Ministry of Education and Research (BMBF) as part of the smart³ research network.

References

- Addington, D. M., Schodek, D., & Schodek, D. L. (2007). *Smart materials and technologies: For the architecture and design professions* (Repr. 2007). Elsevier.
- Aelenei, D., Aelenei, L., & Vieira, C. P. (2016). Adaptive Façade: Concept, Applications, Research Questions. *Proceedings of the 4th International Conference on Solar Heating and Cooling for Buildings and Industry (SHC 2015)*, 91, 269–275. <https://doi.org/10.1016/j.egypro.2016.06.218>
- Aelenei, L., Aelenei, D., Romano, R., Mazzucchelli, E., Marcin, B., & Rico-Martinez, J. M. (2018). *Case Studies—Adaptive Façade Network*.
- Aksamija, A. (2013). *Sustainable façades: design methods for high-performance building envelopes*. John Wiley & Sons, Inc, Hoboken, New Jersey.
- Attia, S., Lioure, R., & Declaude, Q. (2020). Future trends and main concepts of adaptive façade systems. *Energy Science & Engineering*, 8(9), 3255–3272.
- BAFA - Bundesförderung Serielles Sanieren. (2022). Bundesförderung Serielles Sanieren. https://www.bafa.de/DE/Energie/Energieeffizienz/Seriell_Sanieren/serielles_sanieren_node.html
- Biesinger, F., Meike, D., Kraß, B., & Weyrich, M. (2019). A digital twin for production planning based on cyber-physical systems: A case study for a cyber-physical system-based creation of a digital twin. In *12th CIRP Conference on Intelligent Computation in Manufacturing Engineering, 18-20 July 2018, Gulf of Naples, Italy* (Bd. 79, S. 355–360). <https://doi.org/10.1016/j.procir.2019.02.087>
- Bonci, A., Carbonari, A., Cucchiarelli, A., Messi, L., Pirani, M., & Vaccarini, M. (2019). A cyber-physical system approach for building efficiency monitoring. *Automation in Construction*, 102, 68–85. <https://doi.org/10.1016/j.autcon.2019.02.010>
- Broy, M. (2010). Cyber-physical systems—Wissenschaftliche herausforderungen bei der entwicklung. In M. Broy (Hrsg.), *Cyber-physical systems* (S. 17–31). Springer Berlin Heidelberg. http://link.springer.com/10.1007/978-3-642-14901-6_2
- Bui, D.-K., Nguyen, T.N., Ghazlan, A., Ngo, N.-T., Ngo, T.D., (2020). Enhancing building energy efficiency by adaptive façade: A computational optimization approach. *Applied Energy* 265, 114797. <https://doi.org/10.1016/j.apenergy.2020.114797>
- Cerf, V. G. (2010). Building Automation. *Interconnecting Smart Objects with Ip: The Next Internet*, 361–372. <https://doi.org/10.1016/B978-0-12-375165-2.00024-7>
- Chaillou, S. (2022). *Artificial Intelligence and Architecture: From Research to Practice*. Birkhäuser. <https://doi.org/doi:10.1515/9783035624045>
- Decker, M., & Zarzycki, A. (2014). *Designing Resilient Buildings with Emergent Materials*. <https://doi.org/10.13140/2.1.1060.8967>
- Domingues, P., Carreira, P., Vieira, R., & Kastner, W. (2016). Building automation systems: Concepts and technology review. *Computer Standards & Interfaces*, 45, 1–12. <https://doi.org/10.1016/j.csi.2015.11.005>
- Dumitrescu, R., Anacker, H., & Gausemeier, J. (2013). Design framework for the integration of cognitive functions into intelligent technical systems. *Production Engineering*, 7(1), 111–121. <https://doi.org/10.1007/s11740-012-0437-z>
- EUR-Lex—52020DC0098—EN, Nr. COM/2020/98 final (2020). <https://eur-lex.europa.eu/legal-content/EN/TXT/HTML/?uri=CELEX:52020DC0098&from=EN>
- Everything under control: Building with biology*. (2013). Stichting Archis.
- Fox, M. (2016). *Interactive architecture: Adaptive world* (First edition., S. 176). Princeton Architectural Press.
- Gupta, G., & Bose, I. (2019). Digital transformation in entrepreneurial firms through information exchange with operating environment. In *Information & Management* (S. 103243). <https://doi.org/10.1016/j.im.2019.103243>
- Hamedani, A. Z., & Huber, F. (2012). A comparative study of DGNB, LEED and BREEAM certificate systems in urban sustainability. *The sustainable city VII: Urban regeneration and sustainability*, 1121, 121–132.
- Hensel, M. (2013). *Performance-oriented architecture: Rethinking architectural design and the built environment*. John Wiley and Sons, Ltd, Publication.

- Herterich, M.M., Uebernickel, F., Brenner, W. (2015). The Impact of Cyber-physical Systems on Industrial Services in Manufacturing. *Procedia CIRP* 30, 323–328. <https://doi.org/10.1016/j.procir.2015.02.110>
- Herwan, J., Kano, S., Oleg, R., Sawada, H., & Kasashima, N. (2018). Cyber-physical system architecture for machining production line. In *2018 IEEE industrial cyber-physical systems (ICPS)* (S. 387–391). <https://doi.org/10.1109/ICPHYS.2018.8387689>
- Herzog, T., Krippner, R., & Lang, W. (2004). *Façade construction manual*. Birkhauser-Publishers for Architecture.
- IEA. (2021). *Net Zero by 2050—A Roadmap for the Global Energy Sector*. 224.
- In focus: Energy efficiency in buildings*. (2020). European Commission - European Commission. https://ec.europa.eu/info/news/focus-energy-efficiency-buildings-2020-lut-17_en
- Jamaludin, J., & Rohani, J. M. (2018). Cyber-physical system (CPS): State of the art. In *2018 international conference on computing, electronic and electrical engineering (ICE cube)* (S. 1–5). <https://doi.org/10.1109/ICECUBE.2018.8610996>
- Kaelbling, L. P. (1987). An architecture for intelligent reactive systems. Reasoning about actions and plans, 1(2), 395–410.
- Karbasi, A., & Farhadi, A. (2021). A cyber-physical system for building automation and control based on a distributed MPC with an efficient method for communication. *European Journal of Control*, 61, 151–170. <https://doi.org/10.1016/j.ejcon.2021.04.008>
- Kasinalis, C., Loonen, R. C. G. M., Costola, D., & Hensen, J. L. M. (2014). Framework for assessing the performance potential of seasonally adaptable façades using multi-objective optimization. *Energy and Buildings* (Bd. 79, S. 106–113). <https://doi.org/10.1016/j.enbuild.2014.04.045>
- Konis, K., & Selkowitz, S. (2017). *Effective Daylighting with High-Performance Façades*. Springer International Publishing. <https://doi.org/10.1007/978-3-319-39463-3>
- Kragh, M. K., & Jakica, N. (2022). Circular economy in façades. *Rethinking Building Skins* (S. 519–539). Elsevier. <https://doi.org/10.1016/B978-0-12-822477-9.00016-4>
- Kraus, M. A., & Drass, M. (2020). Artificial intelligence for structural glass engineering applications—Overview, case studies and future potentials. *Glass Structures & Engineering*, 5(3), 247–285. <https://doi.org/10.1007/s40940-020-00132-8>
- Loonen, R., Rico-Martinez, J. M., Favoino, F., Brzezicki, M., Menezes, C., La Ferla, G., & Aelenei, L. (2015). *Design for façade adaptability: Towards a unified and systematic characterization*. 10th Conference on Advanced Building Skins, Bern, Switzerland.
- Loonen, R., Trčka, M., Costola, D., & Hensen, J. L. M. (2013). Climate adaptive building shells: State-of-the-art and future challenges. *Renewable and Sustainable Energy Reviews* (Bd. 25, S. 483–493). <https://doi.org/10.1016/j.rser.2013.04.016>
- Luna-Navarro, A., Loonen, R., Juaristi, M., Monge-Barrio, A., Attia, S., & Overend, M. (2020). Occupant-Façade interaction: A review and classification scheme. *Building and Environment*, 106880.
- Mach, T., Grobbauer, M., Streicher, W., & Müller, M. J. (Hrsg.). (2015). *mppf—The multifunctional plug&play approach in façade technology*. Verl. der Technischen Univ. Graz.
- Maleki, B. A. (2011). *Wind Catcher : Passive and Low Energy Cooling System in Iranian Vernacular Architecture*.
- Marchi, L., Antonini, E., & Politi, S. (2021). Green Building Rating Systems (GBRSs). *Encyclopedia*, 1(4). <https://doi.org/10.3390/encyclopedia1040076>
- Mary Reena, K. E., Theckethil Mathew, A., & Jacob, L. (2015). An Occupancy Based Cyber-Physical System Design for Intelligent Building Automation. *Mathematical Problems in Engineering*, 2015, 1–15. <https://doi.org/10.1155/2015/132182>
- Menges, A. (2015). The new cyber-physical making in architecture: Computational construction. *Architectural Design* (Bd. 85, S. 28–33). <https://doi.org/10.1002/ad.1950>
- Menges, A., & Reichert, S. (2015). Performative Wood: Physically Programming the Responsive Architecture of the *HygroScope* and *HygroSkin* Projects: Performative Wood: Physically Programming the Responsive Architecture of the *HygroScope* and *HygroSkin* Projects. *Architectural Design*, 85(5), 66–73. <https://doi.org/10.1002/ad.1956>
- Menges, A., Reichert, S., & Krieg, O. D. (2014). Meteorosensitive Architectures. In M. Kretzer & L. Hovestadt (Hrsg.), *ALIVE* (S. 39–42). Ambra Verlag. <https://doi.org/10.1515/9783990436684.39>
- Merz, H., Hansemann, T., & Hubner, C. (2009). Building Automation. *Building Automation*, 1–282. <https://doi.org/10.1007/978-3-540-88829-1>
- Monostori, L. (2014). Cyber-physical production systems: Roots, expectations and R&D challenges. *Procedia CIRP* (Bd. 17, S. 9–13). <https://doi.org/10.1016/j.procir.2014.03.115>
- Monostori, L., Kádár, B., Bauernhansl, T., Kondoh, S., Kumara, S., Reinhart, G., Sauer, O., Schuh, G., Sihm, W., & Ueda, K. (2016). Cyber-physical systems in manufacturing. *CIRP Annals*, 65(2), 621–641. <https://doi.org/10.1016/j.cirp.2016.06.005>
- Nambisan, S., Wright, M., & Feldman, M. (2019). The digital transformation of innovation and entrepreneurship: Progress, challenges and key themes. *Research Policy*, 48(8), 103773. <https://doi.org/10.1016/j.respol.2019.03.018>
- Negri, E., Fumagalli, L., & Macchi, M. (2017). A review of the roles of digital twin in CPS-Based production systems. In *27th International Conference on Flexible Automation and Intelligent Manufacturing, FAIM2017, 27-30 June 2017, Modena, Italy* (Bd. 11, S. 939–948). <https://doi.org/10.1016/j.promfg.2017.07.198>
- Pasupathy, A. V., & Velraj, R. (2006). Phase Change Material Based Thermal Storage for Energy Conservation in Building Architecture. *International Energy Journal*, 7(2).
- Payne, A. O., & Johnson, J. K. (2013). Firefly: Interactive Prototypes for Architectural Design. *Architectural Design*, 83(2), 144–147. <https://doi.org/10.1002/ad.1573>
- Pisching, M. A., Junqueira, F., Filho, D. J. d. S., & Miyagi, P. E. (2016). An architecture based on IoT and CPS to organize and locate services. In *2016 IEEE 21st international conference on emerging technologies and factory automation (ETFA)* (S. 1–4). IEEE. <https://doi.org/10.1109/ETFA.2016.7733506>
- Prieto, A., Knaack, U., Auer, T., & Klein, T. (2018). Passive cooling & climate responsive façade design: Exploring the limits of passive cooling strategies to improve the performance of commercial buildings in warm climates. *Energy and Buildings*, 175, 30–47. <https://doi.org/10.1016/j.enbuild.2018.06.016>

- Rajkumar, R., Lee, I., Sha, L., & Stankovic, J. (2010). Cyber-physical systems: The next computing revolution. In *Proceedings—Design automation conference* (S. 731–736). <https://doi.org/10.1145/1837274.1837461>
- Sandak, A., Sandak, J., Brzezicki, M., & Kutnar, A. (2019). State of the Art in Building Façades. In A. Sandak, J. Sandak, M. Brzezicki, & A. Kutnar (Hrsg.), *Bio-based Building Skin* (S. 1–26). Springer Singapore.
- Shi, L., Pouramini, S., (2022). Adaptive façade for building energy efficiency improvement by arithmetical optimization algorithm. *Concurrency and Computation*. <https://doi.org/10.1002/cpe.7152>
- Soucek, S., & Loy, D. (2007). Vertical integration in building automation systems. *2016 Ieee 14th International Conference on Industrial Informatics (Indin)*, 81–86. <https://doi.org/Doi 10.1109/Indin.2007.4384735>
- Schneider, M., Waldhör, E.F., Denz, P.-R., Vongsingha, P., Suwannapruk, N., Sauer, C., (2021). Adaptive Textile Façades Through the Integration of Shape Memory Alloy. Presented at the ACADIA 2020 - Distributed Proximities.
- United Nations Department of Economic and Social Affairs. (2021). *The Sustainable Development Goals Report 2021*. <https://www.unlibrary.org/content/books/9789210056083>
- Wang, X., Xi, Q., & Ma, Q. (2021). A review of current work in research of Trombe walls. *E3S Web of Conferences*, 248, 03025. <https://doi.org/10.1051/e3sconf/202124803025>
- Wolf, M. (2012). Embedded computing. *Computers as components* (S. 1–50). Elsevier.

Influence of Automated Façades on Occupants: A Review

Pedro de la Barra*¹, Alessandra Luna-Navarro¹, Alejandro Prieto², Claudio Vásquez³, Ulrick Knaack¹

* Corresponding author, P.delaBarraLuegmayer@tudelft.nl

¹ Delft University of Technology, Netherlands

² Universidad Diego Portales, Chile

³ Pontificia Universidad Católica de Chile, Chile

Abstract

Several studies performing building simulations showed that the automated control of façades can provide higher levels of indoor environmental quality and lower energy demand in buildings, in comparison to manually controlled scenarios. However, in several case studies with human volunteers, automated controls were found to be disruptive or unsatisfactory for occupants. For instance, automated façades became a source of dissatisfaction for occupants when they did not fulfil individual environmental requirements, did not provide personal control options, or did not correctly integrate occupant preferences with façade operation in energy-efficient controls. This article reviews current evidence from empirical studies with human volunteers to identify the key factors that affect occupant response to automated façades. Only twenty-six studies were found to empirically investigate occupant response to automated façades from 1998 onwards. Among the reviewed studies, five groups of factors were found to influence occupant interaction with automated façades and namely: (1) personal factors, (2) environmental conditions, (3) type and mode of operation, (4) type of façade technology, and (5) contextual factors. Overall, occupant response to automated façades is often poorly considered in research studies reviewed because of the following three reasons: (i) the lack of established methods or procedures for assessing occupant response to automated façade controls, (ii) poor understanding of occupant multi-domain comfort preferences in terms of façade operation, (iii) fragmented research landscape, on one hand results are mainly related to similar contextual or climatic conditions, which undermines their applicability to other climates, while on the other hand the lack of replication within the same conditions, which also undermines replicability within the same condition. Lastly, this paper suggests future research directions to achieve a holistic and more comprehensive understanding of occupant response to automated façades, aiming to achieve more user-centric automated façade solutions and advanced control algorithms. In particular, research on the impact of personal factors on occupant satisfaction with automated controls is deemed paramount.

Keywords

Automated control, automated façades, occupant-façade interaction, occupant acceptance, occupant comfort, dynamic façades

DOI

<http://doi.org/10.47982/jfde.2022.powerskin.2>

1 INTRODUCTION

In buildings, façades act as a buffer and connector between indoors and outdoors (Knaack et al., 2014) and affect building energy consumption and occupant multi-domain environmental comfort (Luna-Navarro et al., 2022). In particular, façades can affect occupant satisfaction with the thermal environment (Carmody et al., 2004), acoustic (Tang, 2017), air quality (Izadyar et al., 2020), daylight, and view out (Boyce et al., 2003; Heschong et al., 2013).

Dynamic façade technologies, identified as building systems or façades that can move by forces acting on an object, can vary the visual or solar transmittance (e.g. switchable glazings or movable blinds) or the level of airflow through them (e.g. openable vents) (Barozzi et al., 2016) to effectively respond to changes in outdoor or indoor conditions. Dynamic façades can be manually controlled by occupants (Reinhart & Voss, 2003), or react to changes in environmental conditions, either by passively responding to them (e.g. phase change materials (Balocco & Petrone, 2017)), or by automatically being controlled by actuators and sensors (Bakker et al., 2014). Several automated façades are controlled by a semi-automated logic, which also allow occupants to override the system when they disagree with the control logic (Gunay et al., 2017). Previous work showed that automated controls can assist occupants and overcome the limitations of manual operation by reducing energy consumption (Sullivan et al., 1994; Tzempelikos & Athienitis, 2007) or improving thermal or visual comfort (Hosseini et al., 2019). Contrariwise, the automated control can also negatively impact occupants' satisfaction and behaviour, when the control action does not match individual requirements (Day et al., 2019; Grynning et al., 2017).

In scenarios with automated façades, the type of control logic and the occupant-façade interaction strategy (i.e. the level and mode of interaction) affect occupant behaviour and satisfaction, indoor environmental quality, and energy consumption (Luna-Navarro et al., 2020). Several studies showed that occupant requirements are subjective and individual, affecting occupant response to the control system (Cheng et al., 2016; Gunay et al., 2017). These variances in occupant responses may be explained by a different personal significance of environmental comfort domains (Meerbeek et al., 2014; Cheng et al., 2016) or differences in the level of knowledge of users with automated control (Lee et al., 2012). Therefore, the adaptation of the control logic to individual occupant requirements can be important to achieve occupant environmental comfort and satisfaction, acceptance of automated control strategies, and energy performance of office buildings (Kim et al., 2009).

Four previous studies have performed a literature review on automated controls for automated façades. Konstantoglou & Tsangrassoulis (2016) reviewed automated control strategies of dynamic shading systems and their effects on building energy performance and indoor environmental comfort. This literature review concluded that, even though automated control strategies can enhance energy performance and occupants' comfort, their high level of complexity makes them prone to failure and therefore they often do not achieve the predicted performance. Jain & Garg (2018) analysed the feasibility of various daylight prediction methods and their application in controlling dynamic shading and lighting systems, coming to the conclusion that modified and improved closed loop systems, which include and adapt to user feedback, are better than open loop control strategies based on sensor measurements. However, Luna-Navarro et al. (2020) examined interaction strategies and requirements for satisfactory occupant-façade interaction, pointing out that achieving effective closed-loop operations by satisfactorily engaging the occupant, is challenging since several factors play a role. Tabadkani et al. (2021) reviewed the state-of-the-art regarding occupant-centric control strategies, showing that current interaction strategies are ineffective in improving both user satisfaction and energy efficiency. Ultimately, there is a need to

comprehensively review existing studies on occupant-automated façade interaction and highlight the current evidence of the factors that influence individual occupant response to automated façade controls. This will facilitate the design and operation of automated façades in an occupant-centred manner. *To achieve this*, the aim of this work is to review previous experimental work that evaluates human volunteers' responses to automated façades, either in lab experiments or field studies, and to evaluate current evidence to indicate the directions of future research.

Section 2 explains the review methodology, including selection criteria and the classification scheme that structures this article. Section 3 describes the results of the review, including the discussion of the evidence collected. Finally, Section 4 draws the conclusions, and highlights potential future challenges and investigations based on the review conducted.

2 METHODS

In order to review previous work on the factors that influence occupant preferences regarding automated façade operation, a systematic review was conducted. This section provides a detailed explanation of the inclusion and exclusion criteria and keywords. Advanced queries in all databases based on terms definition were conducted. Therefore, a searching protocol through defined keywords has been used, as shown in Table 1. As a result, all the papers must meet the following requirements: only papers on automated dynamic façade control strategies and that monitor actual occupant response through experiments and monitoring with human volunteers were considered. Occupant response was considered by including the following keywords: user interaction, comfort, satisfaction and acceptance.

The following studies were excluded from this literature review:

- Studies that only considered manually controlled systems that do not incorporate any automated feature;
- studies that only considered façades that passively respond to changes in environmental conditions but do not have active control strategies;
- studies without human volunteers.

Keywords were divided into four groups (Table 1): (1) façade operation, (2) façade technology, (3) experiment placement, and (4) façade control. Consequently, references were searched (WoS (2.328), Scopus (2.795)). Only 127 studies were selected by title and abstract, reduced to 106 after removing duplicates. Full-text revisions assessed the eligibility of articles, applying the inclusion and exclusion criteria described previously. Finally, we ended up with 26 studies that met the requirements for being examined for this literature review, published between 1998 and 2022.

TABLE 1 Search keywords

Database	Date of search	Inclusion searching criteria in Title, Abstract and Keywords			Number of Articles
		1) Façade operation	(2) Façade technology	(3) Experimental testing	
Web of Science	24-2-2022	(adaptive OR responsive OR dynamic OR kinetic OR intelligent OR advance OR smart OR interactive OR active OR automated OR switchable OR climate OR control)	(façade OR envelope OR skin OR shading OR glazing OR glazed OR window OR venetian OR roller OR blind)	(laboratory OR on-site OR field OR experimental OR post-occupancy OR testbed OR test room OR campaign OR monitoring)	2.328
Scopus	22-2-2022	W/3	AND		2.795

Studies were not restricted in terms of geographical location since the scope of the review is also to contextualise the research results and evaluate whether any geographical location is missing in the research landscape to inform future research directions accordingly.

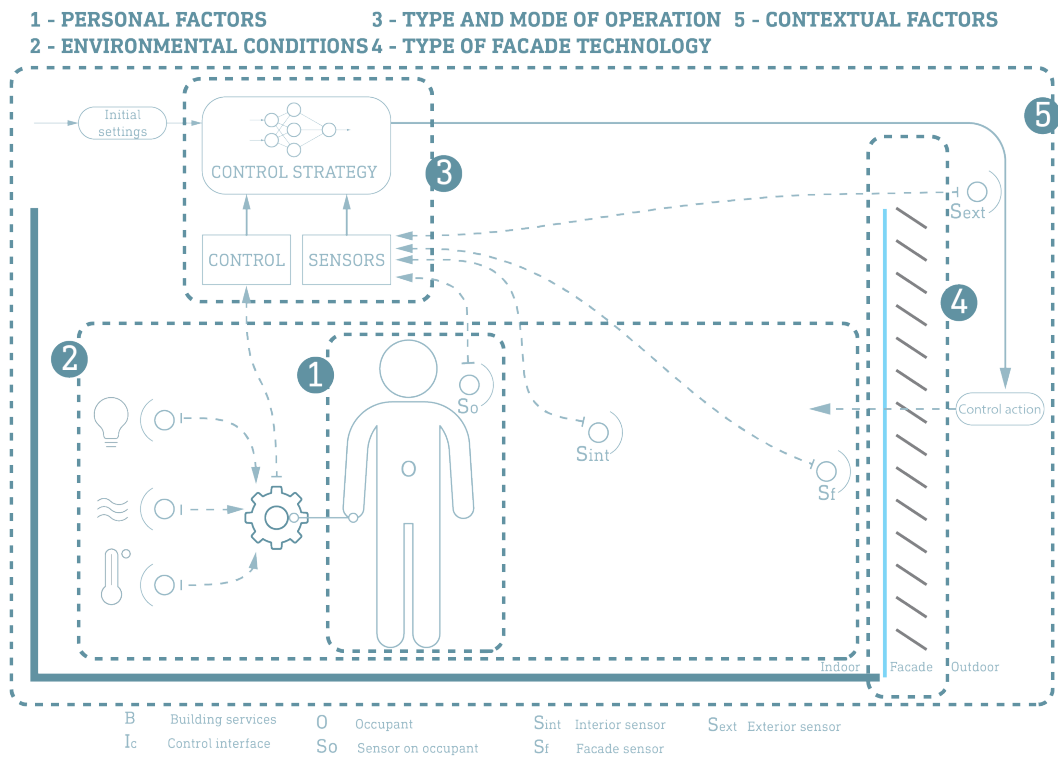


FIG. 1 The classification scheme used in this review to group the factors influencing occupant response that were identified through the literature review (after (Luna-Navarro et al., 2020))

2.1 FACTORS THAT INFLUENCE OCCUPANT RESPONSE

The classification scheme from Luna-Navarro et al. (2020) was used in this review to group the factors that affect users as follows (shown in Fig. 1): 1. personal factors, 2. environmental conditions, 3. type and mode of operation, 4. type of façade technology, and 5. contextual factors (e.g. type of building etc.).

3 RESULTS AND DISCUSSION

3.1 TYPE OF OCCUPANT RESPONSE TO AF STUDIED THROUGH PREVIOUS WORK

Before going to the evidence on factors affecting occupant response, the review results are analysed to identify what type of user response has been considered by previous work.

Occupant response was evaluated in terms of behaviour (13 studies), environmental comfort (20 studies), environmental satisfaction (18 studies), environmental sensation (6), acceptance of the control system or of the indoor environmental conditions (5 studies), and overall satisfaction with the automated control (4 studies). Table 2 shows the type of occupant response considered by each study. These different types of occupant response were studied by previous authors through questionnaires, surveys, and interviews. In addition, occupant behaviour was monitored by tracking occupant override actions (Bakker et al., 2014; Cheng et al., 2016; Goovaerts et al., 2017; Gunay et al., 2017; Lee et al., 2012; Luna-Navarro et al., 2022; Motamed et al., 2019; Sadeghi et al., 2016), or occupant actions to deactivate the control logic (Meerbeek et al., 2014), and set-points (Clear et al., 2006; Guillemain & Morel, 2001, 2002; Vine et al., 1998).

Some studies used the term "comfort" and "satisfaction" interchangeably (Cheng et al., 2013, 2016; Lee et al., 1998; Sadeghi et al., 2016), while other studies used these terms to describe different states of mind. For instance, comfort was intended as the threshold or set-point that defines comfortable environmental conditions, which was often contrasted by surveys of the occupant perception to the environmental quality (Bakker et al., 2014; Cheng et al., 2013, 2016; Clear et al., 2006; Guillemain & Morel, 2001, 2002; Kim et al., 2009; Lee et al., 2012; Meerbeek et al., 2014; Motamed et al., 2017; Sadeghi et al., 2016; Taniguchi et al., 2012; Vine et al., 1998). Satisfaction was used to indicate occupant contentment with the visual environment (Cheng et al., 2013, 2016; Choi et al., 2019; Clear et al., 2006; Day et al., 2019; Guillemain & Morel, 2002; Karlsen et al., 2015; Kim et al., 2009; Lolli et al., 2019, 2020; Luna-Navarro et al., 2022; Meerbeek et al., 2014; Sadeghi et al., 2016; Vine et al., 1998), thermal environment (Choi et al., 2019; Clear et al., 2006; Day et al., 2019; Lolli et al., 2020; Luna-Navarro et al., 2022; Meerbeek et al., 2014; Sadeghi et al., 2016; Wu et al., 2020), acoustic environment (Clear et al., 2006; Lolli et al., 2019; Luna-Navarro et al., 2022), air quality (Luna-Navarro et al., 2022), or overall satisfaction with the automated façade (Cheng et al., 2013, 2016; Clear et al., 2006; Day et al., 2019; Goovaerts et al., 2017; Gunay et al., 2017; Karlsen et al., 2015; Lolli et al., 2020; Luna-Navarro et al., 2022; Meerbeek et al., 2014; Painter et al., 2016). Three studies incorporated acceptance as a descriptor of the level of agreement with the control system implemented. Acceptance was studied in terms of the different modes of operation applied to venetian blinds (Vine et al., 1998) by registering occupant override actions that were intended as a lack of acceptance of the control logic operating the façade (Goovaerts et al., 2017; Gunay et al., 2017). Only one study considered occupant acceptance of the indoor environment (acceptance of the overall indoor environment (Lolli et al., 2019)).

TABLE 2 Summary of type of occupant response reported by studies: overall response to the Control strategy & Façade technology (CS); Occupant response to the Indoor Environmental Quality (IEQ); None (N).

	Occupant response to the indoor environment					
	Behaviour / Interaction Behaviour	Comfort	Satisfaction	Acceptance	Perception	Sensation
(Vine et al., 1998)	CS	IEQ	CS / IEQ	CS	N	N
(Guillemin & Morel, 2001)	CS	IEQ	N	N	N	N
(Guillemin & Morel, 2002)	CS	IEQ	IEQ / CS	N	N	N
(Clear et al., 2006)	CS	N	IEQ / CS	N	N	N
(Kim et al., 2009)	N	IEQ	N	N	N	N
(Lee et al., 2012)	CS	IEQ	CS	N	N	N
(Taniguchi et al., 2012)	N	IEQ	N	N	N	IEQ
(Cheng et al., 2013)	N	IEQ	CS	N	N	N
(Bakker et al., 2014)	CS	IEQ	IEQ / CS	N	CS	N
(Meerbeek et al., 2014)	CS	IEQ	IEQ / CS	N	N	N
(Karlsen et al., 2015)	N	IEQ	IEQ / CS	N	N	N
(Cheng et al., 2016)	CS	IEQ	IEQ	CS	N	N
(Painter et al., 2016)	N	IEQ	CS	N	N	N
(Sadeghi et al., 2016)	CS	IEQ	IEQ	N	CS	N
(Goovaerts et al., 2017)	CS	IEQ	CS	N	IEQ	N
(Gunay et al., 2017)	CS	IEQ	CS	CS	N	N
(Motamed et al., 2017)	N	IEQ	N	N	N	IEQ
(Choi et al., 2019)	N	N	IEQ	N	IEQ	N
(Day et al., 2019)	N	IEQ	IEQ / CS	N	N	N
(Lolli et al., 2019)	N	IEQ	CS	IEQ	N	IEQ
(Motamed et al., 2019)	CS	IEQ	N	N	N	N
(Wu et al., 2020)	N	IEQ	CS	N	N	IEQ
(Bian et al., 2020)	N	IEQ	N	N	N	IEQ
(Lolli et al., 2020)	N	IEQ	IEQ	N	N	IEQ
(Korsavi et al., 2021)	N	IEQ	CS	N	N	N
(Luna-Navarro et al., 2022)	CS	IEQ	IEQ / CS	N	N	N

A few studies also assessed perceived health (Choi et al., 2019) and productivity (Choi et al., 2019; Sadeghi et al., 2016). The least studied aspect of occupant response was sensation. Regarding the visual environment, Glare Sensation Vote (GSV) and Illuminance Rating (IR) were used to capture visual sensation. Thermal Sensation Vote was the subjective rating scale to capture occupant thermal sensation (TSV), which was assessed by using a 5-point Likert scale (from cold to hot) (Lolli et al., 2019, 2020).

3.2 CONTEXTUAL FACTORS AFFECTING OCCUPANT RESPONSE TO AF

All of the studies provide information about the context in which the experiments or the field measurements took place. Table 3 describes the contextual factors summarised from articles, classifying them into location, climate, orientation, testing facility, and floor layout. Regarding location, the studies were conducted in five European countries (14 studies), two North-American

countries (7 studies), and three Asian countries (5 studies). Despite the variety of locations, the climates were limited to temperate and continental conditions (Fig. 2).

TABLE 3 Summary of contextual factors described by previous works to assess the influence of façades on occupant response.

	Climate Location	Orientation							Layout		
		North	West	Southwest	South	Southeast	East	Non-declared	Open plan	2-3 persons office	Single office
(Vine et al., 1998)	Oakland, California - US					✓					✓
(Guillemin & Morel, 2001)	Lausanne - Switzerland				✓						✓
(Guillemin & Morel, 2002)	Lausanne - Switzerland				✓						✓
(Clear et al., 2006)	Berkeley, California - US				✓						✓
(Kim et al., 2009)	Seoul - South Korea		✓		✓		✓		✓		
(Lee et al., 2012)	Berkeley, California - US		✓							✓	
(Taniguchi et al., 2012)	Hiratsuka - Japan							✓			✓
(Cheng et al., 2013)	Beijing - China							✓		✓	
(Bakker et al., 2014)	Eindhoven - The Netherlands		✓								✓
(Meerbeek et al., 2014)	Eindhoven - The Netherlands				✓					✓	
(Karlsen et al., 2015)	Aalborg - Denmark				✓						✓
(Cheng et al., 2016)	Beijing - China							✓			✓
(Painter et al., 2016)	Leicester - U								✓		✓
(Sadeghi et al., 2016)	West Lafayette, Indiana -US				✓						✓
(Goovaerts et al., 2017)	Brussels - Belgium					✓					✓
(Gunay et al., 2017)	Ottawa - Canada			✓							✓
(Motamed et al., 2017)	Lausanne - Switzerland		✓		✓						✓
(Choi et al., 2019)	Toronto - Canada							✓	✓		
(Day et al., 2019)	Charlotte/Richmond/Virginia - US			✓					✓		
(Lolli et al., 2019)	Trondheim - Norway				✓						✓
(Motamed et al., 2019)	Lausanne - Switzerland				✓						✓
(Wu et al., 2020)	Lausanne - Switzerland				✓					✓	
(Bian et al., 2020)	Guangzhou - China					✓					✓
(Lolli et al., 2020)	Trondheim - Norway				✓						✓
(Korsavi et al., 2021)	Plymouth - UK	✓			✓				✓		
(Luna-Navarro et al., 2022)	Cambridge - UK				✓						✓

In terms of the relevance of the weather conditions, Clear et al. (2006) pointed out that two parameters were strongly correlated to occupant behaviour, such as the variation of the sky conditions and the outdoor vertical illuminance. Korsavi et al. (2021) have also reported that occupant behaviour can be impacted by building-related features such as orientation and floor level on automated window operation. Lolli et al. (2019) and Luna-Navarro et al. (2020) showed that orientation and sky condition affect blind occlusion. Moreover, depending on the hemisphere, some orientations can be more challenging. For example, the west and east orientation in the northern hemisphere is challenging due to the low-angle sun situations during the late winter and early spring (Day et al., 2019), while south orientation can be more challenging for overheating. In most cases, the studies were conducted with south-oriented façades (14 studies).

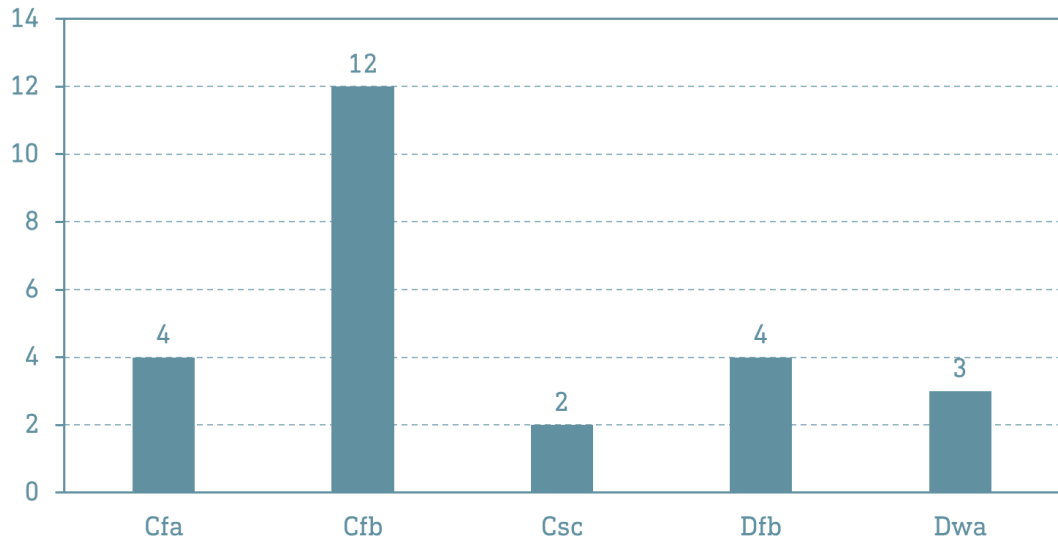


FIG. 2 Climate where the reviewed studies were performed (classification according to the Koppen Climate). The climates are: humid sub-tropical climate (Cfa); temperate oceanic climate (Cfb), cold-summer Mediterranean climate (Csc), warm-summer humid continental climate (Dfb), Monsoon-influenced hot-summer humid continental climate (Dwa).

Concerning where the study took place, two main locations were found: laboratory and real office building (Fig. 3). Laboratory refers to a room fully equipped with sensors and other instruments and that can be adjusted to create the desired experimental conditions and collect relevant data from the indoor environment and occupants. In addition, laboratories are occupied by users only for the purpose of conducting an experiment. In contrast, real office building includes real-world occupied buildings. The studies were split almost equally between field and lab environments.

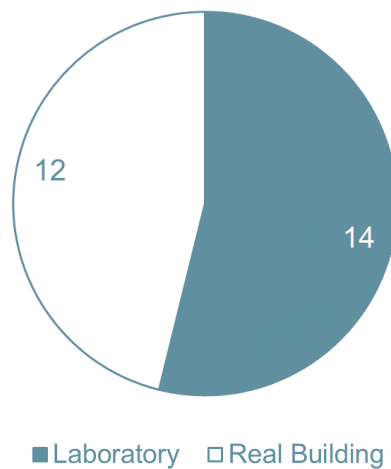


FIG. 3 Pie chart diagram with the number of studies performed on laboratory and real buildings.

Some studies showed that the number of occupants and room characteristics may impact occupant response. Clear et al. (2006) mentioned that visual dissatisfaction reported by occupants was not only produced by the level of sun exposure of the windows but also by the interior walls and object reflection. Additionally, occupants indicated that the room's colour was a source of dissatisfaction.

The weather conditions impact occupant response, and the magnitude of its impact depends on other factors such as orientation, building characteristics, obstructions, window size, and indoor features (Karlsen et al., 2016). Also, indoor room characteristics, such as type of layout, wall colour, amenities, and office features have been proven to affect comfort perception, satisfaction, and occupant response (Bakker et al., 2014; Clear et al., 2006).

Regarding the number of occupants in the same room, Cheng et al. (2016) and Bian et al. (2020) stated that the situation of multiple persons in the general space, performing different tasks should affect the occupant's response to the automated control, even changing throughout the day. However, only a few studies have studied occupant response in shared office spaces.

3.3 PERSONAL FACTORS AFFECTING OCCUPANT RESPONSE TO AF

Personal factors might affect occupants' behaviour and perception, varying from person to person and depending on specific occupants' attributes (Clear et al., 2006). Based on the articles reviewed, personal factors that might affect occupant response are shown in Fig. 4 and are grouped into: "General characteristics", "Personal attitudes", and "Personal significance of the environmental quality". General characteristics refer to the group of features that describe each individual, such as age, gender, profession or work performed, use of glasses, visual disability, handedness, eye colour, and ethnicity (Karlsen et al., 2015). Attitudes refer to the predisposed state of mind of occupants, including habituation to the laboratory or test room, enjoyment of task, pleasantness of the indoor space, rest, and mood (Clear et al., 2006). Finally, personal significance of the environmental quality defines the level of importance that an occupant attributes to a specific environmental domain, such as visual aspects, thermal aspects, air quality, acoustic aspects, privacy, personal control, and room quality, e.g. amenities or services in the room (Sadeghi et al., 2016).

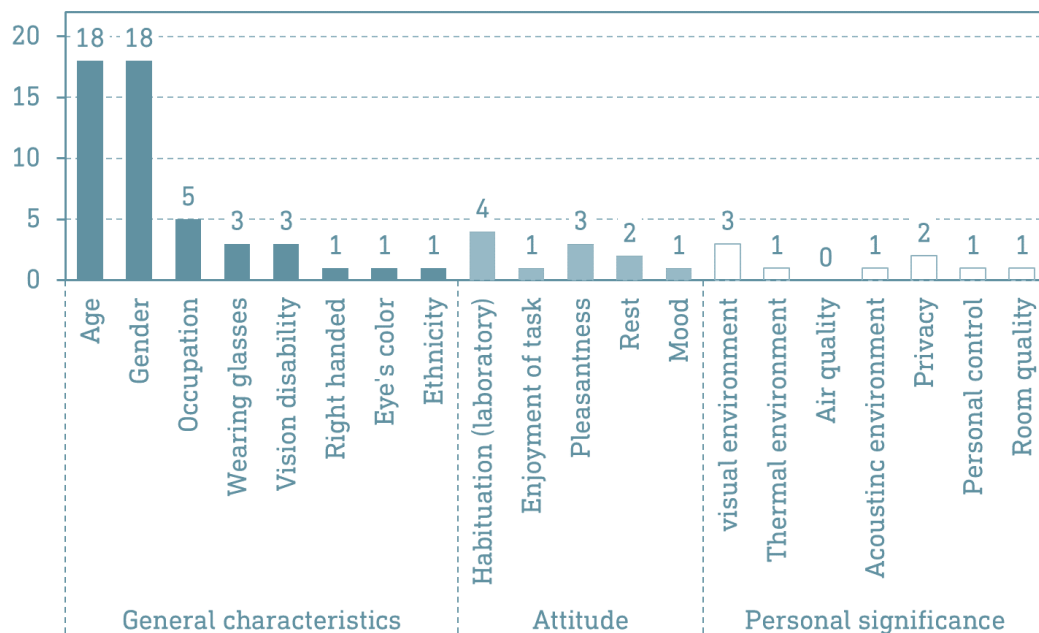


FIG. 4 The number of studies that investigated personal factors in previous works as affecting occupant response to automated façades are shown per type of personal factor studied: general characteristics, attitude, and personal significance of the indoor environmental condition.

The most reported personal characteristics were age and gender, while the level of rest was rarely considered. Five studies included occupants' attitudes (Clear et al., 2006; Karlsen et al., 2015; Luna-Navarro et al., 2022; Motamed et al., 2017; Sadeghi et al., 2016), with Luna-Navarro et al. (2022) being the study that took into account the most attitude descriptors. A few studies considered the personal significance of environmental characteristics, such as visual environment, thermal environment, air quality privacy, personal control and room quality (Clear et al., 2006; Karlsen et al., 2015; Sadeghi et al., 2016). Clear *et al.* (2006) gave a detailed summary about all of them.

Even though most of the studies gathered personal information, the data was often not used to differentiate the results and provide evidence about the importance of occupants' characteristics, attributes, and personal significance in response to automated façades. Overall, three out of twenty-six studies differentiated the data on one or more personal factors to evaluate their impact on occupant response. Clear et al. (2006) reported that age, gender, and other characteristics affected occupants' responses to the electrochromic window operation. This was determined by finding correlations between characteristics of the subjects and appraisals of the different test modes. The main findings were a significant correlation (explained by the level of fitness R^2) between the importance of quiet and sensitivity to environmental noise ($R^2 = 0.48$), the importance of access to outdoor view and the importance of windows ($R^2 = 0.25$), the importance of good lighting and the importance of light and window control ($R^2 = 0.22$), and the importance of good temperature control and the sensitivity to both heat and cold ($R^2 = 0.26$). Karlsen et al. (2015) analysed the percentage of males and females who selected one of the two control strategies (simple and detailed) or the option 'No preference'. Using a Fisher test, the analysis showed no significant dependence between gender and preferred control strategy. Painter et al. (2016) examined the data for studying user interaction, considering that one out of the four participants had a visual condition that affected her vision at times and increased her sensitivity to light. However, no evidence was reported about the effect of the visual conditions in the responses provided by the occupant.

Some authors pointed out that personal factors may determine whether the selected control threshold would lead to a satisfactory indoor environment (Lee et al., 2012; Painter et al., 2016). For instance, personal significance to specific surroundings impacts occupant tolerance to indoor environmental conditions. Karlsen et al. (2015) suggested that the participants might tolerate some glare disturbance depending on the relative importance of access to the outside view. Even the occupants' knowledge (regarding habituation) about the system functionality may impact their ability to interact with the automated façade (Bakker et al., 2014; Lee et al., 2012; Sadeghi et al., 2016). Additionally, specific users' characteristics, such as wearing glasses (Lee et al., 2012) and visual conditions (Painter et al., 2016), could explain why some occupants are more likely to prefer different lighting conditions.

Several studies did not report information on personal factors, both in the laboratory and in field studies. This includes a lack of clear information about general characteristics (e.g. wearing glasses, vision disability, handedness, eye colour), attitude (e.g. habituation, enjoyment, pleasantness, rest, mood), and personal significance (regarding the visual, thermal, air quality, personal control, room, and acoustic environment).

3.4 IMPACT OF OCCUPANT RESPONSE TO INDOOR ENVIRONMENTAL CONDITIONS ON OCCUPANT OVERALL SATISFACTION WITH AF

Occupant response to indoor environmental condition was taken into account in 26 studies when evaluating the performance of AF. The indoor environmental conditions were evaluated by capturing a wide range of comfort domains, particularly in the visual and thermal domains (see Table 4).

TABLE 4 Summary of environmental domains measured by sensors and occupant responses captured by questionnaires investigated in previous works.

	Visual environment						Behaviour and Interaction	Comfort	Satisfaction	Acceptance	Perception	Sensation
	Outside view	Daylight	Glare	Thermal Environment	Acoustic Environment	Indoor air quality						
(Vine et al., 1998)		✓		✓	✓		✓	✓	✓	✓		
(Guillemin & Morel, 2001)	✓	✓		✓			✓	✓				
(Guillemin & Morel, 2002)		✓					✓	✓	✓			
(Clear et al., 2006)		✓					✓	✓				
(Kim et al., 2009)		✓		✓				✓				
(Lee et al., 2012)		✓		✓			✓	✓	✓			
(Taniguchi et al., 2012)		✓						✓				✓
(Cheng et al., 2013)		✓						✓	✓			
(Bakker et al., 2014)	✓	✓		✓			✓	✓	✓		✓	
(Meerbeek et al., 2014)	✓			✓			✓	✓			✓	
(Karlsen et al., 2015)		✓	✓					✓				✓
(Cheng et al., 2016)		✓					✓	✓	✓	✓		
(Painter et al., 2016)		✓	✓					✓	✓			
(Sadeghi et al., 2016)	✓	✓	✓	✓			✓	✓	✓		✓	
(Goovaerts et al., 2017)		✓	✓	✓			✓	✓	✓	✓		
(Gunay et al., 2017)		✓					✓	✓	✓			
(Motamed et al., 2017)		✓	✓					✓				✓
(Choi et al., 2019)		✓						✓			✓	
(Day et al., 2019)		✓	✓	✓				✓	✓			
(Lolli et al., 2019)		✓	✓					✓	✓			✓
(Motamed et al., 2019)		✓	✓				✓	✓				
(Wu et al., 2020)		✓	✓					✓	✓			
(Bian et al., 2020)		✓	✓					✓				✓
(Lolli et al., 2020)		✓	✓					✓	✓			✓
(Korsavi et al., 2021)				✓	✓			✓				
(Luna-Navarro et al., 2022)		✓	✓	✓	✓	✓	✓	✓	✓			
Total	4	24	12	11	3	1	13	20	18	4	4	6

The visual environment was evaluated by measuring daylight levels (24 studies), glare probability (12 studies), and access to outside view (4 studies). Daylight was very often measured on the work plane in terms of horizontal illuminance (18 studies) and vertical illuminance (10 studies). Glare probability was calculated by measuring vertical illuminance at eye level (6 studies) and luminance distribution from the occupant's point of view by HDR imaging (6 studies). Access to outside view was monitored by estimating the visible unobstructed window area (1 study). The thermal environment was

captured by measuring indoor air temperature (9 studies), window surface temperature (2 studies) and vertical irradiance at the window plane (3 studies). The acoustic environment (1 study) and indoor air quality (1 study) were not extensively described since the articles reviewed are talking about dynamic shading devices.

Although several studies captured occupant response to indoor environment, only a few reported that occupant response to indoor environmental conditions affected occupants' response to AF (Fig. 5), either in terms of the visual environment, thermal environment, privacy and acoustic comfort. Several studies showed that occupant response to automated control strategies was significantly driven by occupant dissatisfaction with indoor illuminance control (21 studies). Regarding visual occupant requirements, office occupants tended to prefer higher indoor illuminance levels when the AF was activated (Bakker et al., 2014; Cheng et al., 2013; Clear et al., 2006; Guillemin & Morel, 2002; Lee et al., 2012; Vine et al., 1998). Sadeghi et al. (2016) and Goovaerts et al. (2017) reported that override actions to open the façade were carried out when increasing daylight was needed, while Motamed et al. (2017) described that the preference for the automated mode was driven by the discomfort produced on excessive daylight indoor conditions. Additionally, it was told that occupants' illuminance requirements differ with tasks and areas (Cheng et al., 2016), changing even throughout the day (Bian et al., 2020). Vine et al. (1998) indicated that occupants were satisfied not only with the ability to control the blinds to adjust the amount of daylight but also to adjust the direction and distribution of the daylight in the indoor space.

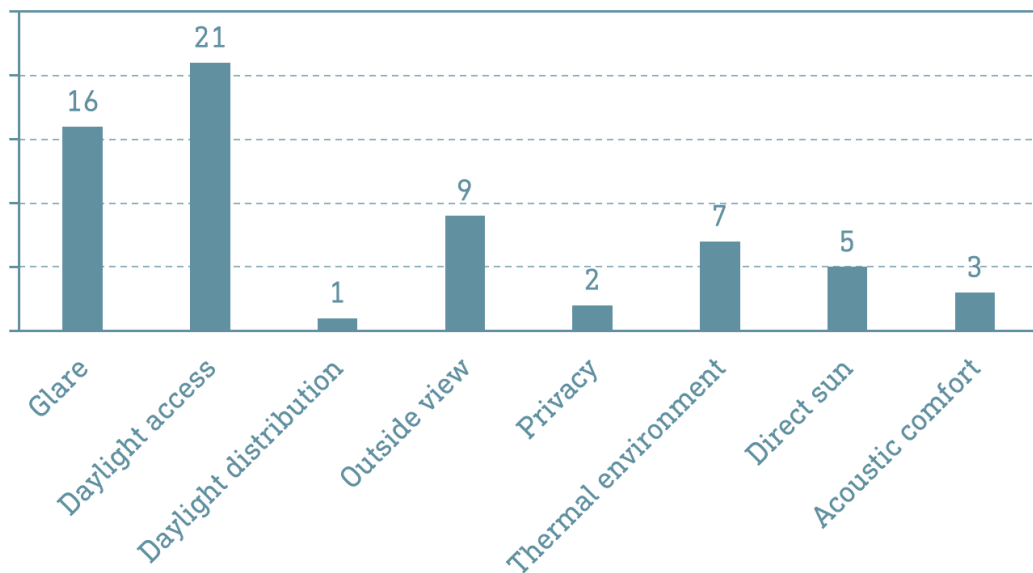


FIG. 5 The number of studies that showed that environmental factors affect occupant response with the AF operation.

Glare discomfort is the most frequent factor affecting occupants' responses to the automated control (16 studies). When the automated control did not effectively protect against glare, occupants overrode (Goovaerts et al., 2017; Gunay et al., 2017; Lolli et al., 2019; Sadeghi et al., 2016) or adjusted the control parameter as allowed (Bian et al., 2020). Glare competes with daylight provision. When the automated control was operated based on glare, occupants intervened to improve daylight quality (Gunay et al., 2017; Meerbeek et al., 2014). When the automated control avoided discomfort from direct sun and or glare, occupants preferred more daylight (Lolli et al., 2019; Meerbeek et al., 2014; Motamed et al., 2017).

Other studies also suggested that the outside view impacts occupants' environmental preferences (9 studies), influencing even the choice of the preferred control strategy (Karlsen et al., 2015; Luna-Navarro et al., 2022). Clear et al. (2006) and Meerbeek et al. (2014) pointed out that the outside view was an important comfort factor for the occupants, who were operating the façade not only to improve the connection with the outside but also to decrease the level of visual stimulus from the exterior. Gunay et al. (2017) described that occupants interfered with the automated control mainly to improve the outside view when the system worked to avoid glare.

A few studies also mentioned that occupant response was impacted by privacy (3 studies). Sadeghi et al. (2016) mentioned privacy as the most important factor affecting lowering blind actions together with glare discomfort. However, privacy depends on contextual characteristics such as the surrounding environment and position in the building. For instance, Meerbeek et al. (2014) explain that the subjects surveyed were not worried about privacy because the office was located on the third floor, far away from the street level.

Dissatisfaction with the thermal environment was mainly related to the ability of the façade to control the incoming solar radiation (Lolli et al., 2019; Sadeghi et al., 2016) or to provide air flow, as suggested by Korsavi et al. (2021) and Lolli et al. (2020). A few studies surveyed occupants to calculate the predicted mean vote (PMV) (Kim et al., 2009).

A few studies also reported acoustic environmental conditions and acoustic satisfaction (4 studies). Luna-Navarro et al. (2022) pointed out that acoustic discomfort was the main driver of occupant dissatisfaction with the façade system.

Studies have also reported that metrics used to capture occupant requirements presented problems when implemented into the automated façade control system. Goovaerts et al. (2017) informed that DGP underestimated the impact of direct sunlight, which generated the set-point lowered by users when direct sunlight was present. A similar problem was reported by Taniguchi et al. (2012) when the algorithm to evaluate indoor luminance overestimated glare sources in the afternoon. Other authors have said people's glare sensation increases gradually from morning until midday but becomes stable or more sensitive to glare in the afternoon (Bian et al., 2020). The majority of the studies investigated the impact of control strategies on occupant's visual domain. On the thermal domain, articles did not report conclusions on how an automated façade affects the thermal environment.

How distance from the façade affects occupant interaction with the façade is still undetermined. Only Day et al. (2019) mentioned that the window's proximity improves occupants' satisfaction. Moreover, the impact of indoor environmental conditions on the occupant response to the automated façade has not been researched sufficiently, making it difficult to extrapolate results, throughout different façade technologies, control logics, and under different weather conditions, to improve current control strategies.

What the main drivers of occupant satisfaction with automated façades are, remains undetermined, in particular whether or not there is an inherent order of importance among different environmental domains. For example, it has been reported that occupants significantly value daylight access (Lee et al., 2012) and outside view (Choi et al., 2019; Wu et al., 2020) and that these factors are often the main reason for overriding an automated façade control system (Meerbeek et al., 2014). The personal level of control also influences occupant environmental requirements. Thus, occupant preferences may be different depending on the interaction level provided by the façade controller (Luna-Navarro et al., 2020). However, there is no clear evidence on whether or not a hierarchy of comfort domains exists.

3.5 THE EFFECT OF CONTROL AND INTERACTION LOGIC ON OCCUPANT RESPONSE TO AF

The control and interaction strategy influences occupant response to the automated façade (Bakker et al., 2014). As a way to improve occupant satisfaction with the automated façade, studies have tested different control strategies. Table 5 summarises the main characteristics of the control logics studied up to now. Additionally, the table gives information on the sensor position (interior/exterior).

TABLE 5 Summary of environmental domains measured by sensors and occupant responses captured by questionnaires investigated in previous works.

	Control loop		Source of information			Control algorithm			Control algorithm					Sensor place			Occupant interaction
	Closed-loop	Open-loop	Sensor-based	Model-based	Others	Rule-based	Adaptive	Predictive	Visual Environment			Thermal Environment	Air quality	Exterior	Interior	On occupant	
									Outside view	Daylight	Glare						
(Vine et al., 1998)	✓		✓		✓				✓	✓					✓		✓
(Guillemín & Morel, 2001)	✓		✓	✓			✓	✓	✓	✓	✓			✓	✓		✓
(Guillemín & Morel, 2002)	✓		✓	✓			✓	✓	✓	✓	✓			✓	✓		✓
(Clear et al., 2006)	✓		✓			✓			✓	✓				✓			✓
(Kim et al., 2009)		✓	✓			✓			✓		✓			✓			
(Lee et al., 2012)	✓		✓	✓		✓			✓	✓				✓			✓
(Taniguchi et al., 2012)	✓		✓	✓	✓	✓			✓	✓				✓			
(Cheng et al., 2013)	✓		✓	✓	✓	✓	✓		✓	✓				✓	✓		
(Bakker et al., 2014)	✓	✓	✓	✓		✓			✓					✓			✓
(Meerbeek et al., 2014)	✓		✓	✓		✓			✓					✓			✓
(Karlsen et al., 2015)	✓		✓	✓		✓			✓	✓	✓			✓	✓	✓	
(Cheng et al., 2016)	✓		✓	✓			✓		✓					✓	✓		✓
(Painter et al., 2016)	✓		✓			✓			✓	✓				✓			
(Sadeghi et al., 2016)	✓		✓	✓		✓			✓					✓			✓
(Goovaerts et al., 2017)	✓		✓	✓		✓			✓	✓				✓	✓		✓
(Gunay et al., 2017)	✓		✓	✓			✓	✓	✓					✓			✓
(Motamed et al., 2017)	✓		✓	✓		✓			✓	✓				✓	✓		
(Choi et al., 2019)	✓		✓			✓			✓					✓			
(Day et al., 2019)	✓		✓			✓			✓					✓			
(Lolli et al., 2019)	✓		✓			✓			✓					✓	✓		
(Motamed et al., 2019)	✓		✓	✓		✓			✓	✓				✓	✓		✓
(Wu et al., 2020)	✓		✓	✓	✓	✓			✓	✓				✓	✓		
(Bian et al., 2020)				✓											✓		
(Lolli et al., 2020)	✓		✓	✓					✓	✓				✓	✓		
(Korsavi et al., 2021)	✓		✓			✓				✓				✓			
(Luna-Navarro et al., 2022)	✓		✓			✓				✓				✓			✓

Sadeghi et al. (2016) reported a dependency between façade configuration (shade position or window transmittance) and occupant satisfaction with the indoor environment. Clear et al. (2006) and Day et al. (2019) pointed out a similar situation for the switchable glazing operation. When electrochromic glazing became opaque, occupants felt more dissatisfied with that configuration, leading to override actions to improve daylight and outside view.

Regarding control loops, studies have described two types: open-loop (12 studies) and closed-loop (14 studies). The control logics used three different sources of information: sensor-based (25 studies), model-based (7 studies), and others (e.g. time, sun profile, weather file, and schedule). The low number of model-based control cases is explained by the fact that this method is computationally intense, lacking in algorithms to develop occupant models inside building controllers (Gunay et al., 2017). The control algorithm implemented in the façade control system was classified into three categories: rule-based (20 studies), adaptive (5 studies), and predictive (3 studies). Most studies implemented rule-based algorithms to control automated façade systems. The adaptive algorithms found were Q-Learning (Cheng et al., 2016) and recursive learning (Gunay et al., 2017). Only three studies implemented a predictive algorithm to analyse and integrate outdoor weather and indoor lighting conditions into a model-based system (Guillemin & Morel, 2001; 2002) to anticipate occupant interaction with the automated façade system (Gunay et al., 2017).

Automated façade control can improve indoor environmental quality (Clear et al., 2006; Kim et al., 2009; Lolli et al., 2019; Motamed et al., 2019), although the effect on occupant satisfaction varies from case to case. For instance, Lolli et al. (2020) reported that automated control improved the desired indoor environmental quality. Similarly, Luna-Navarro et al. (2022) showed that, when the control strategy is properly designed, automated control can provide greater satisfaction than a manually controlled environment. However, if the automated control is disruptive to users, manual controls outperform automated ones. On the contrary, Motamed et al. (2017) showed that the subjects' visual performance was not improved by automated control strategies. Therefore, the type of control strategy is an important factor for occupant satisfaction. The impact of façade control operation affects the indoor space zones differently. Day et al. (2019) reported that occupants placed in the interior, far away from the window did not receive enough daylight when the switchable glazing became dark, and occupants were ultimately displeased with their workspaces.

In regards to determining what aspects of the control strategy most affect occupants, current evidence is fragmented. In terms of control thresholds, Goovaerts et al. (2017) showed that different controls could achieve equal indoor illuminance levels on a desk in the same context but still affect satisfaction among occupants differently. Therefore, personalising the control threshold may not be sufficient to meet individual occupant requirements. In this context, it seems well-established that occupants have individual comfort preference (Cheng et al., 2013) and behavioural responses under different control algorithms (Korsavi et al., 2021). However, to what extent personalisation of control strategies is required is less clear. The automated control's capability to predict occupant preferences is deemed important to improve occupant satisfaction with automated controls (Meerbeek et al., 2014). A predictive lighting and blinds control algorithm can significantly reduce electric lighting consumption in perimeter office spaces whilst maintaining user comfort (Gunay et al., 2017). The predictive control strategy should incorporate as many profiles as there are occupants in the indoor space (Korsavi et al., 2021). Painter et al. (2016) mentioned that a solution might be to develop tools that allow the system to evaluate comfortable and uncomfortable conditions based on physical measurements and occupant control actions. However, capturing more than one user profile and integrating all that information is one of the challenges that adaptive and predictive control strategies currently face.

Few studies advocated for controlling and designing the façade by taking into account the multi-domain influence of façades on users (Luna-Navarro et al., 2022), however, there is still discussion on whether one environmental domain should be prioritised by the control (visual over thermal) or visual aspect (glare over daylight). This is particularly challenging since adjusting one comfort domain can affect the others. For example, Goovaerts et al. (2017) showed that occupants overrode the automated control to increase daylight when it was configured to avoid discomfort glare. Karlsen et al. (2015) mentioned that occupants felt more comfortable with the automated control when it considered indoor environmental parameters affecting their satisfaction perception (in this case, thermal aspects). Gunay et al. (2017) pointed out that occupants intervened to improve the view quality when the system operated based on glare mitigation or building energy efficiency.

Regarding the mode of operation, several studies indicated that the automated façade might influence occupant response because it affected not only the physical parameter defining indoor environmental quality but also impacted the fulfilment of the occupant requirements for personal control (Meerbeek et al., 2014). For instance, Bakker et al. (2014) reported that less frequent, discrete transitions in façade operation are better appreciated than smooth transitions at a higher frequency. However, this topic is largely unexplored. Personal control is key to restoring comfort when the system is not efficient in controlling environmental parameters (Day et al., 2019). Guillemain & Morel (2002) reported that occupants interacted with the automated control as often as the manual control system, reinforcing that comfortable indoor conditions are insufficient for occupants. Occupant environmental requirements and preferences are influenced by the level of control over the system, being able to accept automated control only if they can control it when they need to. Limited indoor environment control has detrimental effects on occupant comfort (Lolli et al., 2020). Furthermore, interaction strategy could work in the opposite direction, being a source of distraction if occupants are involved in the system's operation too frequently (Bakker et al., 2014).

3.6 THE EFFECT OF FAÇADE TECHNOLOGY ON OCCUPANT RESPONSE TO AF

The type of façade technology affects occupant response to automated control strategies because each façade technology offers a different range of dynamic performances, such as controlling visual transmittance, blocking incoming solar radiation, and redistributing daylight in the indoor space. Additionally, different façade technologies have different performances in terms of their ability to balance conflicting requirements, such as glare versus daylight access, solar transmittance versus surface temperature, and privacy versus outdoor view.

Table 6 summarises the façade systems and the position of the shading system. Regarding façade technologies, the main shading system tested in previous work is that of venetian blinds (16 studies), followed by roller shades (8 studies). Switchable glazing has also been evaluated (5 studies), while window opening was the least implemented (2 studies). The automated control controlled a range of façade characteristics, which depended on the technology implemented. In the case of venetian blinds, the system controlled the slats deployment (hold/release) and slat tilt, for roller shades it controlled up and down positions, switchable glazing allowed the modification of glass visual transmittance, while for window opening the window aperture percentage was controlled.

The type of façade also defines how disruptive a control strategy will be. For instance, Luna-Navarro et al. (Luna-Navarro et al., 2022) reported that placing the blinds within the cavity resulted in more effective control of the solar heat gains and was less disruptive to occupants, especially in terms of

their associated noise. Bakker et al. (2014) reported that occupants close to the operation of roller shades were the most disrupted by them. Vine et al. (1998) mentioned that the transition from one position to another, the activation frequency, and the sound generated was considered sources of distraction. Moreover, Wu et al. (2020) also pointed out that the speed of switching also had an impact on occupant satisfaction, who preferred slower and smooth transitions.

TABLE 6 TABLE 6. Summary of façade technologies included by previous works to assess the influence of façades on occupant response.

	Façade system				Shading device placement		
	Switch-able Glazing	Roller shade	Venetian blind	Window opening	Interior	In the cavity	Exterior
(Vine et al., 1998)			✓		✓		
(Guillemin & Morel, 2001)			✓				
(Guillemin & Morel, 2002)			✓				
(Clear et al., 2006)	✓		✓		✓		
(Kim et al., 2009)			✓		✓		
(Lee et al., 2012)	✓						
(Taniguchi et al., 2012)			✓		✓		
(Cheng et al., 2013)			✓				✓
(Bakker et al., 2014)		✓			✓		
(Meerbeek et al., 2014)			✓		✓		
(Karlsen et al., 2015)			✓		✓		
(Cheng et al., 2016)			✓				✓
(Painter et al., 2016)	✓						
(Sadeghi et al., 2016)		✓			✓		
(Goovaerts et al., 2017)			✓		✓		
(Gunay et al., 2017)		✓			✓		
(Motamed et al., 2017)		✓					✓
(Choi et al., 2019)	✓						
(Day et al., 2019)	✓	✓	✓		✓		
(Lolli et al., 2019)			✓		✓		
(Motamed et al., 2019)		✓					✓
(Wu et al., 2020)			✓				✓
(Bian et al., 2020)			✓		✓		
(Lolli et al., 2020)		✓		✓	✓		
(Korsavi et al., 2021)				✓			
(Luna-Navarro et al., 2022)		✓	✓		✓	✓	

4 CONCLUSIONS

This work reviewed twenty-six previous laboratory experiments and field studies that monitored occupant response to automated façades. These studies were reviewed to gather and analyse current evidence on the influence of the following factors on occupant response to AF: (1) contextual factors, (2) personal factors, (3) environmental conditions, (4) control logic, and (5) façade technology.

Throughout the evidence gathered, this literature review shows how occupant response to the AF is captured in terms of occupant behaviour or interaction with the automated control, satisfaction with the interaction strategy, level of acceptance of the automated control logic, perception of the indoor environmental conditions, and sensation regarding specific environmental domains affected by the AF operation. The focus of existing studies was limited to a few climatic conditions and similar types of buildings. In most studies, the experiments took place in single office layouts, and data on occupant response to AFs in open-plan office spaces is scarce.

Regarding the aspects affecting occupant response to AF operation, studies indicated that personal factors impact occupants' behaviour and perception of the indoor environment, varying from person to person and depending on the specific attributes of occupants. Most of the studies reported personal characteristics, but attitudes and personal significance of indoor environmental quality were missed by most of the articles reviewed.

Concerning the control strategy, occupant interaction with the automated control is an essential determinant of occupant requirements for the AF operation. Occupant requirements and preferences are influenced by the level of control over the system, accepting automated control only if they can control it when they need to. Additionally, occupant interaction with the AF is driven primarily to fulfil personal environmental requirements, such as increasing daylight, privacy, access to views, and avoiding glare discomfort. Although AF can provide "comfortable" indoor environmental conditions, it does not properly ensure the achievement of individual environmental requirements and preferences.

In terms of the impact of façade technology, the type of technology affects how disruptive a façade is and depending on the technology, the overall satisfaction could be higher or lower. In particular, differences in façade effects are noticeable when technologies compromise one environmental domain in favour of another.

Overall, several barriers still exist to automated façades that can enhance occupant response, and further research effort is required to answer the following gaps:

- 1 relationship between personal factors and occupant response to AF, in particular there is the need to establish common methods for gathering evidence in this domain, since the majority of the studies do not consider personal factors;
- 2 poor understanding of occupant multi-domain comfort preferences regarding façade operation. Unlocking a holistic and more comprehensive knowledge of occupant response to automated façades should be used to achieve more user-centric automated façade solutions.
- 3 the lack of research to define to what extent learning and personalised control are possible and, in such a case, how to deal with multiple occupants in the same room operating a unique automated façade.

In addition, extending the test scenario to different climates or contextual conditions would be very beneficial, since studies were mainly concentrated on a few climates and conditions. This also undermines generalisation, since larger replication within the same conditions would be beneficial to extend the results.

Ultimately, there is the need for new studies that can demonstrate the benefits of automated façade control strategies and whether personalised controls are necessary to achieve higher occupant satisfaction whilst reducing the energy demand.

References

- Bakker, L. G., Hoes-van Oeffelen, E. C. M., Loonen, R. C. G. M., & Hensen, J. L. M. (2014). User satisfaction and interaction with automated dynamic façades: A pilot study. *Building and Environment*, 78, 44–52. <https://doi.org/10.1016/J.BUILDENV.2014.04.007>
- Balocco, C., & Petrone, G. (2017). Numerical Modelling for the Thermal Performance Assessment of a Semi-Opaque Façade with a Multilayer of Nano-Structured and Phase Change Materials. *Buildings* 2017, Vol. 7, Page 90, 7(4), 90. www.mdpi.com/journal/buildings
- Barozzi, M., Lienhard, J., Zanelli, A., & Monticelli, C. (2016). The Sustainability of Adaptive Envelopes: Developments of Kinetic Architecture. *Procedia Engineering*, 155, 275–284. <https://doi.org/10.1016/j.proeng.2016.08.029>
- Bian, Y., Dai, Q., Ma, Y., & Liu, L. (2020). Variable set points of glare control strategy for side-lit spaces: Daylight glare tolerance by time of day. *Solar Energy*, 201, 268–278. <https://doi.org/10.1016/J.SOLENER.2020.03.016>
- Boyce, P., Hunter, C., & Howlett, O. (2003). *The Benefits of Daylight through Windows Sponsored by: Capturing the Daylight Dividend Program*.
- Carmody, J., Selkowitz, S. E., Lee, E. S., & Arasteh, D. K. (2004). *Window Systems for High-Performance Buildings*. W. W. Norton & Company, Inc..
- Cheng, Z., Xia, L., Zhao, Q., Zhao, Y., Wang, F., & Song, F. (2013). Integrated control of blind and lights in daily office environment. *IEEE International Conference on Automation Science and Engineering*, 587–592. <https://doi.org/10.1109/COASE.2013.6653972>
- Cheng, Z., Zhao, Q., Wang, F., Jiang, Y., Xia, L., & Ding, J. (2016). Satisfaction based Q-learning for integrated lighting and blind control. *Energy and Buildings*, 127, 43–55. <https://doi.org/10.1016/J.ENBUILD.2016.05.067>
- Choi, J. H., Loftness, V., Nou, D., Tinianov, B., & Yeom, D. (2019). Multi-Season Assessment of Occupant Responses to Manual Shading and Dynamic Glass in a Workplace Environment. *Energies* 2020, Vol. 13, Page 60, 13(1), 60. <https://doi.org/10.3390/EN13010060>
- Clear, R. D., Inkarojrit, V., & Lee, E. S. (2006). Subject responses to electrochromic windows. *Energy and Buildings*, 38(7), 758–779. <https://doi.org/10.1016/J.ENBUILD.2006.03.011>
- Day, J. K., Futrell, B., Cox, R., & Ruiz, S. N. (2019). Blinded by the light: Occupant perceptions and visual comfort assessments of three dynamic daylight control systems and shading strategies. *Building and Environment*, 154, 107–121. <https://doi.org/10.1016/J.BUILDENV.2019.02.037>
- Goovaerts, C., Descamps, F., & Jacobs, V. A. (2017). Shading control strategy to avoid visual discomfort by using a low-cost camera: A field study of two cases. *Building and Environment*, 125, 26–38. <https://doi.org/10.1016/J.BUILDENV.2017.08.030>
- Grynning, S., Lolli, N., Wågø, S., & Risholt, B. (2017). Solar Shading in Low Energy Office Buildings - Design Strategy and User Perception. *Journal of Daylighting*, Vol. 4, Issue 1, Pp. 1-14, 4(1), 1–14. <https://doi.org/10.15627/JD.2017.1>
- Guillemin, A., & Morel, N. (2001). An innovative lighting controller integrated in a self-adaptive building control system. *Energy and Buildings*, 33(5), 477–487. [https://doi.org/10.1016/S0378-7788\(00\)00100-6](https://doi.org/10.1016/S0378-7788(00)00100-6)
- Guillemin, A., & Morel, N. (2002). Experimental results of a self-adaptive integrated control system in buildings: a pilot study. *Solar Energy*, 72(5), 397–403. [https://doi.org/10.1016/S0038-092X\(02\)00015-4](https://doi.org/10.1016/S0038-092X(02)00015-4)
- Gunay, H. B., O'Brien, W., Beausoleil-Morrison, I., & Gilani, S. (2017). Development and implementation of an adaptive lighting and blinds control algorithm. *Building and Environment*, 113, 185–199. <https://doi.org/10.1016/J.BUILDENV.2016.08.027>
- Heschong, L., Wright, R. L., & Okura, S. (2013). Daylighting Impacts on Human Performance in School. <http://Dx.Doi.Org/10.1080/00994480.2002.10748396>
- Hosseini, S. M., Mohammadi, M., & Guerra-Santin, O. (2019). Interactive kinetic façade: Improving visual comfort based on dynamic daylight and occupant's positions by 2D and 3D shape changes. *Building and Environment*, 165, 106396. <https://doi.org/10.1016/j.buildenv.2019.106396>
- Izadyar, N., Miller, W., Rismanchi, B., & Garcia-Hansen, V. (2020). Impacts of façade openings' geometry on natural ventilation and occupants' perception: A review. *Building and Environment*, 170, 106613. <https://doi.org/10.1016/J.BUILDENV.2019.106613>
- Jain, S., & Garg, V. (2018). A review of open loop control strategies for shades, blinds and integrated lighting by use of real-time daylight prediction methods. *Building and Environment*, 135(March), 352–364. <https://doi.org/10.1016/j.buildenv.2018.03.018>
- Karlsen, L., Heiselberg, P., & Bryn, I. (2015). Occupant satisfaction with two blind control strategies: Slats closed and slats in cut-off position. *Solar Energy*, 115, 166–179. <https://doi.org/10.1016/J.SOLENER.2015.02.031>
- Karlsen, L., Heiselberg, P., Bryn, I., & Johra, H. (2016). Solar shading control strategy for office buildings in cold climate. *Energy and Buildings*, 118, 316–328.
- Kim, J. H., Park, Y. J., Yeo, M. S., & Kim, K. W. (2009). An experimental study on the environmental performance of the automated blind in summer. *Building and Environment*, 44(7), 1517–1527. <https://doi.org/10.1016/J.BUILDENV.2008.08.006>
- Knaack, U., Klein, T., Bilow, M., & Auer, T. (2014). *Façades: Principles of Construction* (2., rev. e). Birkhäuser. <https://doi.org/doi:10.1515/9783038211457>
- Konstantoglou, M., & Tsangrassoulis, A. (2016). Dynamic operation of daylighting and shading systems: A literature review. In *Renewable and Sustainable Energy Reviews* (Vol. 60, pp. 268–283). Elsevier Ltd. <https://doi.org/10.1016/j.rser.2015.12.246>
- Korsavi, S. S., Jones, R. V., & Fuertes, A. (2021). The gap between automated building management system and office occupants' manual window operations: Towards personalised algorithms. *Automation in Construction*, 132, 103960. <https://doi.org/10.1016/J.AUTCON.2021.103960>
- Lee, E. S., Claybaugh, E. S., & Lafrance, M. (2012). End user impacts of automated electrochromic windows in a pilot retrofit application. *Energy and Buildings*, 47, 267–284. <https://doi.org/10.1016/J.ENBUILD.2011.12.003>
- Lee, E. S., Dibartolomeo, D. L., Vine, E. L., & Selkowitz, S. E. (1998). *Integrated Performance of an Automated Venetian Blind / Electric Lighting System in a Full-Scale Private Office*.

- Lolli, N., Nocente, A., Brozovsky, J., Woods, R., & Grynning, S. (2019). Automatic vs Manual Control Strategy for Window Blinds and Ceiling Lights: Consequences to Perceived Visual and Thermal Discomfort. *Journal of Daylighting*, Vol. 6, Issue 2, Pp. 112–123, 6(2), 112–123. <https://doi.org/10.15627/JD.2019.11>
- Lolli, N., Nocente, A., & Grynning, S. (2020). Perceived Control in an Office Test Cell, a Case Study. *Buildings* 2020, Vol. 10, Page 82, 10(5), 82. <https://doi.org/10.3390/BUILDINGS10050082>
- Luna-Navarro, A., Hunt, G. R., & Overend, M. (2022). Dynamic façades – An exploratory campaign to assess occupant multi-domain environmental satisfaction and façade interaction. *Building and Environment*, 211, 108703. <https://doi.org/10.1016/j.buildenv.2021.108703>
- Luna-Navarro, A., Loonen, R., Juaristi, M., Monge-Barrio, A., Attia, S., & Overend, M. (2020). Occupant-Façade interaction: a review and classification scheme. *Building and Environment*, 177, 371–377. <https://doi.org/10.1016/j.buildenv.2020.106880>
- Meerbeek, B., te Kulve, M., Gritti, T., Aarts, M., van Loenen, E., & Aarts, E. (2014). Building automation and perceived control: A field study on motorized exterior blinds in Dutch offices. *Building and Environment*, 79, 66–77. <https://doi.org/10.1016/J.BUILDENV.2014.04.023>
- Motamed, A., Deschamps, L., & Scartezzini, J. L. (2017). On-site monitoring and subjective comfort assessment of a sun shadings and electric lighting controller based on novel High Dynamic Range vision sensors. *Energy and Buildings*, 149, 58–72. <https://doi.org/10.1016/J.ENBUILD.2017.05.017>
- Motamed, A., Deschamps, L., & Scartezzini, J. L. (2019). Eight-month experimental study of energy impact of integrated control of sun shading and lighting system based on HDR vision sensor. *Energy and Buildings*, 203, 109443. <https://doi.org/10.1016/J.ENBUILD.2019.109443>
- Painter, B., Irvine, K. N., Waskett, R. K., & Mardaljevic, J. (2016). Evaluation of a Mixed Method Approach for Studying User Interaction with Novel Building Control Technology. *Energies* 2016, Vol. 9, Page 215, 9(3), 215. <https://doi.org/10.3390/EN9030215>
- Reinhart, C. F., & Voss, K. (2003). Monitoring manual control of electric lighting and blinds. *Lighting Research and Technology*, 35(3), 243–258. <https://doi.org/10.1191/1365782803LI0640A>
- Sadeghi, S. A., Karava, P., Konstantzos, I., & Tzempelikos, A. (2016). Occupant interactions with shading and lighting systems using different control interfaces: A pilot field study. *Building and Environment*, 97, 177–195. <https://doi.org/10.1016/J.BUILDENV.2015.12.008>
- Sullivan, R., Lee, E. S., Papamichael, K., Rubin, M., & Selkowitz, S. E. (1994). Effect of switching control strategies on the energy performance of electrochromic windows. *Optical Materials Technology for Energy Efficiency and Solar Energy Conversion XIII*, 2255(9), 443–455. <https://doi.org/10.1117/12.185387>
- Tabadkani, A., Roetzel, A., Li, H. X., & Tsangrassoulis, A. (2021). A review of occupant-centric control strategies for adaptive façades. *Automation in Construction*. <https://doi.org/10.1016/j.autcon.2020.103464>
- Tang, S. K. (2017). A Review on Natural Ventilation-enabling Façade Noise Control Devices for Congested High-Rise Cities. *Applied Sciences* 2017, Vol. 7, Page 175, 7(2), 175. <https://doi.org/10.3390/APP7020175>
- Taniguchi, T., Iwata, T., & Ito, D. (2012). *Blind control method based on prevention of discomfort glare taking account of building conditions*. Experiencing Light 2012 International Conference. https://www.researchgate.net/publication/307138640_Blind_control_method_based_on_prevention_of_discomfort_glare_taking_account_of_building_conditions
- Tzempelikos, A., & Athienitis, A. K. (2007). The impact of shading design and control on building cooling and lighting demand. *Solar Energy*, 81(3), 369–382. <https://doi.org/10.1016/J.SOLENER.2006.06.015>
- Vine, E., Lee, E., Clear, R., DiBartolomeo, D., & Selkowitz, S. (1998). Office worker response to an automated Venetian blind and electric lighting system: a pilot study. *Energy and Buildings*, 28(2), 205–218. [https://doi.org/10.1016/S0378-7788\(98\)00023-1](https://doi.org/10.1016/S0378-7788(98)00023-1)
- Wu, Y., Kämpf, J. H., & Scartezzini, J. L. (2020). A survey study of occupants' visual satisfaction on an automated venetian blind based on sky luminance monitoring and lighting simulation. *Proceedings of the ISES Solar World Congress 2019 and IEA SHC International Conference on Solar Heating and Cooling for Buildings and Industry 2019*, 685–692. <https://doi.org/10.18086/SWC.2019.13.05>

CoolSkin

A Novel Façade Design for Sustainable Solar Cooling by Adsorption

Andreas Greiner¹, Olaf Böckmann², Simon Weber³, Martin Ostermann¹, Micha Schaefer²

* Corresponding author, andreas.greiner@ibk2.uni-stuttgart.de

1 Institute for Building Construction, University of Stuttgart, Germany

2 Institute for Building Energetics, University of Stuttgart, Germany

3 Institute for Acoustics and Building Physics, University of Stuttgart, Germany

Abstract

The article investigates the dependencies of façade design and construction in the integration of a sustainable solar-powered cooling system based on closed adsorption. The presented work focuses on the possible design variants of the envelope surface of the façade-integrated adsorber. The principle of adsorption cooling is presented and, based on this, architectural options for façade integration are investigated. This is done both constructively and visually. For each variant, the solar gains are summed up and compared with each other. A functionally designed adsorber, similar to a flat plate collector, serves as a reference and starting point for the modifications. It provides the comparative value for the energy evaluation. The modification is limited to the visible surface of the adsorber. The texture of the solar adsorbing sheet was changed and the glazing used was replaced by ETFE cushions and by a novel ETFE vacuum panel. Finally, the solar simulation results were integrated into the higher-level system simulation to evaluate the resulting gain in cooling capacity. The results show that the system could generate more than 100 W per installed square metre of adsorber façade. Furthermore, higher solar gains compared to the reference case can be obtained at particular times of the day due to geometry and material changes. However, the modifications always lead to a reduction of the total cooling power. In conclusion, the simulation results reveal that design flexibility is possible, but currently the studied design variants have a lower cooling capacity compared to the solely functionally designed adsorber.

Keywords

solar cooling, adsorption, façade integrated cooling

DOI

<http://doi.org/10.47982/jfde.2022.powerskin.3>

1 INTRODUCTION

1.1 MOTIVATION

The world is getting warmer (Masson-Delmotte et al., 2021). Due to the steady progress of global warming, we are experiencing extreme heat events on Earth with increasing frequency. In many parts of the world, temperatures are reaching levels that are life-threatening for people. In order to slow down the global warming that is responsible for this, the consumption of resources in the building mass will be reduced in the future. In addition, the savings in building mass, and thus CO₂, further increases the thermal dynamics of buildings, which in turn leads to faster natural heating of the interior with the risk of over-heating. In the future, we will therefore not be able to operate buildings without active cooling in both existing and new buildings. Current centralized cooling systems have limited retrofit capability due to large pipe cross sections. Decentralized electricity-powered air-conditioning systems cannot be used everywhere due to low heat recovery, noise intensity, and their susceptibility to servicing (Giebeler et al., 2008). In total, air-conditioning systems already consume almost 16 % of final energy consumption in the building sector (about 1885 TWh) in electrical energy in 2020 (IEA, 2021). In order not to further intensify climate change, this cooling energy must be generated in a CO₂-neutral way. In this context, a decentralized adsorption cooling system for buildings was developed as part of the Collaborative Research Center 1244 (SFB 1244) at the University of Stuttgart (Germany), which uses the incident solar energy on the building façade. The use of solar energy is not only sustainable, but it is also an attractive option due to the parallelism of cooling capacity and external cooling load (Giebeler et al., 2008). Because of the integration into the façade, the function of solar energy harvesting becomes a design parameter for the architecture.

There are several different solar-based cooling concepts for buildings. These systems are classified according to their energy sources, which are either electrical, as in the case of photovoltaics (PV), or thermal, as in the case of solar collectors. The electrical energy generated by PV is used for cooling by means of compression units or Peltier elements. The former is currently the most common type of solar-powered cooling (Alexopoulos & Kalogirou, 2022). The direct use of thermal energy sources is divided into closed and open systems. Open systems, which can also be used for dehumidification, are based on liquid absorption or solid adsorption. Closed systems work either thermally and mechanically or on the principle of solid adsorption. The respective advantages and disadvantages of the individual systems and their possible use in buildings have been considered in detail in the past (Prieto et al., 2017a). The fact that the systems have not made their way into the built environment is due to several reasons. The main barrier is the performance, aesthetic, and complexity of the existing developments (Prieto et al., 2017b). In the past, the focus of research was mostly on energy optimization, while the integration of solar thermal collectors into the façade was mostly limited to the constructional side. The mounting of existing collectors on the façade rather than integration into the façade is still practiced today. Integration into mullion-transom façades has been realized in a few cases but has not gained widespread acceptance. On the component level, there are several research projects that deal with further integration methods of different systems (Buker & Riffat, 2015), but there is currently no work known that addresses the design and functional integration with respect to the surface of the solar façade. In particular, the time-dependent influence of the surface structure on the solar gains has not been a subject of research in the context of a solar façade until now. Yet new digital manufacturing methods enable the production of individual elements for a specific task.

The aim of this work is to investigate the possibilities of the novel adsorption cooling façade (ACF) system in terms of the visible façade surface from a design point of view excessively reducing the cooling performance. Publications have shown that a purely functional consideration does not necessarily lead to an application in the building context. An important and often neglected aspect is the design integration into the building concept (Prieto et al., 2017b). In this context, the aesthetic of a building is multifactorial and has occupied architects since the time of Vitruvius (1st century BC) until today. The paper "What makes a façade beautiful?" (Prieto & Oldenhave, 2021) sorts the often-mentioned points of façade aesthetics into intrinsic and extrinsic aspects. Intrinsic aspects like colour, proportions, and texture are as important for a "successful façade" as extrinsic aspects like logic, local context, or conceptual clarity. Due to the individual external dependencies of the extrinsic aspects, the paper can only look at the intrinsic aspects.

As detailed in Section 1.2, there are three components of the ACF that must be integrated into the building: Adsorber, Condenser, and Evaporator. This paper only addresses the integration of the solar absorbing adsorber into the façade. Due to the prevalence of element façades in high-rise building construction, this project assumes the integration of the adsorber into a curtain wall element. The element frame and its material will not be discussed further.

1.2 COOLING PRINCIPLE AND PRELIMINARY WORK

The novel façade-integrated closed low-pressure adsorption system for solar cooling was proposed within the SFB1244, which was first mentioned in Böckmann (Böckmann et al., 2022). This adsorption cooling façade (ACF) uses solar radiation as an energy source. It is therefore suitable as a renewal of the façade during building renovations or directly integrated into new buildings. An advantage of the decentralized system is that it could be installed modularly and is resilient to the failure of individual elements. The shifting of cooling generations to the vertical façade reduces the competition for space on the roof surface between HVAC systems, photovoltaics, terrace use or greenspace applications. Vertical thermal energy harvesting has a 30% (Kasper & Heidler, 2011) lower total energy gain than optimally aligned collectors. However, more decisive for the optimal orientation is the time of solar energy input, to harvest solar energy in the morning for cooling the afternoon. In this case a vertical orientation can achieve more solar energy gains compared to a tilted collector, as the solar zenith is low in the morning. Due to the favourable ratio of footprint to square metre of façade and the avoidance of ambient shading, high-rise buildings are most suitable for the proposed adsorption cooling façade (ACF).

The system consists of three main components: adsorber and condenser, both located on or in the façade, and the evaporator, located below the storey ceiling. It runs through two main phases during each day (Fig. 1): the regeneration phase and the cooling phase. During the regeneration phase, the adsorber is heated up by solar irradiation, initiating the desorption of the adsorbed water. As soon as the adsorber is no longer heated due to the repositioning of the sun, the subsequent cooling phase starts. In this phase, the adsorber is connected to the evaporator, continuously re-adsorbs vapour and thereby lowers the vapour pressure inside the evaporator. Consequently, evaporation is induced in the evaporator, resulting in a temperature decrease of the remaining water and thus provides cooling power to regulate the indoor room/building temperature

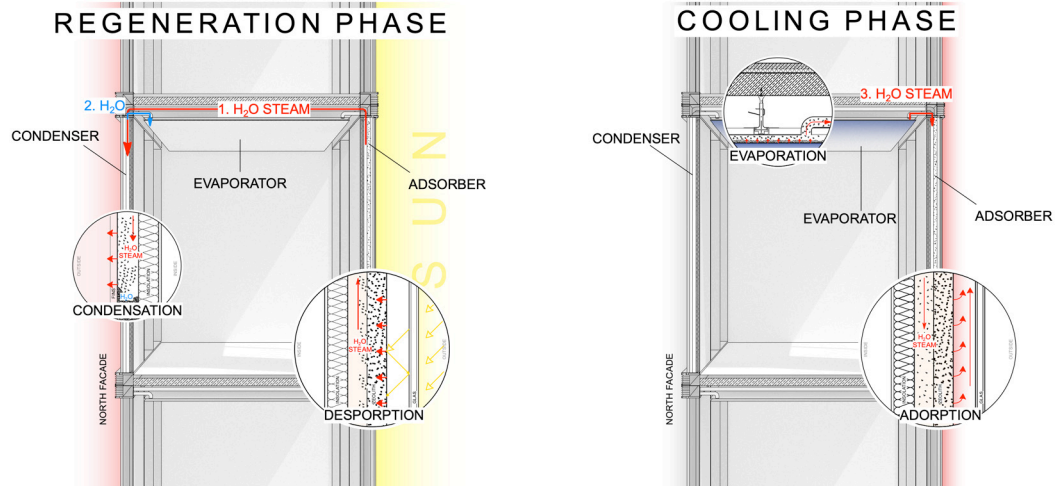


FIG. 1 Integration of the adsorption cooling façade system into one storey of a high-rise building during the regeneration phase (left) and the cooling phase (right)

The simulation of a reference case yields cooling rates of 54 W per installed square metre of adsorber façade, cmp. Figure 2. The cooling power can be maintained for 12 hours, confirming the applicability of the proposed cooling system. However, continuous cooling over the whole day cannot be achieved with only one ACF as the regeneration phase is required. This could be achieved by additional adsorber and condenser elements on the opposite façades of the building, which will be considered in future investigations. The temperatures inside the adsorber reach values of up to 100°C at the end of the regeneration phase, cmp. Figure 2. (Böckmann et al., 2022)

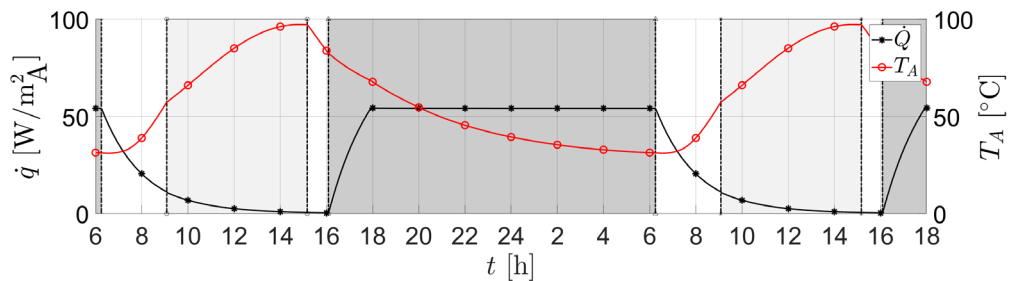


FIG. 2 Evolution of the cooling power (black line) and of the temperature (red line) inside the adsorber over time t . The regeneration phase is shaded light grey and the cooling phase is shaded dark grey.

Additionally, a broad parameter study provided information about possible optimization to increase the cooling rate and cooling capacity. The orientation of the adsorber façade elements, the surface area ratios of the components, and the design of the adsorber were identified as promising optimization parameters. Based on these results, a best-case configuration was identified that revealed cooling rates of up to 150 W per installed square metre of adsorber façade (Böckmann et al., 2022).

2 METHODS

Based on the highest possible energetic gains, a reference collector was developed in a first step, which fulfils the above-mentioned characteristics. This is based on information from the literature for solar collectors and from the functional constraints of the cooling principle. In a second step, the visual and absorptive effects of changes in the different layers of the adsorber are shown by means of two examples. The solar absorptance of the variants was determined simulatively and then each was incorporated into the higher-level component simulation in order to evaluate the effectiveness for the entire ACF.

Rhinoceros 3D software version 7 (Robert McNeel & Associates, Seattle, USA) with the Grasshopper plugin were used to get a three-dimensional parametric model of the Adsorber. The models thereby fulfil the function of a visual assessment and basis for the irradiation simulation. The modelled collectors were 1.5 m by 1.5 m. One square metre centred in it was set as the area to be analysed, to reduce the impact of the frame. The parametric model provides the flexibility for optional optimization steps. The simulation of solar irradiance on the absorbing surface was performed with the plugin Ladybug and with the five-phase method of the Radiance software, used in the environmental analysis plugin Honeybee (Roudsari, 2022) in the Grasshopper graphical programming interface of the Rhinoceros 3D software (Roudsari & Pak, 2013). Ladybug, a tool for analysis of climate data, allows simulation of irradiance on a given surface based on date, location, and geometry. Due to the time-saving simulation method, the subsequent optimization is based on this tool. For a more detailed investigation, the software Radiance was used. The simulation includes the parameter date, location, geometry, colour, reflectance, and transmittance of each specific material to get the hourly effective solar irradiance per square metre. Effects of the frame, back radiation of the environment, and external shading conditions were not considered, as such factors are secondary and must be considered for the individual integration case. The collector efficiency is crucial for the irradiation simulation of the entire system. This depends decisively on the optical efficiency, which relies on the reflectivity and absorptivity of the materials used. The solar absorption coefficient of the highly selective coating is reported to be 96% (Kasper & Heidler, 2011). Since Radiance only calculates the incident radiant energy, all results were multiplied by a factor of 0.96 for the total solar gains. For the absorption sheet, the material was set in Radiance with a specular reflectance of 4%. Both simulations were done with the location as Stuttgart (Germany, 48°44'55.4 "N 9°06'43.2 "E) and the façade orientation of the Collaborative Research Center 1244 demonstrator is approximately south-southeast (SSE) azimuth (-22.5°). The ASHRAE Revised Clear Sky (Tau Model), due to its accuracy for European latitudes, was used as the sky model (Badescu et al., 2013). For the Ladybug simulation, the direct and diffuse radiation were extracted from this model. 26th August was always assumed for both solar simulations.

The evolutionary optimization tool Galapagos (Rutten, 2013) was used to optimize the geometry of the structures in section 3.3.1 with respect to maximum solar gains. The parameters that could be changed with the optimization tool were the height z and the ratio of x_1 to x_2 , which is described in more detail in Chapter 3.3.1. In addition, the results were transferred to the Rhinoceros 3D environment for visualization. The optimized structure was also again simulated more accurately for its solar irradiance by using Radiance, with the specific material properties of each component. The whole workflow process is depicted in a simplified manner in Figure 3.

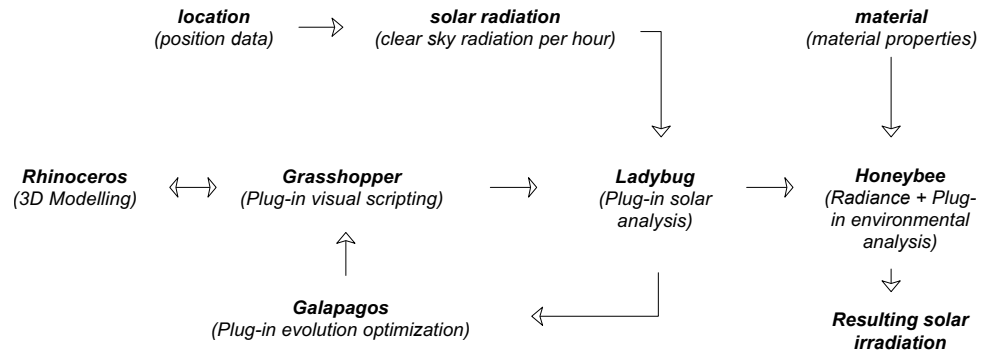


FIG. 3 Workflow diagram for modelling and simulation

The component simulation of the ACF was performed by co-author Boeckmann in (Böckmann et al., 2022) and confirmed the suitability of the system for building applications. Detailed component models were developed for the three main components adsorber, condenser, and evaporator, which are coupled by the vapour flow. The component models describe the internal heat and mass transfer processes as well as the adsorption and condensation/evaporation processes. Simulations of the components were carried out under realistic boundary conditions, applying the evolution of solar irradiation and ambient temperature over time for a summer day in Stuttgart.

3 RESEARCH SET-UP

3.1 BUILDING INTEGRATION PRINCIPLES

On a general level, there are various integration principles for integrating the adsorber element into a façade concept (Fig. 04). Either the system is integrated into the façade level or into the sun protection level. In the case of integration into the façade level, the adsorber element can be located within the insulation layer or in front of it.

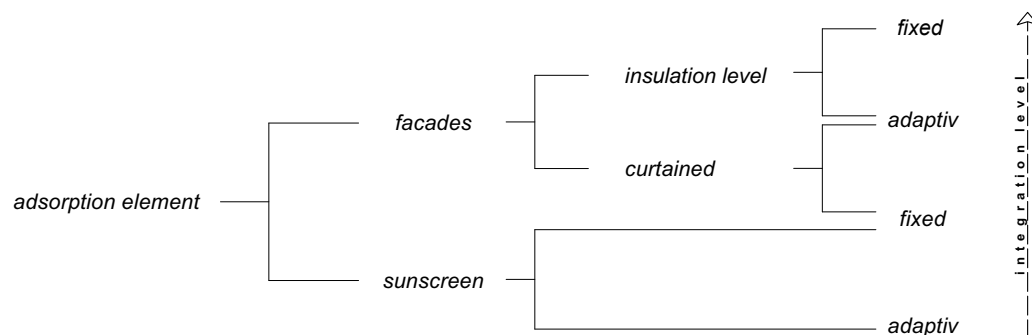


FIG. 4 Integration of an adsorption element

Finally, the various principles are to be considered as both adaptive and fixed elements. With increasing functional integration, the level of integration and also the complexity of the component tend to increase. (Klaiber, Fröhlich, & Vietor, 2019) Regardless of the selected façade system, all principles have in common the design-determining visible surfaces of the components. Since these are the energy harvesting surfaces, they have a large impact on the effectiveness of the overall cooling system. This means that there are functional boundary conditions for the adsorber that must be considered in the design of the adsorber. These are discussed in more detail in Section 3.3.

3.2 REFERENCE ADSORBER DESIGN

The preliminary work (Sect. 1.2) has shown that for the efficient operation of the system, the highest possible temperature difference between the adsorption and desorption phases should be achieved. For this reason, unglazed plastic or stainless-steel adsorbers, as they are already installed in façades today, cannot form the basis of our novel collector. Currently, only vacuum tube collectors and vacuum flat plate collectors reach the temperature range of 100°C or more. (Kasper & Heidler, 2011). In contrast to the decisive maximum temperature difference, vacuum collectors are generally only optimized for maximum energy gain. A possibility for rapid heat dissipation to the environment is not provided. Therefore, based on the principle of a conventional flat plate collector, a new type of collector had to be developed, which allows high-temperature differences between regeneration (charging) and cooling (discharging) phases, which is realized through switchable heat release.

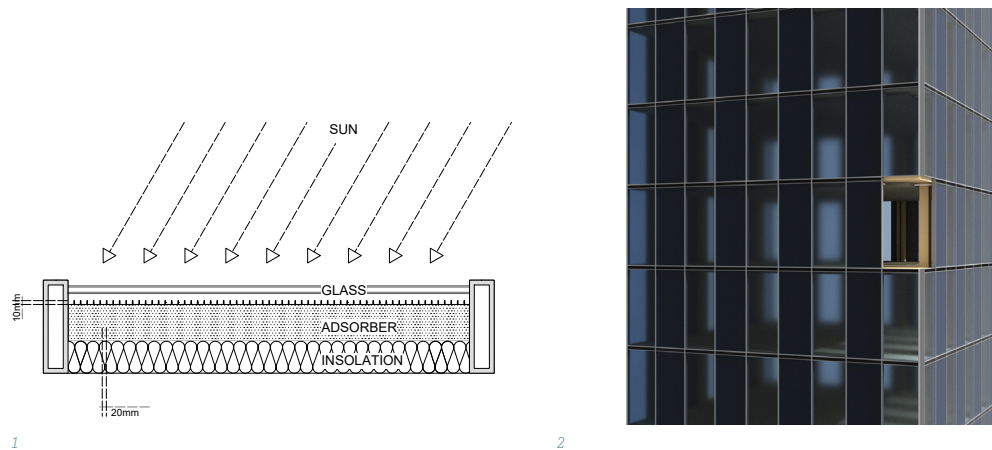


FIG. 5 [1] Top section view adsorption element with reference design, [2] Example of a façade integration of the reference design

Using the general model of product development (VDI 2221, 2019), a reference design (RD) has been constructed (Fig. 5) as a starting point for the investigations. In contrast to a flat plate collector, double insulating glazing with thermal insulation coating in front of the absorbing surface is applied here. For optimal radiation absorption of > 90% (Kasper & Heidler, 2011), this surface is provided with a highly selective coating (Physical Vapor Deposition (PVD) / Chemical Vapor Deposition (CVD)). The absorbing surface is at the same time part of the vacuum adsorber and responsible for the heat transfer. The resulting air-filled space between the glass and the adsorber sheet can be ventilated by means of upper and lower flaps. This vertical convection, which can be activated in the cooling phase, enhances the required heat dissipation and thus facilitates the rapid temperature drop of the adsorber, yielding higher evaporation rates in the evaporator and thus higher cooling power.

The heat release is further enhanced with vertical fins on the adsorber sheet to increase the heat emitting surface area. The effectiveness of this approach has been verified by numerical simulations and experimental validation is currently being conducted.

In This new development of a collector, specific to our system, gives the opportunity to consider the design aspects in the functional design and to explore general approaches for the surface design. As starting points, we have identified two layers on the reference adsorber, which contribute significantly influence the appearance (Fig. 6):

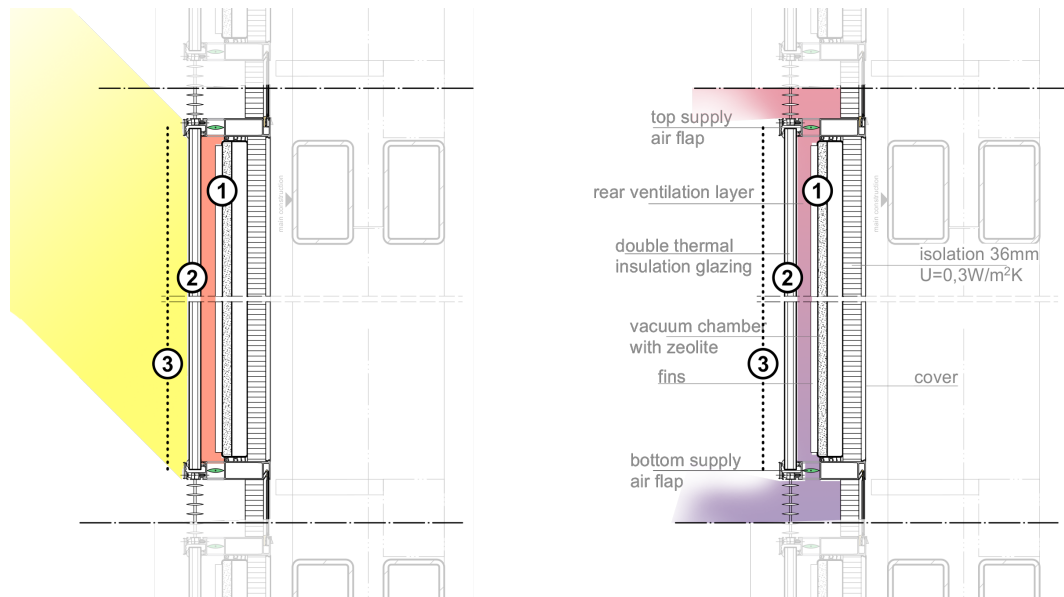


FIG. 6 Section view of the Adsorber element in regeneration phase (left) and cooling phase (right). Layer 1, 2 and 3 are discussed below.

Layer 1 is the highly selectively coated (PVD/CVD) aluminium absorber sheet of the vacuum adsorber, which largely determines the colour of the element through the blue/black shimmering coating and is responsible for solar absorption and thermal transfer into the adsorber. In addition, the absorption sheet is responsible for heat dissipation to the interstitial space during the cooling phase and is thus subject to thermal stress. Mechanically, the vacuum of the adsorber acts on the sheet.

Between Layer 1 and Layer 2 is an air gap, which is used for cooling in the cool-down phase. The gap between them is 10mm. Layer 2 is the double insulating glazing. This determines the “materiality” and surface feel of the element through the reflections and transparency. Both aspects, the solar heat gain coefficient and the thermal transmittance (U), are important factors for the efficiency of the collector. At the same time, the surface also represents the outermost weathering layer and, in addition to thermal loads, the surrounding environmental factors also affect this layer.

of adaptive heat transport of such structures Oei et al., 2019). This folding not only increases the stiffness of the element but can be manufactured from a simple two-dimensional aluminium plate. The former saves the necessary material input and the latter the manufacturing effort. The origami structure is designed to allow vertical airflow (Fig. 8) and maximize the absorbing surface in the defined period (Fig. 7).

The research project "SolarShell" at the University of Leipzig has shown the positive effects that parametric convolution can have on the energy income (Hülsmeier et al., 2017) and, in contrast to our work, investigated the total yield of PV cells. However, due to their structure, the simulations carried out indicate that the thermal solar gain can also be increased by an adjusted alignment. In our case, the maximization of the solar area was performed with the simulation of the solar irradiation with the plug-in Ladybug and optimized using Galapagos. A façade orientation SSE was assumed as an optimization parameter for the Stuttgart (Germany) site and the period from 05:00h to 12:00h for the whole month of August. A width (y) and depth (x) of 100mm and a maximum height (z) of 40mm were defined as the optimization framework (Fig. 9). The initial structure for the convolution was assumed to be $y_1=y_2$ and $x_1=x_2$. For the optimized structure, the ratio x_1 to x_2 was adjusted. In the optimized state, the structure has approx. 50% more surface area than a flat sheet with the same base area. This number can be increased by reducing the width/depth or increasing the height.

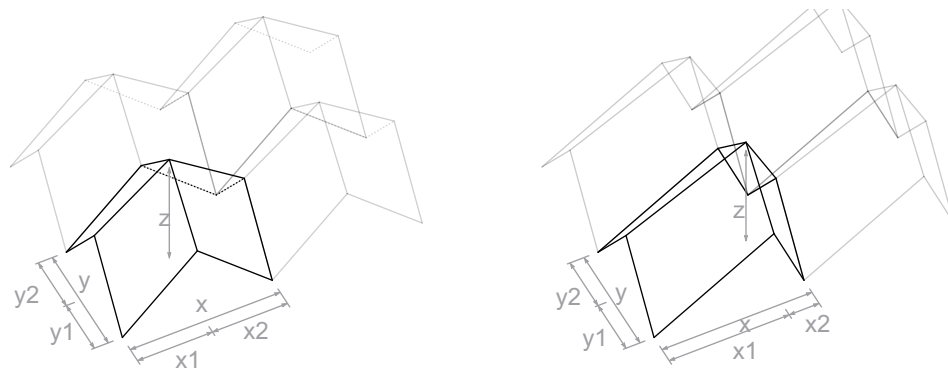


FIG. 9 Optimization method for the isometric folding structure, design/approach based on (Klett, 2013)

3.3.2 Layer 2 – Glass Substitution with an ETFE-Vacuum-Panel (EVP)

Another possibility for design and functional manipulation is the replacement of the double insulating glass pane. Glass is a relatively heavy material, which is in contradiction to the overall goal to reduce resource consumption in the building sector. As a result, especially in the renovation of high-rise buildings, the weight of the façade means that the supporting structure has to be improved. Due to the thermal load on the inside, most highly transparent plastics, such as PE, PP, and PET are not suitable. With a melting point of about 280°C and transmittance of approx. 91%, ETFE (ethylene-tetrafluoroethylene) is very well suited to the class of plastics in the use of a collector. Due to the high e-modulus, resistance to environmental influences and the "lotus" effect of the surface, ETFE has been used in the form of cushions in façades for several years. It could also include, with a 2-layer structure, into the adsorber element (Fig. 10).

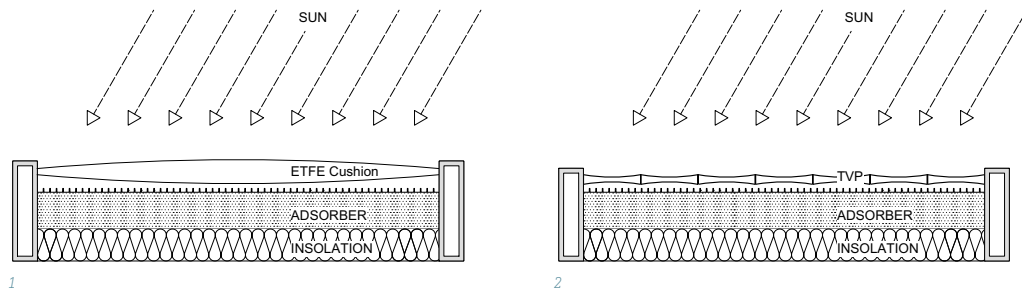


FIG. 10 Top section of the adsorber element with ETFE cushion (left) and transparent vacuum panel (right)

In order to achieve the U-value of double insulating glazing of approx. $1.1W/(m^2K)$, cushion constructions with 3 layers of ETFE are currently used. Since the transmittance decreases with each layer and a pillow construction requires more space volume in the collector, a completely new type of panel was developed with a 2-layer vacuum design (Fig. 10). To ensure the distance between the foils, a supporting structure in between is also needed. This transparent ETFE Vacuum Panel (EVP) thus serves as a design element. By colouring or choosing the material of the internal structure, the appearance can change depending on the angle. This is one of the few possible colour influences, and more complex representations are also possible as a result.

The span (C_d) of the supporting structure depends on the tensile strength (T) of the ETFE foil, the pressure outside ($P(i)$) the height of the structure (h) and the minimum distance (A_z) between the two foils (Fig. 11). For ETFE the tensile strength is $T=30N/mm$, h is set to 30mm and A_z is fixed at 10mm. These values result in a maximum span of approx. 218 mm. In the structures examined, this was limited to 200mm.

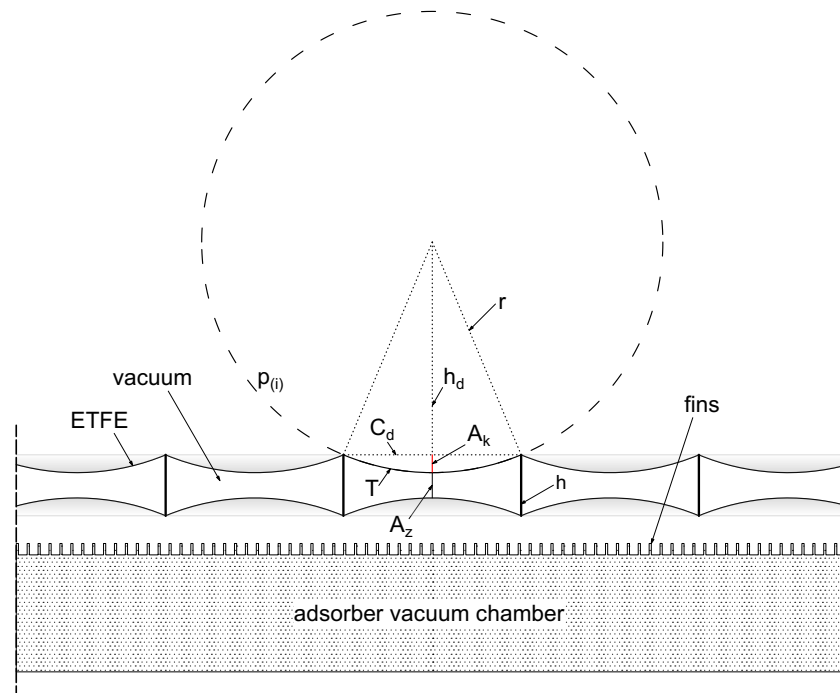


FIG. 11 Calculation sketch for the grid size

Four structures were investigated which could be used as a support structure. Horizontal and vertical lamellas, a grid structure, a hexagon, and a Voronoi structure (Fig. 12). The 2D footprints of the structure are between 0.083% and 0.09% of the total surface. These structures are to be considered exemplary and planners have the freedom to develop their own. The results of the structures obtained here can be used as a reference for geometric principles of new structures.

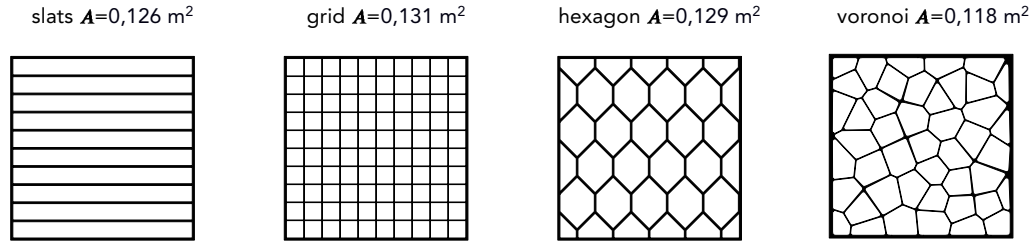


FIG. 12 Simulative studied pattern of support structure

4 RESULTS AND DISCUSSION

4.1 SIMULATION 1 – SOLAR GAINS OF THE REFERENCE DESIGN

In order to classify the absorbed solar energy for the reference design, the solar irradiation of a surface and a surface with solar glass, similar to the structure of a flat collector, were simulated. For the whole of August 26th, the energy simulation in Radiance shows with a south-southeast orientation a total irradiation for a vertical surface of 5108 Wh/m², for a flat plate collector with 4385 W/m², for the reference design with solar glazing (RD - transmission 91%) of 4674 W/m² and for the reference design with double insulating glazing (RD -transmission 83%) of 4214 W/m² (Fig. 13).

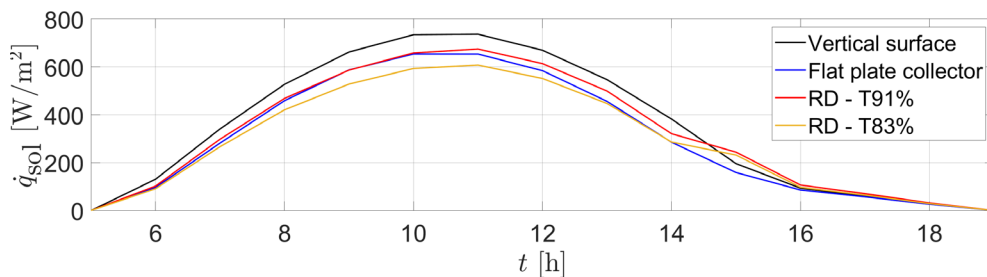


FIG. 13 Solar gains of a vertical surface, flat plate collector, reference design with solarglass T91% and reference design with double glazing T83%

This means that the irradiation on the 'RD - T91%' is 91.5% and on 'RD T-83%' it is 82.5% from the total irradiation on a vertical surface. As expected, the result correlates with the transmission coefficient of the two different glasses. Comparing the flat plate collector with the RD-T91%, the solar gains are almost identical except for the period between 2pm - 4pm. This slightly higher gain of the RD-T91% is due to the marginally better alignment by the fins on the surface of the RD. It can be concluded that the fins on the adsorber surface have a small influence on the optical energy gain, however a much better heat transfer in the cooling phase can be assumed because of the double surface.

By making a comparison between the RD with single-layer solar glazing and the RD with double-layer insulating glazing, the latter is 10% worse overall. In order to compare the two, the thermal losses must be considered in addition to the optical efficiency. These are assumed to be the same except for the glazing. The useful heat output (q_N) can be calculated by the difference between the useful irradiation (E_N) and the thermal losses (q_V) (Kasper & Heidler, 2011).

The thermal losses depend on the temperature difference (ΔT) between the absorber and outside air. If one assumes this very conservatively with ΔT 60° Kelvin at 12 am, a U-value for the solar glass of 5.8 W/m²*K and for the insulating glazing of 1.1W/m²*K (Glaströsch, 2022), the following result is obtained. The RD – T91% has a useful heat output at 12 am of 613 W/m² – 5.8 W/m²*60 = 265 W/m² and the RD – T83% has a useful output of 551 W/m² – 1.1W/m²*60 = 491 W/m². The real power is additionally dependent on the heat losses at the frame and backside. The single-layer solar glazing has a very high heat transfer co-efficiency and the efficiency of the collector decreases due to heat losses through the glass. In addition, condensation on the inside of the single-layer glazing is to be expected, which also reduces the solar gain.

$$q_N = E_N - q_V$$

FIG. 14 Useful heat output to irradiation and thermal losses

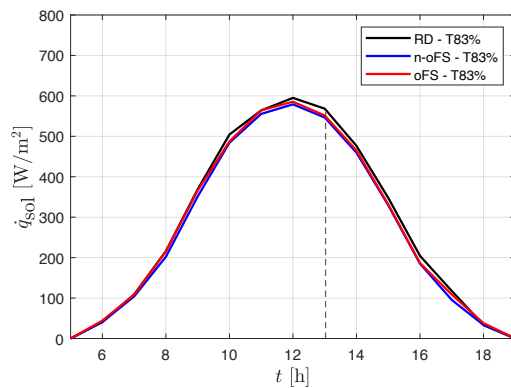


FIG. 15 Comparison RD-T83% with n-oFS and oFS aligned to south

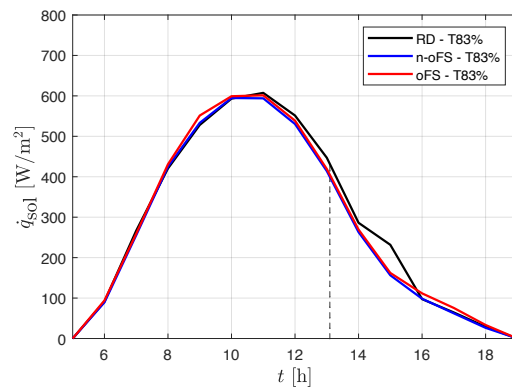


FIG. 16 Comparison RD-T83% with n-oFS and oFS aligned to south-southeast

4.3 SIMULATION 2 – SOLAR GAINS OF THE FOLDING ADSORPTION SHEET

The folds on Layer 1 were simulated for three directions, east (E), south-southeast (SSE) and south (S). In each case, the reference design with double insulation glazing (RD-T83%) was compared with the non-optimized folded sheet (n-oFS) and a folding sheet optimized for orientation (oFS). The period considered was always the full day of August 26th. Looking to the south orientated simulation (Fig. 15), the results are 4146 Wh/m² for the RD-T83%, 3967 Wh/m² for the n-oFS and 4053 Wh/m² for the oFS. Overall, the values are very close to each other and improvement in energy input due to surface optimization is hardly evident. The simulation of the SSE orientated collectors (Fig. 16) resulted in a total solar gain of 4214 Wh/m² for the RD-T83%, 4043 Wh/m² for the n-oFS and 4146 Wh/m² for the oFS. The overall values are also very close to each other, but the optimized surface has a higher gain in the time between 5 am and 10 am. This promotes faster

system dynamics and can thus provide cooling power sooner. A time shift was possible by the oFS. The results of the simulation with east orientation (Fig. 17) have a total solar irradiance of 3511 W/m² for the RD-T83%, 3288 W/m² for the n-oFS and 3641 W/m² for the oFS. The results show a significantly larger solar gain from the optimized convolution to n-oFS with 10% and to RD with 4%.

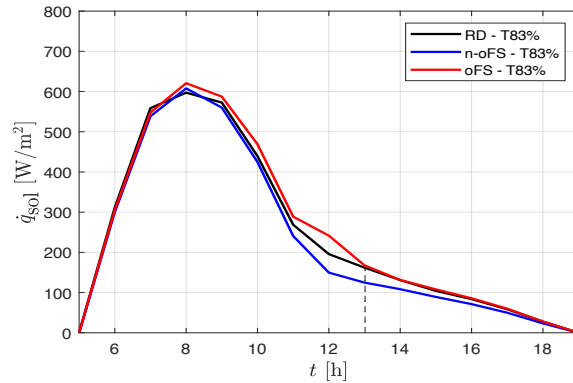


FIG. 17 Comparison RD-T83% with n-oFS and oFS aligned to east

It can be seen that the further the façade is from the optimal orientation to the sun in the south during the desired time period, the greater the additional gain between the non-optimized and optimized folding. In addition, the results show that the optimized folding can shift the solar gain slightly more into the morning hours. It is worthy of discussion whether such a small increase justifies the effort of an individual adjustment of the convolution for alignment and time. But the positive properties from 3.3.1 are also given for an unoptimized convolution.

4.4 SIMULATION 3 - SOLAR GAINS WHEN USING ETFE

The aim of simulation 3 was to investigate the influence of the material ETFE and an internal support structure on Layer 2 (Fig. 18). As with the investigations before, a façade orientation to SSE on August 26th is considered as an example. This shows the values 4214 Wh/m² for the RD, 4121 Wh/m² for an ETFE cushion, 2959 Wh/m² for the EVP with a grid support structure, 2880 Wh/m² for EVP with a hexagon support structure and 3091 Wh/m² for the EVP with Voronoi support structure.

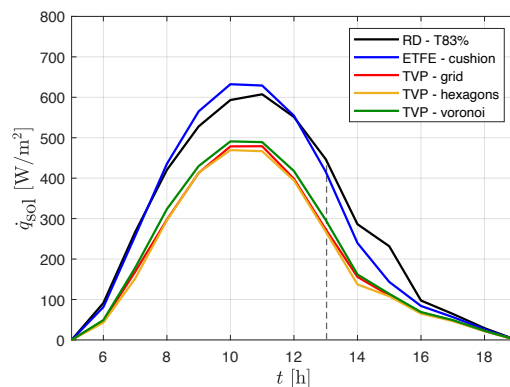


FIG. 18 Comparison RD-T83% with ETFE cushion and EVP with grid/ hexagons/ Voronoi structure aligned to SSE

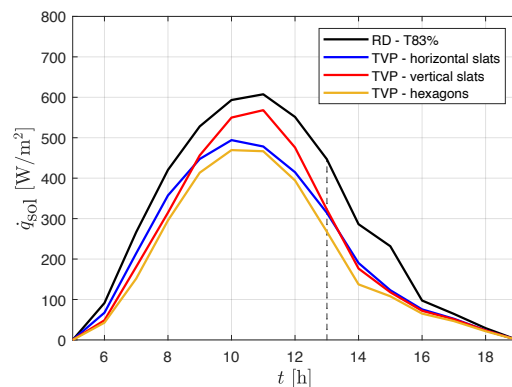


FIG. 19 Comparison RD-T83% with EVP with horizontal and vertical slats and with a hexagon structure aligned to SSE

Using an ETFE cushion, the solar radiation between 5 am and 1 pm is 3% higher than with the RD-T83%. At first glance, this seems to support the use of an ETFE cushion as an outer layer, but, as in Section 4.1, thermal losses must be taken into account. An ETFE cushion has a U-value of approx. 3W/m²K (Knippers et al., 2010) compared to a value of 1.1W/m²K for double glazing. With this in mind, the EVP, with its likely better U-value, is the better choice despite the poorer solar gains. The different results of the structures show a dependence on the solar gain and the geometry. This dependence is further explored in Fig. 19 with vertical and horizontal slats. In particular, the horizontal structures have a 26% negative impact on solar gains until 1 pm. There is still a high degree of geometric optimization of the support structure webs through design minimization, a reflective coating and also tilts adapted to the position of the sun. Further simulative and experimental research must clarify these issues.

4.5 VISUAL IMPACT

The visual impact of a building element is always related to the entire building and its surroundings. Thus, an evaluation is only possible individually according to integration criteria. Based on the integration studies of solar systems (Munari Probst & Roecker, 2019), we have established the following criteria: colour appearance, texture, depth effect, homogeneity. Depending on the façade context, other criteria such as gloss level, roughness and mechanical load-bearing capacity may be of interest. Further research is needed to clarify the influence of these points, as they are more material-specific properties than structural ones. The investigated manipulations were sorted into an evaluation matrix (Table 1) and rated as follows: not influenceable/ low (-), slightly influenceable / medium (o), and strongly influenceable/ high (+).

TABLE 1 Evaluation matrix of the visual criteria with evaluation of the solar gain.

	colour appearance	texture	depth effect	homogeneity (existing)	solar gain
reference adsorber	-	-	-	+	+
Folded sheet	-	o	-/o	+	+
ETFE cushion	-	-	o	+	-
ETFE vac. panel	o	+	+	o	-

It turns out that planners can individualize the ETFE vacuum panel the most. However, the functional values are poor. The folded sheet is the most balanced. For a practical application, further investigations must extend this evaluation matrix and expand it to a catalogue with the most diverse variants. Likewise, further criteria must be added and the presented criteria must be further differentiated. It would be important to have a direct indication of the solar gains depending on the orientation of the building.

4.6 SYSTEM ANALYSIS

Finally, the effect of the different approaches on the cooling rates, achievable with the proposed system, is investigated. For this reason, the different solar irradiation curves, determined in the previous sections, are applied to the model of the system presented in Section 1.2. The focus of the simulation studies is on the cooling power overtime during the cooling phase in the afternoon and the results are shown in Fig.20.

It is found that the highest cooling rates can be achieved with the reference design. The folding of the absorber sheet slightly increases the solar irradiation, but decreases the overall surface, compared to the reference design with the additional fins. This leads to a decreased heat release to the ambient in the cooling phase, which results in a lower cooling rate. Replacing the double insulation thermal glazing with a 2-layer ETFE cushion results in higher thermal losses in the regeneration phase and thus in a lower adsorber temperature. This limits the cooling rate, which is highly influenced by the heat release of the adsorber. The EVP has a comparable insulation effect as the glazing, but this cannot compensate for the much lower solar irradiation. Consequently, the adsorber temperatures and thus the cooling power is reduced.

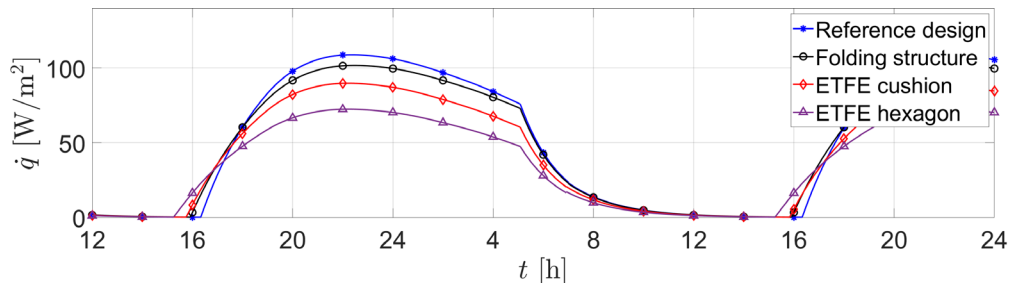


FIG. 20 Cooling power of the investigated reference design with double glazing T83%, folding structure, ETFE cushion and a ETFE hexagon structure

In order to evaluate the design possibilities of the absorber, the variants must meet the necessary cooling power per square metre footprint. This cooling power must be calculated individually for each building and depends strongly on the location (building zone), geometry, construction method, use (internal heat sources), and the control concept (DIN V 18599-2, 2018). Nevertheless, in order to make an initial assessment and evaluation of the various changes, the example of the cooling load calculations of VDI 2078 (VDI 2078, 2015) were looked at more closely and the generally used rough formula of the cooling power calculation was taken (Hanse Handels Haus GmbH, 2021). Thereby, a rough cooling power of 60W/m² for residential buildings and up to approx. 100W/m² for commercial buildings is given. Taking these rough values as a basis, replacing the glazing with an ETFE element is possible, but does not achieve the cooling performance for all usage scenarios. The EVP in particular must be viewed critically, as it only provides more than 60W/m² of cooling capacity over a very short period of time. Since this variant offers the greatest design potential for planners due to the additional support structures, the existing optimization potential must be further explored. The ETFE cushions have the disadvantage that the existing pressure must be maintained. This requires additional energy and technology and is only worthwhile in large-scale use. Manipulation by folding the absorption sheet has the greatest potential in terms of energy, but the optical effect is limited due to localization behind the glass pane.

5 CONCLUSION

In summary, the study has shown that geometric and material surface manipulation of the ACF adsorber is always associated with a loss of cooling performance. Thus, although design manipulation of the surface is possible, it is always subject to functional constraints. Thus, manipulation of the colour was generally ruled out because the highly selective coating only allows

adsorber temperatures above 100°C and was assumed to be unalterable. Any design must take into account both solar irradiance and the fastest possible cooling of the adsorber before the cooling phase. From the present research, trends for surface design parameters can be deduced, but need to be confirmed by further studies. The tendencies are that for layer 1 the light transmission of the material is crucial and any additional structure that can be used for shaping reduces it by shading. For layer 2, the study shows that the surface geometry can have a positive influence on solar energy gain. Unfavourable façade orientations can thus be compensated for to a certain degree. In conclusion, the design of the energy harvesting surfaces is always a balancing act between function and design.

Acknowledgements

The authors thank the Deutsche Forschungsgemeinschaft (DFG, German Research Foundation) for funding under SFB1244-27906422

References

- Alexopoulos, S., & Kalogirou, S. A. (Eds.). (2022). *Solar Thermal Energy*. New York, NY: Springer US. <https://doi.org/10.1007/978-1-0716-1422-8>
- Badescu, V., Gueymard, C. A., Cheval, S., Oprea, C., Baci, M., Dumitrescu, A., ... Rada, C. (2013). Accuracy and sensitivity analysis for 54 models of computing hourly diffuse solar irradiation on clear sky. *Theoretical and Applied Climatology*, 111(3–4), 379–399. <https://doi.org/10.1007/s00704-012-0667-1>
- Böckmann, O., Mamullaku, D., & Schäfer, M. (2022). *Modeling and simulation of a façade-integrated adsorption system for solar cooling of lightweight buildings*.
- Buker, M. S., & Riffat, S. B. (2015). Building integrated solar thermal collectors – A review. *Renewable and Sustainable Energy Reviews*, 51, 327–346. <https://doi.org/10.1016/j.rser.2015.06.009>
- Datentabelle Floatglas Eurowhite [Firmen Homepage]. (2022). Retrieved May 26, 2022, from Glastroesch website: <https://www.glastroesch.com/de/de/datentabellen-ausschreibungstexte/floatglas>
- DIN V 18599-2. (2018). *DIN V 18599-2 (2018-09-00) Energetische Bewertung von Gebäuden—Berechnung des Nutz-, End- und Primärenergiebedarfs für Heizung, Kühlung, Lüftung, Trinkwarmwasser und Beleuchtung—Teil 2: Nutzenergiebedarf für Heizen und Kühlen von Gebäudezonen. (Energy evaluation of buildings - Calculation of useful, final and primary energy demand for heating, cooling, ventilation, domestic hot water and lighting)* Beuth Verlag GmbH.
- Giebeler, G., Fisch, R., Krause, H., Musso, F., Petzinka, K.-H., Rudolphi, A., & Lenzen, S. (2008). *Atlas Sanierung: Instandhaltung, Umbau, Ergänzung (Atlas renovation: maintenance, conversion, addition)* (1. Aufl.). Basel Berlin: Birkhäuser.
- Hanse Handels Haus GmbH. (2021, November 9). Klimacorner.de. Retrieved August 17, 2022, from <https://klimacorner.de/news/auslegung-von-klimaanlagen>
- Hülsmeier, F., Heller, A., Huth, S., Knechtges, S., & Reise, J. (2017). *SOLARSHELL- Die parametrisch optimierte Fassade als Energiequelle (SOLARSHELL- The parametrically optimized facade as an energy source)* (p. 105) [Abschlussbericht]. Leipzig: Hochschule für Technik, Wirtschaft und Kultur Leipzig. Retrieved from Hochschule für Technik, Wirtschaft und Kultur Leipzig website: https://ail.htwk-leipzig.de/fileadmin/portal/m_ail/05_informationen/publikationen/2017-12_solar.shell_schlussbericht_web.pdf
- IEA. (2021). Cooling. Retrieved August 9, 2022, from <https://www.iea.org/reports/cooling>
- Kasper, B.-R., & Heidler, K. (Eds.). (2011). *Solarthermische Anlagen: Leitfaden für das SHK-, Elektro- und Dechdeckerhandwerk, für Fachplaner, Architekten, Bauherren und Weiterbildungsinstitutionen (Solar thermal systems: Guide for the sanitary, heating and air-conditioning, electrical and plumbing trades, for specialist planners, architects, builders and further education institutions)* (9. Aufl., überarb. Neuauf.). Berlin and Frankfurt, Main: DGS Landesverband Berlin Brandenburg and VVEW Energieverl.
- Klaiber, D., Fröhlich, T., & Vietor, T. (2019). Strategies for function integration in engineering design: From differential design to function adoption. *Procedia CIRP*, 84, 599–604. <https://doi.org/10.1016/j.procir.2019.04.344>
- Klett, Y. (2013). *Auslegung multifunktionaler isometrischer Faltstrukturen für den technischen Einsatz (Design of multifunctional isometric folding structures for technical applications)* (1. Aufl.). München: Verl. Dr. Hut.
- Knippers, J., Cremers, J., Gabler, M., Lienhard, J., Cremers, J., & Institut für Internationale Architektur-Dokumentation (Eds.). (2010). *Atlas Kunststoffe + Membranen: Werkstoffe und Halbzeuge, Formfindung und Konstruktion (Atlas Plastics + Membranes: materials and semi-finished products, mold finding and design)* (1. Aufl.). München: Inst. f. Internat. Architektur-Dokumentation.

- Mostapha Sadeghipour Roudsari. (2022). Honeybee · Honeybee Primer [GitBook]. Retrieved April 13, 2022, from <https://mostapharoudsari.gitbooks.io/honeybee-primer/content/text/components/Honeybee.html>
- Mostapha Sadeghipour Roudsari & Michelle Pak. (2013). *Ladybug: A parametric environmental plugin for grasshopper to help designers create an environmentally-conscious design*. Presented at the 13th Conference of International Building Performance Simulation Association, Chambery. Chambery. Retrieved from https://www.ibpsa.org/proceedings/bs2013/p_2499.pdf
- Munari Probst, M. C., & Roecker, C. (2019). Criteria and policies to master the visual impact of solar systems in urban environments: The LESO-QSV method. *Solar Energy*, 184, 672–687. <https://doi.org/10.1016/j.solener.2019.03.031>
- Oei, M., Klett, Y., Harder, N., Flemming, D., & Sawodny, O. (2019). Modelling the Flow and Heat Transfer Characteristics of Perforated Foldcore Sandwich Composites for Application in Room Air Conditioning. *2019 IEEE 15th International Conference on Automation Science and Engineering (CASE)*, 1269–1274. Vancouver, BC, Canada: IEEE. <https://doi.org/10.1109/COASE.2019.8842913>
- Prieto, A., Knaack, U., Auer, T., & Klein, T. (2017a). Solar coolfaçades: Framework for the integration of solar cooling technologies in the building envelope. *Energy*, 137, 353–368. <https://doi.org/10.1016/j.energy.2017.04.141>
- Prieto, A., Knaack, U., Auer, T., & Klein, T. (2017b). Solar façades—Main barriers for widespread façade integration of solar technologies. *Journal of Façade Design and Engineering*, 51–62 Pages. <https://doi.org/10.7480/JFDE.2017.1.1398>
- Prieto, A., & Oldenhave, M. (2021). What makes a façade beautiful? *Journal of Façade Design and Engineering*, 21–46 Pages. <https://doi.org/10.7480/JFDE.2021.2.5540>
- Rutten, D. (2013). Galapagos: On the Logic and Limitations of Generic Solvers. *Architectural Design*, 83(2), 132–135. <https://doi.org/10.1002/ad.1568>
- V. Masson-Delmotte, P. Zhai, A. Pirani, S.L. Connors, C. Péan, S. Berger, ... Y. Chen, L. Goldfarb, M.I. Gomis, M. Huang, K. Leitzell, E. Lonnoy, J.B.R. Matthews, T.K. Maycock, T. Waterfield, O. Yelekçi, R. Yu, B. Zhou (eds.). (2021). *IPCC, 2021: Summary for Policymakers*. In: *Climate Change 2021: The Physical Science Basis. Contribution of Working Group I to the Sixth Assessment Report of the Intergovernmental Panel on Climate Change* [Summary for Policymakers]. Switzerland. Retrieved from https://www.ipcc.ch/report/ar6/wg1/downloads/report/IPCC_AR6_WGI_SPM_final.pdf
- VDI 2078. (2015). *VDI 2078—Calculation of thermal loads and room temperatures (design cooling load and annual simulation)*. Beuth Verlag GmbH.
- VDI 2221 (Ed.). (2019). *VDI 2221—Entwicklung technischer Produkte und Systeme Modell der Produktentwicklung (Design of technical products and systems Model of product design)*. Beuth Verlag GmbH.

Renovating Modern Heritage – The Upgraded Façade of Commerzbank Düsseldorf

Rouven S. Grom^{*}, Andreas W. Putz¹

^{*} Corresponding author, rouven.grom@tum.de

¹ Technical University of Munich, TUM School of Engineering and Design, Germany

Abstract

The post-war building stock is increasingly being transformed. Even at objects protected as listed heritage, renovation usually results in a high degree of material exchange and replacement. This is especially the case in regard to historic curtain wall constructions. Based on the case study of the Commerzbank High-rise and original planning documents by Gartner, the paper focuses on the applied strategy of disassembling and reassembling the curtained aluminium sandwich elements, and the resulting upgrading of the original façade with a newly installed interlayer for insulation. The paper discusses the possible transfer of this strategy, which largely depended on the existing high quality of the aluminium components, their corrosion-resistant properties and low weight. The case study of the former Commerzbank High-rise indicates that a long-term preservation of post-war modern building stock can be achieved without wholesale replacement of original building components. The reuse of existing materials and components represents a promising approach.

Keywords

façade renovation, reuse, retrofitting, aluminium curtain wall, Josef Gartner GmbH, modern building heritage conservation

DOI

<http://doi.org/10.47982/jfde.2022.powerskin.4>

1 INTRODUCTION

The post-war building stock is currently being heavily transformed, repaired, and upgraded. Increasingly stringent requirements and regulations, especially in regard to energy savings, render modern structures unsustainable. After half a century of use, post-war modern structures seem to become obsolete. It does not help that they are generally considered as irreparable. Even with objects protected as listed heritage, renovation usually results in a high degree of material change and replacement. This is especially true in the case of historic building envelopes. In Germany, prominent recent examples of thorough replacement of “light” curtain wall façades through improved replicas include the listed HVB Tower in Munich (1975–1981, architects Walther and Bea Betz), where between 2013 and 2015 the double-pane insulating glass façade has been updated to a box window façade with a total of four layers of glass, while retaining the external appearance (Henn Architects with the support of façade planners R+R Fuchs). Similarly, the listed BMW-Vierzylinder High-rise, BMW’s headquarters in Munich (1968–1972, architect Karl Schwanzer) was re-clad with a new façade between 2004 and 2006 by architects Schweger Associates, copying the original one. The façades of the double high-rises of the Deutsche Bank in Frankfurt (1979–1984, architects Hanig, Scheid, Schmidt) were also replaced by seemingly identical replicas in 2011 (technical architects Volkwin Marg and Hubert Nienhoff, gmp). The new construction allows for the hydraulically assisted opening of windows. With an almost 90% reduction of carbon-dioxide emissions, the renewed edifice was certified LEED Platinum and DGNB gold.

To the passer-by, these new façades are not recognizable as such. In all cases, the greatest attention was paid to preserving the external appearance of the listed buildings. However, it is questionable whether replacing the building fabric so extensively after only 30 to 40 years of service is really sustainable. Arguably and probably, the new façades will hardly last longer. The common approach also contradicts the usual high regard towards historic materiality in Building Heritage Conservation. Conservation and restoration of modern building heritage started in the 1980s and 1990s. Projects concerned largely on iconic buildings from the Modern Movement of the interwar period. Early on, “light” metal-glass-façades were taken care for, like in the prominent examples of Zonnestraal Sanatorium (1927–1931, architects Jan Duiker, Bernard Bijvoet, and Jan Gerko Wiebenga, restoration between 1995 and 2008) and its contemporary Van Nelle Factory (1925–1928, architects Johannes Brinkman and Leendert van der Vlugt, restoration 1998 - 2004), both in the Netherlands, the latter a UNESCO World Heritage Site since 2014. Through trial and error, such projects helped to define conservation approaches which could be applied to “everyday modern” buildings of less historic importance (Jonge, 2017). Based on practical experience, Wessel de Jonge, an authority on the restoration of modern architecture, distinguishes between three principal approaches in dealing with historic light façades. First, the improvement of thermal characteristics by adding secondary glazing or altogether replacement of glazing, resulting in complete change in appearance and considered unsuitable for protected façades. Second, an upgrade of the historic façade itself, retaining some of the original components. And third, by adding a secondary layer on the interior (Jonge, 2017, p. 100). Whereas the restored Zonnestraal Sanatorium is merely a representation of the original idea and design intent, rather than original in material (Meurs & van Thoor, 2010), the restoration of the Van Nelle Factory resulted in a more conservative approach. Here, a secondary internal façade was added which allowed for the buildings’ authentic glazed envelope to be retained in place, as a simple screen against wind, rain, and noise (Kuipers, 2017; Ayón et al., 2019, p. 114-121). In regard to the preservation of post-war high-rise buildings in Germany, a similar development can be traced regarding the eminent restorations of the “Dreischeibenhaus”, the Thyssen High-rise in Düsseldorf (1957–1960, architects HPP), which was renovated in 1994 and again in 2015 by HPP. Whereas the façade, after several previous repairs, was replaced completely by a replica of similar appearance to

the original, but different, construction in the 1990s (Fürst, 1998), the recent renovation was careful not to replace the façade again and instead enhanced it with a new interior layer for isolation.

Preservation of modern architectural icons in general in recent years has proven the significance of original building materials to their conservation, despite them often being machine-made and industrially mass fabricated. Such materials can hardly be reconstituted today and are of essential historic and artistic value to these objects. Considerations of preservation are less alien to the subject of curtain-walled façade and high-rises than one might at first assume. According to a hitherto unpublished analysis of their protection status, the proportion of listed buildings among historic high-rise offices in Germany is higher than average (Rung & Putz, 2021). Of more than 400 such structures built between 1950 and 1980, about a quarter is today legally protected as heritage. Only 10% have been demolished. The extent of the protected fabric is even higher if one looks at envelope surface instead of building units, as mostly large and prominent high-rises have been considered for protection. These results correspond with a parallel statistical survey, also unpublished thus far, of curtain-wall façades built by the prominent manufacturer Josef Gartner GmbH between 1955 and 1985, of which about 10% are currently legally protected as building heritage (Grom, 2021). It is expected that the number of protected edifices of this kind will rise in coming years due to ongoing inventorisation.

With the high percentage of protected heritage objects among curtain-walled high-rise buildings, and increased attention given to the preservation of original appearance and materiality, we conclude that new approaches for the upgrading and conservation need to be developed, but in such a way that these approaches also allow for necessary energy and comfort related improvements. The recent renovation of the former Commerzbank High-rise in Düsseldorf might show a feasible way. Designed by architect Paul Schneider-Esleben and built in the period 1959-1962, it was renovated and preserved in 2021 as one of the city's most outstanding post-war architectural monuments. Whereas the interior was converted into a hotel and lost its original features, the façade was renovated according to building conservation standards. Planned by HPP architects, an office strongly engaged in adaptive reuse and conversion of existing structures in recent years, with the support of Bollinger+Grohmann for structural engineering and façade engineering, the upgrading of the façade was carried out by the same company responsible for the original construction, renowned façade manufacturer Josef Gartner GmbH. It was possible to maintain the original components and appearance while still meeting increased building physics requirements. With its reused and upgraded envelope, the new hotel high-rise was certified as DGNB platinum in 2021.

2 CONSTRUCTION HISTORY

In a brief historical outline, the development of panel constructions is described to place the Commerzbank's façade within the history of construction. In curtain wall construction, a series of developments in the post-war decades basically resulted in two feasible types of construction: stick systems or ladder systems and panel constructions, from which mullion-transom façade systems and unitized systems have been developed. In America, the development of these types of construction took place almost simultaneously, while in Europe, stick systems were increasingly used, mainly due to economic reasons. A façade in stick system construction can be produced economically without expensive machines and in smaller series. For panel elements made of sheet metal, large punches and presses with expensive tools are necessary, which are only worthwhile for large buildings with very high quantities of elements (Gockell, 1964, p. 8).

After World War II, the steel skeleton construction method with a curtain-wall façade of extruded aluminium profile frames – infilled with panels of aluminium sheets and glass – became established in high-rise building construction in the US for weight reasons. Panel constructions made of metal, in aluminium or steel, have been used there since the early 1950s. In Germany, comparable façade constructions made of panels can only be observed a decade later. The architect Schneider-Esleben gained inspiration from various building projects on a study trip to the USA. He ultimately broke away from the idea of a conventional grid façade, as can be seen from numerous preliminary designs. The idea of the Commerzbank façade can probably be traced back to the Alcoa Building in Pittsburgh (USA), designed by the architects Harrison & Abramovitz, which was built between 1950 and 1953 (Gartner, 2021). The Alcoa façade is one of the first high-rise façades worldwide consisting of storey-high anodised aluminium sheet panels with punched-out window openings. Reversible sashes with frames made of extruded profiles are inserted into the openings; the corners of the openings and reversible sashes are rounded and sealed with a compressed air hose. The vertical joints of the panels are made of panel edges butt-screwed together, which allow a component movement when the length changes. At the horizontal joints, the panels overlap. Overall, a fairly even joint pattern is created despite the different joints. The panels are fastened to the faces of the floor slabs with steel brackets. The sheet metal shells are backed with lightweight concrete for thermal insulation, creating a ventilated space between them. In addition, the metal sheets have a striking design feature. They are embossed with a prismatic concave pattern, two square embossments per panel element, which simultaneously create spatial rigidity against wind loads (Schaal, 1961, p. 214). Other American examples of metal panel façades were also mostly made of single-layer sheet metal, stiffening profiles, and initially without integrated insulation. In comparison, the Commerzbank façade of 1962 in Düsseldorf is one of the first examples with a completely prefabricated and flat façade consisting of insulated panels without stiffening profiles or a frame construction. Regardless of this, the French architect, metal construction pioneer and inventor, Jean Prouvé, had already been experimenting with insulated elements made of sheet steel in the 1930s. A first significant application can be found at the Maison du Peuple in Clichy in France from 1935–1939 by architects Eugène Beaudouin and Marcel Lods. The first curtain wall “mur Rideau” made of industrially produced, double-skin panels of formed and folded sheet steel is installed in the office wing of the building, to which the Alcoa façade in Pittsburgh surprisingly bears some similarities. Prouvé’s façade was well known among American architects (Sulzer, 1991, p. 23). Prouvé designed the first noteworthy aluminium façade in Europe in 1951 for the Fédération du Bâtiment building in Paris (France), consisting of insulated, completely prefabricated wall units equipped with horizontal sliding windows and ventilation strips (Aluminium-Zentrale e.V., 1959, p. 12).

This selection of examples can be used to demonstrate the basic construction types of panel constructions. The sheet metal panel of the Alcoa façade stands at the beginning of the constructional development. Here, the embossing stiffens the panel. It has no frame and no insulating layer. The wall units of the Jean Prouvé in Paris are built from a stiffening frame construction, while the insulation is integrated into the panel in spaced shells. The façade of the Commerzbank represents another stage of development, the panel is constructed as a composite element without a frame, the insulation layer alone serves to stiffen it. On closer inspection, however, the Alcoa façade in Pittsburgh is actually a simple cladding made of aluminium sheets, which at first glance can hardly be distinguished from a classic curtain wall. The even more groundbreaking wall unit of the Jean Prouvé in Paris is a skeleton infill, as it was placed between the storey ceilings and not curtained. The façade of the Commerzbank however is a real curtain wall made of sandwich elements.

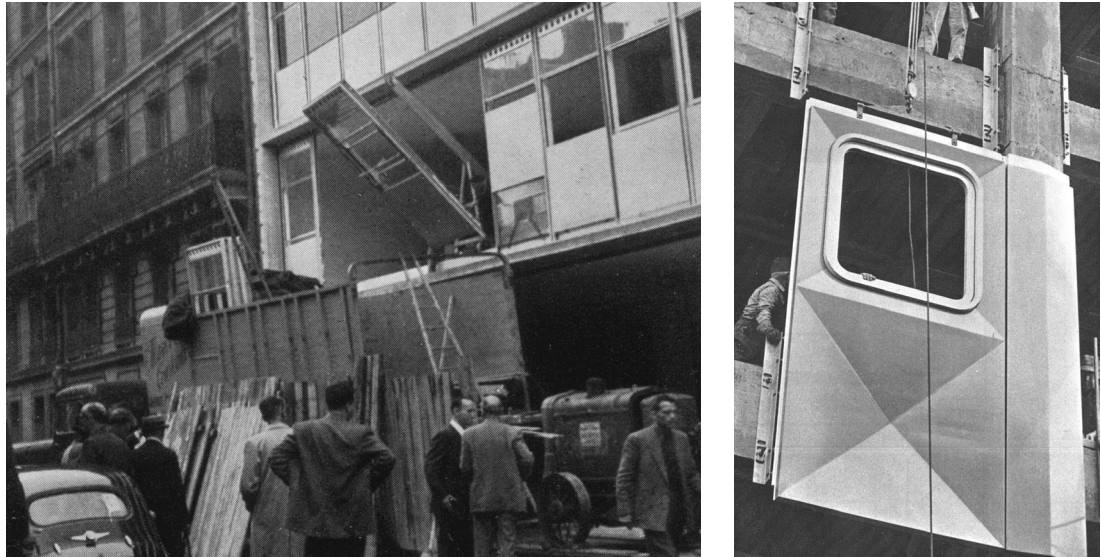


FIG. 1 Mounting of the wall elements in Paris in 1951. Photo in Aluminium-Zentrale e.V., 1959, p.12. (left). Mounting of the wall elements in Pittsburgh in 1953. Photo in Schaal, R. 1961, p. 217. Photo: Alcoa Pittsburg Pa. USA. (right)

In contemporary literature, the façades of these three examples are typologically assigned to panel constructions (Schaal, 1961, p. 213-235; Hofmann, Griese & Meyer-Bohe, 1973, p. 140-141), which, however, are referred to as façade elements or unitized systems according to today's general understanding. However, the designation "façade element" alone says nothing about the constructive structure, the degree of prefabrication and the assembly, because façade elements can also be made from muntin constructions. Rolf Schaal wrote in 1961 that "the construction elements of the panel constructions - like the panels - (...) are in principle enlarged panels of a similar type to those used in muntin constructions. Their construction is essentially the same as that of the panels. In contrast to muntin walls, where the panels rely on the load-bearing and connecting effect of the muntins, the panels are joined together directly without the aid of a visible and dividing muntin framework." (Schaal, 1961, p. 213) The term panel construction is used here to refer to a second type of construction of façade elements. (Gockell, 1964, p. 7) The curtain wall systems that emerged in Germany from the mid-1950s onwards are mostly made of muntin constructions, which are either assembled from individual components or from prefabricated frames. Over the decades, the prefabricated frames, which are possible in a wide variety of variations, have been developed further to create façade elements as we know them today. Unitized systems or façade elements are characterized by a high degree of prefabrication. They are either partially or completely prefabricated, depending on the panel or frame construction. They thus enable an assured quality of production in the factory. They are usually storey-high and one window axis wide. Faster assembly on site is possible with a small number of personnel compared to pure muntin constructions.

3 CASE STUDY: COMMERZBANK HIGH-RISE

3.1 THE FAÇADE OF 1962

The new high-rise office building designed by the architect Paul Schneider-Esleben was built between 1959 and 1962 as an extension to the existing Commerzbank headquarters in Düsseldorf from 1912. Next to the new building, a free-standing concrete tower with lift and stairs was attached,

which was connected to the existing building opposite with an acrylic covered pedestrian bridge above street level. The building was placed with its narrow side facing the street; the parking areas on the right side of the building interrupted the perimeter development allowing for a free view of the structure, with the neighbouring development also being set back. On the left side of the building, Schneider-Esleben designed a two-storey parking garage with a car workshop attached to the rear. Almost covering the entire site, the parking garage continued in the basement. An open drive-in bank counter was built below the high-rise on the ground floor – the chosen static system meant that it was free of supports – which enabled customers to carry out banking transactions smoothly without having to leave their cars. Only a small part of the ground floor was closed-in or glazed. Access to the underground car park, among other things, was behind the drive-in counter.



FIG. 2 The Commerzbank high-rise in Düsseldorf of 1962 by Paul Schneider-Esleben. Photos in Calendar Josef Gartner GmbH, 1963 April 21.-27. (left) + May 19.-25. (right). Photos: Inge Goertz-Bauer. Gartner archives, Gundelfingen (Donau)

The supporting structure of the high-rise office building consists of a twelve-storey structure elevated on three cantilevered concrete slabs. Allowing for free floor plan division without supports in the normal storeys, reinforced concrete slabs – made of prestressed concrete beams – rest on cantilevered ceiling girders. A circumferential reinforced concrete beam and concrete parapets served to reinforce the edges. All structural shell parts of the building and lift tower were finished in exposed concrete, both inside and out, and the monumental supporting structure remained visible in the plinth area (Lepik & Heß, 2015; Schneider-Esleben, 1963). The façade manufacturer Josef Gartner developed a façade made of aluminium panels according to Schneider-Esleben's ideas, which was new at that time in Germany.

Gartner had been responsible for many inventions and standards in façade construction. Traditionally, Gartner developed a customised façade for each client. Schneider-Esleben had already worked with Gartner on the construction of the Mannesmann high-rise in Düsseldorf in 1958 (Gartner, 2021). The futuristic appearance of the new building was in stark contrast to the neoclassical stone façade of the opposite Commerzbank's main administration building. The anodised aluminium façade consisted of lightweight and storey-high elements that were prefabricated in one piece with integrated windows and insulation, as in car body construction, without an additional frame structure, and hung in front of the reinforced concrete skeleton structure (Schneider-Esleben, 1963).

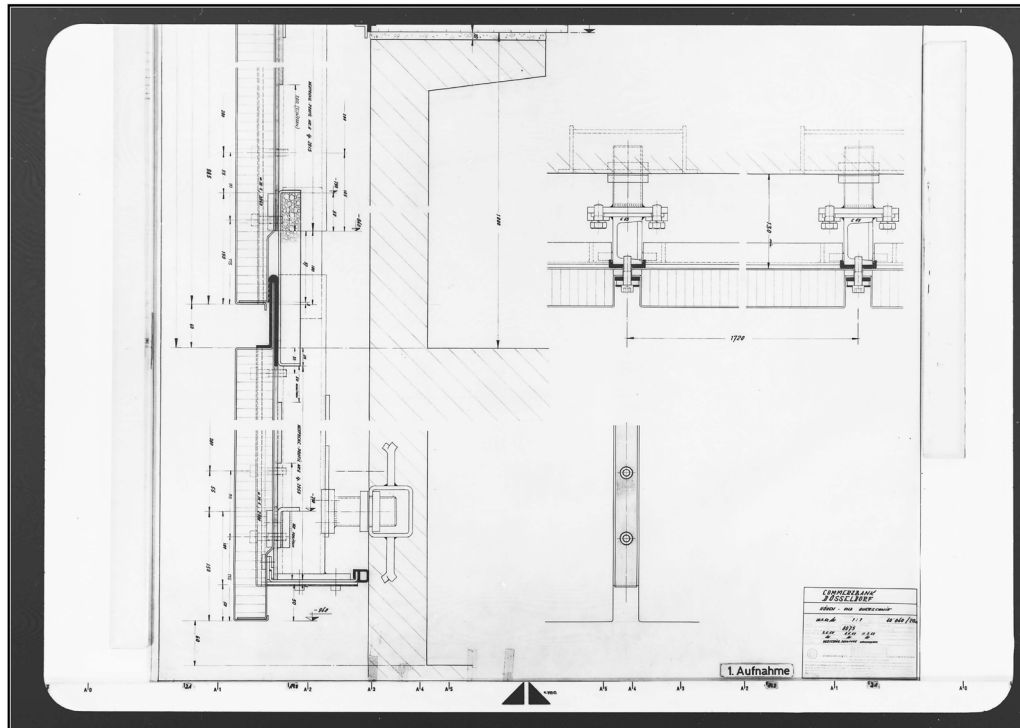


FIG. 3 Working drawings by Josef Gartner GmbH: Horizontal and vertical detail section of the Commerzbank Düsseldorf, 1962. Gartner archives, Gundelfingen (Donau). #40040/20a – 1

The façade of the high-rise consists of 600 identical, 1720 x 3100 mm, flat and jointless wall elements, the inner and outer shells of the elements each made of 2 mm thick aluminium sheets. All aluminium parts are technically anodised in a natural shade of at least 20 µm and are thus particularly resistant to all weathering influences and are maintenance-free. Window openings are pressed out on a factory metal punch and deep-drawn under a press. Air-comb honeycombs from Douglas Air-Craft Corporation, Santa Monica (USA) were used as insulation filling. The paper honeycomb structure was developed for sandwich panels in aircraft construction for its low weight and high rigidity. However, since these panels were less suitable for insulation, the Gartner company developed a process to fill the air spaces of the honeycombs with synthetic resin foam. For the sandwich construction, Gartner built its own heating press to hot-bond the inner and outer shells with the synthetic resin foam-filled Air-Comb honeycomb core to form a thermal insulation panel. The panels achieved an insulation value of 0.05 W/(mK). The stabilizing paper honeycomb core was originally impregnated with phenolic resin, which acted as a moisture and fire retardant. In addition, a concrete parapet was built to prevent fire flashover. The panel shells were edged on all sides in order to achieve the most airtight closure possible through bonding.

The horizontal sliding joints of the panels were sealed with a surrounding neoprene flap and were very wide in order to compensate for possible dilatation caused by the projecting concrete slabs. The horizontal joints were additionally backed with polystyrene boards to compensate for thermal bridges. The sandwich elements, which were only 60 mm thick, were fixed exclusively at the vertical joint using clamping strips enclosed in Neoprene, which were screwed to the flange of a vertically continuous steel U-profile. To compensate for the structural tolerances, a steel façade anchor patented by Gartner was encased in concrete into the edge beam, which also allowed adjustment in all three axes. The resulting gap, an air space of over 130 mm, was closed in the area of the window openings with aluminium profiles and neoprene seals. Rounded "railway windows" were integrated into the punched openings of the aluminium sheets at the corners.

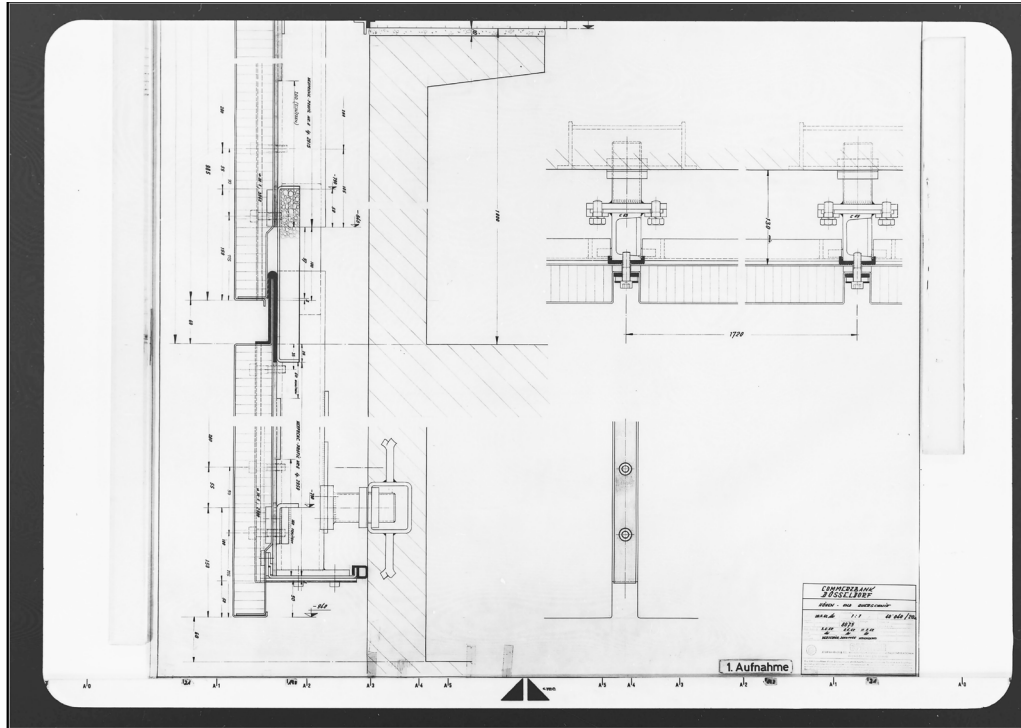


FIG. 4 Working drawings by Josef Gartner GmbH: Horizontal and vertical detail section of the Commerzbank Düsseldorf, 1962. Gartner archives, Gundelfingen (Donau). #40040/20a – 2

The reversible sashes of the windows consisted of single-pane glazing and were dry-glazed with roll-in neoprene profiles; conventional window putty was dispensed with. Plastic external venetian blind slats on the room side served as sun protection. Consistently following the curvature, insulated and round aluminium elements were also developed for the rounded corners of the building. The glazing of the elements was already carried out at the factory in Gundelfingen in Bavaria before being transported to Düsseldorf, where the elements were assembled ready for installation. The assembly work was carried out swiftly using relatively few workers (Schneider-Esleben, 1963).

3.2 RECENT UPGRADING OF THE FAÇADE

Due to its innovative and full-surface aluminium façade, as well as its solitary position in the urban fabric, the Commerzbank Tower was listed as a historical monument in 1998. After remaining vacant for many years, an American investor bought the building in 2015 with the intention of revitalizing it and converting it into a sustainable hotel. The goal and challenge of the revitalization was to preserve the historic appearance of the façade insofar as possible according to its protected status and to upgrade the main components of the structure according to current requirements. The architects who were commissioned for the renovation involved the Josef Gartner company very early on in the redesign process of the façade, and were able to draw on the planning documents from the company's own drawing archive and use them to develop an initial renovation idea (Romig & Rothkopf, 2022). Initially, only the upgrading of the existing façade was discussed. During the planning process, a completely new construction of the façade was also considered, but was rejected for economic reasons. Moreover, an identical reconstruction would hardly have been technically feasible (Romig, 2022).

An initial renovation concept by Gartner considered retaining the existing façade, while adding to it a contemporary layer with appropriate structural-physical properties. For this purpose, new façade elements were to be installed in the 130 mm wide space between the existing panels and the concrete parapet. The existing panels were to be integrated into this to preserve the outer shell. The existing panels were not to be dismantled and the honeycomb insulation would not be exposed. The windows were to be replaced with the same external geometry. For this purpose, parallel opening windows with insulating glazing were proposed. The ready-to-install elements were to be transported to Düsseldorf and installed on site. In order to be able to implement this renovation concept, the shell structure and the existing façade anchors would have to be able to bear the additional loads of the new façade elements, with a higher weight of glazing and an integrated new insulation layer. Before the new substructure was to be installed, the fixings were to be reworked for new structural protection so that they could be used further. The steel substructure was to be completely removed, and the new façade elements were to be hung directly on the façade anchors.

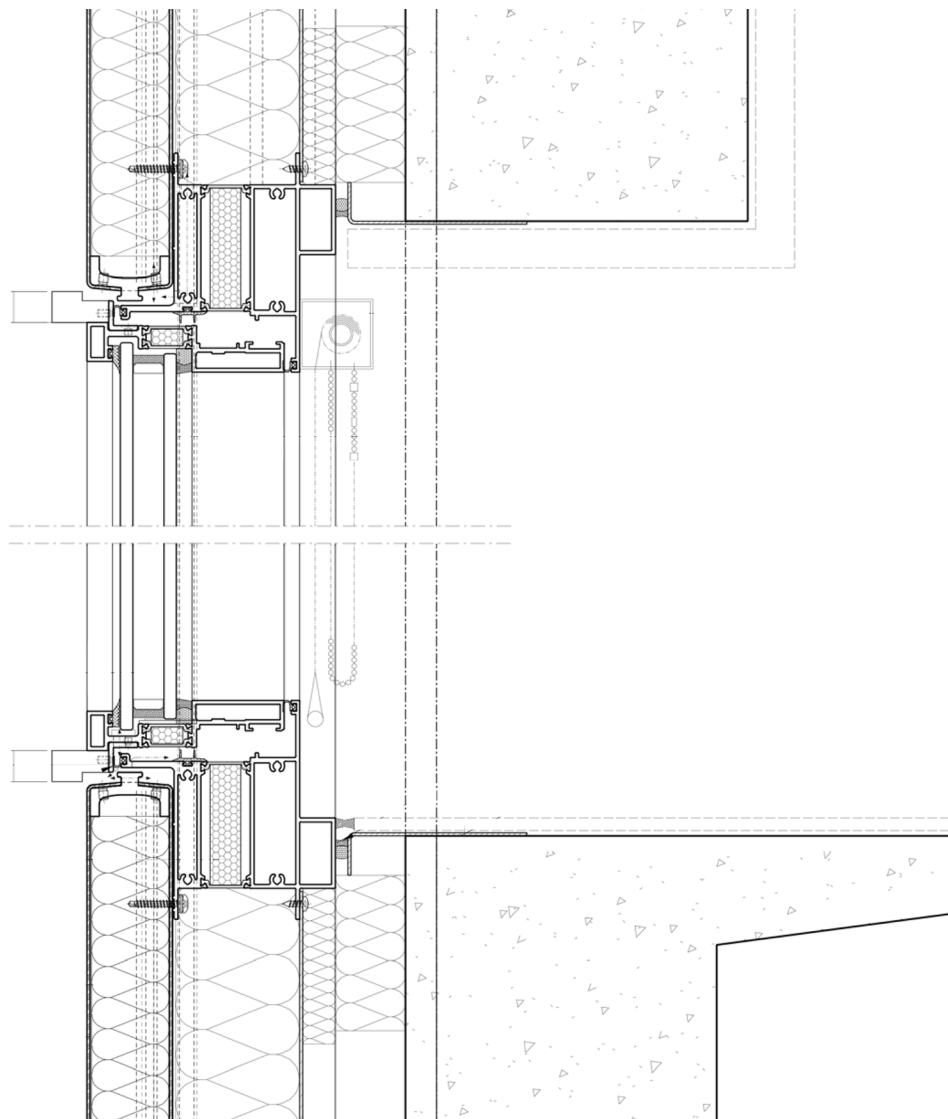


FIG. 5 The upgraded façade. Drawing by Josef Gartner GmbH: Vertical detail section of the Commerzbank Düsseldorf, 2022. Josef Gartner, Gundelfingen (Donau)

In the implementation of this concept, the existing panels would be brought to Gundelfingen, the existing window wings dismantled and disposed of. After inspecting the individual panels for damage, individual panels would be remanufactured. All aluminium surfaces were to be cleaned and resealed. Subsequently, the new façade elements were to be manufactured and the refurbished panels mounted in or on the new façade elements. Before the elements were delivered back to Düsseldorf, the new window sashes were to be mounted. Insulation of panels that could not be reused were to be disposed of (Gartner, 2016).

The renovation concept was not implemented as described because of major deviations in the fixing anchors on site, the position of which did not match the as-built plans, among other things. The new façade could simply not be mounted directly on the old fixing anchors. New façade fixings were required, which then also had to be modified because the concrete structure was dimensionally very inaccurate. Therefore, the façade elements including the steel substructure first had to be dismantled and transported to the main factory site in Gundelfingen. After dismantling and disposing of the existing window casements the elements were opened, disassembled, and inspected for damage. The paper honeycomb construction used for insulation was intact, even after more than 60 years, except for a few damaged panels; these were exposed and could be removed without leaving any residue, and then disposed of according to regulations. Non-combustible and dimensionally stable rock wool insulation panels were now used as new insulation. The aluminium sheets with the aged aluminium surface were resealed after abrasive cleaning. Even though the metal surface could not be compared to the natural and irregular grain of a material such as wood or stone, at the time of completion in 1962 there are nevertheless very slight colour nuances that can be attributed to the chemical surface treatment. After cleaning, however, the differently patinated and aged surface has a detrimental effect on the new façade appearance, which now appears slightly blotchy and less homogeneous in its new shine. After the fabrication of a new aluminium supporting framework, which is thermally broken, the repaired metal sheets could be put back in place. The shoring is attached to the back of the newly refurbished panels and thus almost completely fills the gap of more than 130 mm between the aluminium panel and the concrete parapet. Prior to this, sealing was carried out inside and outside and a parallel extension sash was installed in the element. After inserting the insulation and inlaying the rubber, the newly prepared elements were sealed. Afterwards, the elements were delivered to Düsseldorf. Before the new substructure was installed, the façade fixings had to be reworked. The elements are now fixed using newly placed stainless-steel anchors. The existing reversible sashes with single-pane glazing were replaced with parallel vent windows with double insulating glazing. This type of window is suitable for natural ventilation concepts; above all, mirror effects in the façade are avoided in comparison to tilt and turn windows. Gartner developed a special fitting here in the form of a xy-scissor, which enables manual operation with a continuously adjustable opening width of up to 200 mm. The old fittings of the reversible sash, which were also part of the façade elevation, were replaced with rubber dummies similar to those of historic appearance. By using the parallel opening windows, it was possible to preserve the very narrow view of the original optics. In total, the area of the new façade covers approx. 3100 m², the size of the elements remained unchanged, but they now weigh up to 280 kg. Since the new elements were hung in the same position, the exterior cubature remains unchanged (Romig & Rothkopf, 2022).

However, the conversion of the office tower into a hotel brought with it a number of constraints. Newly required ventilation ducts were laid in two shafts on the western front sides of the building, and the service core originally located there was removed and now provides a new room for housekeeping. A new second escape staircase in accordance with fire protection regulations is located on the south-west side, resulting in the breaking through of all ceilings. The integration of

the new, necessary staircase into the building also means a loss of over 130 sq.m of hotel space. The free-standing lift tower next to the building was also upgraded and continues to be used for access to the individual floors.

The formerly open ground floor now contains the hotel lobby with reception and dining area. It was enclosed with a 6 m high fully glazed façade with stiffening glass gravity beams. Following the rounded corners of the upper storeys, curved glass was installed in the corners of the ground floor glazing. The thick glass wall and glass fins are connected to each other via special toggle brackets. The frameless glass construction creates a quite homogeneous glass band, and the vertical joints are thus almost completely recessed. The refurbished exposed concrete supporting structure was selectively covered with acoustic panels in a few places; the character of the monumental supporting structure remains somehow intact and visible. The idea of a base that is as glazed as possible is understandable, but the new glass envelope set flush with the outer edge of the aluminium elements completely changes the original appearance and design intention of the elevated structure.



FIG. 6 The former Commerzbank high-rise after the recent upgrade and conversion, 21.11.2021. Photos: Rouven Grom

4 CONCLUSIONS

The 1960s façade of the Commerzbank in Düsseldorf was remarkable for its significant innovations in façade construction. The Josef Gartner company developed one of the first elemental façades of its kind in Germany. At the time, specially developed insulation was bonded between two aluminium sheets. A special feature is the façade skin, which was completely insulated at a very early stage and runs in one plane. The panel construction can hardly be compared with the frame constructions common at the time, referred to in a broader sense as “façade elements”. In the 1960s, stick systems or ladder systems were very common in Germany. In comparison, thermally broken profiles were only increasingly used from the 1970s onwards. Gartner is known for its high-quality façade constructions, and this façade also proved to be particularly durable. For the most part, the

old façade was still functional at the time of the renovation, but no longer complied with updated thermal insulation regulations. The preservation of the shell and the façade could be achieved with a minimally invasive intervention within the existing gap between raw structure and envelope, leading to little replacement and loss of original material substance. The façade was indeed refurbished according to heritage conservation aspects, and, according to a rough calculation, a value of more than 200 tons of carbon dioxide was saved by reusing the existing aluminium sheets.¹ This value is even higher when considered in terms of the transport and further processing of aluminium from the semi-finished product to the finished element. Carbon-dioxide of approximately 600 tons bound in the raw structure of the tower also contributes positively to the ecological balance.²

In order to be able to discuss the transferability of the executed façade renovation concept, we define the following conditions and criteria that should be fulfilled. First, the building's owner and involved planners must, in general terms, aim for the preservation of the existing building; in the case of the Commerzbank, this meant a voluntary, and probably also financial, additional effort for the investor, who was comfortable with the conservation of the façade. Another driving force was the existing monument protection of the property, which additionally obliges the owner to care for the edifice. Demolition is actually only permitted if the costs of renovation cannot be recovered, or if the property is in poor structural condition. Responsible protection agencies should ask for preservation of material and structural properties and not just aesthetics. A historical and constructive understanding on the part of all those involved in the planning and construction process is of absolute importance. In addition, historical investigation and a thorough building survey on site are necessary to clarify the façade system and the condition of the façade. It must be possible, as has been the case in Düsseldorf, to dismantle the façade. High quality building components in good condition and of sufficient material thickness are helpful. In Düsseldorf, the aluminium sheets, for example, showed corrosion-resistant properties and were of low weight, and thus offered great potential for further reuse. Inserting a new layer for isolation as substructure asks for sufficient space between raw structure and original skin, a feature which often can be found in curtain walled façades of that period. However, irregularities and tolerances of the concrete structure are common and have to be identified in advance. Last but not least, it should also be mentioned that the builder, in this case the façade company, must have a high degree of professional and technical know-how in order to be able to plan and implement this type of special solution at all. Even if these conditions cannot be met in all respects, the reuse of existing materials and components for future renovation tasks represents a promising and transferable approach.

Acknowledgements

Research on this paper was partly funded by the BBSR Innovationsprogramm ZukunftBau and a research fellowship by the Wüstenrot Stiftung.

We would like to thank the Josef Gartner GmbH for its comprehensive support.

1 A standard aluminum sheet wall element of the Commerzbank has an area of approx. 7 m². The density of aluminum is 2,700 kg/m³. A 2 mm thick aluminum sheet weighs approx. 5.4 kg/m². The production of 1 kg of aluminum generates approx. 8-10 kg of CO₂.

2 The structure of the building has a volume of approx. 1,800 m³. The production of 1m³ of reinforced concrete emits approx. 320 - 340 kg of CO₂.

Reference list

- Aluminium-Zentrale e.V. (1959). *Aluminium-Fassaden*. Bericht der Aluminium-Zentrale e.V. Band 5 [Aluminium-Façades. Review of the Aluminium-Zentrale e.V. Volume 5]. Düsseldorf, MA: Aluminium-Zentrale e.V..
- Ayon, A., Pottgiesser, U., Richards, N. (2019). *Neue Fassaden im Bestand. Sanierungsstrategien für Klassiker der Moderne* [New facades in existing building stock. Renovation strategies of modern classics], Birkhäuser Verlag GmbH.
- Fürst, T. M. (1998). *Das Thyssen-Haus in Düsseldorf: Die Modernisierung eines Nachkriegsmonuments* [The Thyssen-House in Düsseldorf: The Modernization of a post-war monument]. Conservation of Modern Architecture? ICOMOS Journals of the German National Committee XXIV, 77–89.
- Gartner, Dr. F. (2021). Interview 27.05.2021.
- Gockell, B. (1964). *Über die Verwendung von vorgehängten Fassaden (Curtain Walls) in gestalterischer, konstruktiver und technischer Hinsicht* [About the usage of curtain walls in terms of design, construction and technology]. (Doctoral Dissertation).
- Grom, R. (2021). *Findbuch Josef Gartner (1955–1985)*. [Inventory Josef Gartner (1955-1985)] Unpublished study, funded by Wüstenrot Stiftung.
- Hoffmann, K., Griese, H., & Meyer-Bohe, W. (1975). *Fassaden. Die Bauelemente V [Façades. The Building Components V]*. Stuttgart, MA: Julius Hoffmann.
- de Jonge, W. (2017) Sustainable renewal of the everyday Modern, *Journal of Architectural Conservation*, 23:1-2, 62-105, DOI: 10.1080/13556207.2017.1326555
- Josef Gartner GmbH. (2016). *Sanierung Fassade Commerzbank Düsseldorf [Renovating façade Commerzbank Düsseldorf]*. Unpublished internal study.
- Kuipers, M. (2017). *Van Nellefabriek Rotterdam: World Heritage of a World Port*. MA: nai010 publishers.
- Lepik, A., & Heß, R. (2015). *Paul Schneider Esleben. Architekt [Paul Schneider Esleben. Architect]*. Hatje Cantz.
- Meurs, P., & van Thoor, M. (2010). *Sanatorium Zonnestraal. History and Restoration of a Modern Monument*. NAI Publishers.
- Roming, M. (2022). Discussion and E-Mail 07.03.2022.
- Roming, M., & Rothkopf, C. (2022). *Revitalisierung Commerzbank Düsseldorf. Sanierung einer denkmalgeschützten Hochhausfassade* [Revitalization of Commerzbank Düsseldorf. Refurbishment of a listed high-rise façade]. FASSADE / FAÇADE: Fachzeitschrift für Fenster- und Fassadenbau / Revue technique pour fenestres et façades, 02, 45-50.
- Rung, H., & Putz, A. (2021). *Potentialanalyse des Bauvolumens von Bürohochhäusern (1950 – 80)* [Potential analysis of the construction volume of high-rise office buildings (1950 - 80)]. Unpublished study. Funded by Stiftung Bayerisches Baugewerbe.
- Schaal, R. (1961). *Vorhangwände. Curtain Walls. Typen Konstruktionsarten Gestaltung [Curtain Walls. Design Manual]*. Georg D. W. Callwey.
- Schneider-Esleben, P. (1963). *Verwaltungshochhaus der Commerzbank, Düsseldorf = Bâtiment administratif de la Commerzbank à Düsseldorf = Administrative building of the Commerzbank, Düsseldorf*. Bauen + Wohnen = Construction + habitation = Building + home : internationale Zeitschrift, 17(8), 344-347. doi:10.5169/seals-331661
- Sulzer, P. (1991). *Jean Prouvé : Meister der Metallumformung ; das neue Blech* [Jean Prouvé : Master of metalforming ; the new sheet metal]. Rudolf Müller GmbH.

Timber-based Façades with Different Connections and Claddings: Assessing Materials' Reusability, Water Use and Global Warming Potential

Miren Juaristi¹, Ilaria Sebastiani¹, Stefano Avesani¹

* Corresponding author, Miren.JuaristiGutierrez@eurac.edu

¹ Institute for Renewable Energy, European Academy of Bolzano, Italy

Abstract

Timber-based façade technologies have the potential to effectively reduce the carbon footprint, reduce water use in construction, and minimize waste, when their manufacturing process is highly prefabricated. Additionally, avoiding glue parts can enhance the sustainability of the façade as its elements can be replaced (extending the durability of façades and therefore buildings) and separated once that they reach their end of life (to re-use or recycle them). Thus, the connection between materials might have a considerable impact on the façade's sustainability. Moreover, timber-based façades can have different claddings, impacting on the water needed for the technology and their Global Warming Potential (GWP). This paper assesses, through a novel methodological approach, materials' reusability, water use, and GWP for different façade connections and claddings. Four prototypes with different connections (staples, screws, timber nails, and geometrical assembly) were built. Experimental activities representing façade elements' substitution and disassembly provided qualitative and quantitative information about production, extraordinary maintenance, and end-of-life phases. Through these tests, the quantity of material that could be re-used and disposed in such phases was quantified and then inserted in a Life Cycle Analysis (LCA). LCA was conducted using EF v.3.0 impact method and components were modelled with EPD information and Ecoinvent cut-off 3.7 database. According to the results, a timber-based façade with timber nails and wood cladding is the most promising of reusable façade materials, decreasing the water use and GWP.

Keywords

Wood construction, extraordinary maintenance, disassembly, End of Life, Climate Change Potential

DOI

<https://doi.org/10.47982/jfde.2022.powerskin.5>

1 INTRODUCTION

According to the Circularity Gap Report of 2022, to keep the planet on a 1.5-degree trajectory, Greenhouse Gas Emissions (GHG) should be reduced by 39% from 2019 levels (Circle Economy, 2022). To reach such an ambitious target is of paramount importance to shrink global material use and extraction by 28%. As highlighted in that report, buildings and construction industry are one of the most impacting sectors in this regard, and thus interventions related to them are critical in reaching the aforementioned reductions. The Circularity Gap Report detected highly impacting interventions involving façade technologies: (i) treating construction materials in a circular way (reusing, recycling, or reducing the quantity), (ii) having resource efficient construction, and (iii) increasing durability of the façade technologies and thus of buildings.

With this evidence, when developing or comparing façade systems, special attention should be paid to (a) the emissions related to the selected technologies during their whole life cycle and water use, a precious resource, (b) the durability of façade elements, and (c) the possibility of reusing the façade materials once they reach their end-of-life. While a well-known method to quantify the emissions and water use exists, i.e. environmental Life Cycle Analysis (Hildebrand, 2014; Pittau et al., 2019), there are few works giving methods to measure the potential re-use of materials (Gubert et al., 2021; Heesbeen et al., 2021) and their application is not widespread. Moreover, end-of-life modelling might heavily impact the overall LCA results, and thus needs to be carefully investigated. LCA methods have already been used to compare a single-use façade against a reusable one (Cruz Rios et al., 2019). Yet, understanding which elements of the façade systems are reusable in a second life is still a difficult task and increases the uncertainty of modelled end-of-life scenarios. To overcome the lack of experience in façade reusability, Cruz Rios et al. (2019) proposed to evaluate the impact of the reusability rate thanks to hybrid LCA approach based on sensitivity analysis.

Façade systems should be designed not only for assembly, but also for their effective disassembly to (i) decrease the disposal of façade materials when their reach their end-of-life and (ii) to lengthen the lifespan of the façade system by substituting and upgrading their elements during their service life. However, the literature on design for assembly and disassembly is scarce. Denis and Dogan (2014) proposed a pioneer methodology to design façade systems with increased deconstruction capacity. According to this work, the connection types of façade systems influence assembly and disassembly sequences, and they suggest simple mechanical and dry jointing connections to allow disassembly without the destruction of adjacent parts. Another research work proposed an end-of-life tool for building product development, structured following the 4Rs of the Circular Economy Concept: Reduce/Reuse/Recycle/Recover (Gubert et al., 2021). This tool establishes a set of indicators to map the impacts of the evaluated building technology. From the technology point of view, Gubert et al. proposed connection systems, lifespan of the components and separability of the elements as the main parameters defining the suitability for the 4Rs .

The sparse literature on design methods boosting detachable façade systems and the lack of practical experience to evaluate replacement, disassembly, and reuse potential, makes it difficult to frame which connection systems and façade features are the optimal ones for the effective separation of the façade elements and future materials reuse. To face this gap of knowledge, the aim of this work was twofold: (i) developing experimental tests and LCA approach to assess façade technologies options' reusability and sustainability; (ii) evaluating the environmental performance of timber-based prefabricated façade systems with different connections among layers thanks to the new approach.

To the state of the art, these kind of assessment methods including prototyping and experimental tests are still uncommon but necessary to understand the disassembly and reusability potential of façade systems, to update façade elements through materials' substitution (increasing the overall façade service life), and to gain knowledge on the possible end-of-life scenarios for the façade elements, thus having more reliable data for the LCA modelling of this phase.

2 METHODOLOGY

This work assesses materials' reusability, water use, and GWP based on two methodological pillars: (i) prototyping and experimental testing of assembly and disassembly activities of different timber-based prefabricated façade options and (ii) LCA assessment of environmental impacts, using the information gathered in the experimental tests for the end-of-life modelling. The assessment compared timber-based prefabricated façade technologies with variations in the two key-features: the connections among façade layers and façade claddings.

The research activity was structured as follows:

- 1 Prototyping:
 - a Identification of possible connections among the façade layers of a timber-based prefabricated façade system and design of the functional prototypes.
 - b Monitoring the duration of the manufacturing process for each façade prototypes with different connections among layers.
- 2 Testing maintenance (removing and replacing) and end-of-life disassembly phases:
 - a Installation of the prototypes in the experimental test facility
 - b Monitoring the duration of the on-site partial disassembly, removal and substitution of materials. Visual control to identify damaged and non-reusable materials and quantification (% of the total area).
 - c Monitoring the duration of the off-site disassembly. Visual control to identify damaged and non-reusable materials and quantification (% of the total area).
- 3 Life Cycle Analysis
 - a Quantification of GWP and water use for the variations of timber-based prefabricated façades with different connections and cladding materials. LCA without and with a window.
 - b Illustrating the benefits of reusing façade materials: merging the impact of their second life with the first life-cycle.

2.1 PROTOTYPING

According to the literature exposed in section 1, different ways of assembling the façade layers impact on the elements' substitution and separation activities. To quantify the impacts of ways of assembling with experimental data, this research compared a state-of-the-art multi-layered timber based prefabricated façade technology (Fig.1) with façade systems with alternative connections. The proposition of the alternative connection system came out from the iterative discussions among the researchers and a timber-based façade manufacturer.

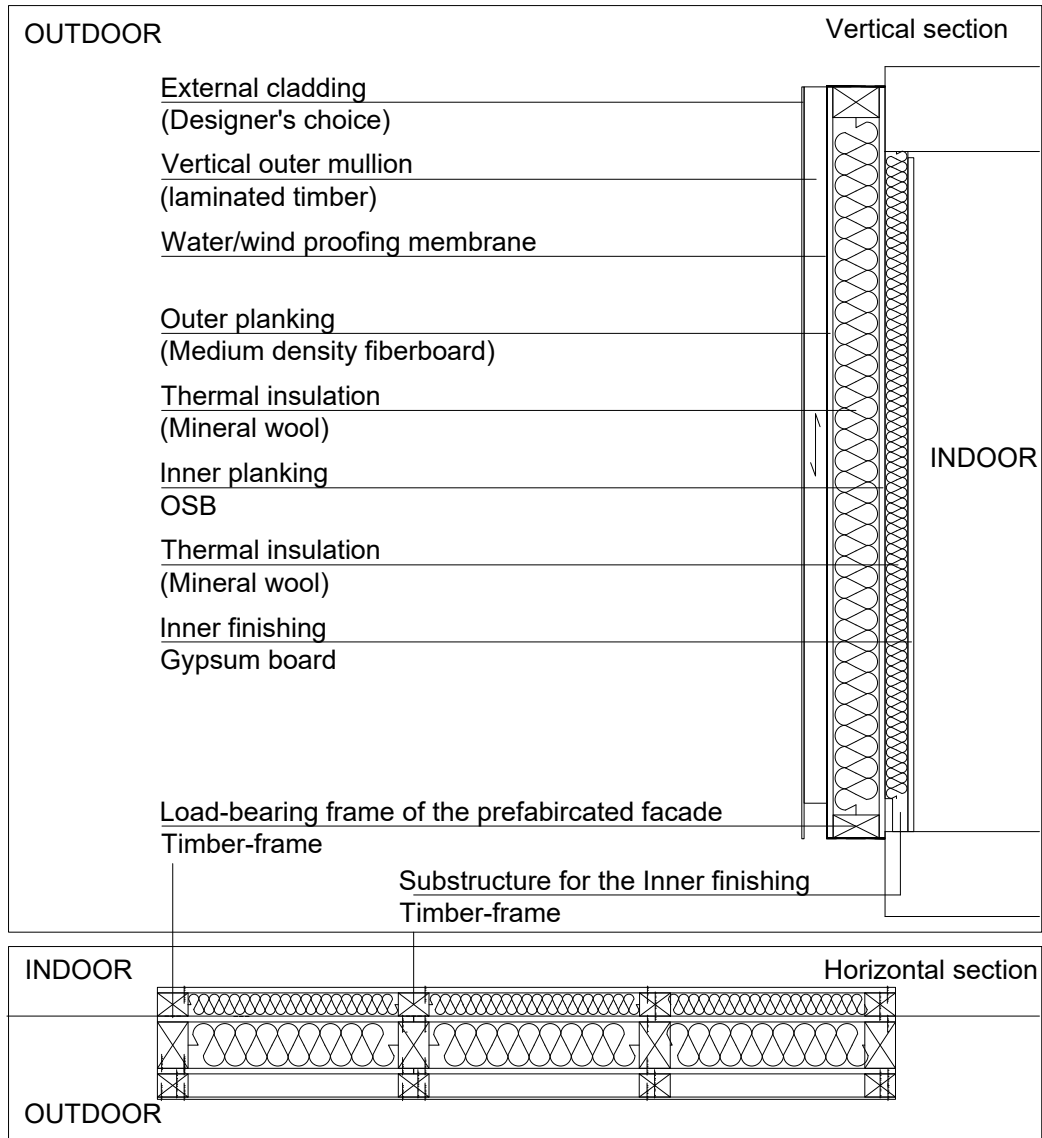


FIG. 1 Prefabricated timber-based multi-layer façade

2.2 TESTING

Four prefabricated timber-based façade prototypes were designed and manufactured as specimen for being tested through a dedicated experimental campaign. The duration of each activity related to the prototypes' manufacturing was monitored to quantitatively compare the differences between the façade connections. The specimens were then installed onto a metallic structure which emulates the slabs of a building, in order to carry out a partial on-site disassembly and insulation materials' substitution (Fig. 2).



FIG. 2 *Experimental activity to test the replacement of a façade layer. Image by Fiorentino.*

On-site partial disassembly and substitution of materials aimed at emulating a possible extraordinary maintenance activity. Even if nowadays the removal or substitution of the insulation layer is an uncommon maintenance activity, it might be a realistic operation in the future to optimize the façade performance to adapt to changes in boundary conditions or indoor requirements. For instance, it could happen that the original insulation levels are no longer the optimal ones because of climate change and/or due to a change in the building use. Eventual technology developments could also bring novel insulation systems and replacing the existing static insulation layer could be a good strategy to reduce the energy demand of the buildings (Juaristi et al., 2022). If the other façade materials are still in good condition, as a result of extraordinary maintenance activity they could be kept until they reach their end-of-life. Thus, this experimental test enabled the understanding of the separability of the different façade layers with different connectors when the façade is installed on the building. It also enabled the identification of the materials that could be re-installed once the insulation panel was replaced.

Afterwards, end-of-life activities were emulated to test the ease of separation of materials and their potential future reuse. For this activity it was assumed that it would not be done on site, but in a dedicated facility. Therefore, the four prototypes were dismantled from the metallic structure (Fig. 3) and the prefabricated façade elements were transported to a shed. There, the four prototypes were completely disassembled by workers, who were asked to separate the majority of the undamaged material in a reasonable amount of time (Fig. 4). The duration of this activity was monitored. Once the façades were disassembled, it was possible to visually check the materials that were damaged and to quantify the % of the area which was damaged by measuring the amount. Thanks to this qualitative and quantitative evaluation, potential reuse of material and the eventual reasons that could lead to a downgrading were established.



FIG. 3 Prefabricated façade elements were disassembled and transported to a shed to separate materials, to realistically emulate an end-of-life scenario.



FIG. 4 PEmulating disassembly activities in the end-of-life phase.

2.3 LIFE CYCLE ANALYSIS: BOUNDARY CONDITIONS & ASSUMPTIONS

To understand if the effective separation of the façade elements and reuse of future materials has a significant impact in the GWP and water use, a LCA must be done. Thus, OpenLCA software was used to quantify the aforementioned impact categories. EF v.3.0 adapted method was implemented along a cradle-to-grave/cradle life cycle and the four façade systems were modelled by using the EPDs of the façade elements, as provided by the supplier to the timber façade manufacturer. When EPDs were not available, Ecoinvent cut-off v.3.7 database was used. The information in this database was also used to model the "standard" processes related to the façade (e.g. transport, disposal activities...). The durability of each façade element was considered thanks to the EPD information and German information portal for sustainable buildings (*Nutzungsdauern von Bauteilen Für Lebenszyklusanalysen Nach Bewertungssystem Nachhaltiges Bauen (BNB)*, n.d.) [Lifespan of building components for Life Cycle Analyses according to the Sustainable Building Assessment System].

Table A, available in the Appendix, summarizes the characteristics of the multi-layered timber-based façade systems and the information used for LCA modelling, and highlights the parameters that were changed for each façade system. When analysing the differences between the connectors, no cladding system was modelled at all. This is because analysed prefabricated façade technologies offer high flexibility in terms of the cladding system. To assess the impact that the selection of the cladding would have, three representative façade claddings were modelled for a timber-based prefabricated panel with state-of-the-art connectors: two options for the ventilated façades, HPL claddings and wood claddings, and plaster claddings with no airgap.

The variations of the timber-based prefabricated façades were modelled for a functional unit of 15 m² and a U value of 0.15 W/m²K. The system boundary considered the following life cycle phases: Production, Construction, Maintenance, and End-of-Life. These phases were modelled according to the following assumptions:

- A **Production:** Façade manufacturing site is in Brixen (Italy). All the façade materials are purchased ready to be integrated in the façade systems. The origin of the materials was established based on the current suppliers of the timber-based façade manufacturer. This information was also used to model the transport accordingly (from the selling point to Brixen). EURO 3 transport of different dimensions were modelled according to the material's weight and dimension and the distance never exceed the 500km. On the other hand, the information from providers' EPDs enabled the modelling of the transformation processes from raw materials to façade elements. Specific manufacturing processes to transform façade elements into a timber-based prefabricated façade include cutting these elements to fit the size of the prefabricated module and to connect the different layers. In this phase, some mineral wool and plastic-based waste is generated (from insulation, joint-sealing tapes, water-tightness membrane, and packaging). The energy needed for this transformation included the electricity of the turning table and hand machines. 30% of this electricity comes from the photovoltaic panels installed in the factory, while the remaining 70% comes from a medium voltage electricity grid.
- B **Construction:** a hypothetical construction site is located 300km from the factory. Thus, a >32tonnes EURO 3 lorry transport was modelled. In the installation process, the electricity consumed by the crane placing the prefabricated façade and the diesel for the lifting platform was considered, based on the calculations made by the timber-based façade manufacturing company. This phase also included the waste related to the packaging.
- C **Maintenance:** according to the EPD, only wood claddings need maintenance activities. Two different analyses were carried out for two possible maintenance scenarios:

- Coating treatment of the wood cladding 7 times during its lifespan. For this activity, the diesel for the lifting platform was considered.
 - Deinstallation of the wood cladding at the middle of its lifespan, substituting it with a new wood cladding and incinerating the old one. For this activity, the diesel for the lifting platform was considered. The transport was modelled considering a 16-32 tonnes EURO 4 lorry, both for the new cladding and old cladding transportation.
- D **End-of-Life:** in this phase, it was hypothesized that prefabricated façade panels would be dismantled as a single element to be transported to the manufacturing factory in which disassembly and waste separation are expected to happen. Therefore, this phase includes a >32tonnes EURO 3 lorry transport, the electricity consumed by the crane removing the prefabricated façade, and the diesel for the lifting platform. To determine the way in which separated damaged material needs to be modelled, EPD information regarding disposal and recycling processes was considered. Not all of the materials are disposed or recycled; end-of-life phase was modelled considering the disposal and recycling of the materials that were identified as non-reusable in the experimental tests. Initial LCA results referred only to the first life cycle of the façade systems and their materials. Re-usable materials were expected to have a second life and therefore, the impacts of using re-used materials instead of virgin materials would be accounted for when modelling their second life cycle. However, this way of illustrating the results did not highlight clearly enough the potential reduction of GWP and water use when the re-use of façade components is boosted. Therefore, the benefits of reusing façade materials were illustrated by merging the impact of their second life into the first life cycle. To do so, the positive impacts of integrating re-used materials in future façade systems were directly subtracted from the total impacts of the first life cycle.

3 RESULTS

3.1 POSSIBLE CONNECTIONS AMONG LAYERS

Currently, staples are used as connectors among layers. However, they do not allow such an effective disassembly of the different façade layers with the minimum harm, which is an essential characteristic of reused materials in their second life. For this reason, three timber-based façade systems with different layers' connections were proposed and compared with a state-of-the-art timber-based multi-layered façade. Proposed alternative connectors were (i) screws, expected to increase the duration of assembly and disassembly phases but causing less harm to materials when separating the façade elements; (ii) timber nails, expected to be similar to staples in terms of assembly and disassembly, but would have a lesser impact when disposing of them, and (iii) geometrical assembly (with milled mullions and no connectors at all), which is a more complex fabrication but the materials are not harmed when disassembling them.

3.2 PROTOTYPING AND EXPERIMENTAL TESTS: DURATION OF EACH PHASE AND ASSESSMENT OF REPLACEMENT, DISASSEMBLY, AND REUSABILITY POTENTIAL

The fabrication of the prototypes and experimental tests enabled the production times to be monitored as well as the validation of the hypothesis with which they were proposed. This production

was mainly based on handcraft. Therefore, the results shown in Table 1 could be slightly different if specific automatized machinery was used for each process, adapted to each connection types.

TABLE 1 Duration differences for fabrication, extraordinary maintenance and disassembly activities (the percentages represent the difference of that façade option respect the fastest solution in each phase)



Connections	Stapples (1_SA)	Screws (2_S)	Timber Nails (3_TN)	Geometrical assembly (4_NC)
Production time	Best opt	+ 36%	+ 7%	+ 67%
Maintenance (Removing)	+ 500%	+ 125%	+ 50%	Best opt
Maintenance (re-installing)	+ 22%*	+ 111%	+ 44%**	Best opt
End-of-Life Disassembly	+ 98%	+ 35%	Best opt	+ 6%

* The same outer planking panel could not be re-placed in the façade again. A new board and staples were needed for the extraordinary maintenance activity

** New timber nails were needed in the extraordinary maintenance activity

The results demonstrate that state-of-the-art connections, the staples, are the fastest options to manufacture. However, as expected, they also are the slowest options when the components of this façade system need to be removed in an extraordinary maintenance activity (Fig. 2) or separated when they reach their end-of-life (Fig. 5 a). Fig. 2b highlights how the outer enclosure panel cannot be replaced if removed in an extraordinary activity because the holes of the staples are too many and too big. If staples are substituted with screws the disassembly time is shortened, and the same holes might be used for re-fixing the layers. Yet, the extraordinary maintenance (removing the insulation layer and re-installing disassembled elements) remains time-consuming. Timber nails showed overall better results, their production time being almost comparable to the staples; they are easily separable when reaching their end-of-life and need a reasonable time in an eventual extraordinary maintenance activity. The best option to ensure a fast and effective extraordinary maintenance was, as expected, the façade with geometrical assembly. However, it was also the most time-consuming in terms of its fabrication and the façade with timber nails had similar disassembly times.

Visual check of the façade components after the substitution and disassembly activities was essential to understand the reusability potential of the different types of connections of the four façades. Fig. 5 illustrates how, when disassembling the façade with the staples, part of the material was lost, such as the internal finishing plasterboard and the borders of the OSB and medium-density wood fibre boards (which were cut for a faster disassembly process). Moreover, part of the plaster remained attached to the wood mullions. On the contrary, when disassembling the façade with no connectors at all, the panels remained complete and free of damage. Only part of the waterproof membrane remained attached to the mullions. Regarding the façade elements with screws and timber nails, they were separated without harming them, except from the holes of the connections (Fig. 6).



FIG. 5 Façade layers after the disassembly activity, for a prefabricated multi-layer timber-based façade joint with (a) 1_SA staples and (b) NC geometrical assembly. Images by Fiorentino.

The outcomes of disassembly activities were a useful input for the Life Cycle Assessment of different timber-based prefabricated façade options, as it enabled the detection of the material quantity that could be reused or recycled in the end-of-life phase. The measurement of the waste from disassembly process stated that for the façade with staple connectors, 75% of the area of the medium-density wood fibre boards and OSB panels could be reused, whereas for the other three connector types 100% would be reusable if the holes were not a problem in their future applications.



FIG. 6 OSB panels and wood mullions after the disassembly activity. The tests were carried out for four different connections between façade layers (a) staples and nails, (b) screws, (c) timber nails, and (d) interlockings. Images by the author.

3.3 LIFE CYCLE ASSESSMENTS FOR DIFFERENT OPTIONS OF PRE-FABRICATED TIMBER-BASED FAÇADES AND END-OF-LIFE SCENARIOS

Life Cycle Assessment results show the GWP differences of the analysed variations of timber-based prefabricated façades (for different connections and cladding materials). As illustrated in Fig. 7, the production phase is the one with the highest impact in the equivalent kg of CO₂ emissions. Surprisingly, when looking at total GWP results (Fig. 7a), the timber-based prefabricated façade with a plaster cladding (4_SA_P) is the one with the lesser impact during production, even less than the evaluated façade technologies with no cladding at all (1_SA, 2_S and 3_TN). This is because 4_SA_P does not have a medium-density wood fibre board panel as a front enclosure, because it is not commonly used when plaster finishing is adopted. Instead, the insulation layer is closed with wood fibre insulating boards, to which the outer plaster is applied. Thus, this result highlights the significant impact that medium-density wood fibre boards have in the GWP of the studied façades. Regarding the total GWP of the evaluated cladding materials, HPL panels are the most impactful ones. However, it should be noted that, according to the information given by the fabricators in the EPDs and the German information portal for sustainable buildings (*Nutzungsdauern von Bauteilen Für Lebenszyklusanalysen Nach Bewertungssystem Nachhaltiges Bauen (BNB)*, n.d.) [Lifespan of building components for Life Cycle Analyses according to the Sustainable Building Assessment System], the three façade claddings are not expected to have the same lifespan and maintenance requirements. A timber-based prefabricated façade with a plaster cladding (4_SA_P) is expected to last for a maximum of 40 years and coatings are the only expected maintenance activity in that timeframe. HPL can last 50 years, the same duration that is expected for the timber-based prefabricated façade systems. Wood façade claddings can also last up to 50 years if they are regularly painted (6_SA_Wp) or if just the cladding is replaced once during the façade system's lifetime (7_SA_Wr). Taking these lifespans, the GWP results were normalized per year. Likewise, a timber-based prefabricated façade with a plaster cladding (4_SA_P) is no longer the façade option with the smallest equivalent emissions of CO₂, but that with the timber claddings (Fig. 7b).

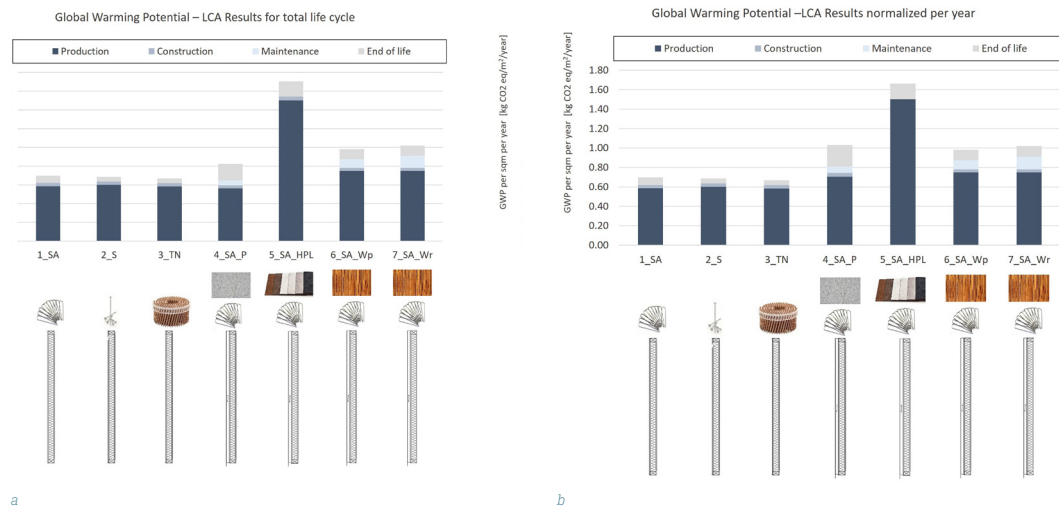


FIG. 7 Global Warming Potential (GWP) per square meter for total life cycle of different prefabricated multilayer opaque façade systems with different connection and cladding materials. 1_SA, 2_S, 3_TN scenarios have no finishing. (a) Total life Cycle Analysis results and (b) Total life Cycle Analysis results normalized per year for 40 years of lifespan (for 4_SA_P) and 50 years (for all other cases).

Life Cycle Assessment were also done for a calculation unit including a window of 1.2m² in the calculation unit of 15m², and an installation layer (made of insulating material and internal wooden mullions), to better understand the impact of each façade component in the GWP. Furthermore, the obtained results were compared to those in the existing literature (Hildebrand, 2014). The impacts of three opaque façade typologies with a window were used from this research work and re-calculated by increasing their insulation layer to reach the same U-value considered for the timber-based prefabricated façades. The insulation material was estimated to be the same as proposed by Hildebrand in her work and only its thickness was modified to reach a U-value of 0.15W/m²K. To quantify the GWP of the additional insulation, the GWP calculated by Hildebrand for those specific materials was considered.

The results of Fig. 7 report the total GWP, that is not normalized to the expected lifespan. According to these results, the timber-based panel with HPL claddings would have a higher GWP than lightweight concrete façades with a with an External Thermal Insulation Composite System (ETICS) made of extruded polystyrene (XPS). On the other hand, timber-based prefabricated façade systems have lower GWP than a façade made of bricks and EIFS insulated with mineral wool. Its GWP is also lower than for ventilated façades with a concrete core, mineral wool, and aluminium substructure.

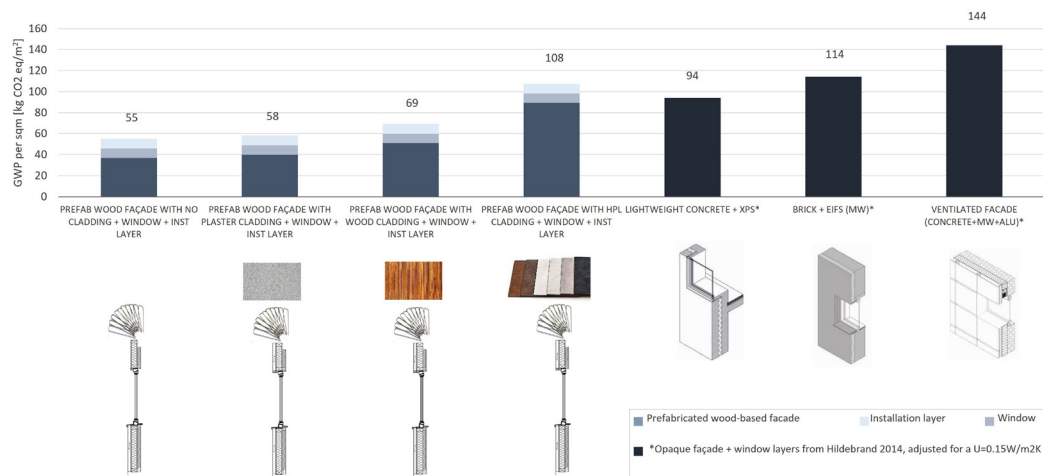


FIG. 8 Global Warming Potential (GWP) per square metre for total life cycle of different multi-layer opaque façade layers (U=0.15W/m²K) which include a window. Total Life Cycle Analysis results for Production, Maintenance, and End of Life Phases.

Fig. 7 and Fig. 8 give interesting insights about the GWP of different variations of the timber-based prefabricated façades, but explaining how the reusability of its components could have a significant impact on the GWP and water use is not straightforward. With this aim, further Life Cycle Assessment calculations were done by considering in the analysed life cycle the benefits of reusing the façade components in a second life. The savings from not manufacturing these elements again are illustrated in Fig. 9, which shows the overall GWP and water use for all scenarios and their potential reduction according to the aforementioned method. According to the results of these graphs—which are not normalized to the annual impacts—if HPL cladding panels are reused once they reach their end of life, their GWP use is lower than for wood cladding. However, to do so, business models compatible with reusability should be applied and it is not clear how the HPL could be reused, as, theoretically, they would have reached their lifespan as façade cladding materials. Regarding the results for different façade layer connections, screws (2_S) and timber nails (3_TN) would enable a more significant reduction of the studied environmental parameters compared to the state-of-the-art connections (1_SA).

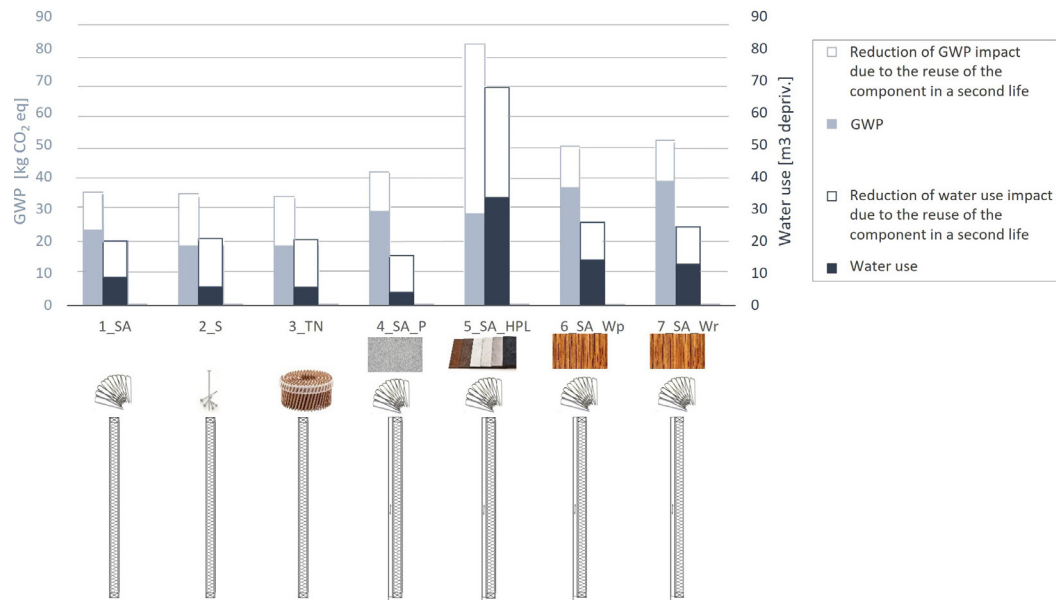


FIG. 9 Global Warming Potential (GWP) and water use per square metre and its possible reduction if the components are reused in a second material life. Global results for total life cycle of different prefabricated multi-layer opaque façade systems with different connection and cladding materials.

4 LIMITATIONS AND FUTURE WORKS

One of the biggest limitations of the present work was that façade materials were still new (not aged) when doing experiments for replicate extraordinary maintenance and end-of-life disassembly activities. Future works should find a method to age components of the façade elements before disassembling it, to perform disassembly activities under more realistic conditions. The results of these experiments suggest that timber nail connections might facilitate the disassembly of prefabricated timber-based façades without compromising their fabrication time nor the analysed environmental aspects. However, more detailed static evaluations are needed to guarantee that these connections are also suitable to meet the structural requirements. Similarly, the façade system with geometrical assemblies should be evaluated to test whether it provides enough structural safety against horizontal impact and suction effects in the ventilated chamber.

According to the LCA results, medium-density wood fibre board panels have a significant impact on the GWP. The maintenance of wood cladding with the evaluated coatings also have a substantial impact. Future works should investigate more environmentally friendly coatings for the maintenance of wood claddings. They should also identify cost-effective alternative materials for the front-enclosure of prefabricated timber frames, with the ability to give enough structural stability. Moreover, the emissions related to the transport of prefabricated elements can be reduced if the overall weight of the prefabricated façade element is reduced by optimizing the timber frame substructure and material quantity. Life Cycle Analysis quantified the possible reduction of the GWP and water use if the materials were reused instead of disposed of when they reach the end of their life. However, to reuse these components, the capacity to easily disassemble it is not the only target that must be pursued; the reusability of façade components will be only possible if the market is interested in it. Thus, future works should also focus on the possible business models aligned with the circular economy to sell the materials coming from dismantlable timber-based façade systems.

5 CONCLUSIONS

The contribution of the presented work to the research field was a novel methodology to consider crucial aspects of sustainability in the façade system, namely potential façade disassembly for a future re-use of materials and how it impacts on the Global Warming Potential and water use of the façade system. These aspects were evaluated and quantified thanks to the real-scale prototyping activities (production, maintenance-removing and -replacing, and end-of-life disassembly phases) and LCA calculations. The results showed that current state-of-the-art connections (staples) enable a faster fabrication than studied alternative solutions (screws, timber nails, and geometrical assemblies, with milled mullions and no connectors between layers). The fabrication time of timber-based prefabricated façades with timber nail connections was only slightly longer than with staples. Surprisingly, façade systems with timber nail connections were the fastest ones when disassembling them in the end-of-life activity. Disassembled panels, though, remained with the holes where the nails had previously been placed, which could be a problem for some potential reusability, whereas the façade systems with geometrical assembly didn't have this problem. This last system had the best duration considering the extraordinary maintenance activities, but its overall suitability seems limited as its fabrication is more complex and longer in comparison to the other analysed façade systems. Besides, the reusability of the milled mullions could be limited due to its particular geometry.

Overall, according to the results of the present work, timber-based prefabricated façade systems have a lower Global Warming Potential (GWP) than other opaque façade typologies (taken as reference from other scientific studies) regardless the type of connections between layers. However, the selection of the cladding has a big impact on the GWP and water use. Timber-based prefabricated façade systems with HPL cladding have a much higher impact than those with wood claddings or plaster claddings, this last one being the one with the lowest equivalent CO₂ emissions. Timber-based façade with HPL cladding also has a higher GWP than a comparable lightweight concrete façade with an External Thermal Insulation Composite System (ETICS). On the other hand, HPL cladding requires less maintenance than wood and plaster claddings and have a longer lifespan. Indeed, the lifespan of the façade system has a great impact on GWP results. This is why the normalized results, according to the lifespan declared by the fabricators, show how plaster claddings are the less suitable option compared to the wood claddings, in terms of reducing the CO₂ emissions, because of their longer durability if expected maintenance activities are followed. This work also quantified the potential CO₂ emissions and water use reductions if the façade components were re-used in a second life. In such a scenario, timber nail connections and HPL claddings show a great opportunity to reduce environmental impacts if reused, and in this scenario, they would become the timber-based prefabricated façade system with the least equivalent CO₂ emissions.

Acknowledgments

This paper represents the results of the research project entitled "Development of a Technology and Market Radar for industrialized Wood-Based Façade Systems", funded by Fondazione Cassa di Risparmio di Bolzano and Rubner Holzbau Srl. Special thanks to Florian Borho for the support in the data collection.

References

- Circle Economy. (2022). *The Circularity Gap Report 2022*. <https://www.circularity-gap.world/2022#Download-the-report>
- Cruz Rios, F., Grau, D., & Chong, W. K. (2019). Reusing exterior wall framing systems: A cradle-to-cradle comparative life cycle assessment. *Waste Management, 94*, 120–135. <https://doi.org/https://doi.org/10.1016/j.wasman.2019.05.040>
- Deniz, O. S., & Dogan, E. (2014). Building Façade System for Deconstruction. *Journal of Sustainable Architecture and Civil Engineering, 8*(3). <https://doi.org/10.5755/j01.sace.8.3.7231>
- Gubert, M., Toniato, G., Papaiz, L., & Avesani, S. (2021, September 22). End of Life tool for building product development: the Solar Window Block case study. *XV Convegno Della Rete Italiana Di LCA 2021*.
- Heesbeen, C., Zabek, M., & Hildebrand, L. (2021). A Definition of Essential Characteristics for a Method to Measure Circularity Potential in Architectural Design. In T. Auer, U. Knaack, & J. Schneider (Eds.), *Powerskin Conference Proceedings* (pp. 165–174). TU Delft open Journals.
- Hildebrand, L. (2014). *Strategic investment of embodied energy during the architectural planning process*. Delft University of Technology, Faculty of Architecture and the Built Environment.
- Juaristi, M., Favoino, F., Gómez-Acebo, T., & Monge-Barrio, A. (2022). Adaptive opaque façades and their potential to reduce thermal energy use in residential buildings: A simulation-based evaluation. *Journal of Building Physics, 45*(5), 675–720. <https://doi.org/10.1177/17442591211045418>
- Nutzungsdauern von Bauteilen für Lebenszyklusanalysen nach Bewertungssystem Nachhaltiges Bauen (BNB)*. (n.d.). Retrieved May 19, 2022, from <https://www.nachhaltigesbauen.de/austausch/nutzungsdauern-von-bauteilen/>
- Pittau, F., Amato, C., Cuffari, S., Iannaccone, G., & Malighetti, L. E. (2019). Environmental consequences of refurbishment vs. demolition and reconstruction: A comparative life cycle assessment of an Italian case study. *IOP Conference Series: Earth and Environmental Science, 296*(1). <https://doi.org/10.1088/1755-1315/296/1/012037>

Annex

ROLE	ELEMENT	MATERIAL	DURABILITY (years)	SOURCE FOR LCA MODEL
External cladding*	Variable 1	Plaster	40	EPD-SON-20150247-IBA1-EN**
	Variable 2	HPL	50	EPD-FMX-2012111-EN
	Variable 3	Wood	60	
Connection of external cladding and water/wind proofing membrane**	Vertical outer mullion	Solid structural wood	50	EPD-RUB-20180059-IBB1-EN
Water/wind proofing	Foil-Membrane	Polyester and acrylic coating	50	Modelled by the authors with database's flows
Closing layer of the insulation, rigidity	Outer planking	Medium Density Fibreboard **, =615 kg/m ³	50	EPD-EGG-20140196-IBA1-DE
Thermal performance	Thermal insulation	Mineral Wool, density =60kg/m ³	50	EPD-RUB-20180059-IBB1-EN
Load-bearing frame of the prefabricated façade	Timber-frame	Solid structural wood	50	EPD-RUB-20180059-IBB1-EN
Closing layer of the insulation and vapour barrier, rigidity	Inner planking	Wood based panels	50	EPD-EGG-20180107-IBD1-EN
Fastening of the inner insulation and connection of the inner cladding***	Vertical inner mullion	Solid structural wood	50	EPD-RUB-20180059-IBB1-EN
Inner finishing***	Gypsum	Gypsum	50	EPD-FER-20160218-CAD1-EN
Daylight, ventilation***	Window (transparent part, U=1.1 W/m ² K, frame U=1.5W/m ² K)	Glass and wood (frame)	25	Database

*For the supporting board. Plaster layer was modelled by the authors with database's flows.

** The EPD to model plaster cladding refers to the supporting board. Plaster layer was modelled by the authors with database's flows. Moreover, the façade system with the plaster cladding does not include vertical outer mullions nor an outer planking made of medium-density wood fibre board.

***Installation layers and windows were a variable parameter; thus they were not always modelled.

The Potential of Static and Thermochromic Window Films for Energy Efficient Building Renovations

A.J.J. Kragt^{1,2*}, E.R. van den Ham¹, H. Sentjens³, A.P.H.J. Schenning³, T. Klein¹

* Corresponding author, a.j.j.kragt@tudelft.nl

1 Delft University of Technology, Netherlands

2 ClimAd Technology

3 Eindhoven University of Technology, Netherlands

Abstract

The type of glazing implemented in a building plays an important role in the heat management of a building. Solar heat entering through glazing causes overheating of interior spaces and increases building's cooling load. In this work, the energy saving potential of window films based on Cholesteric Liquid Crystals (CLC) is explored. This emerging technology allows for the fabrication of static and thermochromic solar heat rejecting window films and can provide a simple renovation solution towards energy efficient buildings. Simulations on a model office showed that static CLC-based window films can save up to 29% on a building's annual energy use in warm climates. In climates with distinct summer and winter seasons, static solar heat rejecting windows films cause an additional heating demand during winters, which reduces the annual energy savings. In these climates, the benefit of thermochromic CLC-based window films becomes evident and an annual energy saving up to 22% can be achieved.

Keywords

glazing, solar heat rejection, window films, thermochromic, energy savings

DOI

<http://doi.org/10.47982/jfde.2022.powerskin.6>

1 INTRODUCTION

The world population and people living in urban areas is growing (United Nations, 2018; 2019). To host and keep hosting this growing population, high-rise buildings are increasingly dominating the city landscape. These buildings should provide comfort and well-being to its occupants, be sustainable and simultaneously positively impact the urban environment. To this end, large glazing areas are increasingly used in building façade designs, as this allows natural daylight, which positively impact the health and productivity of occupants (Chen, Zhang, & Du, 2019; Knoop et al., 2020). However, solar heat entering through glazing causes overheating of indoor spaces and increases the demand for artificial cooling loads. Buildings are already responsible for 36% of worldwide energy consumption. Despite increasing population and floor area, reductions in energy consumption have been realized between 2010 and 2018 for space heating, lighting, appliances, cooking, and domestic hot water. In contrast, the energy use for space cooling has increased by 33% in this period, which is likely related to increased glazing area, rising temperatures, and an increasing demand for thermal comfort, and is expected to increase even further (Glass for Europe, 2019; IEA, 2018). Due to this steep increase in cooling demand, the overall energy consumption of buildings is still increasing at 1 to 2% per year (Dennis, 2018; IEA, 2019; Pérez-Lombard et al., 2008; Prieto et al., 2017). Therefore, it is of increasing importance to implement measures that reduce the energy use for space cooling in the built environment. This need is also recognized by policies which prescribe reduction of CO₂-emissions in the building sector. In view of this, the European Commission aims to at least double the renovation of existing building stock for the next ten years. Therefore, 35 million buildings in Europe should be renovated by 2030 (European Commission, 2020). These regulations have led to an increasing demand for innovative materials to reduce the environmental impact and increase the sustainability of new and existing buildings. In this respect, there is a lot to gain by renovation of existing glazing and glazing designs in new buildings. If all EU buildings were equipped with high-performance glazing by 2030 a total of 29% of energy use can be saved annually. This corresponds to an annual CO₂-emission reduction of up to 94.2 million tonnes (Glass for Europe, 2019).

Thermal losses and heat gains through glazing determines for a large extent the energy consumption performance of a building. On cold days (e.g. in winter), thermal losses from inside to outside a building should be reduced as much as possible to decrease energy use on heating systems. Simultaneously, on warm days (e.g. in summer), solar heat gains through glazing from outside to inside a building should be prevented to reduce the required energy for space cooling (Long & Ye, 2014). Solar radiation contains UV-light (300 - 400 nm), visible light (400 - 700 nm) and near-infrared (near-IR) light (700 - 2500 nm, Figure 1) (Jelle et al., 2015; Rezaei et al., 2017). UV-light has the ability to affect other materials, such as furniture inside a building, causing discolouration and degradation and interacts with the human skin with a potential negative impact on people's health (Gonzaga, 2009; Kim & Kim, 2010). Therefore, a window element or material should preferably block UV-light. The visible light part of the spectrum accounts for 43% of the solar energy. Interaction of a window with this part of the solar spectrum will determine the tinting or colouring of a window and therefore the appearance of the building and the daylight comfort of its occupants. The near-IR light accounts for 52% of the solar energy and causes heating of interior spaces. Therefore, glazing technologies that focus on the reduction of solar heat gains through glazing focus on rejection of solar near-IR light, while allowing sufficient visible light to ensure daylight comfort.

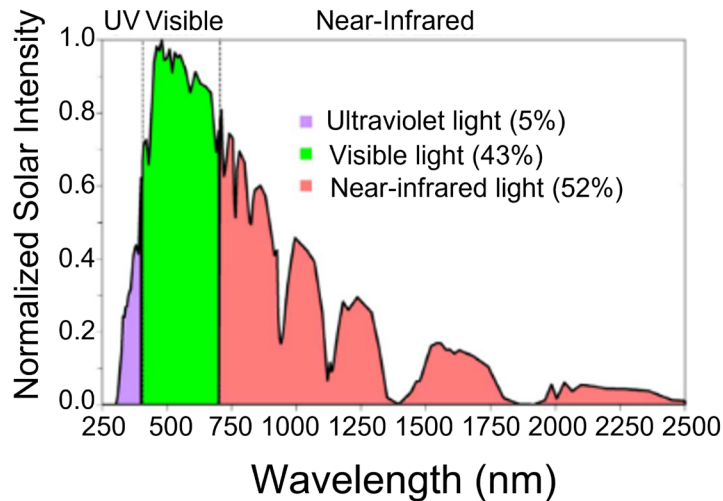


FIG. 1 The solar energy distribution. Adapted from Rezaei et al., 2017

Various glazing solutions are developed to impact the heat management of buildings. Next to shutters and blinds, a common solution is the use of low-emissivity (Low-E) coatings. Such Low-E materials usually consist of various layers of metals (typically silver) and metal oxides, which can for instance be applied to a glass pane via sputtering or other deposition techniques (Ding & Clavero, 2017; Jelle et al., 2012). Their main function is to re-direct long-wave radiation from inside a building back into the building to reduce the amount of heating required on cold days. These coatings thus increase the insulating properties of a glazing units (Long & Ye, 2014). In addition, various Low-E coatings exist which not only insulate glazing, but also reject solar heat to keep a building cool on warm days and reduce the energy use on artificial cooling (Al-Obaidi et al., 2014; Jelle et al., 2015; Mohelníková & Altan, 2009; Rezaei et al., 2017; Xu et al., 2017). Nowadays, most new building designs in cold or temperate climates are equipped with Low-E coated insulating glass units (IGUs) (Selkowitz, 1999).

Another solution that reduces the solar heat gains through glazing is the use of solar heat rejecting window films. Such films are simply adhered to existing IGUs to upgrade a building's glazing performance without the need to replace any glass panes (Bahadori-Jahromi et al., 2017; Curcija et al., 2017). Window films can be fabricated via roll-to-roll methods on flexible substrates at high throughput. Over the years, companies in this field, such as 3M and Saint-Gobain, developed a variety of window films having various gradations of tinting and near-IR reflection based on reflective metal-containing coatings or absorptive metal oxides (Jelle et al., 2015; Kim et al., 2021). These films are designed and optimized for various climates around the world. For instance, a warm and sunny climate requires a film with more tinting and near-IR reflection, whereas a colder and less sunny climate requires more visible light transmission and less near-IR reflection, in order to optimize the balance between solar heat gains in winter and rejection in summer (Hui & Kwok, 2006; Li et al., 2015; Sedaghat et al., 2021). As such films are fabricated in a cost-effective way and can be applied to existing window panes, they are an appealing and easy-to-install renovation option.

Low-E coated glazings and solar heat rejecting window films do not adapt their optical properties with the outdoor weather conditions. In winter, when solar heat is desired to enter a building, these solutions also reject solar heat, causing an additional energy use on heating the indoor space to a comfortable temperature. Therefore, climates with distinct summer and winter seasons would benefit from dynamic glazing solutions (Casini, 2014). Several pilot and simulation studies revealed

that such dynamic glazing solutions could realize an annual energy saving between 8 and 53% in temperate climates compared to traditional glazing solutions depending on variables, such as building geometry, orientation, and the used reference glass (General Services Administration, 2014; Khandelwal et al., 2015; Mann et al., 2021; Mann et al., 2020; Dussault et al., 2012; DeForest et al., 2017). A recent development is the electrically switchable glazing. These glazings can be switched from a transparent to tinted state on demand of the end-user or coupled to a sensor to tint autonomously depending on the outdoor sunlight intensity (Al Dakheel & Aoul, 2017). These systems are effective in maintaining a comfortable light illumination throughout the day and also allow an energy benefit compared to non-responsive glazing units (Arbab et al., 2017; Clear et al., 2006; Day et al., 2019; General Services Administration, 2014; Mardaljevic et al., 2016; Painter et al., 2016; Piccolo & Simone, 2009). Electrically switchable materials can be prepared from electrochromic metal oxides, such as tungsten oxide (WO_3), but also include examples of conjugated polymers and switchable liquid crystal (LC) devices (Baetens et al., 2010; Casini, 2018; Ke et al., 2019; Khandelwal et al., 2015; Khandelwal et al., 2017; Marchwinski, 2014; Wang et al., 2016). The fabrication of these systems requires sandwiching of the responsive material between two glass plates with electrically conductive layers and requires electronic wiring, which causes high fabrication and installation costs (Brzezicki, 2021). Dynamic glazing solutions that require a simpler installation are systems that respond autonomously to outdoor weather conditions, such as thermochromic glazing solutions (Mann et al., 2020; Seeboth et al., 2010; Serpe, 2019). These materials can consist of inorganic pigments that can change their absorptive properties with temperature, such as VO_2 -based thermochromic materials (Calvi et al., 2021; Cui et al., 2018; Ke et al., 2018; Long & Ye, 2014; Yeung et al., 2021). These systems are usually laminated between two glass plates and are installed similar to regular IGUs.

This work discusses the energy saving potential of an emerging technology, namely Cholesteric Liquid Crystal (CLC) based coatings, for solar heat management in buildings. LCs are materials that possess both solid-like as well as liquid-like properties. LC molecules have some level of organisation similar to the crystal structure of a solid, but are also able to change organisation easily and flow like a liquid. When incorporating a chiral molecule inside an LC, a rotation in the molecular organisation can be induced and a periodic helical organization of the molecules can be created, called a CLC phase (Figure 2) (Liang, 2015). This helix provides an optical structure with periodically altering refractive indices, which is able to reflect light of a specific wavelength and circular polarization. Therefore, a CLC material can reflect 50% of incoming unpolarized light around a specific central wavelength. This wavelength is determined by the periodicity of the cholesteric helix structure, which can be tuned by the concentration and type of chiral dopant (Balamurugan & Liu, 2016; Dierking, 2014; Liu et al., 2016; Mitov, 2012; White et al., 2010). A CLC material can thus be tuned to reflect only in the near-IR range of the solar spectrum, while leaving the visible light transmission unaffected. This property makes them appealing as solar heat rejecting glazing material. Furthermore, the wavelength range to be reflected can be broadened to lower the solar heat gain coefficient (SHGC) of the glazing. This can be achieved by coating multiple CLC layers reflecting at different wavelengths on top of each other, but might also be achieved by creating a pitch gradient in a single CLC layer (Khandelwal et al., 2014; Kim et al., 2018; Liu et al., 2016; Mitov, 2012; Ranjkesh & Yoon, 2021; Van Heeswijk et al., 2019). Such a pitch gradient might be achieved by polymerization induced diffusion methods, in which one creates a concentration difference of the chiral dopant throughout the thickness of the CLC material (Broer et al., 1999; Fan et al., 2008; Khandelwal et al., 2017). Another possible route could be the stepwise polymerization at various specific temperatures of a thermochromic CLC material (Duan et al., 2017; Guo et al., 2010; Mitov et al., 2004; van Heeswijk et al., 2020; Wu et al., 2011; Xiao et al., 2016). In this way various pitch lengths, and thus reflective wavelengths, are established inside one CLC layer. Using these methods, CLC

broadband reflectors spanning a wavelength range of up to 13 μm have been fabricated (Zhang et al., 2016). To decrease the SHGC further, the 50% reflection limit of a regular CLC-based device can be exceeded by including both a left- and right-handed helical CLC structures into one window film device (Khandelwal et al., 2014; Mcconney et al., 2011; Ranjkesh & Yoon, 2021; Zhao et al., 2015). Another option would be to insert an achromatic optical half-waveplate material in between two broadband CLC reflectors of the same handedness (Komanduri et al., 2013; Kraemer & Baur, 2019; Ortiz-Gutiérrez et al., 2001). Such a waveplate converts the transmitted circularly polarized light of the first CLC broadband layer to the opposite handedness, which then can be reflected by the second CLC broadband layer (Khandelwal et al., 2014; Kragt et al., 2019; Mitov, 2012).

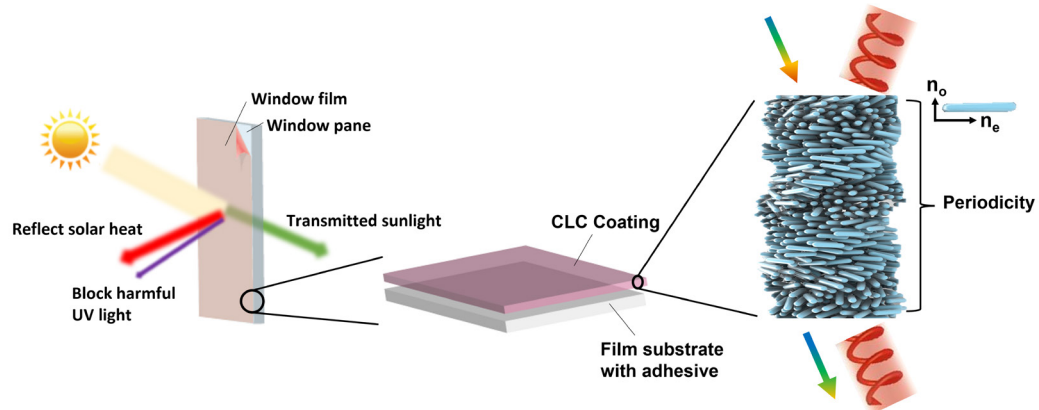


FIG. 2 Simplified representation of a solar heat rejecting window film based on a CLC reflective coating. (left) A solar heat rejecting window film adhered to glass. (middle) A zoom-in on a simple window film build-up comprising a CLC coating on an adhesive film substrate. In practice, the window film might consist of multiple coating layers bearing various functionalities. (right) A representation of the periodic helix structure inside a CLC coating. The molecules are represented by the blue bars. The periodic rotation of the extraordinary and ordinary refractive indices (n_e and n_o , respectively) causes the CLC material to reflect light of a specific wavelength and circular polarization. Many of these periodic helices are present in one coating layer to reach the 50% reflection limit of a single CLC coating layer. The CLC helical structure is adapted from Liang, 2015.

Besides static reflectors, the organisation, and thus optical properties of CLC materials, can also be tuned by external stimuli, such as electric fields and temperature (Khandelwal et al., 2017; Zhang et al., 2021). This property also makes them appealing for dynamic glazing solutions that can respond to outdoor weather conditions. By modifying the chemical composition and processing conditions CLC-based materials can be fabricated that can, for example, shift their reflective wavelength upon changes in temperature (Khandelwal et al., 2019; Kragt et al., 2019; Ranjkesh & Yoon, 2019; White et al., 2010; Zhang et al., 2021). In particular, CLC materials that show a phase transition from a non-reflecting smectic liquid crystal phase to a reflective cholesteric phase are prone to show huge wavelength shifts towards lower wavelengths upon increasing the temperature (van Heeswijk et al., 2019; Yang et al., 2022; B. Zhang et al., 2019; P. Zhang et al., 2018; W. Zhang et al., 2017; Zhang et al., 2021). In a smectic phase the molecules are organized in a two-dimensional order, not bearing the periodic helical structure of a CLC phase. As soon as the material undergoes a phase transition from a smectic to a cholesteric phase, the cholesteric pitch starts to form and gradually becomes shorter, causing a shift of the reflective properties towards smaller wavelengths. Such materials have shown reflection band shifts of over 1100 nm (Tzeng et al., 2010). The transition temperature and reflective wavelength position of such materials can be tuned by varying the chemical composition of the thermochromic CLC material. In addition, one could even design a material that is able to shift from a narrow to broadband reflector by partly polymerizing a thermochromic material (Khandelwal et al., 2016; Yang et al., 2003; Yuan et al., 2010). In this way, CLC-based materials can be used to regulate the level of solar heat rejection based on the outdoor temperature conditions.

In this work, the energy saving potential of both static and thermochromic CLC-based window films in both warm and temperate climates is explored. The window films are based on a CLC coating applied on a flexible substrate providing a static near-IR reflecting film that can be adhered to a glass plate (Figure 2). Such window films are interesting for energy efficient building renovations. The impact on a building's energy consumption when developing these films into a full broadband reflector and thermochromic window film is evaluated using an office building simulation. This provides insights on further material developments towards effective energy saving window film products based on CLC coating technology.

2 METHODOLOGY

To explore the potential impact of CLC-based window film technologies on the energy performance of a building various static and thermochromic window films are designed to represent the theoretical optical performance limits of CLCs. The glazing characteristics, such as visible light transmission (T_{vis}), solar heat gain coefficient, (SHGC) and U-value, of these window films in combination with a double clear IGU and a Low-E coated IGU are calculated. These glazing characteristics are then used to specify the glazing performance of a building model in DesignBuilder representing a standard office floor. The monthly and annual energy use for lighting, heating, and cooling of this building is calculated and the energy performances with various glazings inserted are compared to each other to quantify the energy saving potential of the CLC-based window films.

2.1 CHOLESTERIC LIQUID CRYSTAL WINDOW FILMS

Several static window films, as well as one thermochromic window film, are designed based on empirical findings during laboratory fabrication and methods described in literature. For the CLC-based window film that is actually fabricated in a laboratory, the film is adhered to a single glass pane and the optical properties are measured by spectrophotometry. This data is imported in LBNL software Optics6 to determine its optical characteristics and subsequently in Window 7.7 to translate these to glazing characteristics. For the CLC-based window film designs that are based on methods described in literature, the transmission and reflection spectra are not measured, but plotted by hand. In this process realistic values for reflection band broadness and depth are taken based on findings in literature representing the limits of CLC-based technology. For the thermochromic window film design potential transition temperatures and wavelength shifts found in literature are taken as a reference. These simulated optical data are then imported similarly as the actually fabricated CLC-based window film into the LBNL softwares Optics6 and Window 7.7 to determine the glazing characteristics.

The optical properties of Cholesteric Liquid Crystals (CLCs) can be custom designed by using various processing methods. The first CLC-based window film design consists of a single CLC coating layer on a polyethylene terephthalate (PET) substrate based on a CLC ink formulation provided by ClimAd Technology and is actually fabricated in a laboratory. This ink was coated on a UV-blocking polyethylene terephthalate (PET) film having a thickness of 50 μm by means of wire-bar coating and subsequent drying and UV-curing steps. An optically clear adhesive was laminated at the non-coated side of the film, which was then adhered to a 4 mm thick single clear glass plate (10 x 12 cm, Stolker Glas). The transmission spectrum of this window was measured on a Perkin Elmer Lambda 750 UV/Vis/NIR spectrophotometer over a wavelength range between 400 and 2500 nm (Figure 3A, black

solid curve, CLC narrow). In addition, the reflection spectra of the glazing device were measured from both sides of the sample over the same wavelength range. The CLC narrow band window film device has a central reflective wavelength at 920 nm at which it reaches a transmission of 48%. Adhered to a single clear glass plate, the CLC narrow band window film has a visible light transmission of 88% and a solar heat gain coefficient (SHGC) of 0.79 as determined with LBNL software Optics6 and Window7.7.

The SHGC of CLC-based window films can be decreased by broadening the reflection band of the CLC material (Liu et al., 2016; Mitov, 2012). To explore the energy saving potential of such broadband reflectors, transmission and reflection spectra were plotted by hand. The depth of the transmission spectrum in the reflected wavelength range as well as the baseline of a single glass pane is based on the measured spectra of the actually fabricated CLC narrow band window film device. The bandwidth of the plotted broadband CLC-based window film device reflected a full width at half height between 840 and 1570 nm. (Figure 3A, yellow curve, CLC broad). Broadband reflectors spanning a similar or even larger wavelength range are also described in literature and can be fabricated by creating a pitch gradient in a single CLC material layer by polymerization induced diffusion methods or by polymerizing a thermochromic CLC material at various temperatures (Fan et al., 2008; Duan et al. 2017; Xiao et al., 2016; L. Zhang et al., 2016). Therefore, the chosen wavelength range of the simulated broadband CLC-based window film device is believed to be feasible in practice when optimized as a coating on a window film. Adhered to a single clear glass this device has a SHGC of 0.72, while the visible light transmission is still at 88%. To decrease the SHGC of CLC-based window films further one could fabricate a broadband reflector exceeding the 50% reflection limit of a single layer of CLC material by superimposing multiple layers of opposite handedness of the CLC helix structure or sandwiching a half waveplate material in between two CLC layers reflecting similar handedness (Khandelwal et al., 2014; Komanduri et al., 2013; Kraemer & Baur, 2019; Kragt et al., 2019; Mcconney et al., 2011; Mitov, 2012; Ortiz-Gutiérrez et al., 2001; Ranjkesh & Yoon, 2021; Zhao et al., 2015). In this way, CLC-based reflectors are created, reflecting nearly all incoming light within the reflected wavelength range. Therefore, the third static CLC-based window film device used in this work consists of two CLC-based broadband reflectors superimposed on top of each other to create a broadband reflector that reflects nearly all incoming light. This design represents the limits of CLC-based window films that could be achieved in practice after optimization. This simulated full broadband reflector reflects over the same wavelength range as the simulated broadband reflector described above, but reaches a transmission as low as 5% over the reflected wavelength range (Figure 3A, green curve, CLC full broad). Adhered to a single clear glass plate this CLC-based window film device reaches a SHGC of 0.54 with a visible light transmission of 85%.

CLC materials not only allow for the fabrication of static IR reflectors, but could also be processed to thermochromic devices (Khandelwal et al., 2016; Tzeng et al., 2010; van Heeswijk et al., 2019; Yang et al., 2022; Zhang et al., 2018; Zhang et al., 2021). To simulate the potential limits of thermochromic CLC-based window film we combined several literature findings into one design. This design is based on CLC materials that show large reflection band shifts spanning hundreds of nm in a temperature range between 12 and 20 °C (Tzeng et al., 2010; Yang et al., 2022). By applying a processing method in which such thermochromic CLC material is only partly polymerized one could create a device that is changing from a narrowband to a broadband upon increasing the temperature, as the thermochromic response of the polymerized portion of the material is inhibited, while the non-polymerized part still shifts its reflected wavelength (Khandelwal et al., 2016; Yang et al., 2003; Yuan et al., 2010). Similar to the simulated static full broadband reflector design, two such thermochromic CLC layers could be superimposed on top of each other to fabricate a thermochromic CLC-based window film reflecting nearly all incoming light over the reflected wavelength range.

Combining these materials and methods described in literature and optimizing those into a single device, one could imagine a thermochromic CLC-based window film that is not reflecting at 10 °C, turns into a full narrowband reflector at 12 °C, and gradually changes to a full broadband reflector at 20 °C. The spectral data of such a thermochromic window film on a single glass pane are plotted by hand in which the baseline is based on the actually measured glass pane subtracted by the overall absorption one could expect from two CLC coating layers based on the actually measured static CLC narrow band window film. For a fair comparison between the static and the thermochromic window film device, the thermochromic window film starts to reflect a narrowband at 1500 nm at 12 °C and turns into a full broadband reflector at 20 °C, covering the same wavelength range as the static CLC-based window film design (Figure 3B). These simulated spectral data at the various temperatures are imported into the LBNL softwares Optics6 and Window 7.7. The SHGC of the thermochromic CLC based window film changes instantly and reversibly from 0.82 to 0.79 to 0.54 as soon as the temperature of the thermochromic coating layer is altered from 10 to 12 to 20 °C, respectively, by daily fluctuations of outdoor air temperature and solar radiation. The visible light transmission of the thermochromic CLC based window film remains unchanged (85%) at the various temperatures.

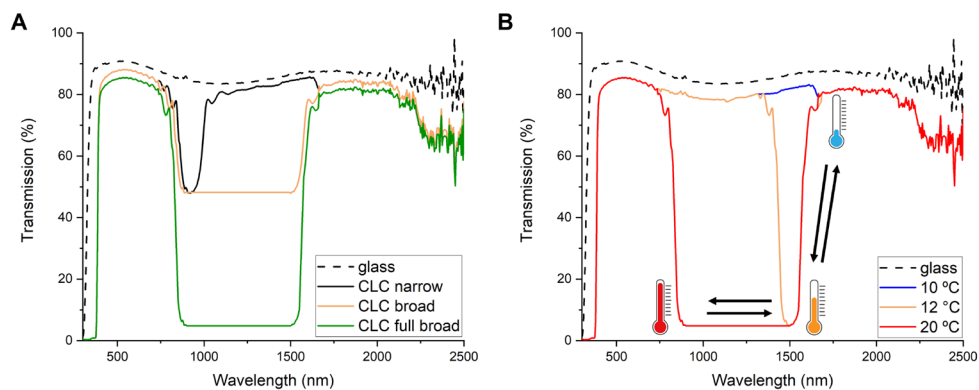


FIG. 3 Transmission spectra of static CLC-based window films adhered to a single clear glass plate (4 mm) of (A) various static window films and (B) a thermochromic window film. The CLC narrowband reflector film is measured from a fabricated sample. The other data are derived from this spectrum and represent the potential of CLC-based window film technology.

2.2 GLAZING DESIGN CHARACTERISTICS

Two IGUs were selected as reference glazing systems; a double clear glass system and a Low-E coated glass system. The glass characteristics of the clear glass were calculated by importing transmission and reflection spectra of a 4 mm glass plate (Stolker Glas) in the LBNL software Optics6. The glass characteristics of the Low-E coated glass were taken from the International Glazing Database (Saint-Gobain Eclaz 4 mm). The IGU glazing characteristics were calculated in the software DesignBuilder according to ISO 10292 and consisted of two glass plates (clear or Low-E coated) filled with argon (16 mm). The Low-E coating was placed on the inner side of the inner glass pane (position 3). The double clear and Low-E coated IGUs were equipped with CLC-based window films by replacing the outside glass pane with a user-defined glazing defined by the glazing characteristics as calculated in the previous section, so that the window film faces the outdoor environment (position 1, Figure 4). For the thermochromic CLC-based window film the outside glass pane has to be defined as a 'pane group' instead of a static 'pane'. Within this pane group the glazing characteristics of the glazing at different temperatures can be defined in a similar way as for a static glass pane. The calculated glazing characteristics of the double clear and Low-E coated IGUs

equipped with various CLC-based window films are tabulated in Table 1 and Table 2, respectively. In practice, the window film might also be integrated inside the IGU unit (e.g. position 2) or integrated as a laminate between two glass plates. The glazing characteristics could be somewhat affected in these configurations, but this is beyond the scope of this work.

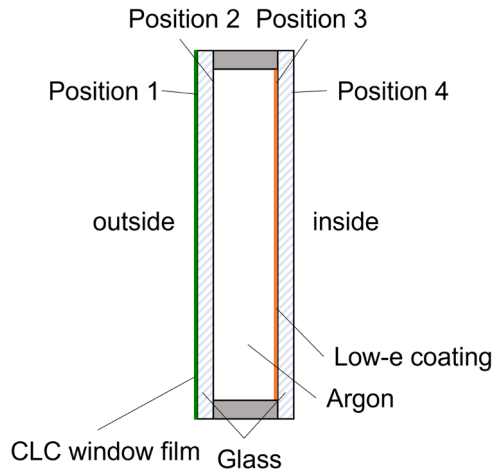


FIG. 4 Schematic build-up of the Low-E coated IGU equipped with a CLC-based window film

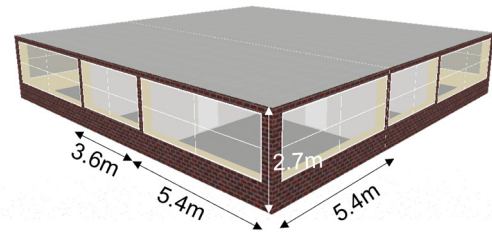


FIG. 5 Schematic representation of the model office used in the DesignBuilder simulations

TABLE 1 Glazing characteristics of double clear IGU equipped with various CLC window films.

The SHGC for the thermochromic window glazing system is given at various temperatures (10, 12, and 20 °C). The visible light transmission remains constant at various temperatures.

glazing type	Double clear	+ CLC narrow	+ CLC broad	+ CLC full broad	+ thermochromic
Tvis (%)	83	80	80	78	78
SHGC	0.79	0.71	0.65	0.50	0.73 > 0.71 > 0.50
U-value (W/(m2K))	2.6	2.6	2.6	2.6	2.6

TABLE 2 Glazing characteristics of the Low-E coated IGU equipped with various CLC window films.

The SHGC for the thermochromic window glazing system is given at various temperatures (10, 12, and 20 °C). The visible light transmission remains constant at various temperatures.

glazing type	Double clear	+ CLC narrow	+ CLC broad	+ CLC full broad	+ thermochromic
Tvis (%)	84	81	81	79	79
SHGC	0.70	0.64	0.59	0.46	0.65 > 0.63 > 0.46
U-value (W/(m2K))	1.1	1.1	1.1	1.1	1.1

2.3 DESIGNBUILDER SIMULATIONS

The building's energy performance was simulated using the software DesignBuilder. A model office was designed having side offices (3.6 x 5.4 x 2.7 m) with one outdoor facing window and corner offices (5.4 x 5.4 x 2.7 m) with two outdoor facing windows. The four identical sides of the office are oriented towards the North, East, South and West (Figure 5). The window-to-wall ratio of the model office was 60%. The floor and ceiling of the office were designed to be adiabatic, to

mimic an office space with adjacent building levels. The outdoor walls are medium weight walls having a U-value of 0.25 W/(m²K). The building is equipped with an LED lighting system having a normalised power density of 2.5 W/m² per 100 lux and is turned on when the illuminance level drops below 400 lux at a working height of 0.8 m during occupied hours. The HVAC system is based on the 'Best practice' template defined in DesignBuilder. The heating system runs on natural gas and has a coefficient of performance (CoP) of 1.0 and is activated when the indoor temperature of a room drops below 20 °C. For operation schedule the DesignBuilder template 'Office_OpenOff_Heat' is used. The cooling system runs on electricity from the grid and has a CoP of 2.5 and is activated when the indoor temperature rises above 25.5 °C during occupied hours (DesignBuilder template 'Office_OpenOff_Cool'). The mechanical ventilation is turned on when the air rate drops below the minimum requirement of 10 l/s per person and follows the 'Open_OpenOff_Occ' schedule defined in DesignBuilder. Natural ventilation is turned off. Furthermore, the activity is based on the 'Generic Office Area' template defined in DesignBuilder. The model office has an occupation density of 0.111 people/m² and operates according to the standard open office occupancy schedule (DesignBuilder template 'Office_OpenOff_Occ'). During the operational hours defined by this occupancy schedule office equipment is used with a power density of 11.77 W/m².

During the simulations, all modelling parameters are kept constant. Only the glazing system is varied according to the characteristics described in the previous section. The building's energy use for lighting, heating, and cooling is gathered for the building equipped with various glazing designs. For the thermochromic glazing, DesignBuilder varies the glazing characteristics according to the outdoor temperature. In this case, the glazing characteristics are defined at 10, 12, and 20 °C. At the average between two defined switching temperatures DesignBuilder switches to the corresponding glazing characteristics. This means that <11 °C the glazing characteristics as set for 10 °C are used, at outdoor temperatures between 11 and 16 °C the glazing characteristics as set for 12 °C are used, and at outdoor temperatures >16 °C those as set for 20 °C are used. The energy use calculations were done for the climates of Guangzhou and Lisbon, which have warm and sunny conditions throughout almost the entire year, and for Amsterdam and Beijing, which have variable seasons with fluctuating temperatures. The weather data files are downloaded from www.climate.onebuilding.org, which provided Typical Meteorological Year (TMY) datasets for the specific locations, which were then imported into the DesignBuilder model.

3 RESULTS

3.1 ENERGY SAVING POTENTIAL OF CLC WINDOW FILMS ON DOUBLE GLAZING

The energy consumption of the model building equipped with double glazing and various CLC-based window films was calculated for the climates of Guangzhou, Lisbon, Amsterdam, and Beijing. The energy use for lighting, heating, and cooling was included and the total energy consumptions are compared to each other (Figure 6A). These simulations show that in climates with warm temperatures all year through (e.g. Guangzhou and Lisbon) almost no energy use for space heating is required to maintain a comfortable indoor temperature and the building's energy consumption is mainly due to space cooling. When applying static CLC-based window films to the glazing, an increasing amount of energy can be saved with decreasing SHGC. This translates to an energy saving of up to 24 and 26% in Guangzhou and Lisbon, respectively, when applying the CLC full broadband

film to the glazing (Figure 6B). In these climates there is no additional benefit of applying a thermochromic window film, as rejection of solar heat is beneficial almost all year through.

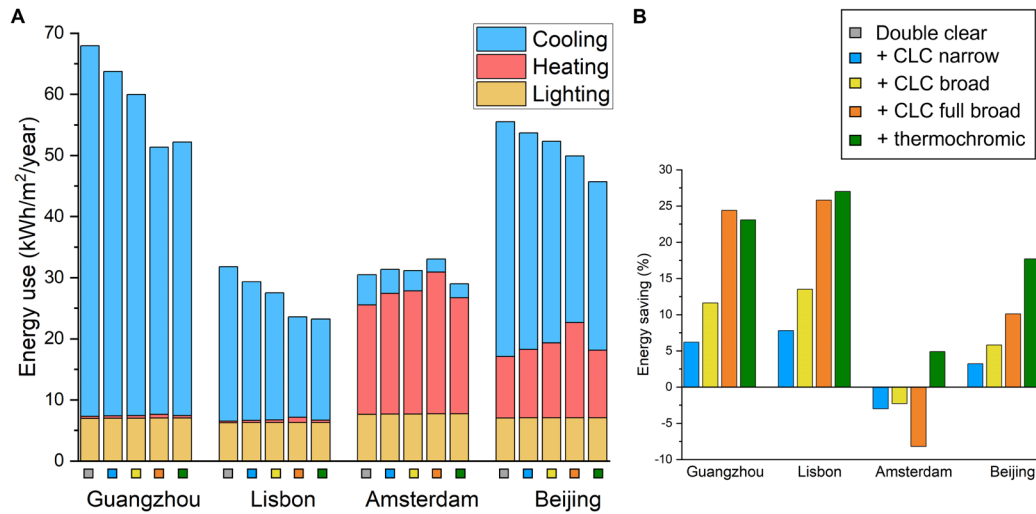


FIG. 6 (A) Annual energy use for lighting, heating, and cooling of the simulated building equipped with double glazing and various CLC window films in various climates. The legend in panel (B) also corresponds with the squares below the bars, which indicate the implemented glazing type. (B) Energy saving percentage of the simulated building compared to double glazing.

This outcome changes when performing the simulation in climates in which outdoor temperature conditions fluctuate more heavily between seasons (e.g. Amsterdam and Beijing). In these climates the energy use for space heating makes up a significant portion of the building's annual energy consumption and can even become the main source of energy consumption, such as in Amsterdam. The simulations reveal that applying a static CLC-based window film to the double glazing of the model building decreases the energy use for space cooling. However, the energy use for space heating increases. This effect is caused by the additional energy use required for space heating in winter (Figure 7). As solar heat is also rejected on colder days (e.g. winter) it takes more energy for the heating system to remain a comfortable indoor temperature. In Beijing, where cooling energy use is still the main source of the building's energy consumption, the energy savings on cooling are still larger than the additional required energy use for space heating, and an overall annual energy saving of 10% is achieved. In Amsterdam, where heating is the main source of the building's energy consumption, the additional required energy use for space heating when applying a static CLC-based window film is larger than the energy savings on space cooling, which results in an increase of the annual energy use. To prevent the additional required energy use for space heating in climates like Amsterdam and Beijing, a thermochromic window film can be applied to the glazing of the model building. When doing so, solar heat is rejected on warm days, which saves energy use on cooling, whereas solar heat is allowed to enter the building on cold days, which prevents the additional required energy use for space heating (Figures 6 and 7). In this case, an overall annual energy saving of 5 and 18% can be achieved in Amsterdam and Beijing, respectively, compared to double glazing. When comparing the energy saving performance of the thermochromic film to that of a static CLC-based window film reaching the same SHGC (e.g. the CLC full broadband film), the thermochromic film improves the energy efficiency of the building, at 13% and 8% in Amsterdam and Beijing, respectively.

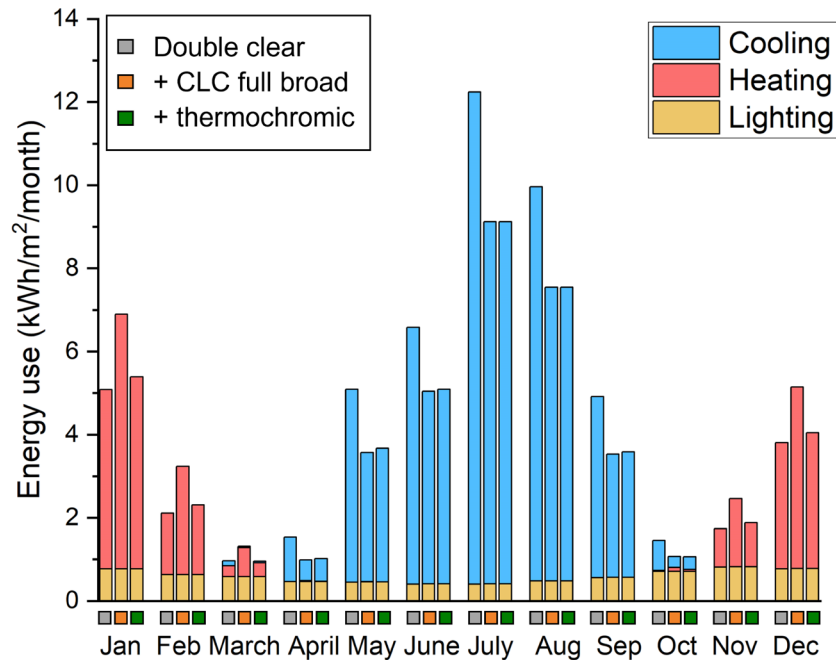


FIG. 7 Monthly energy use for lighting, heating, and cooling of the simulated building equipped with double glazing and a CLC full broadband or thermochromic window film in Beijing.

3.2 ENERGY SAVING POTENTIAL OF CLC WINDOW FILMS ON LOW-E COATED DOUBLE GLAZING

Similar simulations were carried out for a model building that is equipped with Low-E coated double glazing. Low-E coatings increase the insulating value of the glazing and thus lower the U-value. (Jelle et al., 2012; Rezaei et al., 2017) Therefore, the energy use for space heating on cold days (e.g. winter) decreases. Simultaneously, the energy use for space cooling on warm days (e.g. summer) increases, as indoor heat cannot leave the building as easily. In warm climates, such as Guangzhou and Lisbon, this effect causes an increase in overall annual energy consumption of the model building when compared to double glazing. In climates bearing distinct summer and winter seasons, such as Amsterdam and Beijing, replacing double glazing with Low-E coated double glazing does enhance the energy efficiency of a building.

When implementing the CLC-based window films to the Low-E coated glazing of the model building in Guangzhou and Lisbon, similar trends can be discovered as in the case of double glazing (Figure 8A). The energy use for space cooling decreases with decreasing SHGC. Overall annual energy savings of up to 25% and 29% can be reached when equipping the glazing with a CLC full broadband film (Figure 8B). Additionally, in the case of Low-E coated glazing there is no additional benefit of applying a thermochromic glazing in these climates.

With the model building being equipped with a Low-E coated double glazing, the energy use for space heating decreases to a large extent. Therefore, space cooling becomes the major source of energy consumption both in the climates of Amsterdam and Beijing. When applying static CLC-based window films to the glazing of the model building, the energy savings on cooling on warm days (e.g. summer) remains larger than the additional required energy use for space heating on cold days (e.g. winter, Figure 8). This results in an overall annual energy saving up to 12% and 19% for Amsterdam and Beijing, respectively, when using the CLC full broadband film. In the case where a

thermochromic CLC-based window film is used, the energy savings could even increase further to 18% and 22%, respectively.

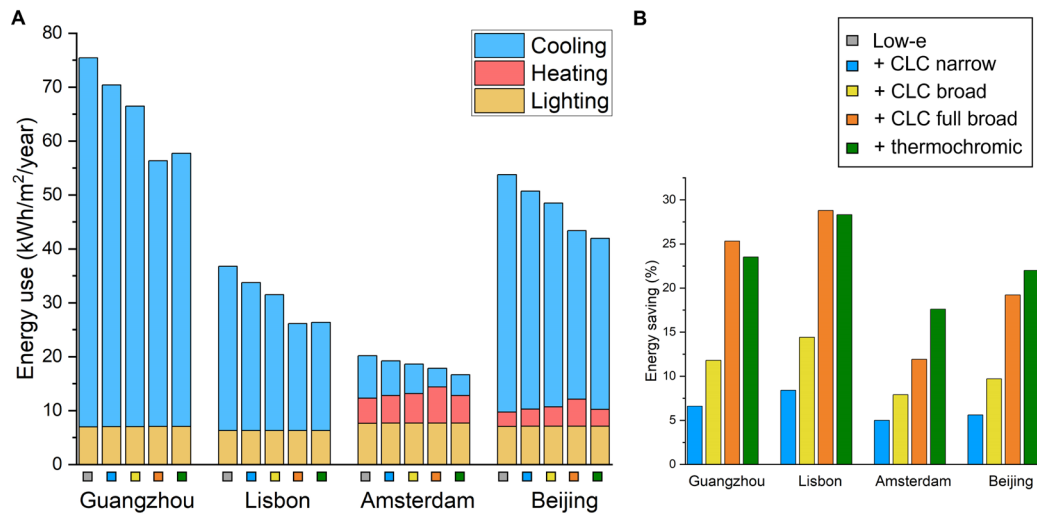


FIG. 8 (A) Annual energy use for lighting, heating, and cooling of the simulated building equipped with Low-E coated double glazing and various CLC window films in various climates. The legend in panel (B) also corresponds with the squares below the bars, which indicate the implemented glazing type. (B) Energy saving percentage of the simulated building compared to Low-E coated double glazing.

4 CONCLUSIONS

When renovating our model office with static CLC-based window films an annual energy saving between 24% and 29% can be achieved in warm climates, such as Guangzhou and Lisbon by reducing the cooling load. In climates with distinct summer and winter seasons, the energy saving increases when decreasing the SHGC of the film. In climates with fluctuating weather conditions throughout the year, such as Amsterdam and Beijing, the application of static CLC-based window films also reduces the cooling load of our model office, but simultaneously increases the heating demand during cold periods. Therefore, the annual energy savings are smaller compared to that in warm climates, especially when combined with double glazed buildings, in which heating contributes a large portion of a building's energy use. In these climates, one would benefit from the renovation of buildings using thermochromic CLC-based window films; a thermochromic film can improve the annual energy saving between 3% and 13% compared to a renovation with a static CLC-based window film. An annual energy saving between 5% and 22% can be achieved when renovating our model office with a thermochromic CLC-based window film.

The simulation results also show that the energy performance of a building in warm climates, such as Guangzhou and Lisbon, does benefit from a Low-E coating compared to clear double glazing. In these climates, renovations that add solar heat rejection to currently installed double glazing, such as with the addition of CLC-based window films, are preferred over improving the glazing's U-value. However, in climates with distinct summers and winters, such as Amsterdam and Beijing, Low-E coated double glazing has an energy efficiency benefit over clear double glazing. Here, combining good insulating properties with adaptive solar heat rejection results in the best energy performance.

For these climates, renovations are thus recommended in which clear (single or double) glazing is replaced by Low-E coated double glazing with adaptive solar heat control. These findings are in line with earlier reported building simulations, which report an energy saving between 15 and 30% of thermochromic glazing in combination with a Low-E coating compared to clear double glazing in the climate of The Netherlands (Mann et al. 2020, 2021).

Although glazing plays a significant role in the energy efficiency of buildings, the renovation of buildings has to be an integral solution that also includes other elements, such as the opaque elements of buildings, the efficiency of HVAC installations, and the thermal and daylight comfort of occupants. The introduction of other building materials for the walls and roofs (with different insulation values), as well as the introduction of screens and blinds to improve daylight comfort, are likely to influence the outcome of the energy performance simulations and thus the impact of the CLC-based window films studied in this work. Therefore, we advise conducting further studies to understand the interplay between various building use cases and the proposed window films.

Nevertheless, based on the findings presented in this work, optical window films based on CLC materials have real potential as an energy-saving renovation solution. To optimize the energy saving potential for various climates around the world, it is recommended to drive the material development of CLC-based window films towards both static as well as thermochromic solar heat rejection films. To be competitive in performance and energy saving to current window film products on the market, it is necessary to fabricate films with full broadband reflection properties and large optical contrast between cold and warm states, while maintaining the benefit of a highly visible light transmission. In addition, it should be ensured that the films are fabricated in a cost-effective way and at high throughput, such as via roll-to-roll fabrication methods.

References

- Al-Obaidi, K. M., Ismail, M., & Rahman, A. M. A. (2014). A review of skylight glazing materials in architectural designs for a better indoor environment. *Modern Applied Science*, 8(1), 68–82. Retrieved from <https://doi.org/10.5539/mas.v8n1p68>
- Al Dakheel, J., & Aoul, K. T. (2017). Building applications, opportunities and challenges of active shading systems: A state-of-the-art review. *Energies*, 10(10), 1672–1704. Retrieved from <https://doi.org/10.3390/en10101672>
- Arbab, S., Matusiak, B., Martinsen, F., & Hauback, B. (2017). The impact of advanced glazing on colour perception. *Journal of the International Colour Association*, 17, 50–68.
- Baetens, R., Jelle, B. P., & Gustavsen, A. (2010). Properties, requirements and possibilities of smart windows for dynamic daylight and solar energy control in buildings: A state-of-the-art review. *Solar Energy Materials and Solar Cells*, 94(2), 87–105. Retrieved from <https://doi.org/10.1016/j.solmat.2009.08.021>
- Bahadori-Jahromi, A., Rotimi, A., Mylona, A., Godfrey, P., & Cook, D. (2017). Impact of window films on the overall energy consumption of existing UK hotel buildings. *Sustainability (Switzerland)*, 9(5), 1–23. Retrieved from <https://doi.org/10.3390/su9050731>
- Balamurugan, R., & Liu, J. H. (2016). A review of the fabrication of photonic band gap materials based on cholesteric liquid crystals. *Reactive and Functional Polymers*, 105, 9–34. Retrieved from <https://doi.org/10.1016/j.reactfunctpolym.2016.04.012>
- Broer, D. J., Mol, G. N., Haaren, J. A. M. M. Van, & Lub, J. (1999). Photo-Induced Diffusion in Polymerizing Chiral-Nematic Media. *Advanced Materials (Deerfield Beach, Fla.)*, 11(7), 573–578. Retrieved from [https://doi.org/10.1002/\(SICI\)1521-4095\(199905\)11:7<573::AID-ADMA573>3.0.CO;2-E](https://doi.org/10.1002/(SICI)1521-4095(199905)11:7<573::AID-ADMA573>3.0.CO;2-E)
- Brzezicki, M. (2021). A systematic review of the most recent concepts in smart windows technologies with a focus on electrochromics. *Sustainability*, 13(17), 9604–9628. Retrieved from <https://doi.org/10.3390/su13179604>
- Calvi, L., Leufkens, L., Yeung, C. P. K., Habets, R., Mann, D., Elen, K., ... Buskens, P. (2021). A comparative study on the switching kinetics of W/VO₂ powders and VO₂ coatings and their implications for thermochromic glazing. *Solar Energy Materials and Solar Cells*, 224(February), 110977–110986. Retrieved from <https://doi.org/10.1016/j.solmat.2021.110977>
- Casini, M. (2014). Smart windows for energy efficiency of buildings. *Proceedings of the Second International Conference on Advances in Civil, Structural and Environmental Engineering*, 2(1), 273–281. Retrieved from <https://doi.org/10.5593/SGEM2015/B62/S26.040>
- Casini, M. (2018). Active dynamic windows for buildings: A review. *Renewable Energy*, 119, 923–934. Retrieved from <https://doi.org/10.1016/j.renene.2017.12.049>

- Chen, X., Zhang, X., & Du, J. (2019). Exploring the effects of daylight and glazing types on self-reported satisfactions and performances: a pilot investigation in an office. *Architectural Science Review*, 62(4), 338–353. Retrieved from <https://doi.org/10.1080/00038628.2019.1619068>
- Clear, R. D., Inkarojrit, V., & Lee, E. S. (2006). Subject responses to electrochromic windows. *Energy and Buildings*, 38(7), 758–779. Retrieved from <http://www.sciencedirect.com/science/article/B6V2V-4JWFGY5-1/2/c6f79ad78484e5ad7bd2686c332f4ef7>
- Cui, Y., Ke, Y., Liu, C., Chen, Z., Wang, N., Zhang, L., ... Long, Y. (2018). Thermochromic VO₂ for Energy-Efficient Smart Windows. *Joule*, 2(9), 1707–1746. Retrieved from <https://doi.org/10.1016/j.joule.2018.06.018>
- Curcija, C., Goudey, H., & Mitchell, R. (2017). *Low-e Applied Film Window Retrofit for Insulation and Solar Control*. Retrieved from https://www.gsa.gov/cdnstatic/GPG_-_Low-e_Solar_Film_Report_-_final_2.28.2017.pdf
- Day, J. K., Futrell, B., Cox, R., & Ruiz, S. N. (2019). Blinded by the light: Occupant perceptions and visual comfort assessments of three dynamic daylight control systems and shading strategies. *Building and Environment*, 154(February), 107–121. Retrieved from <https://doi.org/10.1016/j.buildenv.2019.02.037>
- DeForest, N., Shehabi, A., Selkowitz, S., & Milliron, D. J. (2017). A Comparative Energy Analysis of Three Electrochromic Glazing Technologies in Commercial and Residential Buildings. *Applied Energy*, 192, 95–109. Retrieved from <https://doi.org/10.1016/j.apenergy.2017.02.007>
- Dennis, A. (2018). *Global trends in thermal comfort in air conditioned and naturally ventilated offices in six climates*. UC Berkeley. UC Berkeley. Retrieved from <https://doi.org/10.11436/mssj.15.250>
- Dierking, I. (2014). Chiral Liquid Crystals: Structures, Phases, Effects. *Symmetry*, 6, 444–472. Retrieved from <https://doi.org/10.3390/sym6020444>
- Ding, G., & Clavero, C. (2017). Silver-Based Low-Emissivity Coating Technology for Energy-Saving Window Applications. In N. Nikitenkov (Ed.), *Modern Technologies for Creating the Thin-film Systems and Coatings* (pp. 409–431). IntechOpen. Retrieved from <https://doi.org/http://dx.doi.org/10.5772/57353>
- Duan, M., Cao, H., Wu, Y., Li, E., Wang, H., Wang, D., ... Yang, H. (2017). Broadband reflection in polymer stabilized cholesteric liquid crystal films with stepwise photo-polymerization. *Physical Chemistry Chemical Physics: PCCP*, 19, 2353–2358. Retrieved from <https://doi.org/10.1039/C6CP07066C>
- Dussault, J. M., Gosselin, L., & Galstian, T. (2012). Integration of smart windows into building design for reduction of yearly overall energy consumption and peak loads. *Solar Energy*, 86(11), 3405–3416. Retrieved from <https://doi.org/10.1016/j.solener.2012.07.016>
- European Commission. (2020). *A Renovation Wave for Europe - greening our buildings, creating jobs, improving lives*. European Commission. Retrieved from https://energy.ec.europa.eu/topics/energy-efficiency/energy-efficient-buildings/renovation-wave_en
- Fan, B., Vartak, S., Eakin, J. N., Faris, S. M., Fan, B., Vartak, S., ... Faris, S. M. (2008). Broadband polarizing films by photopolymerization-induced phase separation and in situ Swelling Broadband polarizing films by photopolymerization-induced phase separation and in situ Swelling. *Applied Physics Letters*, 92, 061101–061105. Retrieved from <https://doi.org/10.1063/1.2838299>
- General Services Administration. (2014). *Electrochromic and Thermochromic Windows*. *Public Building Services* (Vol. GPG-010). Retrieved from https://www.gsa.gov/cdnstatic/GPG_Findings_010-Smart_Windows.pdf
- Glass for Europe. (2019). *Glazing Potential - Energy Savings & CO₂ emission reduction*. Retrieved from <https://glassforeurope.com/glazing-saving-potential-2030-2050/>
- Gonzaga, E. R. (2009). Role of UV light in photodamage, skin aging, and skin cancer: Importance of photoprotection. *American Journal of Clinical Dermatology*, 10(SUPPL. 1), 19–24. Retrieved from <https://doi.org/10.2165/0128071-200910001-00004>
- Guo, R., Li, K., Cao, H., Wu, X., Wang, G., Cheng, Z., ... Yang, H. (2010). Chiral polymer networks with a broad reflection band achieved with varying temperature. *Polymer*, 51(25), 5990–5996. Retrieved from <https://doi.org/10.1016/j.polymer.2010.10.025>
- Hui, S. C. M., & Kwok, M. K. (2006). Study of thin films to enhance window performance in buildings. In *Proceedings of the Sichuan-Hong Kong Joint Symposium 2006* (pp. 158–167).
- IEA. (2018). *The Future of Cooling Opportunities for energy-efficient air conditioning*. Retrieved from https://iea.blob.core.windows.net/assets/0bb45525-277f-4c9c-8d0c-9c0cb5e7d525/The_Future_of_Cooling.pdf
- IEA. (2019). *2019 Global Status Report for Buildings and Construction*. *UN Environment programme* (Vol. 224). Retrieved from <https://doi.org/https://doi.org/10.1038/s41370-017-0014-9>
- Jelle, B. P., Hynd, A., Gustavsen, A., Arasteh, D., Goudey, H., & Hart, R. (2012). Fenestration of today and tomorrow: A state-of-the-art review and future research opportunities. *Solar Energy Materials and Solar Cells*, 96(0), 1–28. Retrieved from <http://www.sciencedirect.com/science/article/pii/S0927024811004685>
- Jelle, B. P., Kalnæs, S. E., & Gao, T. (2015). Low-emissivity materials for building applications: A state-of-the-art review and future research perspectives. *Energy and Buildings*, 96(7491), 329–356. Retrieved from <https://doi.org/10.1016/j.enbuild.2015.03.024>
- Ke, Y., Chen, J., Lin, G., Wang, S., Zhou, Y., Yin, J., ... Long, Y. (2019). Smart Windows: Electro-, Thermo-, Mechano-, Photochromics, and Beyond. *Advanced Energy Materials*, 9(39), 1–38. Retrieved from <https://doi.org/10.1002/aenm.201902066>
- Ke, Y., Zhou, C., Zhou, Y., Wang, S., Chan, S. H., & Long, Y. (2018). Emerging Thermal-Responsive Materials and Integrated Techniques Targeting the Energy-Efficient Smart Window Application. *Advanced Functional Materials*, 28(22), 1800113–1800130. Retrieved from <https://doi.org/10.1002/adfm.201800113>
- Khandelwal, H., Loonen, R. C. G. M., Hensen, J. L. M., Debije, M. G., & Schenning, A. P. H. J. (2015). Electrically switchable polymer stabilised broadband infrared reflectors and their potential as smart windows for energy saving in buildings. *Scientific Reports*, 5, 11773–11782. Retrieved from <https://doi.org/10.1038/srep11773>
- Khandelwal, H., Loonen, R. C. G. M., Hensen, J. L. M., Schenning, A. P. H. J., & Debije, M. G. (2014). Application of broadband infrared reflector based on cholesteric liquid crystal polymer bilayer film to windows and its impact on reducing the energy consumption in buildings. *Journal of Materials Chemistry A*, 2(35), 14622. Retrieved from <https://doi.org/10.1039/C4TA03047H>
- Khandelwal, H., Schenning, A. P. H. J., & Debije, M. G. (2017). Infrared Regulating Smart Window Based on Organic Materials. *Advanced Energy Materials*, 7(14), 1–18. Retrieved from <https://doi.org/10.1002/aenm.201602209>

- Khandelwal, H., Timmermans, G., Debije, M. G., & Schenning, A. P. H. J. (2016). Dual electrically and thermally responsive broadband reflectors based on polymer network stabilized chiral nematic liquid crystals: the role of crosslink density. *Chemical Communications*, 52(66), 10109–10112. Retrieved from <https://doi.org/10.1039/C6CC04721A>
- Khandelwal, H., Van Heeswijk, E. P. A., Schenning, A. P. H. J., & Debije, M. G. (2019). Paintable temperature-responsive cholesteric liquid crystal reflectors encapsulated on a single flexible polymer substrate. *Journal of Materials Chemistry C*, 7(24), 7395–7398. Retrieved from <https://doi.org/10.1039/c9tc02011j>
- Kim, D.-Y., Lee, K. M., White, T. J., & Jeong, K.-U. (2018). Cholesteric liquid crystal paints: in situ photopolymerization of helicoidally stacked multilayer nanostructures for flexible broadband mirrors. *NPG Asia Materials*, 10, 1061–1068. Retrieved from <https://doi.org/10.1038/s41427-018-0096-4>
- Kim, G., & Kim, J. T. (2010). UV-ray filtering capability of transparent glazing materials for built environments. *Indoor and Built Environment*, 19(1), 94–101. Retrieved from <https://doi.org/10.1177/1420326X09358020>
- Kim, J., Baek, S., Park, J. Y., Kim, K. H., & Lee, J. (2021). Photonic Multilayer Structure Induced High Near-Infrared (NIR) Blockage as Energy Saving Window. *Small*, 17, 2100654–2100662. Retrieved from <https://doi.org/10.1002/sml.202100654>
- Knoop, M., Stefani, O., Bueno, B., Matusiak, B., Hobday, R., Wirz-Justice, A., ... Norton, B. (2020). Daylight: What makes the difference? *Lighting Research and Technology*, 52(3), 423–442. Retrieved from <https://doi.org/10.1177/1477153519869758>
- Komanduri, R. K., Lawler, K. F., & Escuti, M. J. (2013). Multi-twist retarders: broadband retardation control using self-aligning reactive liquid crystal layers. *Optics Express*, 21(1), 404–420. Retrieved from <https://doi.org/10.1364/oe.21.000404>
- Kraemer, M., & Baur, T. (2019). Achromatic devices in polarization optics. *Optical Engineering*, 58(8), 082406-1–15.
- Kragt, A. J. J., van Gessel, I. P. M., Schenning, A. P. H. J., & Broer, D. J. (2019). Temperature-Responsive Polymer Wave Plates as Tunable Polarization Converters. *Advanced Optical Materials*, 7(21), 1901103–1901109. Retrieved from <https://doi.org/10.1002/adom.201901103>
- Kragt, A. J. J., Zuurbier, N. C. M., Broer, D. J., & Schenning, A. P. H. J. (2019). Temperature-Responsive, Multicolor-Changing Photonic Polymers. *ACS Applied Materials & Interfaces*, 11(31), 28172–28179. research-article. Retrieved from <https://doi.org/10.1021/acsami.9b08827>
- Li, C., Tan, J., Chow, T. T., & Qiu, Z. (2015). Experimental and theoretical study on the effect of window films on building energy consumption. *Energy and Buildings*, 102, 129–138. Retrieved from <https://doi.org/10.1016/j.enbuild.2015.04.025>
- Liang, Y. (2015). Liquid Crystals. Retrieved from <http://www.beautifulchemistry.net/liquid-crystals/>
- Liu, C., Fuh, A. Y., Chen, Y., Chen, J., Chen, L., Chen, J., & Chen, L. (2016). Research progress of cholesteric liquid crystals with broadband reflection characteristics in application of intelligent optical modulation materials. *Chinese Physical B*, 25(9), 096101–096111. Retrieved from <https://doi.org/10.1088/1674-1056/25/9/096101>
- Long, L., & Ye, H. (2014). How to be smart and energy efficient: A general discussion on thermochromic windows. *Scientific Reports*, 4, 6427–6436. Retrieved from <https://doi.org/10.1038/srep06427>
- Mann, D., Yeung, C., Habets, R., Vroon, Z., & Buskens, P. (2021). Building energy simulations for different building types equipped with a high performance thermochromic smart window. *IOP Conference Series: Earth and Environmental Science*, 855(1), 12001–12005. Retrieved from <https://doi.org/10.1088/1755-1315/855/1/012001>
- Mann, D., Yeung, C., Habets, R., Vroon, Z., & Buskens, P. (2020). Comparative Building Energy Simulation Study of Static and Thermochromically Adaptive Energy-Efficient Glazing in Various Climate Regions. *Energies*, 13, 2842–2859.
- Marchwinski, J. (2014). Architectural evaluation of switchable glazing technologies as sun protection measure. *Energy Procedia*, 57, 1677–1686. Retrieved from <https://doi.org/10.1016/j.egypro.2014.10.158>
- Mardaljevic, J., Kelly Waskett, R., & Painter, B. (2016). Neutral daylight illumination with variable transmission glass: Theory and validation. *Lighting Research and Technology*, 48(3), 267–285. Retrieved from <https://doi.org/10.1177/1477153515620339>
- Mcconney, M. E., Tondiglia, V. P., Hurtubise, J. M., Natarajan, L. V., White, T. J., & Bunning, T. J. (2011). Thermally Induced, Multicolored Hyper-Reflective Cholesteric Liquid Crystals. *Advanced Materials*, 23, 1453–1457. Retrieved from <https://doi.org/10.1002/adma.201003552>
- Mitov, M., Nouvet, E., & Dessaud, N. (2004). Polymer-stabilized cholesteric liquid crystals as switchable photonic broad bandgaps. *The European Physical Journal E*, 15(4), 413–419. Retrieved from <https://doi.org/10.1140/epje/i2004-10058-4>
- Mitov, M. (2012). Cholesteric Liquid Crystals with a Broad Light Reflection Band. *Advanced Materials*, 24(47), 6260–6276. Retrieved from <https://doi.org/10.1002/adma.201202913>
- Mohelníková, J., & Altan, H. (2009). Evaluation of optical and thermal properties of window glazing. *WSEAS Transactions on Environment and Development*, 5(1), 86–93.
- Ortiz-Gutiérrez, M., Olivares-Pérez, A., & Sánchez-Villicaña, V. (2001). Cellophane film as half wave retarder of wide spectrum. *Optical Materials*, 17(3), 395–400. Retrieved from [https://doi.org/10.1016/S0925-3467\(00\)00102-6](https://doi.org/10.1016/S0925-3467(00)00102-6)
- Painter, B., Irvine, K. N., Waskett, R. K., & Mardaljevic, J. (2016). Evaluation of a mixed method approach for studying user interaction with novel building control technology. *Energies*, 9(3), 1–23. Retrieved from <https://doi.org/10.3390/en9030215>
- Pérez-Lombard, L., Ortiz, J., & Pout, C. (2008). A review on buildings energy consumption information. *Energy and Buildings*, 40(3), 394–398. Retrieved from <https://doi.org/10.1016/j.enbuild.2007.03.007>
- Piccolo, A., & Simone, F. (2009). Effect of switchable glazing on discomfort glare from windows. *Building and Environment*, 44(6), 1171–1180. Retrieved from <https://doi.org/10.1016/j.buildenv.2008.08.013>
- Prieto, A., Knaack, U., Klein, T., & Auer, T. (2017). 25 Years of cooling research in office buildings: Review for the integration of cooling strategies into the building façade (1990–2014). *Renewable and Sustainable Energy Reviews*, 71(May 2015), 89–102. Retrieved from <https://doi.org/10.1016/j.rser.2017.01.012>
- Ranjekesh, A., & Yoon, T. H. (2019). Fabrication of a Single-Substrate Flexible Thermoresponsive Cholesteric Liquid-Crystal Film with Wavelength Tunability. *ACS Applied Materials and Interfaces*, 11(29), 26314–26322. research-article. Retrieved from <https://doi.org/10.1021/acsami.9b05112>

- Ranjesh, A., & Yoon, T. H. (2021). Ultrathin, transparent, thermally-insulated, and energy-efficient flexible window using coatable chiral-nematic liquid crystal polymer. *Journal of Molecular Liquids*, 339, 116804. Retrieved from <https://doi.org/10.1016/j.molliq.2021.116804>
- Rezaei, S. D., Shannigrahi, S., & Ramakrishna, S. (2017). A review of conventional, advanced, and smart glazing technologies and materials for improving indoor environment. *Solar Energy Materials and Solar Cells*, 159, 26–51. Retrieved from <https://doi.org/10.1016/j.solmat.2016.08.026>
- Sedaghat, A., Abbas Oloomi, S. A., Malayer, M. A., Alkhatib, F., Sabri, F., Sabati, M., ... Chowdhury, S. (2021). Effects of Window Films in Thermo-Solar Properties of Office Buildings in Hot-Arid Climates. *Frontiers in Energy Research*, 9, 1–22. Retrieved from <https://doi.org/10.3389/fenrg.2021.665978>
- Seeboth, A., Ruhmann, R., Mühling, O., Seeboth, A., Ruhmann, R., & Mühling, O. (2010). Thermotropic and Thermochromic Polymer Based Materials for Adaptive Solar Control. *Materials*, 3(12), 5143–5168. Retrieved from <https://doi.org/10.3390/ma3125143>
- Selkowitz, S. E. (1999). High Performance Glazing Systems : Architectural Opportunities for the 21 st Century High Performance Glazing Systems : Architectural Opportunities for the 21 st Century. In *Glass Processing Days Conference* (pp. 1–11).
- Serpe, M. J. (2019). Gel sandwich smartens up windows. *Nature News & Views*, 565, 438–439.
- Tzeng, S. T., Chen, C., & Tzeng, Y. (2010). Thermal tuning band gap in cholesteric liquid crystals. *Liquid Crystals*, 37(9), 1221–1224. Retrieved from <https://doi.org/10.1080/02678292.2010.492247>
- United Nations. (2018). *The World's Cities in 2018*. Retrieved 10 January 2020 from <https://digitallibrary.un.org/record/3799524>
- United Nations. (2019). *World Population Prospects 2019. Department of Economic and Social Affairs. World Population Prospects 2019*. Retrieved from <http://www.ncbi.nlm.nih.gov/pubmed/12283219>
- Van Heeswijk, E. P. A., Kloos, J. J. H., Grossiord, N., & Schenning, A. P. H. J. (2019). Humidity-gated, temperature-responsive photonic infrared reflective broadband coatings. *Journal of Materials Chemistry A*, 7(11), 6113–6119. Retrieved from <https://doi.org/10.1039/c9ta00993k>
- van Heeswijk, E. P. A., Meerman, T., de Heer, J., Grossiord, N., & Schenning, A. P. H. J. (2019). Paintable Encapsulated Body-Temperature-Responsive Photonic Reflectors with Arbitrary Shapes. *ACS Applied Polymer Materials*, 1(12), 3407–3412. Retrieved from <https://doi.org/10.1021/acspap.9b00841>
- van Heeswijk, E. P. A., Yang, L., Grossiord, N., & Schenning, A. P. H. J. (2020). Tunable Photonic Materials via Monitoring Step-Growth Polymerization Kinetics by Structural Colors. *Advanced Functional Materials*, 30, 1906833–1906840. Retrieved from <https://doi.org/10.1002/adfm.201906833>
- Wang, Y., Runnerstrom, E. L., & Milliron, D. J. (2016). Switchable Materials for Smart Windows. *Annual Review of Chemical and Biomolecular Engineering*, 7(1), 283–304. Retrieved from <https://doi.org/10.1146/annurev-chembioeng-080615-034647>
- White, T. J., McConney, M. E., & Bunning, T. J. (2010). Dynamic color in stimuli-responsive cholesteric liquid crystals. *Journal of Materials Chemistry*, 20(44), 9832–9847. Retrieved from <https://doi.org/10.1039/c0jm00843e>
- Wu, X., Yu, L., Cao, H., Guo, R., Li, K., Cheng, Z., ... Yang, H. (2011). Wide-band reflective films produced by side-chain cholesteric liquid-crystalline elastomers derived from a binaphthalene crosslinking agent. *Polymer*, 52(25), 5836–5845. Retrieved from <https://doi.org/10.1016/j.polymer.2011.10.036>
- Xiao, L., Cao, H., Sun, J., Wang, H., Wang, D., Yang, Z., & He, W. (2016). Double UV polymerisation with variable temperature-controllable selective reflection of polymer-stabilised liquid crystal (PSLC) composites. *Liquid Crystals*, 43(10), 1299–1306. Retrieved from <https://doi.org/10.1080/02678292.2016.1172351>
- Xu, X., Zhang, W., Hu, Y., Wang, Y., Lu, L., & Wang, S. (2017). Preparation and overall energy performance assessment of wide waveband two-component transparent NIR shielding coatings. *Solar Energy Materials and Solar Cells*, 168, 119–129. Retrieved from <https://doi.org/10.1016/j.solmat.2017.04.032>
- Yang, H., Mishima, K., Matsuyama, K., Hayashi, K.-I., Kikuchi, H., & Kajiyama, T. (2003). Thermally bandwidth-controllable reflective polarizers from (polymer network/liquid crystal/chiral dopant) composites. *Applied Physics Letters*, 82(15), 2407–2409. Retrieved from <https://doi.org/10.1063/1.1567809>
- Yang, T., Yuan, D., Liu, W., Zhang, Z., Wang, K., You, Y., ... Zhou, G. (2022). Thermochromic Cholesteric Liquid Crystal Microcapsules with Cellulose Nanocrystals and a Melamine Resin Hybrid Shell. *ACS Applied Materials & Interfaces*, 14(3), 4588–4597. Retrieved from <https://doi.org/10.1021/acsmi.1c23101>
- Yeung, C. P. K., Habets, R., Leufkens, L., Colberts, F., Stout, K., Verheijen, M., ... Buskens, P. (2021). Phase separation of VO₂ and SiO₂ on SiO₂-Coated float glass yields robust thermochromic coating with unrivalled optical properties. *Solar Energy Materials and Solar Cells*, 230, 111238–111249. Retrieved from <https://doi.org/10.1016/j.solmat.2021.111238>
- Yuan, X., Zhang, L., & Yang, H. (2010). Study of selectively reflecting characteristics of polymer stabilised chiral nematic liquid crystal films with a temperature-dependent pitch length. *Liquid Crystals*, 37(4), 445–451. Retrieved from <https://doi.org/10.1080/02678291003646207>
- Zhang, B., Lin, X., You, Y., Hu, X., de Haan, L., Zhao, W., ... Yuan, D. (2019). Flexible thermal responsive infrared reflector based on cholesteric liquid crystals and polymer stabilized cholesteric liquid crystals. *Optics Express*, 27(9), 13516–13526. Retrieved from <https://doi.org/10.1364/oe.27.013516>
- Zhang, L., Wang, M., Wang, L., Yang, D., Yu, H., & Yang, H. (2016). Polymeric infrared reflective thin films with ultra-broad bandwidth. *Liquid Crystals*, 43(6), 750–757. Retrieved from <https://doi.org/10.1080/02678292.2016.1142013>
- Zhang, P., Kragt, A. J. J., Schenning, A. P. H. J., Haan, L. T. De, & Zhou, G. (2018). An easily coatable temperature responsive cholesteric liquid crystal oligomer for making structural colour patterns. *Journal of Materials Chemistry C*, 6, 7184–7187. Retrieved from <https://doi.org/10.1039/c8tc02252f>
- Zhang, W., Kragt, S., Schenning, A. P. H. J., De Haan, L. T., & Zhou, G. (2017). Easily Processable Temperature-Responsive Infrared-Reflective Polymer Coatings. *ACS Omega*, 2(7), 3475–3482. Retrieved from <https://doi.org/10.1021/acsomega.7b00454>

- Zhang, W., Froyen, A. A. F., Schenning, A. P. H. J., Zhou, G., Debije, M. G., & de Haan, L. T. (2021). Temperature-Responsive Photonic Devices based on Cholesteric Liquid Crystals. *Advanced Photonics Research*, 2, 2100016–2100043. Retrieved from <https://doi.org/10.1002/adpr.202100016>
- Zhang, W., Schenning, A. P. H. J., Kragt, A. J. J., Zhou, G., & De Haan, L. T. (2021). Reversible thermochromic photonic coatings with a protective topcoat. *ACS Applied Materials and Interfaces*, 13(2), 3153–3160. Retrieved from <https://doi.org/10.1021/acsami.0c19236>
- Zhao, Y., Zhang, L., He, Z., Chen, G., Wang, D., Zhang, H., & Yang, H. (2015). Photoinduced polymer-stabilised chiral nematic liquid crystal films reflecting both right- and left-circularly polarised light. *Liquid Crystals*, 42(8), 1120–1123. Retrieved from <https://doi.org/10.1080/02678292.2015.1025871>

Additively Manufactured Urban Multispecies Façades for Building Renovation

Iuliia Larikova¹, Julia Fleckenstein¹, Ata Chokhachian¹, Thomas Auer¹, Wolfgang Weisser², Kathrin Dörfler¹

- * Corresponding author, larikova.y@gmail.com
- 1 TUM School of Engineering and Design, Germany
- 2 TUM School of Life Sciences

Abstract

This research investigates the potential of additive manufacturing and digital planning tools for the creation of location-specific façade redesigns that can host cavity-dependent animal species and develops methods for their realization. The proposed approach is explored based on a case study of a student dormitory in need of renovation in the urban area of Munich. Based on theoretical knowledge and design experimentations that link the fields of architecture, climate-responsive design, terrestrial ecology, and digital fabrication, a set of design principles for the additive manufacturing of inhabitable ceramic tiles is conceived and transferred into a computational design tool. The conception of single tiles and the overall façade design are developed in terms of their positive climatic impact on both the animal species and humans, their nesting opportunities, their structural feasibility, and their integrability with standard ceramic façade systems. To verify the fabricability of the proposed design, a façade fragment was additively manufactured as a prototype in 1:1 scale. The initial findings presented in this paper provide a glimpse of how emerging digital technologies could provide new ways to expand current habitual architectural planning and fabrication tools, to enable the creation of site-specific solutions, and to bring together human and animal needs.

Keywords

Additive Manufacturing, Computational design, Climate-aware design, Terrestrial ecology, Building renovation

DOI

<https://doi.org/10.47982/jfde.2022.powerskin.7>

1 INTRODUCTION

The preservation of biodiversity is considered one of the key factors in mitigating climate change. Urbanization, which displaces native wildlife and replaces it with impermeable surfaces, is one of the most significant contributors to the global decrease in biodiversity. Paved areas, lack of greenery, and significant resource consumption – buildings being one of the largest energy consumers (Bauer et al., 2013) – are all factors in cities that have a negative influence on biodiversity and, hence, the global climate (McDonald et al., 2013). Beyond the positive impact of biodiverse environments on the climate, juxtaposing human habitats with animals' can also have positive psychological impacts on humans (Sandifer et al., 2015). However, the human relationship with non-humans throughout human history has often been one of fighting against or even conquering nature (Tsing et al., 2017). This approach is reflected in the built urban context through infrastructure and buildings that are primarily tailored to overt human needs; that is, today's building envelopes consider attributes that serve human requirements, such as spatial organization, insulation, and aesthetics, and present themselves as hostile to the requirements of native wildlife. Another problem that most cities deal with today is the ageing of the buildings; many of them no longer satisfy modern ecological, energy-efficiency, or comfort requirements. In 2020, according to the European Commission report, building renovation rates in the European Union will be doubled by 2030, resulting in 35 million buildings renovated by 2030 and will maintain at this level after achieving European Union climate neutrality by 2050. Among others, energy efficiency, decarbonization, and life-cycle thinking are named the main principles of renovation (European Commission, 2020). These foundations could be seen as an opportunity to rethink the approach to urban renewal and to integrate new solutions into the existing urban fabric, enabling a shift towards a harmonious relationship with nature and the coexistence of humans with non-humans. Creating new envelopes for buildings needing renovation could be a chance to rethink and redesign façades toward the inclusivity of different species in the envelopes: small animals and birds, and the creation of positive microclimate conditions with the help of the surface design, for the wellbeing of both humans and other species. In this context, this research proposes to explore whether digital technologies could be used as a powerful tool to help build – literally and figuratively – a new way of co-habitation. It addresses the question of whether digital technologies could provide the necessary tools to extend the usual architectural tools for creating human habitats to create animal-friendly habitats, with the particular focus of this research being the development of such tools to accommodate nesting sites for selected species within building envelopes.

As such, the presented research provides initial findings of exploring an integrative approach that combines expertise in architecture, digital fabrication, climate-responsive design, and terrestrial ecology to redesign and transform building envelopes to host, breed, and protect cavity-dependent wildlife species in the urban context. In particular, the integration of microclimate performance and animal inclusion within a bespoke façade redesign using the possibilities of digital technologies and additive manufacturing is explored. Departing from a standard ceramic façade system, a digital design tool is developed, which allows for individually adapting the standard façade tiles towards a context-specific geometry, aimed at incorporating cavities for both self-shading effects and animal housing. The tool also enables the analysis of the static feasibility and its climatic performance through simulations. A functional prototype, at 1:1 scale, was produced with robotic extrusion 3D printing using clay and ceramic firing to test the fabricability of the proposed design principles. This research aims to create and demonstrate a preliminary design approach for a site-specific, wildlife-inclusive, and climate-performative urban façade design, as part of a global ecosystem that could be adapted and reproduced in different contexts using digital design and fabrication technologies.

The main body of this paper is organized by presenting the main stages of the research: Section 2 gives an overview of the research method; Section 3 contains the analysis, which contextualizes this research and provides an overview of the project's origins; Section 4 presents the design studies, which explain the development of the design tool (Section 4.1), details of the design explorations and their results (Section 4.2), and the validation of the proposed fabrication process, which documents the process, its limitations, and result (Section 4.3). Section 5 gives an evaluation of the proposed research method and process and discusses the design framework. Finally, Section 6 highlights the perspective of future work.

2 METHOD

To investigate the feasibility of wildlife-friendly and climate-conscious design for façade renovation, we apply a Research through Design (RtD) methodology, defined as “the possibility for design to be based on design practice, i.e., through artistic and creative design objects, interventions, and processes, to gain insights” (Bang et al., 2012) (Fig. 1), and an experimental case study based methodology by experimentally testing and validating aspects of the proposed method for a specific location in the urban context of Munich.

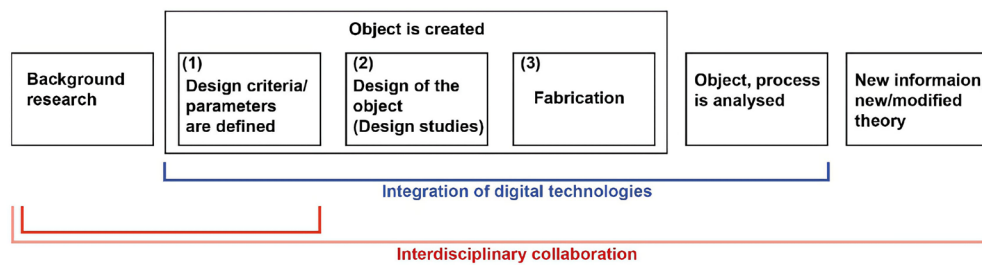


FIG. 1 Research through Design (RtD) method, as defined by (Herriott R., 2019), expanded by (1) the determination of design criteria, parameters, design systems, and fabrication methods and their primary analysis and evaluation; (2) the design of the object, including various parameter studies on different scales; and (3), the fabrication process, where the object is realised in real-scale to testify the legitimacy of the design solutions and the proposed fabrication process.

The interdisciplinary collaboration between architects, ecologists, and façade specialists is crucial to address the multiple aspects that define the scope of this research, comprising the topics of cavity-dependent species integration, microclimate considerations, as well as the application of clay extrusion 3D printing for custom ceramic tiles. The background research, referred to in the case of this project as “State of the Art” (Section 3), includes a literature review and the study of similar projects and research in this field, which forms a basis for the design process, in particular for the definition of sub-criteria and parameters. The practical experience and theoretical knowledge of the specialists from the research areas involved also formed a solid basis for the experimental research method of the project (Whitelaw et al., 2021).

To conduct the proposed RtD process, the experimental case study is set in a specific urban context – a student residence in Munich, Germany. Provided by the terrestrial ecology research (see Section 3), three main target species for the selected urban context are chosen: the bird species House Sparrow and Black Redstart, and the bat species Common Pipistrelle. The species' specific needs set the main boundary conditions for the project, which we have consecutively converted into parameters for the conception of design principles and the generation of design proposals.

In line with Multi-Objective Optimization techniques (Bertagna et al., 2021, Brown & Mueller, 2017), digital technologies are implemented at all design stages to guide the design process (Fig. 1). This technique allows evaluation, re-evaluation, and adjustment processes to be integrated into all design stages and to provide an optimal choice of sub-options. To fundamentally address the problem at various scales, the design of the single façade element and the design of the whole façade pattern are conceived and evaluated in terms of climate efficiency and fabricatability with the help of simulations. For the purpose of renovation, a retrofitting design approach is used – the elements are designed to fit into existing ventilated façade systems such that standard-sized tiles can be replaced with bespoke tiles of added functions at required locations. Additive manufacturing with clay was chosen for the realization of bespoke tiles, which have the ability to realize complex, high-resolution geometries. In addition, clay was considered the best option for initial investigations as a robust and potentially species-innocuous material. To verify the design for realization feasibility, i.e., to verify its fabricatability and evaluate the limitations and prospective of the selected digital fabrication method, a set of ceramic tiles are additively manufactured, fired, and assembled into a façade fragment prototype at 1:1 scale.

3 STATE OF THE ART

3.1 ARTIFICIAL HABITS IN THE BUILT ENVIRONMENT

The focus on inhabitable building envelopes, such as previously shown with the concept of Animal Aided Design (AAD) (Hauck & Weisser, 2015), has received increasing attention in recent years. Key objectives of AAD link urban planning disciplines with technical solutions to permanently keep and protect urban wildlife (Weisser & Hauck, 2015). Wildlife inclusive design strategies are characterized by a multidisciplinary approach, in which all aspects of the project, such as the choice of target species, landscape, and open spaces design, are planned as a united system and aligned with each other in architectural solutions (Apfelbeck et al., 2020). Built examples such as the social residential housing with integrated children's facilities in Laim – Germany, designed by the Munich architects bogevisches buero (bogevisches buero & GEWOFAG Projektgesellschaft mbH, 2019) in collaboration with Prof. Weisser and Prof. Hauck, already show this interdisciplinary approach of carefully designed habitats for hedgehogs, house sparrows, green woodpeckers, and pygmy bats (Figure 2) (Apfelbeck et al., 2019).



FIG. 2 Integration of nests into buildings' facades, Weisser & Hauck, bogevischs buero architects, 2015.

The design of the project focused on the wall's built-in elements to fulfil a single function: to provide shelter for birds. However, the design does not offer any additional visual or climate performative qualities. Moreover, the built-in elements cannot be temporarily removed from the façade, making cleaning and revising processes difficult. Therefore, in the experimental design study presented, we aim to extend the currently deployed solution with a multifunctional approach that includes multiple functions at the level of the single element, making this element the starting point of architectural explorations.

3.2 ADDITIVE MANUFACTURING PROCESSES FOR WILDLIFE INCLUSIVE DESIGN

Additive Manufacturing (AM) technology has been increasingly promoted as a sustainable production technology over the past decade (Jiang et al., 2018). Its potential for waste-free production, great material variety, and design freedom are now becoming increasingly prominent in the construction sector (Willmann et al., 2018). The production process of AM building elements typically occurs through the digitally controlled layer-by-layer application of material, providing a high degree of individualization and reducing material waste (Kloft et al., 2021). In combination with computational design and simulation, AM allows for the expansion of architectural possibilities, enabling the integration and customization of multiple functions through geometric and material freedom on a par (Dunn, 2012). Ceramic materials, due to their robustness, recyclability, and implementation in the building industry in the form of handy components for façade constructions, are particularly attractive in terms of their potential for AM (Wolf et al., 2022). In this context, the project Cabin of Curiosity has demonstrated the production of bespoke geometries of varying façade elements produced with clay extrusion 3D printing (Rael et al., n.d.). Each of the three typologies of elements incorporates a different mounting principle; moreover, each element integrates several functions: hosting vegetation, rain protection, and shade – made possible through the application of computer-aided technologies combining design with fabrication. The research defining framework for computer-aided design and manufacturing of habitat structure for cavity-dependent animals (Parker et al., 2022) explores an interdisciplinary approach on par with the possibilities of generative design and 3D Printing in terms of creating artificial cavities. In the case study of the owl (Parker et al., 2022), researchers tested several generative design variations and evaluated them before fabrication. The final selected geometry was adjusted for the owls' and stakeholders' needs. Modular components were produced in different manufacturing techniques: 3D Printing with wood and CNC cutting. This study presents the potential of digital technologies in terms of conservation initiatives. The research explores hanging nest structures, however, in cities or dense urban conditions, there is a limit of free available trees for placing the nests. Therefore, possible development of this idea could be expanding structural variety for placing the nests in diverse urban contexts.

3.3 DESIGN STRATEGIES FOR CLIMATE-RESILIENT URBAN FAÇADES

Urban climate phenomena, such as the Urban Heat Island Effect (UHIE), are strongly related to and amplified by the built environment (Roesler & Kobi, 2018). Materiality, shape, and morphology of buildings, greenery, global radiation, and evaporative cooling are parameters that influence the outdoor climate (Perini et al., 2017). By precisely controlling and planning such parameters, the outdoor climate comfort could be positively influenced with the help of computational design and fabrication. For example, the Climate Active Brick project (Fleckenstein et al., 2022) has investigated possibilities to reduce solar exposure and, hence, solar radiation, by integrating self-shading patterns

into the classic rat-trap bonded brickwork. With the help of climate simulations, the optimal context-specific self-shading brick pattern was found, characterized by differentiated frontal brick rotations. The fabrication of the brick assemblies' customized pattern was then achieved with the help of a robotic arm. The focus of the current approaches lies on creating better microclimate conditions for humans; therefore, to improve biodiversity, it is important to include the needs of species in microclimate design.

4 EXPERIMENT - CASE STUDY PROJECT

4.1 SELECTION OF THE LOCATION

As defined by Apfelbeck et al. (2020), the choice of the urban context and a systematic approach are significant components of a successful wildlife-inclusive design. Therefore, the search for a suitable building was the first step in the research project development. The criteria for the building choice for the experimental project within the Munich urban area were defined based on the background research and desired goals: the building should be located in a dense urban zone to study the possibility of improving biodiversity/microclimate in dense urban conditions through the envelope design, with available greenery in proximity needed for nurturing the selected species, and a minimum of 40% wall-to-window-ratio, since glass façades are not suitable for integrating nests. A suitable prototypical site influenced by UHIE was found in the Maxvorstadt area of Munich based on UHIE study provided by Funk, et al. (2014), a student dormitory with available east and north façade surfaces and in need of renovation.

4.2 DEFINITION OF DESIGN CRITERIA

In a preliminary design phase, based on the state-of-the-art research and project goals, the following main design criteria that can influence the geometric differentiation and architectural idea are being determined: species requirements, including the microclimatic improvements for the selected species and humans, the façade system and structure, and fabricatability. Each criterion has its own set of parameters which are reviewed, analyzed, and contextualized before being merged and converted to design parameters, as described below.

4.2.1 Species Needs

As land-use modification pushes many bird species away from land areas, many species, such as the Common Redstart, are now located in urban environments (Droz et al., 2008). Wildlife-inclusive architectural design could help to provide species in the cities with suitable conditions within the built fabric. Some factors for the nests, such as the size of the nest, the height from the ground, and if the species prefer to live alone or near their neighbours, could be addressed directly through geometry – with the correct position of a nest on the façade, the right size of the nest, and correct size of the nest openings. Other factors, such as temperature and protection from the wind, could be devoted to the microclimate parameters, which cannot be solved directly by geometry or placement on the façade; however, they could be influenced by creating a design that would reduce the amount of radiation or protect the nest from the wind, reducing the façade pressure.

TABLE 1 Selected species need matrix (Larikova I., 2021)

	Species	Size of the species	Height of the nest from the ground	Number of nests	Distance between nests	Building orientation	Avoid	other
	House Sparrow	15-17 cm	3-10 m	Colonies with 5-10 nests	Min 0,5 m	W, N, E	High temperature, strong wind	Nests need to be cleaned once in 2-3 years
	Black redstart	13-15 cm	1-4 m	Prefer to live alone (or in couples)	-	W, N, E	High temperature, strong wind	Nests need to be cleaned once in 2-3 years
	Common Pipistrelle	3.5 – 5 cm	3-6 m	Groups from 3 to 5 caves	Min 0,6 m	S	Too low temperature, dryness, strong wind	Nests could be self-cleaning

TABLE 2 Geometrical requirements of the nests

	Species	The shape of the nest	Size of the nest	The shape of the entrance	Size of the entrance
	House Sparrow	Sphere or rectangular	20-30 cm * 15-20 cm *15-20 cm	Round or rounded rectangular	D = 3-6 cm
	Black redstart	Sphere or rectangular	20-30 cm * 18-24 cm *18-22 cm	Oblong, balcony-like	W = 12-18 cm, H = 8-15 cm
	Common Pipistrelle	Oblong and narrow parallelogram	20-30 cm * 30-60 cm *12-18 cm	Oblong and narrow	W = 18-20 cm, H = 5 -7 cm

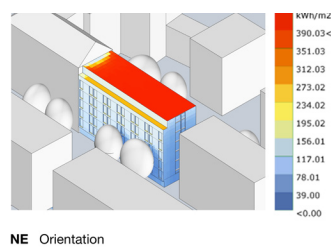
Based on the data collected by researchers in the field of ecology (Bischer et al., 2017.; Droz et al., 2008; Koryakina, 2018; Londoño, 2007; Weggler, 2006), and the direct consultations with specialists and industry professionals, the most important criteria for three selected species – the Black Redstart, the House Sparrow, and the Common Pipistrelle - are defined and summarised in Table 1, whereas geometric requirements for the nests are summarised in Table 2.

4.2.2 Microclimate Improvements for Species and Humans.

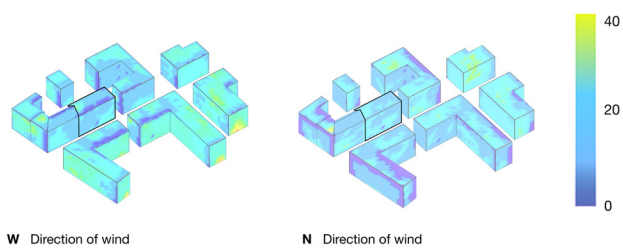
Although there is some data on preferred temperatures and humidity levels for the selected species, finding the perfect conditions for nest placement in dense urban environments is not straightforward. Digital analytical tools implemented from the early design stages make the decision-making process more precise and conscious and also serve as a base to create a design that would help to improve given climate conditions toward the species' requirements and needs.

However, to model and quantify the contribution and effects of every single parameter, both in the site selection and façade design process, several detailed computational models would be required. To reduce the computational complexity and focus on the geometry-driven parameters, two main environmental forces are selected to be simulated in this project. First, the amount of radiation incident on the building influences the microclimatic conditions of the façade. In general, this radiation should be reduced, both to protect the built-in nests from overheating and to avoid general overheating of the façade, to contribute to a well-designed microclimate for humans. Second, the wind façade pressure incident on the building influences parameters such as weathering. Here, too, the wind pressure should generally be reduced in habitable areas.

To address the selected microclimate parameters, the reduction factor is used as a basis for subsequent design developments. To proceed with developing and exploring a site-specific design solution, first, the existing state of solar radiation and the wind façade pressure are analyzed with the help of computational tools: The Ladybug plugin for solar radiation and Eddy 3D plugin for façade wind pressure are used within the architectural design environment Rhino (McNeel & Associates, n.d.) and Grasshopper, using the EPW (energy-plus) map for Munich. The simulations are done for the time frame of June to August, between 11am to 4pm, as the potentially hottest temperature possible in that time frame. The focus of the analysis is made on the west façade, as it is the street façade, which provides a higher potential for exploring visual qualities of wildlife-inclusive design in the urban context.



NE Orientation
 FIG. 3 Solar radiation analysis, June-August; 11am – 4 pm (Larikova I., 2021)



W Direction of wind N Direction of wind
 FIG. 4 Wind facade pressure analysis, west and north directions of wind, June-August; 11am – 4 pm (Larikova I., 2021)

Figure 3 depicts the output of the solar radiation analysis, in which dark blue zones receive little or no solar radiation while red zones are significantly affected. As the simulation shows, the vertical façade surface exhibits a progression from blue to green from the lower to the upper part of the façade, greenish especially in the higher areas, which would be ideal for the placement of nests due to their height and orientation. These green zones, indicating a high level of solar exposure, therefore need solutions that can reduce the amount of solar radiation for better comfort of the species to be housed and for better microclimate comfort for humans. Figure 4 shows the result of wind simulation for north and west winds. Dark blue zones depict areas with no or low wind façade pressure, whereas yellow zones show high levels of this pressure; hence, they would need to be adjusted to host nests. In sum, the analysis serves to detect façade areas which are directly suitable for placing nests for the selected species and areas which need microclimate improvement. Areas that are highly affected by wind or solar exposure are locally improved with the help of the design of the single façade elements and conscious elements' distribution (see Section 4.3).

4.2.3 Façade System

Based on background research, a Ventilated Façade Systems (VFS) with ceramic wall elements was selected. Though External Thermal Insulation Composite Systems (ETICS) are the most common systems in renovation projects in Europe, particularly in Germany (Asam, 2017) VFS have high efficiency in insulating properties, and are relatively easy to install (Bernhard Rudolf, 2012). Key parameters that influenced the choice of the façade systems are presented in Table 3: VFS have the advantage of having additional air space between the façade surface and insulation, and thus, a flexible layer thickness, which is crucial for the project, as this additional space has potential to integrate the nesting part of the tile behind the façade surface. VFS also shows good compatibility with ceramic façade tiles. Moreover, the idea of the experimental project is to mix standard industrially fabricated ceramic tiles with customized additively manufactured ones for higher cost and time efficiency. Therefore, the selected VFS sets several parameters for the design of a single façade element: a rear part must fit into the substructure profile, while the dimensions of custom elements should match standard tiles.

TABLE 3 Duration differences for fabrication, extraordinary maintenance and disassembly activities (the percentages represent the difference of that façade option respect the fastest solution in each phase)

	Building costs efficiency	Thermal insulation properties	Flexibility of the layers thickness	Revision possibility after installation
ETICS	√	√		
VFS		√	√	√

4.2.4 Fabricatability

The selected AM manufacturing process of robotic clay 3D printing also has specific limitations that need to be considered in the design and parametric studies, i.e., the process requires material to be deposited continuously in layers, the elements must be stable during extrusion 3D printing and drying, and the overall geometry is limited to round edges, specific printing path lengths, specified layer height and thickness, and maximum overhang angles. Parameters from a literature search served as a basis. During a series of digital studies and test prints, the parameters were adjusted according to the experimental results.

4.3 DESIGN STUDIES AND RESULTS

4.3.1 Microscale – Experimental Design of a Single Element

The design of a single element departs from the geometry of an industrially fabricated ceramic tile of a ventilated façade system, which is based on a hollow core and is hung vertically onto a substructure (Fig. 5, left). This ceramic tile can be produced using the typical industrial extrusion method, but due to its geometric features, it can also be produced using the proposed extrusion 3D printing method, either with its standard shape or with geometric variations to integrate the proposed multi-species requirements, that is, to integrate the self-shading effect for contributing

to the positive influence on the façade microclimate, and to integrate nesting opportunities, which, additionally to the climate-active function, can host the nests for the selected species. All tiles have the same outer boundary of 35x20cm to fit into the standard size of the ventilated façade system for ceramic tiles. In order to reduce both the solar exposure through self-shading effects and the pressure of the wind on the façade, the front surface of the climate-performative tiles is deformed outwards with a fold of varying depth and angle. According to selected studies addressing the topic of wind pressure, vertical folds are more effective in terms of wind façade pressure reduction (Kwok & Grondzik, 2007; Lignarolo et al., 2011; Simiu, 2011), and also effective for conceiving a self-shading effect. With the help of three parametrically controlled points that create a depth from 2 to 10 cm, corresponding with the amount of radiation or wind pressure needed to be reduced, the folded frontal surface of the tile can be shaped at varying depths (Fig. 5). The climate-performative tiles with nests incorporate openings at the bottom of the front surface which can be parametrically adjusted from species to species (based on data from Table 2: Geometrical requirements of the nests), without changing the overall tile geometry (Fig. 6). These openings are connected directly with the hollow core incorporating the nests as depicted in Fig. 7.

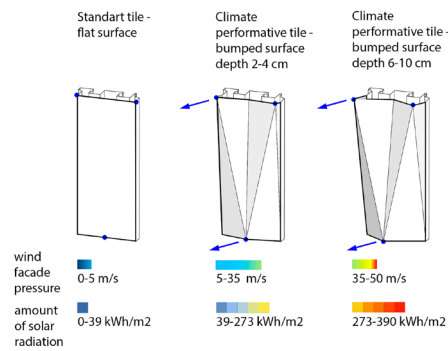


FIG. 5 Climate performative tile, front surface formation principals

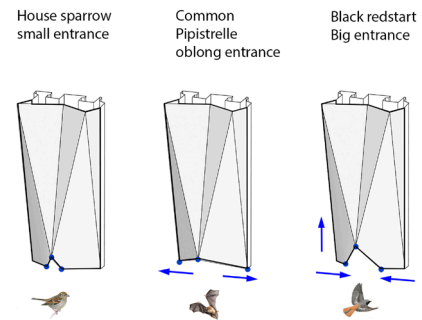


FIG. 6 Climate performative tile with nest, front surface entrances for species principal

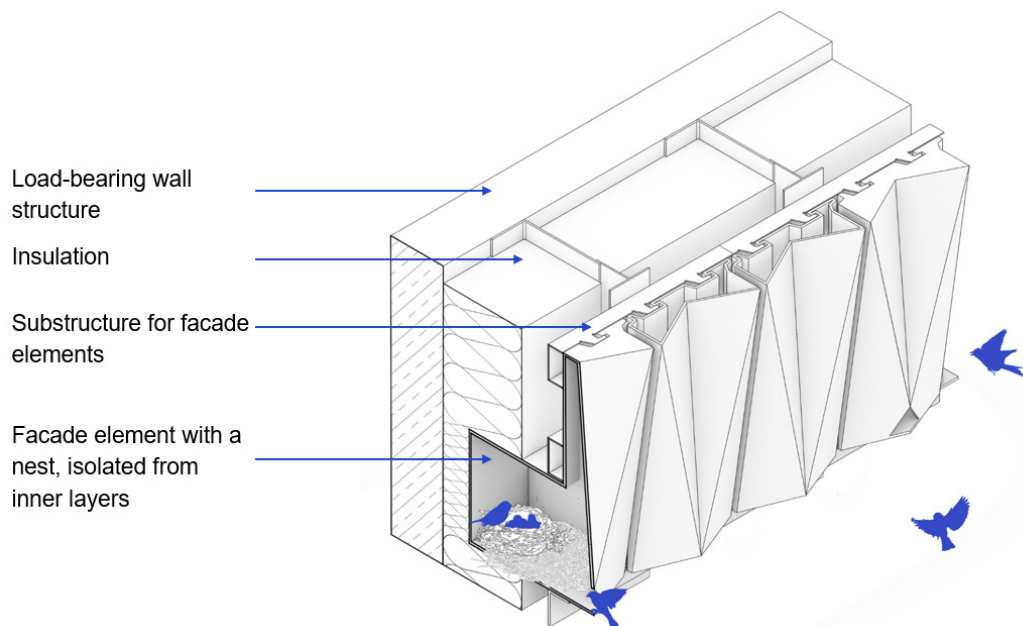


FIG. 7 Axonometry section of the façade fragment (Larikova I., 2021)

Each tile has the same structural profile on the back side as the standard tiles to be installed onto the standard sub-structure. Moreover, the tiles for hosting the animal species integrate the nests into the back side, whose sizes could also vary for different species without the need to change the substructure (Fig. 7).

The air layer and reduced insulation layer allow the incorporation of the nest parts into the ventilated system without interfering with the wall structure, therefore, making the approach relevant for renovation purposes. Unlike the other tile types, the tiles with nests have permanently closed cover tops and temporarily closed bottoms to protect the internal façade systems from birds and litter. The advantage of using the ventilated façade system over built-in components is the ability to provide easier access to the nests after assembly (elements could be taken out individually from any place of the façade after mounting) and thus provide more flexibility in terms of the periodic cleaning required (Table 1: Selected species needs matrix).

4.3.2 Macroscale – Context-Specific Parametric Façade Design

To test the features and potential impact of bespoke tile designs on larger surfaces, the west street façade of the student dormitory building is chosen for more detailed façade design studies. Three façade maps, namely 1) to simulate solar radiation, 2) to simulate wind façade pressure, and 3) to indicate the preferred heights of the species (Fig. 8a), were merged into one map (Fig. 8b) as a basis for the distribution of the custom tiles.

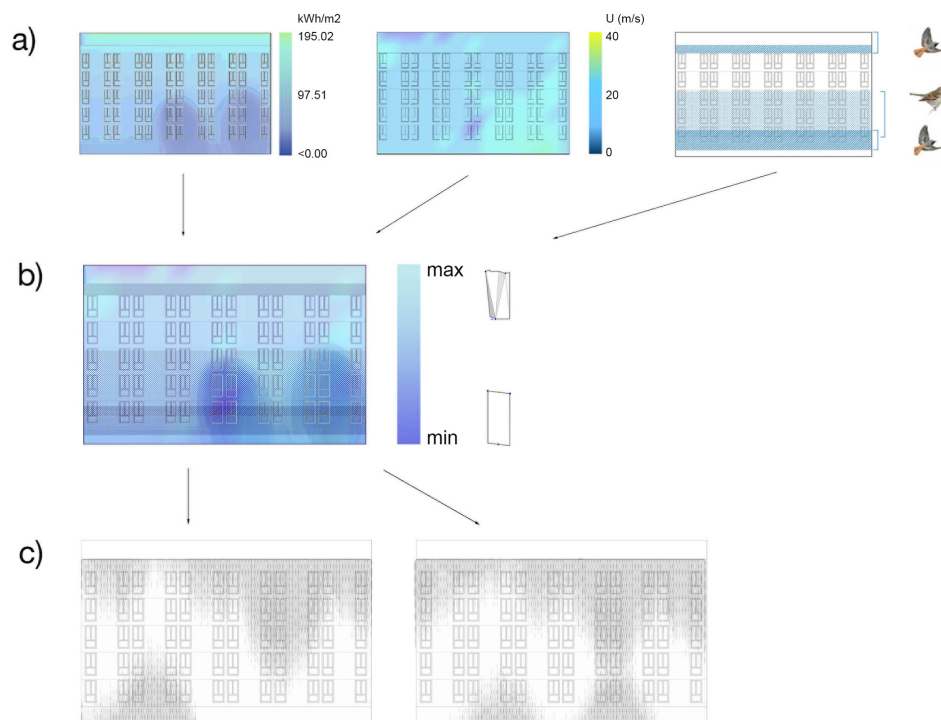


FIG. 8 a) Maps with climate simulations, solar and wind exposure, and the required height for species, b) merged façade maps, and c) generated façade patterns based on the information given in a)/b)

In Fig. 8b, lighter zones correspond with a higher amount of solar radiation and wind pressure, therefore, climate-performative tiles are distributed there; in the darker zones, standard tiles are used, whereas the climate-performative tiles with nests are distributed according to the species' needs. The rule for avoiding undesirable interactions between humans and species and preventing the invasion of litter into apartments was implemented as an additional input parameter: nests were not allowed to be placed directly under windows or balcony doors. Different options of the tiles' distribution resulted in differentiated façade patterns (Fig. 8c), one of which was chosen, manually revised, adjusted for the urban context, and transferred into the final façade design (Fig. 9).



FIG. 9 Visualisation in the urban context (Larikova I., 2021)

To verify the assumption of the microclimatic behaviour of the proposed façade design, namely, solar radiation reductive behaviour, simulations with the façade fragment are conducted. As depicted in Fig. 10, according to the simulations undertaken with the Ladybug plugin within the architectural design environment Rhino (McNeel & Associates, n.d.) and Grasshopper, as a result of the self-shading effects caused by tiles with folds, the solar radiation could be reduced from 200- 150 kWh/m² to an average of 0-50 kWh/m² within the analyzed time frame (June to August between 11am and 4pm), the most performative are the tiles with the protrusion/depth ratio more than 7cm.

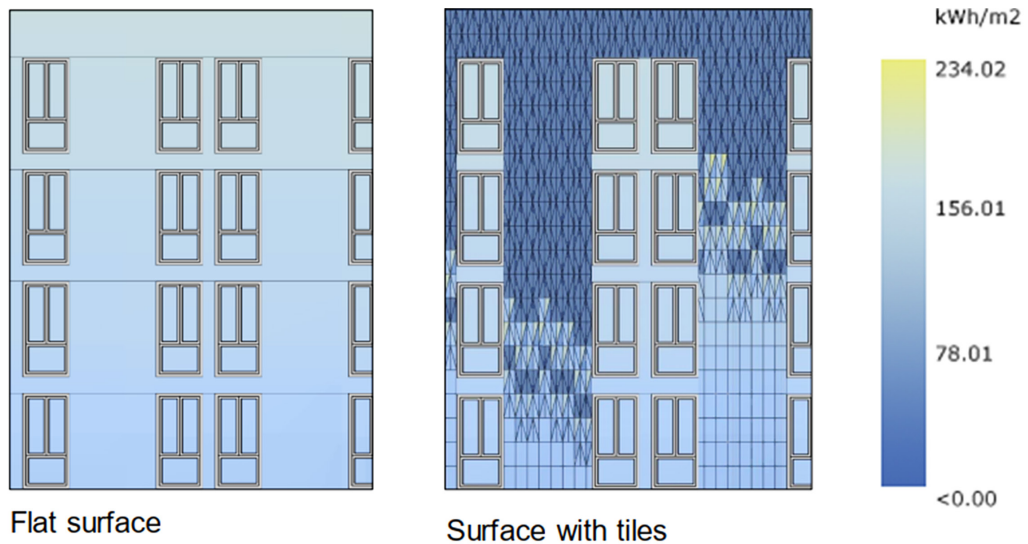


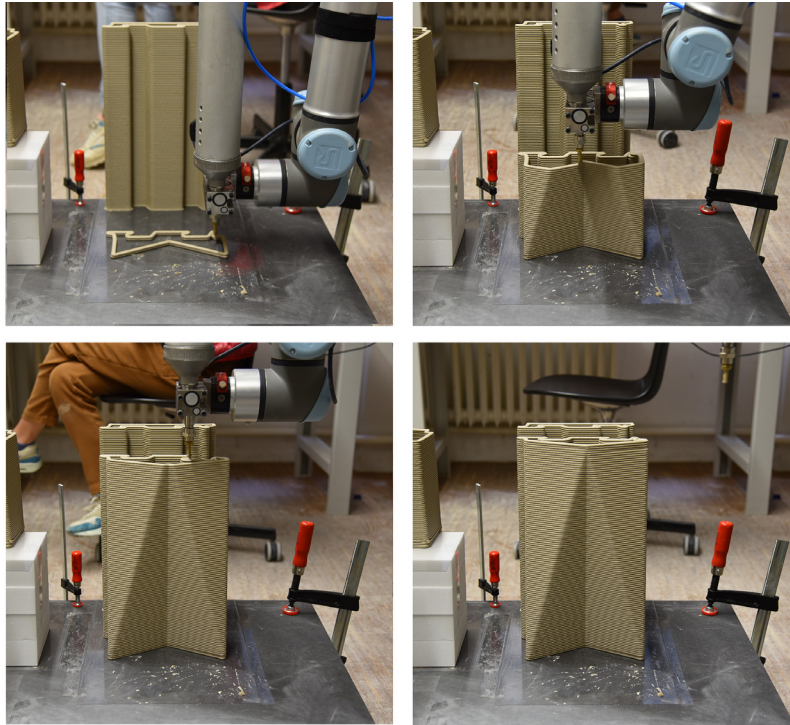
FIG. 10 As intended in the façade design, the simulation demonstrates a reduction in the amount of solar radiation of the façade when fitted with self-shading tiles in areas of higher solar exposure. (Larikova I., 2021)

4.4 PROTOTYPE FABRICATION

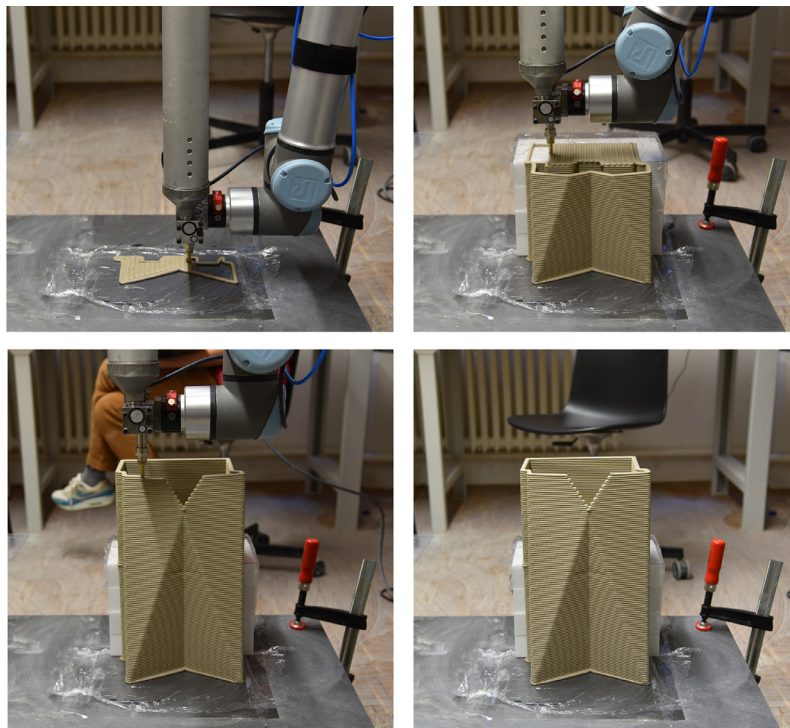
To verify fabricability and evaluate the limitations and prospects of the chosen digital fabrication process, a set of ceramic tiles of a selected area of the designed façade was additively manufactured and assembled into a 1:1 scale prototype. The production of the ceramic tiles includes the following processes: After the 3D extrusion process (4.1.1), the elements have to be dried (4.4.2), which requires defined conditions and preparations. These two processes are followed by the firing of the ceramic tiles (4.4.3), necessary to achieve maximum strength properties and allow the elements to withstand outdoor weather conditions for assembly (4.4.4). During the prototype manufacturing process, 15 tiles were 3D printed; nine of these, found to be of the best quality after firing, were mounted onto the substructure of a standard ventilated façade system of the final 60 x 108 cm prototype. Three of the tiles produced are the tiles with nests for two of the three selected species – the Black Redstart and House Sparrow.

4.4.1 3D Ceramic Extrusion 3D Printing

The original geometry of the tiles is represented by a surface-based geometry that is sliced to generate the paths for 3D Printing. With the nozzle diameter of 5 mm, the required slicing height of the layers is determined as 35 mm; the potential shrinkage from the drying and firing processes is calculated and planned prior to manufacture so that the tiles are produced approximately 11% larger than the final target size. The material used for the tiles is a grossed, ready-made ceramic body from the company Witgert with around 20% chamotte to gain maximum durability after firing. The printing time of one average layer with an average length of 55-70 cm of the bespoke tiles took around 40 seconds, which resulted in a printing time of around 70 minutes for one tile and allowed about three tiles to be produced on average in 8 working hours. Fig. 11.a documents the 3D printing process of a climate-performative tile, and Fig. 11.b documents the fabrication of a climate-performative tile with an integrated nest, which required temporary support for printing the nest cover to be added manually.



a Climate performative tile



b Tile with the nest

FIG. 11 Documentation of 3D printing (Larikova I., 2021)

4.4.2 Drying

The 3D printing process is followed by a drying process with the aim that the elements do not deform unevenly or crack due to shrinkage of the material. The geometry of the elements caused uneven shrinkage of the ceramic material, which became a major problem during the manufacturing process. The lab used for Printing and drying contained about 50% humidity. This low humidity level resulted in a very rapid and heterogeneous drying process, which caused significant deformations, especially twisting, of the vertical elements, with deviations of 5% to 15% from the original shape being observed (Fig. 12). Therefore, some of the elements were printed on a non-absorbent board, as it was believed that allowing this board to absorb water from a printed element would result in further deformation. However, no differences were observed between the elements printed and dried on these two types of boards. The next iteration thence included stiffening bridges within the geometry of the elements to provide better balance and less deformation. The final drying took about two weeks, after which the elements were carefully transported in order to subject them to the first so-called bisque firing in industrial plants. Another issue was the fragility of the elements after drying, which caused some tiles losses during transportation.

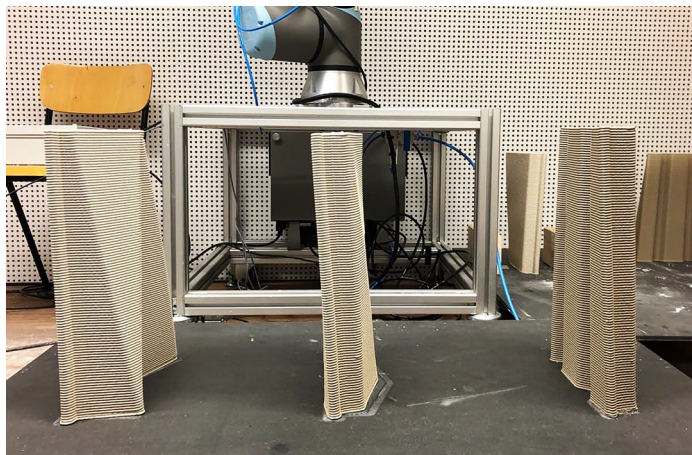


FIG. 12 During the drying process, deformations of the tiles were observed, caused by the low humidity level of the space and the uneven drying process. (Larikova I., 2021)



FIG. 13 Fired ceramic tile with a nest

4.4.3 Firing

To harden the raw ceramic element and to give the material maximum strength, elements were bisque fired at around 900°C. Firing was uneventful – no cracks appeared. The elements were glazed again and fired at 1200°C to achieve maximum durability of the elements enabled by the industrial production facilities. After firing, ceramic elements are typically more durable and stable compared to their dried state. However, they remain fragile, which can lead to further damage during transport and assembly operations. Fig. 13 shows a fired element with an integrated nest before assembly.

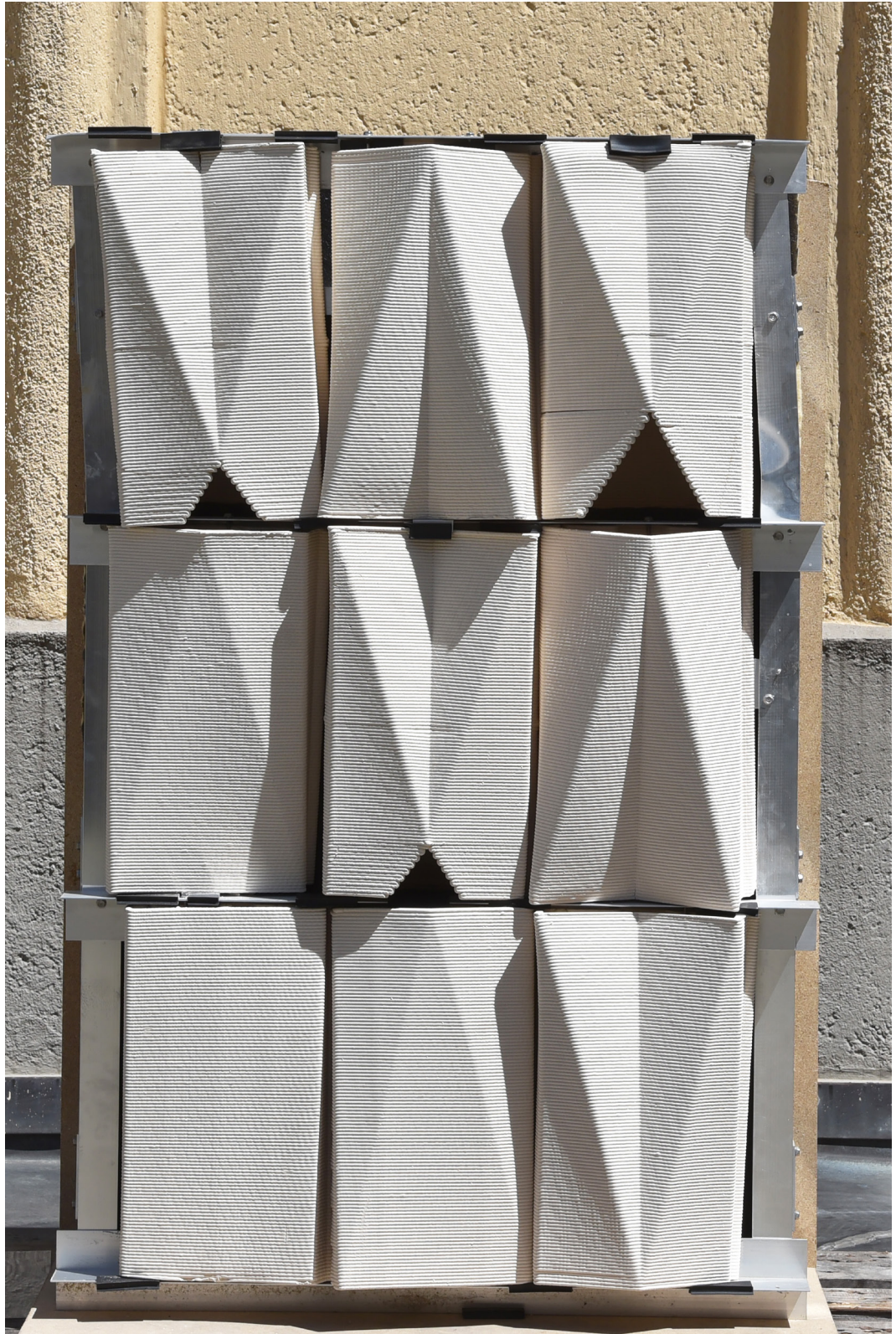


FIG. 14 Final assembled prototype

4.4.5 Assembly

As depicted in Fig. 14 and 15, a final prototype was assembled consisting of: nine tiles, eight of which were climate-performative, and three of the eight include nests; the insulation steel substructure; and the planned insulation layer behind it. Deformations caused mainly by the drying process did not prevent the final assembly, however, they made it significantly more difficult. It demanded additional fastening elements, making it laborious to take one element out for required future cleaning.



FIG. 15 Final assembled prototype

5 RESULTS AND CONCLUSION

5.1 SUMMARY OF RESULTS

This research presented preliminary results of the integrative design method and digital fabrication for wildlife-inclusive façade design. An analytical-based design approach with the integration of digital tools throughout the whole planning process was tested, validated, and analyzed; the AM tools have shown their potential for facilitating wildlife-inclusive façade design in terms of species needs, design quality, and the retrofitting of buildings in the urban contexts.

5.2 INTEGRATIVE DESIGN APPROACH

The integrative design approach for enabling wildlife-inclusive façade renovation has shown that the implementation of digital tools from the early design stages helps to link and collect the information of different disciplines and contributors within one computational design model. In particular, it contributed to the better integration of different functions both within a single façade element and the entire façade retrofitting design through the synthesis of different design criteria. Thus, the thorough analysis and simulation in the preliminary design phases formed a basis for well-founded design investigations, the evaluation of various options, and finding and selecting solutions. Together with experimental studies concerning the fabrication, and feedback loops of design adaptations and optimization cycles with respect to the fabricability of the tile designs, a continuous digital design-to-fabrication process could eventually be achieved. The experimental project has proven that for the successful development of the wild-live inclusive design for façades it is essential that several aspects of façade designs are investigated and improved simultaneously, in comparison with a sequential design approach where different disciplines are integrated on different design stages. Therefore, multifunctionality and visual architectural qualities distinguish the result of the approach. However, the integrative design approach in its current state also has certain limitations. For example, simulation of the actual behaviour of species and evaluation of the design in terms of its wildlife-friendly suitability cannot be performed due to the lack of sufficient background information and data. Due to the experimental nature of the project, the definition of design parameters related to animal behaviour was rather superficial, based on standard design principles and general information about the animal behaviour. The suitability can therefore only be analyzed experimentally on real-world prototypes and then returned to a digital model as part of future research.

5.3 FABRICATABILITY

Digital fabrication, namely extrusion 3D printing AM, has preliminarily proven its feasibility perspective in terms of site-specific animal-inclusive design solutions, which facilitate variability and local differentiation. The experimental project has shown that AM could contribute to the crucial improvement of retrofitting strategies and multifunctionality compared to the current traditional techniques. Manufacturability was demonstrated by producing a 1:1-scale prototype (Fig. 15), in which the tiles could be manufactured, fired, and assembled into the intended façade segment, despite manufacturing-related deformations. Some manufacturing obstacles encountered during the process, such as the shrinkage caused by the drying process and the fragility of the elements, would have to be addressed by more process and optimization iterations in the future. A short summary of the evaluated fabricability criteria could be seen in Table 4: the strongest feature of the AM production is a very high accuracy and resolution of the printed geometry, whereas a major challenge relates to deformation during drying. This obstacle could potentially be addressed by extended process simulation prior to production or by a selection of another cladding system or substructure that is more tolerable to potential deformations.

TABLE 4 Fabricability parameters evaluation

	Accuracy of 3D printed Geometry	Durability after drying	Deformations caused by drying	Durability after firing	Deformations caused by firing	Compatibility with the selected façade system
high	√		√			
medium				√		√
low		√			√	

6 OUTLOOK

Exploring a new experimental topic that integrates several disciplines evokes many questions and discussions about its further scientific development and possible practical application. The chosen methodology has proven its feasibility, however, many aspects of the future work could be optimized. The research was conducted on different scales, and further issues could be addressed regarding scales from urban to macro and include a variety of potential research directions.

On the urban scale, it would be necessary to understand the possibility of species integration not only on the urban block level but on the city planning level; theoretical research, simulations, integration, and interdisciplinary planning on a city scale could facilitate more viable architectural solutions in the future.

On the macroscale, several topics need to be researched further. First, the fabrication process could be improved for future projects in several ways. For example, more suitable drying conditions should be tested, deformations could be precalculated, and the geometry could be adjusted more precisely to prevent deformations (e.g., as tested with stiffness bridges). Another possible direction for further research could be testing other AM or digital fabrication techniques, such as particle bed 3D printing or casting moulds. Second, real-life on-site tests are needed for further development of the design basis. Fig. 16 demonstrates a vision of a façade test bed, that is, to depict that it will be essential to test demonstrators in real-world scenarios, document the behaviour of a species and verify the correlation between assumption and actual practice of the nest usage by the species of interest, as well as analyze on-site climate parameters. Such data would be required to serve as an essential basis for subsequent design iterations.



FIG. 16 Collage of the future vision of multispecies facades for human and non-human urban cohabitation.

Acknowledgements

The research received support from the industrial side, enabling to test the approach on a real-scale mockup: Tonality GmbH, LEIPFINGER-BADER GmbH.

References

- Apfelbeck, B., Hauck, T. E., Jacoby, C., Piecha, J., Rogers, R., Schröder, A., & Weisser, W. W. (2019). Animal-Aided Design im Wohnumfeld Einbeziehung der Bedürfnisse von Tierarten in die Planung und Gestaltung städtischer Freiräume [Animal-Aided Design in residential Environment Incorporating the needs of animal species into the planning and design of urban open spaces].
- Apfelbeck, B., Snep, R. P. H., Hauck, T. E., Ferguson, J., Holy, M., Jakoby, C., ... Weisser, W. W. (2020). Designing wildlife-inclusive cities that support human-animal coexistence. *Landscape and Urban Planning*, 200(March), 103817. <https://doi.org/10.1016/j.landurbplan.2020.103817>
- Asam C. (2017). Dämmmaßnahmen an Gebäudefassaden | Einsparpotenziale durch energetische Gebäudesanierung [Insulation measures on building facades | Savings potentials through energy-efficient building refurbishment.]. BBSR-Analysen Kompakt 11/2017
- Bang, A.L., Krogh, P., Ludwigsen, M., Markussen, T., (2012) The role of hypothesis in constructive design research. *Proceedings of the art of research IV Online*.
- Bauer, M., Mösele, P., & Schwarz, M. (2013). Green Building - Leitfaden für nachhaltiges Bauen [Guide to sustainable building]. Retrieved from <http://link.springer.com/10.1007/978-3-642-38297-0>
- Bernhard, R. (2012). Breathing Façades: Technologies for Decentralized Natural Ventilation. *Detail*, 7+8.
- Bertagna, F., D'Acunto, P., Ohlbrock, P.O., & Moosavi, V. (2021). Holistic Design Explorations of Building Envelopes Supported by Machine Learning. *Journal of Façade Design and Engineering*, 9(1), 31-46.
- Bischer, R., Hauck, T. E., Mühlbauer, M., Piecha, J., Reischl, A., Scherling, A., & Weisser, W. (n.d.). Animal-Aided Design für den Stadtpark Donau in Ingolstadt-Entwürfe von Studentinnen [Animal-Aided Design for the Donau City Park in Ingolstadt – design projects by students.]. Kassel.
- bogevischs buero, & GEWOFAG Projektgesellschaft mbH. (2019). Geförderte Wohnanlage mit Kindertagesstätte [Subsidised housing complex with day care centre], Brantstraße, München.
- Droz, B., Arnoux, R., Rey, E., Bohnenstengel, T., & Laessler, J. (2008). Characterizing the habitat requirements of the Common Redstart (*Phoenicurus phoenicurus*) in moderately urbanized areas. Retrieved from <http://sitn.ne.ch>.
- Dunn, N. (2012). *Digital fabrication in architecture*. Laurence King.
- European Commission. (2020). A Renovation Wave for Europe - greening our buildings, creating jobs, improving lives. *European Commission*, COM(2020), 1–26.
- Fleckenstein, J., Molter, P. L., Chokhachian, A., & Dörfler, K. (2022). Climate-Resilient Robotic Façades: Architectural Strategies to Improve Thermal Comfort in Outdoor Urban Environments using Robotic Assembly. *Frontiers in Built Environment*, 8. <https://doi.org/10.3389/fbuil.2022.856871>
- Funk, D., Groß, G., & Trute, P. (2014). Stadtklimaanalyse Landeshauptstadt München [City climate analysis of the City of Munich]. Landeshauptstadt München - Referat Für Gesundheit Und Umwelt, 61.
- Güneralp, B., McDonald, R. I., Fragkias, M., Goodness, J., Marcotullio, P. J., & Seto, K. C. (2013). Urbanization forecasts, effects on land use, biodiversity, and ecosystem services. *Urbanization, Biodiversity and Ecosystem Services: Challenges and Opportunities: A Global Assessment* (pp. 437–452). Springer Netherlands. https://doi.org/10.1007/978-94-007-7088-1_22
- Herriot, R., (2019). What kind of research is research through design? *International Association of Societies of Design Research Conference Design Revolutions*
- Jiang, J., Xu, X., & Stringer, J. (2018). Support structures for additive manufacturing: A review. *Journal of Manufacturing and Materials Processing*, Vol. 2. MDPI. <https://doi.org/10.3390/jmmp2040064>
- Kwok A. & Grondzik W. (2007). *The Green Studio Handbook: Environmental strategies for schematic*. Elsevier, Oxford
- Kloft, H., Gehlen, C., Dörfler, K., Hack, N., Henke, K., Lowke, D., ... Raatz, A. (2021). TRR 277: Additive Fertigung im Bauwesen. *Bautechnik*, 98(3), 222–231. <https://doi.org/10.1002/bate.202000113>
- Koryakina, T. N. (2018). Features Gastostomy and Characteristics of Nests of the Great Tit (*Parus Major L.*) and the Common Redstart (*Phoenicurus Phoenicurus L.*) *The Urbanized Landscape of the City Of Monchegorsk. V Mire Nauchnykh Otkrytiy*, 10(1), 52. <https://doi.org/10.12731/wsd-2018-1-52-63>
- Larikova I. (2021). Animal-inclusive design for digitally fabricated facades in Munich's buildings renovation. *Master Thesis*. TUM School of Engineering and Design, Technical University of Munich. Retrieved from https://mediatum.ub.tum.de/1631371?-show_id=1659627
- Lignarolo L., Lelieveld C., Teuffel P. (2011), Shape morphing wind-responsive facade systems realized with smart materials. *Adaptive Architecture: An International Conference*, London, UK, March 3-5, 2011
- Londono, G. A. (2007). Effects of Temperature and Food on Avian Incubation Behavior. *A thesis presented to the graduate school of the University of Florida in partial fulfilment of the requirements for the degree of master of science*, University of Florida. Retrieved from https://ufdcimages.uflib.ufl.edu/UF/E0/02/14/65/00001/londono_g.pdf

- Parker, D., Roudavski, S., Jones, T. M., Bradsworth, N., Isaac, B., Lockett, M. T., & Soanes, K. (2022). A framework for computer-aided design and manufacturing of habitat structures for cavity-dependent animals. *Methods in Ecology and Evolution*, 13(4), 826–841. <https://doi.org/10.1111/2041-210X.13806>
- Perini, K., Chokhachian, A., Dong, S., & Auer, T. (2017). Modeling and simulating urban outdoor comfort: Coupling ENVI-Met and TRNSYS by grasshopper. *Energy and Buildings*, 152, 373–384. <https://doi.org/10.1016/j.enbuild.2017.07.061>
- Rael, R., San Fratello, V., Arja, L., Cao, H., Curth, S., Darweesh, B., ... Wilson, K. (n.d.). *Cabin of 3D Printed Curiosities*. Retrieved May 27, 2021, from Emerging Objects website: <http://emergingobjects.com/project/cabin-of-3d-printed-curiosities/>
- Roesler, S., & Kobi, M. (2018). *The Urban Microclimate as Artifact: Towards an Architectural Theory of Thermal Diversity*. Birkhäuser. <https://doi.org/10.1515/9783035615159>
- Sandifer, P. A., Sutton-Grier, A. E., & Ward, B. P. (2015). Exploring connections among nature, biodiversity, ecosystem services, and human health and well-being: Opportunities to enhance health and biodiversity conservation. *Ecosystem Services*, Vol. 12, pp. 1–15. Elsevier B.V. <https://doi.org/10.1016/j.ecoser.2014.12.007>
- Simiu E. (2011). *Design of buildings for wind. A Guide for ASCE 7-10 Standard Users and Designers of Special Structures. Second Edition*. John Wiley & Sons, Inc., Hoboken, New Jersey
- Tsing, A., Swanson, H., Gan, E., & Bubandt, N. (2017). *Arts of Living on a Damaged Planet :Ghosts and Monsters of the Anthropocene*. University of Minnesota Press
- Weggler, M. (2006). Constraints on, and determinants of, the annual number of breeding attempts in the multi-brooded Black Redstart *Phoenicurus ochruros*. *Ibis* (Vol. 148).
- Weisser, W., & Hauck, T. (2015). *Animal Aided Design*. 49. Retrieved from <https://www.tum.de/die-tum/aktuelles/pressemitteilungen/detail/article/32308/>
- Whitelaw, M., Hwang, J., & le Roux, D. (2021). Design Collaboration and Exaptation in a Habitat Restoration Project. *She Ji*, 7(2) 223–241. <https://doi.org/10.1016/j.sheji.2020.08.011>
- Wolf, A., Rosendahl, P. L., & Knaack, U. (2022). Additive manufacturing of clay and ceramic building components. *Automation in Construction*, Vol. 133. Elsevier B.V. <https://doi.org/10.1016/j.autcon.2021.103956>

Retrofitting Potential of Building envelopes Based on Semantic Surface Models Derived From Point Clouds

Edina Selimovic¹, Florian Noichl¹, Kasimir Forth^{*1}, André Borrmann¹

* Corresponding author, kasimir.forth@tum.de

¹ Technical University Munich, Germany

Abstract

To meet the climate goals of the Paris agreement, the focus on energy efficiency needs to be shifted to increase the retrofitting rate of the existing building stock. Due to the lack of usable information on the existing building stock, reasoning about the retrofitting potential in early design stages is difficult. Therefore, deconstructing and building new is often regarded as the more reliable and economical option. Digital methods are missing or not robust enough to capture and reconstruct digital models of existing buildings efficiently and automatically derive reliable decision-support about whether demolition and new construction or retrofitting of existing buildings is more suitable. This paper proposes a robust, automated method for calculating existing buildings' life cycle assessments (LCA) using point clouds as input data. The main focus lies in bridging the gap between point clouds and importing semantic 3D models for LCA calculation. Therefore, the automation steps include a geometric transformation from point cloud to 3D surface model, followed by a semantic classification of the surfaces to thermal layers and their materials by assuming the surface elements by building age class.

Keywords

retrofitting potential, LCA, point cloud, semantic enrichment

DOI

<https://doi.org/10.47982/jfde.2022.powerskin.8>

1 INTRODUCTION

The construction sector is responsible for a large share of the overall situation of increasing emissions. In 2019, the amount of waste produced by the construction industry in Germany alone amounted to 230.9 million tons in 2019 (Umweltbundesamt, 2021). Most used materials are from non-renewable resources, mainly found in the existing building stock. At the same time, landfill capacities are decreasing and pose an additional environmental challenge to this industry sector (Hillebrandt, 2018; Rosen, 2018). Furthermore, the manufacturing, transportation, construction, and disposal of newly built assets, including buildings and infrastructure, contribute to 11% of the total carbon emissions worldwide (WorldGBC, 2019). For this reason, a particular emphasis is placed on the consideration of retrofitting instead of demolishing and building new. Consequently, retrofitting is regarded the most sustainable and ecologically most significant solution for the previously described problems in industrialized countries (Lottner, 2014; WorldGBC, 2019).

Due to the lack of usable information on the existing building stock, reasoning about the retrofitting potential in early design stages is difficult. Therefore, deconstructing and building new is often regarded as the more reliable and economical option (Matthias Hüttmann, 2018). Robust methods are missing to efficiently capture and reconstruct digital models of existing buildings (Deutscher Abbruchverband, 2007). The automatic derivation of reliable decision-support about whether demolition and new construction or retrofitting of existing buildings is more suitable is currently not supported (Matthias Hüttmann, 2018).

With the introduction of digital methods in the construction sector, such as Building Information Modeling (BIM), many conventional planning processes were facilitated (Borrmann, 2015). Synergies from many different disciplines have been identified, such as in the field of sustainability (BBSR & BBR, 2019). Since then, model-based sustainability analysis, for example, Life Cycle Assessment (LCA), can be realized in early design stages. However, previous research focused on pre-existing BIM models and neglected the existing building stock (Akbarieh et al., 2020).

The current way of creating a quantity take-off of an existing building is mostly a manual process, representing only an estimation and focused mainly on costs (Deutscher Abbruchverband, 2007). Remodeling would be highly time-consuming. To circumvent this, techniques have been developed in recent years that use digital methods to automatically generate 3D building models of a building through point cloud capture and processing. Automated processes for 3D Reconstruction and object recognition are therefore needed. These are yet not fully mature or applicable for the case of LCA calculation of existing buildings (Chen, 2021).

Addressing the mentioned problems, this paper proposes a method for bridging the gap between point clouds and importing semantic 3D models into tools for holistic calculation of the environmental impact of different scenarios. This research proves the opportunity to compare the environmental impacts and emissions between an existing building and a retrofitting variant and supports future decision-making without extensive manual preparation.

2 BACKGROUND AND RELATED WORK

This section discusses the background, related work, and the research gap for our proposed methodology. Firstly, we discuss the limitations of BIM in the end-of-life phases of building design. Secondly, we introduce the topic of geometric reconstruction of point clouds. In the end, we show approaches of object classification with a focus on windows as an exemplary addition and essential contribution to LCA calculations.

2.1 BIM IN THE END OF LIFE (EOL) DESIGN PHASE

Akbarieh et al. investigated the application of BIM in the EoL phase of buildings and to what extent BIM is used for planning in the EoL phase (Akbarieh et al., 2020). However, their research showed that most studies on BIM-based EoL topics were based on existing BIM models and did not investigate a simplified automated remodeling for different use cases. The applications developed mostly represent Application Programming Interfaces (APIs) for specific proprietary BIM tools in the form of Plug-Ins connected to LCA software. A direct data transfer between the 3D model and the LCA tool is often missing and not applicable without a workaround that includes specialized third-party software.

Studies conducted on existing buildings to investigate an EoL-related topic and therefore create a 3D model were carried out by Ge et al. (2017). They manually reconstructed the model with the help of plans, point clouds, and pictures, which is time-consuming. Volk et al. (2018) investigated an automatic approach that enabled the 3D reconstruction of the interior of a building based on a point cloud collected by a depth sensor. The building components were detected automatically, and the quantity take-off was calculated based on standard values and experience data to eventually perform a deconstruction analysis. Nevertheless, at some points, manual intervention was still needed.

2.2 3D RECONSTRUCTION

Employing digital surveying methods, existing buildings can be captured as point clouds. Reconstructing a 3D model from these point clouds has been a challenge in computer vision and computer graphics for years and is still an active field of research (Chen, 2021). The Poisson reconstruction by Kazhdan & Hoppe (2013) creates watertight surfaces from oriented point clouds. However, this approach requires complete data free of outliers, which is rarely the case for real-world measurements. Other papers address the problem of Manhattan-world scene reconstruction (Coughlan & Yuille 2000; Li et al., 2016), which represents the 3D scene with axis-aligned non-uniform boxes. Li et al.'s (2016) method successfully creates faithful reconstructions from various data sources. Still, this approach dramatically simplifies the geometric complexity of the real world. Nan & Wonka (2017) developed PolyFit, an approach that allows robust results for simple geometries with a slicing method. For this purpose, in a first step, the RANSAC algorithm (Schnabel et al., 2007) detects planes in the dataset. The next step clips the model with the detected planes in polyhedral cells, representing the candidates' faces. Described as an integer programming problem, the results of this approach are watertight and manifold. The only disadvantage lies in the scalability due to the extensive computation time needed for complex geometries (Nan & Wonka, 2017).

2.3 OBJECT CLASSIFICATION: WINDOW CLASSIFICATION

More semantic information can be added to create a model representation beyond the pure geometry of the building envelope. The window-to-wall ratio provides important information for energy simulation (Schneider & Coors, 2018). Therefore window classification is a suitable extension for a pure 3D reconstruction process.

There are many studies concerning window classification. Volk et al. use an image rendering of the point cloud walls to extract the windows (Volk et al., 2018). Yang et al. (2016) create a binary image to detect "holes" in the image Taraben & Kraemer (2021) use a deep learning approach to map the detected windows from 2D images on a previously generated surface model. Schneider & Coors (2018) recognize windows directly in the point cloud using a contouring algorithm.

Nevertheless, most studies treat windows as “holes” in the building hull and do not consider further features as radiometric properties. One advantage of point cloud acquisition by laser scanning is the ability to record intensity values. Intensity represents the amount of light reflected from a surface and is usually stored per point with a value from 0 to 255. It is assumed that each material can be approximated through a range of intensity values (Macher et al., 2021). The evaluation of intensity features is robust to light changes or shading but depends on scanner position, distance to object, and object colour (Macher et al., 2021; Park & Cho, 2021).

Park & Cho developed a deep learning method for material classification on 3D point clouds that consider intensity values in addition to geometric information and colour values (Park & Cho 2021). Macher et al. (2021) used intensity values to segment the windows from the facade based on a Histogram analysis. For this study, a laser scan point cloud should be used to investigate window classification based on intensity values.

3 METHODOLOGY

This section proposes a methodology for geometrically reconstructing surface models using point clouds as input, semantically enriching these models and importing them into an LCA tool. The acquisition of the point cloud derived from terrestrial laser scanning (TLS) is out of scope for this paper, as it is only used as the input for the proposed methodology. The geometric transformation from point cloud to 3D surface model is conducted using the PolyFit approach (Nan & Wonka, 2017). Transparent elements such as windows are identified through laser intensity values of the points. In the next step, the faces of the model can be assigned to thermal surface classes and finally imported into LCA software. The materials and material layers of the model faces are approximated by assuming the building age class. Figure 1 shows an overview of the workflow. The following subchapters introduce the steps of this workflow in more detail.

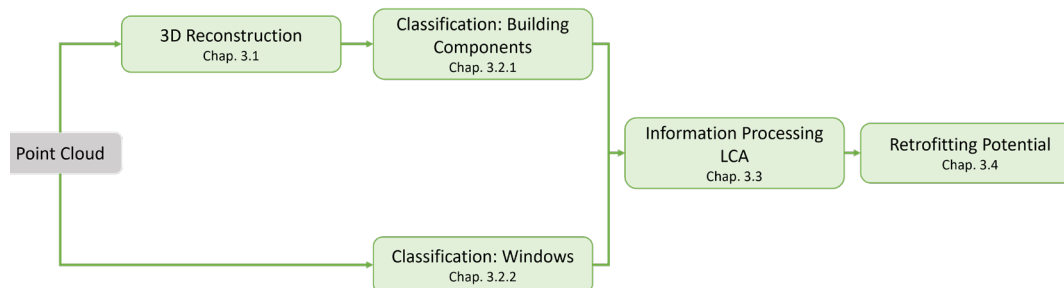


FIG. 1 The general workflow

3.1 3D RECONSTRUCTION

The process of creating the 3D shape and appearance of real objects is referred to as 3D reconstruction. In the following, the steps for reconstructing a 3D model out of a point cloud are explained in more detail. The entire methodology is shown in Figure 2.

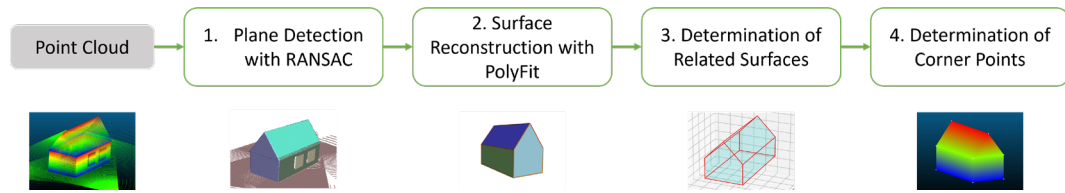


FIG. 2 Methodology for the 3D Reconstruction

To perform 3D reconstruction, the PolyFit approach is used. This approach is based on the RANSAC algorithm (Schnabel et al., 2007), which can identify planes from the point cloud. Thus, building surfaces, such as walls or roofs, can be captured individually. In PolyFit, the previously detected planes intersect with the point cloud's bounding box. This results in several faces, referred to as face candidates (Figure 3 - left). To determine the faces from the face candidates that form a common surface, PolyFit converts the reconstruction problem into a binary linear programming problem, resulting in the right picture of Figure 3.

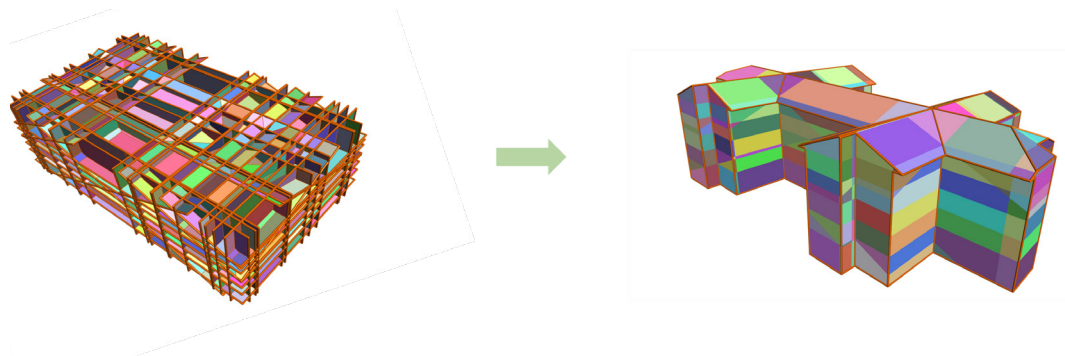


FIG. 3 PolyFit Result: Face Candidates (left) and selected face candidates (right)

The result can be exported as an OBJ-file (fileformat.info, 2022). The OBJ file contains information about all exterior surfaces and their corner points. The surfaces in the file represent the selected face candidates pictured on the right in Figure 3. However, for further applications, the combined building surfaces are more valuable. Hence, step 3 determines the combined surfaces formed by the selected face candidates. To identify them, this study uses the face normals. Face orientation can be determined using the dot product, starting from an XY-plane. In the last step the faces with the same normal orientation and at least one same point can be merged. After the related faces were detected, inner surfaces, in this case floors, are estimated using the building height. For this purpose, a floor height was assigned manually, which allowed the number of floors and their respective height coordinates to be estimated. The area of the floors is assumed to be identical to the ground floor.

Consequently, the corner points of the resulting surfaces are identified, as they are needed for further processing in LCA tools. Because the surface edges represent an intersection of straight lines, the condition can be set that corner points whose count is odd in the total set of points will represent a corner point of the total surface. This condition will take convex as well as concave polygonal surfaces into account. In this step, the order in the clockwise (CW) or counterclockwise (CCW) direction gets lost, and the corner points are listed in a random sequence. However, it is impossible to define a polygonal surface only by the point coordinates, so the order has to be rebuilt. To accomplish this, the point-edge relationships are considered beforehand. Consequently, the identified corner points can be ordered in a CW or CCW order.

3.2 OBJECT CLASSIFICATION

The surface model provides purely geometric information. To further use the model for LCA calculation, semantic information has to be added for a retrofitting potential analysis. In a first step, each surface is assigned to a thermal surface class, which will be later enriched with more material assumptions. In a second step, windows are classified to derive the window-to-wall ratios for the model.

3.2.1 Thermal Surface Classification

Each surface is assigned to a thermal class. The thermal surface classes describe the boundary conditions of each surface, e.g., wall to exterior or wall to the ground. There are 13 different classes existing (Hollberg et al., 2018). In this study, the following assumptions are made:

- 1 There is no basement floor
- 2 The flat and the pitched roof are referred to as the roof class
- 3 The walls considered only represent the walls to exterior
- 4 There is no distinction between ceilings
- 5 There is no distinction between windows in walls and roof windows

The thermal classes considered in this study can be classified based on simple geometric conditions, collected along with the thermal classes in Table 1. The basis for this classification is normalized surface normal vectors, rounded to one decimal. The classes are determined through the surfaces' orientation to the XY-plane, where rounding to one decimal leads to a tolerance of 2.8° for single-axis rotation and 4.0° rotation around two axes.

TABLE 1 Thermal Surface Classification

Thermal surface class	Condition 01	Condition 02
Floor to Ground	Orientation parallel to XY-plane	Lowest z-coordinates
Flat Roof	Orientation parallel to XY-plane	Not the Floor surface
Pitched Roof	Orientation neither parallel nor perpendicular to XY-plane	
External-Wall	Orientation perpendicular to XY-plane	
Ceiling	Assumed floor height and floor number, dependent on total building height	Orientation parallel to XY-plane and equally shaped as the floor to ground

3.2.2 Window Classification

The window classification is carried out using intensity values. These are obtained from the laser scan and stored with the points in the point cloud. Therefore, the window classification is performed directly on the point cloud in contrast to the thermal surface classification. For the LCA calculation, the window-to-wall ratio was estimated. An accurate geometric representation was not needed. Figure 4 shows a summary of the classification process.

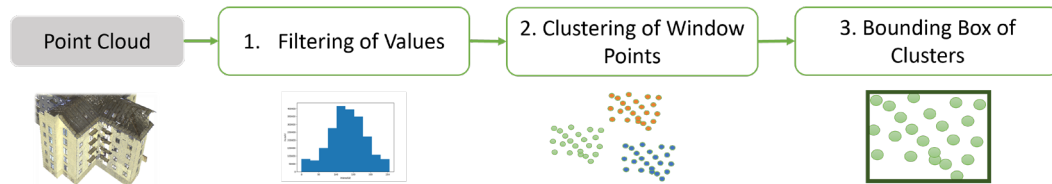


FIG. 4 Process for the Window Classification

In this study, the window points are extracted by their intensity values. Therefore, the values of the whole point cloud are analyzed in a histogram. Hence giving an initial range for the façade values, from which the range of values for the windows can be approximated. The range must be adjusted specifically to the project and is refined within the case study (Chapter 4.3). The range with the most window points and the fewest false points is iteratively filtered out. False points refer to points whose intensity values overlap with the window points. To define a clear assignment of points to each window, the points defining one window are clustered into a group, which is necessary to extract the windows individually. The window points are clustered with the density-based DBSCAN-Clustering by Ester et al., (1996). The algorithm depends on the parameter eps, which describes the minimal radius that combines all points within this radius to a cluster. A weakness of the intensity-based approach is that the window points are not fully captured in the point cloud processing due to the transparent material property of glass, which leads to an inaccuracy in the detected clusters and thus only represents an approximation. Consequently, the bounding boxes around the clusters, determined in the last step, were not perfectly rectangular.

3.3 INFORMATION REQUIREMENT AND PROCESSING FOR THE LCA

Certain information is required to perform an LCA from a semantic enriched 3D model. The information can be represented in alphanumeric numbers, coordinates, etc., and is needed for different reasons within the LCA calculation. Table 2 gives an overview of the required types of information.

TABLE 2 LCA required Input Information

Information	In the form of	Usage for LCA calculation
Surfaces	XYZ-coordinates of the corner points	Essential for whole LCA
Area of the surface	Alphanumerical number	Essential for whole LCA
Surface material	By assumption of the surface elements by building age class	Essential for whole LCA
Thermal Layer of the surface	Text label	Calculation of the use phase
Outward-facing surface normal	Vector	Calculation of the use phase
Window openings in surface	Number of the surface area and ID of the window	Essential for whole LCA Window-to-wall ratio

The surface area of the polygonal surfaces and windows is calculated based on the corner point coordinates. Therefore, the surface is split into triangles, which allows taking convex as well as concave surfaces into account. The area can be calculated using the cross product of each triangle. The sum of all triangle areas determines the total area. Afterwards, the window-to-wall ratio is calculated by dividing the previously classified window area by the total area. In the last step, the outward-facing normal of every surface is defined, needed to calculate the use phase in the LCA.

This computation represents a common problem, which is solved with the Trimesh library (Dawson-Haggerty et al. 2019) and is not applicable for objects with high geometric complexity. As a final step, in the LCA calculation tool, the material layers and material thicknesses of the model faces are approximated by assuming the building age class. Therefore, the information from the TABULA database is combined with the LCA database using OEKOBAUDAT (BBSR 2022).

3.4 CALCULATION OF THE RETROFITTING POTENTIAL

The calculated retrofitting potential in this study aims to compare the environmental impacts of the existing building with a retrofitting variant using LCA. To simplify and enable the comparability of the variants, the following assumptions as well as system boundaries and boundary conditions were made:

- No consideration of the lifecycle phase C for the demolition of reconstructed old substances according to the Rating System Sustainable Building (BMUB, 2017)
- Considered useful lifespan of the building: 50 years
- Chosen environmental indicators: primary energy non-renewable and global warming potential (GWP)
- Manual specification of an identical energy system

In summary, the retrofitting potential will compare only newly installed materials in all lifecycle phases. A detailed analysis for recycling and demolitions efforts of existing building components is out of scope, as in this early design phase, no reliable assumptions can be made.

4 CASE STUDY

4.1 DATASET AND PREPROCESSING

To test and validate the proposed method, this study conducted a case study on a point cloud (see Figure 5.a) obtained by a TLS of an existing 5-storey multi-apartment building from the 1960s (MERKO 2022). The point cloud of the abandoned building, situated in Adazi, Latvia, was acquired due to the building's need for retrofitting. First of all, the point cloud with 10.315.268 points was subsampled within the open source software CloudCompare (CloudCompare 2022) through the specification of space between the points to 0.1 m. In the used point cloud, the points of the interior of the building were also contained. To simplify computation, these points were removed manually. To reconstruct the 3D model, the planes were detected with the RANSAC algorithm (see Figure 5.b) and the surface model was generated using the PolyFit software. Here the complexity was reduced with the provided PolyFit parameters, allowing simplified further processing. The obtained surface model consisted of selected face candidates from PolyFit (see Figure 3 right). In the next step, related faces were combined with building surfaces (see Figure 5.c), allowing the extraction of the corner points' coordinates.

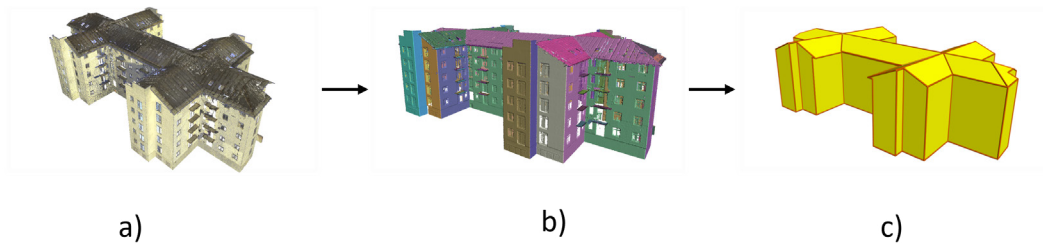


FIG. 5 a) The Point Cloud with b) the Detected Planes from RANSAC and c) the Reconstructed Surface Model from PolyFit

4.2 SEMANTIC ENRICHMENT AND WINDOW CLASSIFICATION

Subsequent steps deal with semantic enrichment. Thermal surface classification is conducted on the geometric surface model. Due to simplified assumptions, the implemented classification system classified all walls as exterior walls and the floor as floor-to-ground. A building with a cellar is not considered here. Furthermore, the ceiling structure is always the same, and there is no ceiling against unheated space. In addition, recesses in the ceilings cannot be taken into account. Extensions or garages with flat roofs are excluded since only one roof is assumed.

The windows were detected separately in the point cloud file, providing the laser intensity information. After the performed Histogram analysis of intensity values, it was observed that the intensity values of window elements were heavily spreading. Nevertheless, almost all window intensity points lay in a range from 0 to 40, with some outliers at value 255. In between, there were virtually no window points detected. However, choosing all points in a range [0;40] would lead to many false points, mainly from the roof and the building edges (see Figure 6.b). This is most likely the case due to standard sensitivity factors of laser scanners, such as the scanner position, the incidence angle, and the distance to the acquired object. The determination of the window range is thus project-specific, and a range of [0;25] was iteratively set as the most accurate for this point cloud.

On this basis, the window points were extracted, and the DB-Scan Clustering was performed to further extract the windows individually (see Figure 6.c). Here the parameter describing the minimal distance of a point to a cluster was set to 0.4 m. This value is set to prevent nearby window points from being merged into one cluster. The clustering results still showed that some windows were merged, but on the downside, some were neglected totally. Nevertheless, this was largely compensated in the overall results.

Due to the intensity-based approach, some false points that were not describing windows, but overlapping in intensity values, were extracted too. This led to falsely detected clusters from these points. Some were removed based on their orientation parallel to the XY-plane, as they were representing balconies. Others were removed based on their very low height, which is not common for windows, thus representing the lower building edge.

In the last step, the bounding boxes were defined around each cluster (see Figure 6.d). Due to some missing window points, the boxes were not perfectly rectangular but also rhomboid-shaped. This was acceptable since only the ratio is to be examined, and the geometrical form of the recognized windows is of secondary importance. Consequently, the corner points were determined and the area calculated. The results showed a detection rate of approximately 94 %, with a total window area of 1129.62 m² compared to the correct area of around 1200 m².

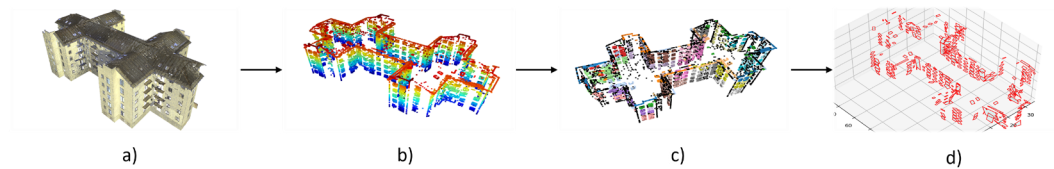


FIG. 6 a) point cloud with b) filtered window points and c) clustered windows, and d) cluster-fitted bounding boxes

4.3 LCA CALCULATION OF RETROFITTING POTENTIAL

Subsequently, the gained information was processed as input in an LCA tool. Due to its LCA-based direct variant comparison function, the LCA software used in this study was CAALA (CAALA 2020). Moreover, CAALA enables the calculation of the total emissions, embodied and operational energy, using a single-zone calculation approach. For this purpose, the data was converted into a CAALA-JSON file. Therefore, the area, the surface outward normal, and the window-to-wall ratio was calculated, as described in Chapter 2.3.

After the geometry was read in the software, the material layers were assumed by building age class. The investigated building complex was assumed to be building type NBL_MFH_E (1958-1968) according to the TABULA building type defined by the institute for housing and environment in the course of an EU project (Loga et al., 2015).

In the next step, the retrofitting variant was developed considering the building age, including the following measures, which CAALA suggests for this construction:

- 1 Wood fibre insulations in an external thermal insulation composite system (ETICS)
- 2 Triple glazing windows with a wooden frame, $U=0.8$, $g=0.6$
- 3 the energy system of a condensing gas boiler

The refurbished variant leads to much better results regarding energy performance as well as greenhouse gas emissions. This is represented in Table 3 with the total non-renewable primary energy consumption (PENRT) and the greenhouse gas emissions (GWP) of the existing building in comparison to the emissions of the refurbished variant. All lifecycle phases were considered for the calculation as described in Section 3.4.

Furthermore, Figure 7 depicts the cumulative emissions of the GWP over the whole lifecycle. Here the existing building starts with no emissions and finishes the first year with 78.53 kg CO₂-eq./ (m²NGF*a) from the building's operational phase B6. The retrofitted variant starts with -24.0 kg CO₂-eq./ (m²NGF*a) resulting from phases A1-3 due to sustainable materials used and increases annually by 26.56 kg CO₂-eq./ (m²NGF*a) on account of the operational phase B6. In contrast to the retrofitted variant, the emissions from the end of life phase C of the existing building are not considered as described by the considered systematic of the sustainable rating system (BMUB, 2017). This can be seen in Figure 7 from the different incline at the end of the two graphs. Only simple retrofitting measures were chosen to validate the workflow, as the focus is on the automated generation of geometric and semantic information rather than on different and complex retrofitting scenarios.

TABLE 3 LCA results of the variant comparison

LCA indicator	Unit	Existing Building	Retrofitted variant
Primary energy non-renewable (PENRT)	[kWh/(m ² NGF*a)]	358.74	129.14
Global Warming Potential (GWP)	[kg CO ₂ -eq./ (m ² NGF*a)]	78.53	28.43

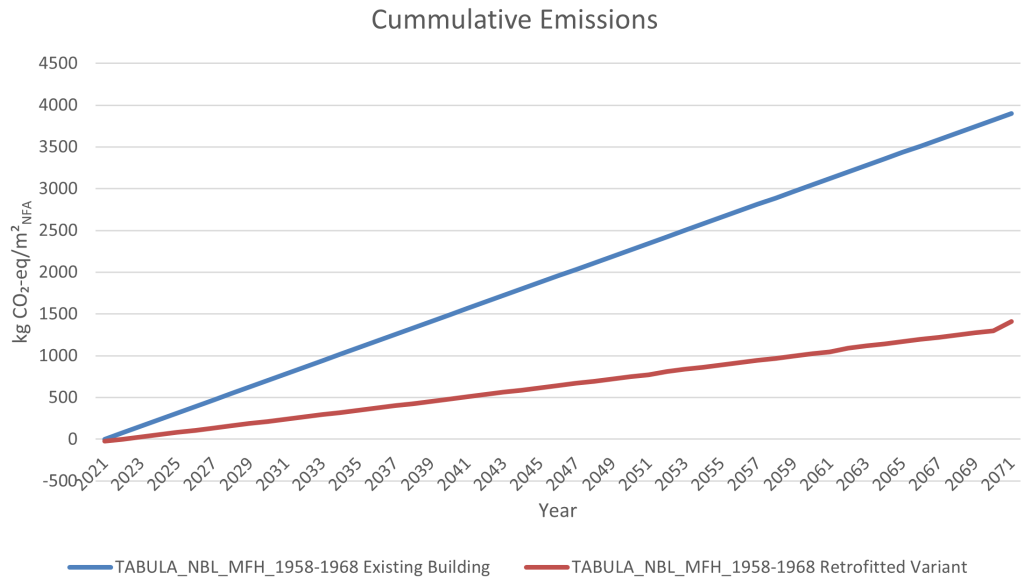


FIG. 7 Cumulative Emissions of the GWP of the Compared Variants

5 DISCUSSION

The proposed method enables LCA calculation of retrofitting scenarios on the basis of semantic 3D models generated and enriched from point clouds. The method was tested on a 5-storey multi-apartment building. The study verified that a point cloud of the building's envelope could be processed in such a way that the minimum geometric and semantic requirements needed for an LCA calculation and the import into an LCA tool can be obtained. The proposed methodology leads to widening the scope of action for construction decisions on retrofitting the existing building stock already in early design stages. Moreover, the ability of semantic enrichment of 3D models with intensity values for window classification was demonstrated.

Limitations of the developed method can be faced if the geometric complexity is too high, resulting in an inaccurate surface model or a wrong surface outward normal computation. The latter would lead to an incorrect LCA calculation of the use phase and, therefore, only enable the calculation of the embodied energy, which is insufficient for the making of a meaningful decision.

Furthermore, the classification of the windows requires manual adjustment for filtering the intensity values of the window points. The investigation of laser intensity values restricts the digital surveying technology to laser scanning and the results to the quality of the acquired window points. It has to be mentioned that the results of the window classification represent a window-to-wall ratio and not an accurate geometric shape, which is, however, sufficient for a simplified LCA calculation in an early design phase.

The LCA results strongly depend on the selected materials and thicknesses and on the assumptions of the TABULA building typology. Furthermore, the material allocation is not performed independently but requires this function in the software.

6 CONCLUSION AND OUTLOOK

Regarding the building sector's climate goals and environmental impacts, the retrofiting rate needs to be increased instead of the number of new constructions. Hence, this paper proposes an automated method to calculate the LCA of existing buildings by using point clouds as input data to close the gap between point clouds and LCA software. To validate the method, a point cloud acquired with a laser scanner of an existing building was used, containing the intensity values of each point. The geometrical reconstruction was conducted using the PolyFit approach. The semantic enrichment of the building components was based on geometrical information, while the windows were classified using intensity values. For this study, the window-to-wall ratio was sufficient. Thus, the geometric representation of the windows was not needed. The developed method detected around 94 % of the total window area and mapped the windows to the appropriate walls.

In future works, the importance of 3D reconstruction, and similarly, Scan-to-BIM processes, will increase, opening up a wide synergy potential for many research fields, such as sustainability. Furthermore, radiometric features such as intensity should be investigated in future studies, especially in the promising field of deep learning. The consideration of intensity values could enable a material classification from the point cloud and therefore help to identify more information about surface materials. This could lead to a direct assumption of building classes. Besides, the window classification can be more sensitized to determine the geometric shape. Thus, a combination of the usage of intensity values with a deep learning technology could lead to promising results.

References

- Akbarieh, A., Jayasinghe, L. B., Waldmann, D., & Teferle, F. N. (2020). BIM-Based End-of-Lifecycle Decision Making and Digital Deconstruction: Literature Review. *Sustainability*, 12(7), 2670. <https://doi.org/10.3390/su12072670>
- BBSR, & BBR (2019). *Ökobilanzierung und BIM im Nachhaltigen Bauen [Life Cycle Assessment and BIM in Sustainable Construction]*. Retrieved from <https://www.bbsr.bund.de/BBSR/DE/forschung/programme/zb/Auftragsforschung/2NachhaltigesBauenBauqualitaet/2019/oekobilanz-bim/01-start.html>
- BBSR, Ö. (2022, May 20). ÖKOBAUDAT. Retrieved from <https://www.oekobaudat.de/en.html>
- BMUB (2017). *Bewertungssystem Nachhaltiges Bauen (BNB). Büro- und Verwaltungsgebäude. Modul Komplettmodernisierung. BNB_BK 1.1.1: Ökologische Qualität. Wirkungen auf die globale und lokale Umwelt. Treibhausgaspotential (GWP) [Sustainable Building Rating System (BNB). Office and administration buildings. Module whole-building modernization. BNB_BK 1.1.1: Environmental quality. Effects on the global and local environment. Greenhouse gas potential (GWP)]*. Retrieved from <https://www.bnb-nachhaltigesbauen.de/bewertungssystem/buerogebaeude/steckbriefe-bnb-bk-2017/>
- Borrmann, A. (2015). *Building Information Modeling: Technologische Grundlagen und Industrielle Praxis [Building Information Modeling: Technological Basics and Industrial Practice]*. VDI-Buch Ser. Wiesbaden: Springer Fachmedien Wiesbaden GmbH. Retrieved from <https://ebookcentral.proquest.com/lib/kxp/detail.action?docID=3567925>
- CAALA (2020, August 3). Ihr digitaler Assistent für ganzheitliches Entwerfen. – CAALA [Your digital assistant for holistic design. – CAALA]. Retrieved from <https://caala.de/>
- Chen, Z. (2021). *Learning to Reconstruct Compact Building Models from Point Clouds* (Master Thesis). Delft University of Technology. Retrieved from <https://repository.tudelft.nl/islandora/object/uuid:e33e7fa1-118e-41d8-904f-5f03eb36e887?collection=education>
- CloudCompare (2022). CloudComapre (Version 2.12.1) [Computer software]. CloudCompare: CloudCompare. Retrieved from <http://www.cloudcompare.org/>
- Coughlan, J. M., & Yuille, A. L. (2000). *The Manhattan World Assumption: Regularities in scene statistics which enable Bayesian inference*.
- Dawson-Haggerty et al. (2019). Trimesh (Version 3.2.0) [Computer software]. Retrieved from <https://trimsh.org/>
- Abbrucharbeiten: Grundlagen, Vorbereitung, Durchführung [Demolition work: Fundamentals, preparation, execution]*. (2., aktualisierte und erw. Aufl.) (2007). Köln: R. Müller.
- Fileformat.info (2022, May 11). Wavefront OBJ: Summary from the Encyclopedia of Graphics File Formats. Retrieved from <https://www.fileformat.info/format/wavefrontobj/egff.htm>
- Ge, X. J., Livesey, P., Wang, J., Huang, S., He, X., & Zhang, C. (2017). Deconstruction waste management through 3d reconstruction and bim: A case study. *Visualization in Engineering*, 5(1), 1–15. <https://doi.org/10.1186/s40327-017-0050-5>

- Hollberg, A., Lichtenheld, T., Klüber, N., & Ruth, J. (2018). Parametric real-time energy analysis in early design stages: A method for residential buildings in Germany. *Energy, Ecology and Environment*, 3(1), 13–23. <https://doi.org/10.1007/s40974-017-0056-9>
- Kazhdan, M., & Hoppe, H. (2013). Screened poisson surface reconstruction. *ACM Transactions on Graphics*, 32(3), 1–13. <https://doi.org/10.1145/2487228.2487237>
- Li, M., Wonka, P., & Nan, L. (2016). Manhattan-World Urban Reconstruction from Point Clouds. In (pp. 54–69). Springer, Cham. https://doi.org/10.1007/978-3-319-46493-0_4
- Loga, T., Diefenbach, N., & Born, R. (2015). *Deutsche Gebäudetypologie: Beispielhafte Maßnahmen zur Verbesserung der Energieeffizienz von typischen Wohngebäuden [German building typology: Exemplary measures for improving the energy efficiency of typical residential buildings]*. Darmstadt.
- Macher, H., Roy, L., & Landes, T. (2021). Automation of windows detection from geometric and radiometric information of point clouds in a scan-to-BIM process. *The International Archives of the Photogrammetry, Remote Sensing and Spatial Information Sciences, XLIII-B2-2021*, 193–200. <https://doi.org/10.5194/isprs-archives-XLIII-B2-2021-193-2021>
- Matthias Hüttmann (2018). *Graue Energie Abreißen oder sanieren? [Demolishing or retrofitting embodied energy?]* BUND-Jahrbuch 2018 Ökologisch Bauen Und Renovieren: Nachhaltige Orientierung für Bauherren, 16–19. Retrieved from chrome-extension://efaidnbmnnnibpajpogcblefindmkaj/viewer.html?pdfurl=https%3A%2F%2Fwww.bund-bawue.de%2Ffileadmin%2F-bawue%2FDokumente%2FThemen%2FKlima_und_Energie%2FOekologisch_Bauen_und_Renovieren_2018_Graue_Energie_Abreissen_oder_sanieren.pdf&clen=913329&chunk=true
- MERKO (2022, May 11). DEMO DATA | Drupal. Retrieved from <http://www.merko.lv/en/demo-data>
- Nan, L., & Wonka, P. (2017). *PolyFit: Polygonal Surface Reconstruction from Point Clouds*. <https://doi.org/10.1109/ICCV.2017.258>
- Park, J., & Cho, Y. K. (Eds.) (2021). *Laser Intensity-assisted Construction Material Classification in Point Cloud Data using Deep Learning*. Orlando, FL.
- Schnabel, R., Wahl, R., & Klein, R. (2007). Efficient RANSAC for Point-Cloud Shape Detection. *Computer Graphics Forum*, 26(2), 214–226. <https://doi.org/10.1111/j.1467-8659.2007.01016.x>
- Schneider, S., & Coors, V. (2018). *Automatische Extraktion von Fenstern in 3D Punktwolken mittels einer hierarchischen Methode [Automatic extraction of windows in 3D point clouds using a hierarchical method]* (38. Wissenschaftlich-Technische Jahrestagung der DGPF und PFGK18 Tagung in München No. 27). München. Retrieved from https://www.researchgate.net/publication/323749844_Automatische_Extraktion_von_Fenstern_in_3D_Punktwolken_mittels_einer_hierarchischen_Methode
- Taraben, J., & Kraemer, K. (2021). *Automatisierte Generierung von Stadtmodellen aus UAS-Befliegungen für die energetische Bewertung von Quartieren [Automated generation of city models from UAS flights for the energetic evaluation of neighborhoods]* (32. Forum Bauinformatik 2021).
- Umweltbundesamt (2021, November 29). *Abfallaufkommen [Volume of Waste]*. Retrieved from <https://www.umweltbundesamt.de/daten/ressourcen-abfall/abfallaufkommen#bau-abbruch-gewerbe-und-bergbauabfalle>
- Volk, R., Luu, T. H., Mueller-Roemer, J. S., Sevilimis, N., & Schultmann, F. (2018). Deconstruction project planning of existing buildings based on automated acquisition and reconstruction of building information. *Automation in Construction*, 91, 226–245. <https://doi.org/10.1016/j.autcon.2018.03.017>
- Yang, J., Shi, Z.-K., & Wu, Z.-Y. (2016). Towards automatic generation of as-built BIM: 3D building facade modeling and material recognition from images. *International Journal of Automation and Computing*, 13(4), 338–349. <https://doi.org/10.1007/s11633-016-0965-7>

Suntex: Weaving Solar Energy Into Building Skin

Pauline van Dongen*¹, Ellen Britton¹, Anna Wetzel¹, Rogier Houtman², Ahmed Mohamed Ahmed¹, Stephanie Ramos¹

* Corresponding author, pauline@paulinevandongen.nl

¹ Pauline van Dongen, Netherlands

² Tentech, Netherlands

Abstract

The key objective of this research project is to "create a new architectural textile, Suntex, by interweaving thin film solar cells and electrically conductive yarn into a structural technical textile, so it can generate energy while it is providing shade, structure or an aesthetic update to a building."

Textile has strong potential as a sustainable building material because it can be lightweight, material efficient, and low carbon. Moreover, its flexibility provides great design freedom and its transparency makes it very suitable for façade applications, maintaining views to the outside while providing solar shading. Suntex is a solar textile, currently in development, intended for textile architecture applications like textile façades. By combining three qualities, namely providing the building with energy generation, solar shading, and a unique aesthetic appearance, which also promotes the acceptance of solar technology, it offers a positive climate impact.

Suntex can be considered as a new type of membrane material for Building Integrated Photovoltaics (BIPV). With this innovative, constructive fabric, enormous surfaces that are still unused can be outfitted with energy-generating potential.

This paper presents a design case to analyse the potential impact of Suntex as a textile façade. Based on insights into the development process and experiment results so far, it evaluates the feasibility and impact from a technical and design perspective.

Keywords

Textile architecture, solar textile, energy innovation, lightweight structures, BIPV

DOI

<https://doi.org/10.47982/jfde.2022.powerskin.9>

1 INTRODUCTION & OBJECTIVES

1.1 INTRODUCTION

Buildings generate nearly 40% of annual global carbon dioxide (CO₂) with operational emissions (including energy used to heat, cool, and light buildings) accounting for another 28% (UN Environment and International Energy Agency, 2017). To achieve the target of the Paris Agreement, approximately two thirds of the existing building stock will need to be modernised by 2040 (Architecture 2030, 2022). Buildings must become climate-positive by producing their own renewable energy and become climate-proof through intelligent thermal management.

As stated by the International Energy Agency, solar energy is “becoming the lowest-cost option for new electricity generation in most of the world” (IEA, 2020) and thus holds great promise for a sustainable future. One of the characteristics of solar systems is that they can be decentralised with the installations for the production of energy located closer to the place of energy consumption, a factor that has become particularly appealing in light of the global energy crisis (World Economic Forum, 2022). However, photovoltaic panels on the roofs of homes and offices alone, especially in high-rise buildings, are insufficient to meet the energy demand (TNO, n.d; Middelhaue, 2021). Façades have great potential, especially in low-latitude urban areas where the low sun on the vertical surface generates greater solar potential in the winter months than on roofs (Horn et al. 2018), so long as façades are carefully selected to maximise incident irradiance and minimise shading from nearby buildings or other obstructions.

Traditional silicon solar photovoltaic modules are rigid, heavy and have a one-size-fits-all design. This makes it a challenge to integrate them both functionally and aesthetically into existing buildings. New generations of thin-film solar cells mark a turning point in solar harvesting possibilities for buildings. These solar films are lightweight and flexible and can be custom fit for many more applications, such as applying them on existing (architectural) surfaces, including low-load-capacity roofs and curved surfaces, or integrating them into other flexible materials like textiles. In comparison to other materials like steel, concrete, aluminium or glass, textile is a more sustainable building material with very low embodied carbon due to its lightweight structural properties (Van Hinte & Beukers, 2020) and low energy consumption (Shareef Al-Azzawi et al., 2021). Furthermore, its flexibility and transparency provide great design freedom and usage, also in architecture. A second skin façade, from textile for example, enables views to the outside while mitigating and controlling excessive solar radiation. In addition, these façades can save energy through their isolation and ventilation properties during the cooling or heating period of a building. (Ahriz et al., 2022).

Combining (thin-film) solar technology with textiles is not new (Smelik et al., 2016; Kuhlmann et al., 2018; Nathanson, 2021) and the solutions range from highly experimental lab-stage research to more applied approaches that are already commercially available (Satharasinghe et al., 2020). The simplest, most common approach is to attach the flexible solar panel to the surface of the textile, for example through adhesives, sewing or laminating (Mather & Wilson, 2017; Nathanson, 2021). However, these assembly processes are difficult to scale industrially and present limitations for architectural applications in terms of their mechanical properties, modularity, and design potential (Mather & Wilson, 2017). To date, this method is used commercially within an architectural context by the US-based company Pvilion.

Suntex, an architectural textile currently under development, takes a different approach. Thin-film solar panels and electrical circuits (composed of conductive yarn) are integral to the construction of the textile by being directly combined in the weaving process. With the aim of being both a standardised and easily customizable architectural textile that increases the energy-harvesting potential of otherwise untapped surface area. Intended as a (retrofitted) façade second skin, Suntex has the potential to make a building more energy efficient through thermal insulation and through harvesting additional energy with integrated photovoltaics. Additionally, it brings completely new aesthetic qualities such as colour, transparency, and texture, which can help drive the adoption of photovoltaic technology (Reinders et al., 2020). A Suntex façade, in common with other façade solutions, can become a valuable addition for energy autonomy and grid reliability. By applying Suntex to existing infrastructure it is not in competition with agricultural land, industrial estates, or housing unlike space-consuming solar farms. Further, solutions such as Suntex have the potential to improve urban habitats, by de-reflecting glass windows, a primary source of bird-building collisions (Klem, 2006).

The key objectives of this paper are to explore the feasibility of Suntex and potential impact of this new textile when applied as a textile façade. The feasibility will be investigated by evaluating the textile samples created so far, against the requirements of a type I architectural fabric. The potential impact of this new textile will be investigated through an implementation analysis, which includes a case study, wherein the quantified benefit of energy generation will be explored alongside the qualitative benefits.

It should be noted that the initial phase of the research project is currently planned to run for two years, and is at the midpoint of one year at the time of writing.

2 RESEARCH METHODOLOGY

In order to develop a smart technical textile for application in textile architecture, this research is carried out at the intersection of textile design, design engineering and textile architecture. The design process is therefore hands-on, iterative, and highly collaborative. As a result of this interdisciplinary approach, both scientific research methods and design research methods are combined in the textile development process, which follows an iterative cycle.

As detailed in section 2.2, the textile design process follows an adapted version of the 'design thinking' approach (System Concepts, n.d) in that it is an iterative process in which testing informs the next steps. First, materials are selected according to pre-defined criteria. Next, a weave pattern is designed alongside a strategy to integrate the OPV film, and a sample is created. This sample is mechanically tested and reviewed against the textile requirements (Section 2.1). Conclusions from this process inform the first steps of the next iteration; the material selection and sample design. The latest iteration of the textile is then further evaluated through the development of a case study that reveals the potential impact of applying Suntex as energy harvesting building skin. In general, a case study combines data from multiple sources to explore a problem or scenario (Methodspace, 2021). While design cases or case studies can be built on expected, speculative data alone, this paper also shows the actual data gathered through experimental testing on woven textile samples. This process is done in an effort to contribute to the field of smart, technical textile development by sharing the details of the textile design and development process. In this case, the mechanical strength values achieved in the textile sample evaluation (Section 3.1) and the inherent nature of

weaving to produce rectilinear textiles indicated that a second-skin façade would be a worthwhile design case study to investigate (Section 3.3) as an initial application. The Westraven Rijkswaterstaat building in Utrecht (The Netherlands) was selected as the particular building to explore as it is a prominent example of a textile second-skin façade and it already demonstrates the environmental benefits of retrofitting a building in this way, in terms of thermal management.

2.1 TEXTILE REQUIREMENTS FOR SUNTEX

From a structural standpoint, textiles used in architecture are required to meet strength and stiffness criteria as well as water, UV-light, and fire resistance for durable load bearing applications. Typical architecture textiles are coated fabrics such as polyvinyl chloride (PVC) coated polyester (PES) fabrics and polytetrafluoroethylene (PTFE) coated glass fabrics, where the coating provides protection against weathering agents, and the fabric weave within the coating is the load-carrying element. Uncoated fabrics are similarly used in an architectural context but to a limited extent since without a coating, achieving comparable durability becomes challenging. In terms of strength, architecture fabrics are classified into categories from type I to type V, corresponding to tensile strengths of about 3000 N/5cm to 10,000 N/5cm, respectively. The strength should be verified in both weave directions and in areas of seams using relevant standardised tensile strength tests. Type I fabric, thus, offers the minimum required tensile strength for a viable fabric. It is also necessary that the fabric does not show too much remaining strain under loading so as not to lose functionality prior to failure. In addition, architecture fabrics are required to provide a sufficient level of fire retardancy which is demonstrated by the fabric's ability to undergo combustion, the extent of smoke production, and the production of molten droplets, as indicated by the Euroclasses for fire reaction classification. A polymeric coating is considered sufficient for water and UV-light resistance; however, for uncoated fabrics, these properties should be verified.

In light of the aforementioned criteria, the Suntex fabric is designed to be a type I fabric with a strength of approximately 3000 N/5cm in both warp and weft directions. The fire behaviour objective is set to meet at least EN 13501 class B-S2, D0.

To guarantee a functional solar fabric, not only is the structural behaviour important, but the practicality and environmental impact are also crucial. These aspects were translated into the following preset objectives that have informed the R&D process of Suntex:

- 1 A lightweight material of up to 1200 g/m² with a solar panel active area to textile surface ratio of approx. 50/50;
- 2 A material that can be rolled up;
- 3 A modular system that can be put together in (differently shaped) strips to form 3D curved fabrics, whereby the various electrical circuits are connected by means of interconnects;
- 4 An energy yield of approximately 20 W_p/m² (Peak watt at STC) of composite solar textile (given this is only 50% coverage of active OPV area), which may seem relatively little compared to traditional silicon solar panels, but the characteristics of OPV mean it can be used in this context in a way traditional silicon solar panels could not;
- 5 A sunlight transmission factor of 20 - 30%;
- 6 A fully recyclable material, whereby the solar cell structures can be separated from the textile, with a lifespan of 10 - 15 years.

Deeper consideration of the textile requirements also reveals the challenges involved in developing this new material. For instance, the uniformity of the textile is being challenged by the integration of solar cells. This further complicates the general inhomogeneity and anisotropy possible in textile fabrics, meaning tensile and bending properties differ between warp and weft. Further, the integration of electrical hardware components in a soft flexible textile can cause stress concentrations and weak points. To mitigate these challenges, the textile is being developed in an iterative process using high tenacity yarns, the selection of which is informed by extensive tensile testing to meet the requirements for a type I architectural textile. In addition, when implementing the Suntex textile, certain design guidelines may need to be recommended, regarding the loading directions.

Aside from the design and construction challenges, consideration must be given to the route to mass manufacturing. In order for the textile to have maximum impact and accessibility, the production should be efficient and cost-effective. Ongoing conversations with industry partners are informing design decisions which affect the production, to ensure design for manufacture is an inherent part of the development process.

2.2 TEXTILE DESIGN PROCESS

The design process of the textile itself is informed by the requirements outlined in Section 2.1, and broadly follows these steps repeatedly (forming an iterative loop):

- 1 Material selection (as detailed in section 2.2.1).
 - a Photovoltaic technology selection
 - b Yarn selection
- 2 Textile development process (see section 2.2.2).
 - a Structure/Weave design (including solar panel integration method).
 - b Sample creation.
- 3 Sample evaluation (Testing, as detailed in section 3.1).
- 4 Analysis and review of the materials and weave design (as detailed in section 3.1), then return to the material selection stage.

2.2.1 Material Selection

A *Photovoltaic Technology Selection*

As a first step, the type of photovoltaic technology to be integrated had to be selected. Organic photovoltaic film (OPV) was chosen for a number of reasons; it is a flexible, thin-film material (as can be seen in Fig. 1) produced in a low-carbon, roll-to-roll manufacturing process, and, it is composed of organic, non-toxic materials which are abundant and can be recovered at end-of-life. Due to this composition, it is semi-transparent and can be created in different colours (see Fig. 2). Additionally, the materials and production process mean that this technology has the theoretical potential to provide electricity at a lower cost than first- and second-generation solar technologies (USA Department of Energy, 2022), and it can have an energy payback time (the time required by an application to generate as much energy as is consumed during its production) around 10 times shorter than that of other solar technologies (ASCA®, EPBT 2021).

Furthermore, OPV technology is rapidly improving. For example, the ASCA® OPV film which is currently available can produce approximately $20\text{--}50 \text{ W}_p / \text{m}^2$ (depending on chosen colour), but the company has recently achieved outputs of $70 \text{ W}_p / \text{m}^2$ in pilot scale and expect to translate that to production by year end 2022 (ASCA®, Efficiency Increase, 2021). For comparison, the most efficient monocrystalline N-Type silicon solar technology on the market can produce $220 \text{ W}_p / \text{m}^2$ (Clean Energy Review, 2022), but of course the characteristics of OPV technology enable it to be used in contexts where monocrystalline silicon solar panels would not be used. In addition to these promising results under Standard Testing Conditions, OPV technology has also been shown to be less sensitive to some 'real world' factors than traditional silicon solar. Especially relevant to outdoor façade applications, as shown by Dolara et al.'s (2022) research at Polimi's SolarTechLAB; OPV has high performance in lower light conditions and with light from different angles (as occurs with vertical installation on a façade), and it is not adversely affected by increased temperatures. In fact, during their five-month outdoor testing period in Milan, the OPV modules showed improved performance (shown by an increasing P_{mpp} , maximum power point) with increasing temperature in all the considered irradiance range, whereas the monocrystalline and CIS modules tested in the same conditions showed a linear decrease with the cell's temperature. Finally, on a practical level, the nature of the OPV film technology means that custom sizes and shapes can be created, and smaller order quantities are possible which is essential for early-stage prototyping and testing. For this project, OPV strips of 45cm length and 2.5cm width were available for initial prototyping and testing, to later inform the design of a custom part.

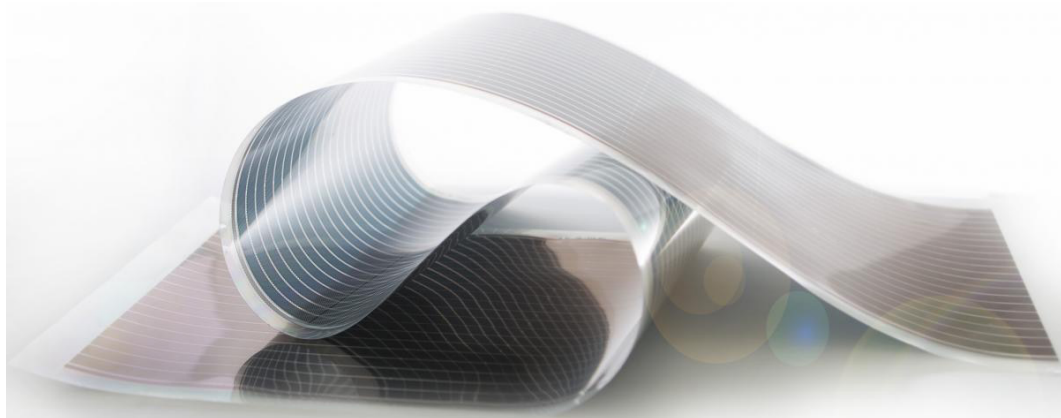


FIG. 1 ASCA Organic Photovoltaic Film, flexibility apparent. (Image courtesy of ASCA®)

B Yarn Selection

The continuous challenge with Suntex is the requirement to combine several "unusual" materials in one weaving process to make up the functional module. Alongside the OPV films (which mechanically, act like PET film), materials like a conductive track (that connects the solar panels), transparent monofilament (to secure the solar film), and high-tenacity yarns (that give the required tensile strength) are inevitable to use when making Suntex. All of the materials have rather different properties in terms of flexibility, elasticity, or breaking-load, which all need to be considered before, during, and after the textile has been woven. During the hands-on research, materials were assessed on how well they harmonise and complement each other so that their properties combine in the weave to make Suntex an energy-harvesting architecture type 1 fabric. The important factors for the selection of materials and structure of the fabric include:

- A high-tenacity main yarn, used in warp and weft, that is readily available and has a textile look and touch
- A high-tenacity main yarn, used in warp and weft, that when woven has a tensile strength of 3000N/5cm (criteria type 1 architectural fabric)
- A transparent warp yarn (“float yarn”) in combination with a specific weave pattern to hold the OPV films in place without putting strain or load on them or covering them entirely
- A conductive yarn, used in warp and weft, that enables a functioning circuit which connects the OPV films with each other and enables a connection to transfer the energy to an outlet
- All materials complying with fire-retardancy, durability, and weather resistance standards for textile architecture

Based on these factors, examples of chosen yarns and their mechanical properties can be seen in Table 1.

TABLE 1 An example selection of yarns to suit the set criteria, and their mechanical properties.

	Example	Diameter (mm)	Linear Density (dTex)	Breaking Force (N)	Breaking Tenacity (cN/dTex)
Main Yarn	MSP rPET	n/a (flat yarn)	1100	84.3	7.54
Float Yarn	Filva Monofilament	0.40	1600	27.45	1.72
Conductive Yarn	Karl Grimm High Flex 3981	0.42	2325	27.468	1.181



FIG. 2 ASCA Organic Photovoltaic Film; transparency, colour and freeform possibilities apparent. (Image courtesy of ASCA®)

2.2.2 Textile Development Process

A *Weave design*

The main focus of the textile development is the weave structure which is designed strategically around the integration of the OPV film. This makes it similar to the Texenergie/Texenergy research project by Saxion University (Hurenkamp, 2020), in which OPV films were woven into a textile to make indoor window blinds (among other applications). Since these use cases differ significantly the material choices for Suntext and the weave structure are also different.

The main aim for Suntext is that the high-tenacity yarns described in Section 2.2.1 B must take the majority of the tensile load, and the “float” structures around and on top of the OPV hold the film strips in place without putting excessive load on these strips or shading them. The purpose of this is to prevent electrical efficiency losses of the OPV. Therefore, an iterative process began, in which different material combinations, patterns, and weave-set-ups were tested and evaluated regarding processability and functionality of Suntext, first on a handweaving loom and later an industrial sampling loom. As detailed in Section 3.1, these woven demonstrators and specimens were extensively tested to investigate their structural and tensile behaviour and therefore verify or eliminate material choices, weave patterns, and set-ups.

Throughout the design process, the aim was to retain a textile look and touch as opposed to a heavily coated industrial composite-like material. This is because such composite materials are difficult to disassemble, repair and recycle and, further, have limited opportunities for surface and colour design. Suntext remains uncoated, so the chosen pattern and (coloured) yarns will define the unique look and give it a tactile feel as opposed to a flat and printed coated textile. Removing the entire step of coating during the manufacturing process can compensate for the extra time needed for the more complex weaving process.

Because Suntext is unique and new, there is little (empirical) research that could be referenced when planning and anticipating the challenges of weaving, except for the above named Texenergie/Texenergy project. This makes the textile development process variable, as one change in fabric construction may affect the entire look, feel, behaviour, and functionality of Suntext.

B *Sample Creation*

In addition to the choice of materials, the weaving loom plays a major role. Industrial looms tend to be fit for one purpose only and cannot be tweaked to switch from one material to another, especially regarding the preparation of warp beams and general setup which can take months. Therefore, to facilitate a more agile development process, most Suntext samples were initially tested on a handweaving loom (Louët Erica) and later recreated on an industrial sampling loom (CCI Evergreen). On both looms a maximum fabric width of 50cm can be woven and the maximum fabric length varies, depending on the length of the warp yarns used. On the handweaving loom, the length of those yarns is chosen by the weaver and for the CCI Evergreen loom, the warping machine available for these trials automatically limits the total length of the textile to 2m. The number of shafts on the looms also differs, from a maximum of 4 (Louët Erica) to 24 (CCI Evergreen). The number of shafts (and the carefully planned warp threading through these shafts) determine the addressability of the warp yarns, and therefore more shafts can realise more complex weave structures in which several yarns need to be lifted or lowered individually. With Suntext, this is necessary for integrating the OPV film and the conductive tracks.



FIG. 3 Louët Erica Handweaving Loom



FIG. 4 CCI Evergreen Sampling Loom

Strategic use of both technologies enabled quick control and production of small samples within days that varied in complexity. A choice of these samples and the analysis thereof can be found in Section 3.1 Textile Evaluation. Further, using the CCI Evergreen sampling loom has made it possible to experiment and test solutions for weaving Suntext in an industrial setting and being able to assess the limitations that would be present in larger industrial productions like warp and weft yarn tensions, warp beam setup, gripper system, and more. Making the transition from a sampling loom to an industrial loom is the next step in the process to make Suntext widely available for use in textile architecture.

3 EXPERIMENTAL TESTING & RESULTS

As mentioned in Section 2, experimental testing is an essential part of the iterative design process. This section outlines the experimental tests and its results. More precisely, it reports textile evaluation tests and electrical and mechanical behaviour of the OPV film. A case study is then carried out in order to analyse and compare the impact of Suntext on a building façade.

3.1 TEXTILE EVALUATION

The evaluation of the textile's mechanical properties was performed using tensile strip tests in which fabric specimens, of at least 5cm widths and 20 cm lengths, were mounted onto the clamps of a tensile testing machine and stretched until failure. From these tests, the failure load, and the elongation at break can both be measured for assessing the strength and stiffness of the specimens. Additionally, the tests provide insight into the interaction between the fabric and the solar cell tape, which gives an indication of whether the solar cells will undergo stress during loading. Multiple test series were carried out on composite fabrics with different yarn strengths to examine whether the strength of the configuration meets the strength objective. See Table 2 for brief overview.

TABLE 2 A summarised overview of Suntext iterations.

Iteration Name	Loom	Material Combination	Weaving Pattern Notes	Evaluation Notes
Suntex V1.1	Louët Erica handweaving loom	TPU main yarn	Plain Weave with double-sided floats	Progress to machine weaving (CCI Evergreen)
Suntex V1.2	CCI Evergreen Sampling Loom (automatic)	TPU main yarn, Monofilament float yarn	2/2 Twill, Plain Weave with single-sided floats (with plain/twill backing)	Coated yarn creates an open mesh structure which is interesting for optical properties but the strength is insufficient, so must review material choices.
Suntex V2	Louët Erica handweaving loom	Twisted rPET main yarn and float yarn	Plain Weave with single-sided floats (with plain/twill backing)	Strength promising and denser weave possible with this yarn, progress to machine weaving and test with monofilament float yarns.
Suntex V3	CCI Evergreen Sampling Loom (automatic)	Twisted rPET main yarn, monofilament float yarn	Plain Weave with single-sided floats (with plain/twill backing)	Conclusive testing has not yet been completed; weave is denser than V2 which suggests high strength, but weaker monofilament material included may counteract this benefit.



FIG. 5 Suntext V1.2 sample.

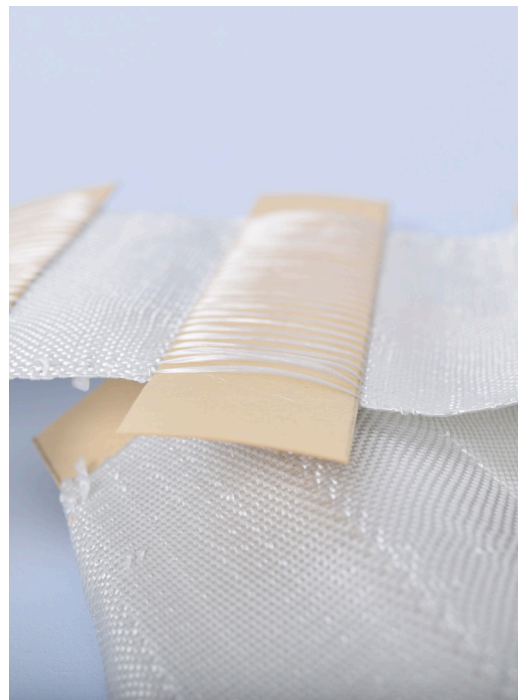


FIG. 6 Suntext V2 sample with card strips in place of solar film.

The initial fabric composite Suntext V1 (Figure 5), made with thermoplastic polyurethane (TPU) coated polyester yarns, demonstrated insufficient strength and in some cases large elongations. Consequently, the main yarn, which is the most prevalent in a weave, had to be replaced by a higher tenacity yarn in the subsequent fabric prototype. Suntext V2 (Figure 6) was, thus, hand-woven from recycled high-tenacity polyester (rPET) yarns. To acquire a quick indication of the strength behaviour and the impact on the solar film, only warp specimens were woven. The tensile tests of Suntext V2 consisted of six fabric specimens, three of which were regular plain-woven fabric (Suntext V W1 - W3) and an additional three with PET film strips inserted to mimic the presence of the solar film, hereby referred to as 'solar film' or 'SF' (for example, 'Suntext V2 SF W1' in Table 3). All specimens were coated with a speckling pattern prior to testing to enable digital image correlation (DIC) analysis

during the tests. This analysis type provides the strain field over the specimens' area throughout the loading process until failure which helps identify whether the mode of failure is valid and if non-uniform stressing occurs, therefore revealing the effect of integrating the solar film into the woven textile. After specimen preparation, each specimen was mounted onto the clamps of an Instron 1122 tensile machine, and an initial 10 N prestress was applied. The initial length was then measured, and the tests carried out with an extension rate of 100 mm/min.

3.1.1 Results of Textile Evaluation

The results are summarised in Table 3, and can be seen in the graph in Figure 8. The data showed substantial failure loads, averaging 2781.4N for the regular specimens and 2545.2N for the specimens with 'solar film' (SF) integrated in 'float' structures (Figure 7). This strength reduction of only 8.49% in the more irregular 'solar film' (SF) specimens, verifies the weaving strategy of implementing single-sided floats (with plain/twill backing) to integrate the solar films.

TABLE 3 Suntex V2 specimen information and tensile test results (as logged by Instron 1122 tensile testing machine used)

General Information		Weave specifications			Test Results	
Category	Specimen Name	Pattern	Warp density (yarns/cm)	Weft density (yarns/cm)	Elongation (%)	Failure Load (N/5cm)
Regular Specimens	Suntex V2 W1	Plain weave	10	11	13.3	2646.23
	Suntex V2 W2		10	11	15.0	2959.46
	Suntex V2 W3		10	11	12.7	2738.56
Solar Film (SF) Specimens	Suntex V2 SF W1	Plain/Twill backing layer at SF 'floats'	10	16.6	9.7	2263.44
	Suntex V2 SF W2		10	16.6	10.6	2547.77
	Suntex V2 SF W3		10	16.6	10.2088	2542.64



FIG. 7 Suntex V2 Specimens after testing to failure. Regular specimens labelled "Twisted rPET W1-3" are referred to as "Suntex V2 W1-3" in this paper, and Solar Film specimens labelled "Twisted rPET SC W1-3" are referred to as "Suntex V2 SF W1-3" in this paper.

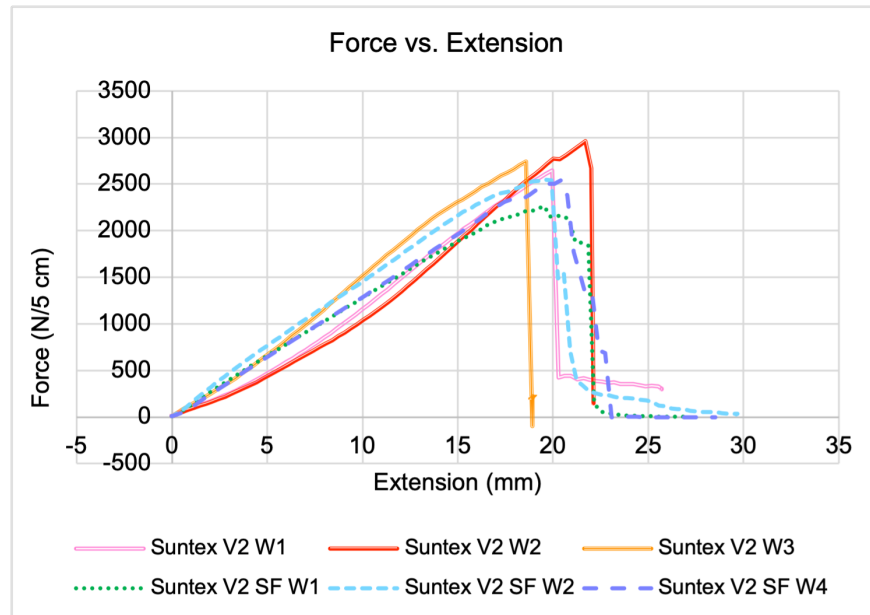


FIG. 8 Suntex V2 specimens' force-extension behaviour.

The digital image correlation (DIC) analysis (Figures 9 and 10) data correlates with the data logged by the Instron 1122 tensile testing machine used (summarised in Table 3). The DIC analysis of the solar film specimens is particularly interesting (Figure 10); lower strain can be observed at the solar film sections compared to the adjacent woven sections, which implies that the solar cells are not under any stresses that could cause a loss of function before fabric failure. This indicates that the weave design strategy to integrate the solar film in a way that it would not be subject to large tensile loads is successful, and supports the viability of this approach and the textile itself.

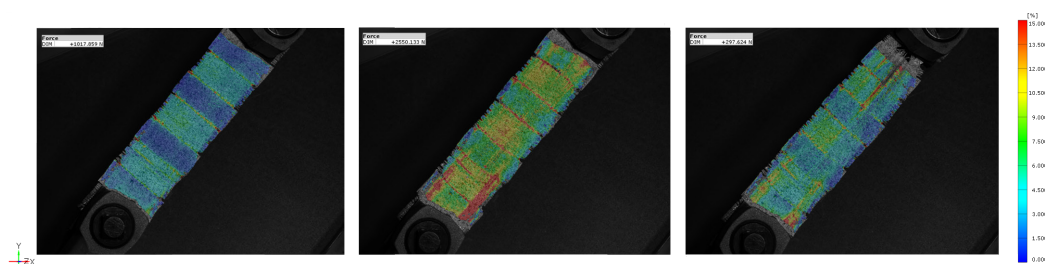


FIG. 9 Specimen 'Suntex W3' strain field along the longitudinal direction at failure (left) & directly after failure (right).

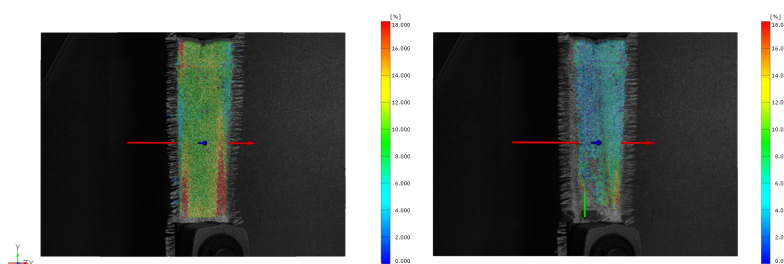


FIG. 10 Specimen 'Suntex V2 SF W2' strain field at approximately 1 kN load (left), at maximum load (middle), and after failure (right).

The results are, however, limited to the warp direction only, and to verify the fabric strength, the weft direction should also be tested. Furthermore, due to the samples being handwoven, non-uniform stressing of the specimens is most likely to happen, which might cause failure at a lesser load than potentially possible. Upcoming tests, therefore, should be performed on fabrics woven on a power loom. Nonetheless, these results show the rPET Suntex V2 is a promising configuration to achieve the desired strength, and inform the next iteration, Suntex V3.

Suntex V3 samples have been woven on a power loom (CCI Evergreen), using the same rPET yarn as Suntex V2 for the 'main yarn' but with some of these warp yarns replaced with monofilament (which is used as the float yarn to hold the solar film in place). Weaving it on the power loom facilitated a denser weave, which should result in a stronger overall textile. However, the weaker monofilament replacing some of the rPET warp yarns may counteract this effect. Conclusive mechanical testing has not yet been performed, to investigate these theories and the mechanical strength of this latest iteration.

3.2 ELECTRICAL AND MECHANICAL BEHAVIOUR OF THE OPV FILM

In addition to evaluating the tensile properties of the surrounding woven textile, certain properties of the OPV film were also investigated, to understand how it would behave within the textile. The material data sheets generally provide figures for the electrical properties, thickness, weight, flexibility, impact resistance and operating conditions. However, as the material is not intended to be tensioned (as is the case with all photovoltaic technology), tensile strength and elongation data is not provided.

The OPV film is a composite in itself; it is a laminated stack of a substrate, conductive material, printed active material within a polymer encapsulant. Fan et. al (2013) demonstrated with a certain OPV film sample that the inner laminated stack tends to be more sensitive to straining compared to the encapsulant, so it is expected electrical failure occurs at a lesser tensile force and strain than mechanical failure. However, each company producing OPV may be implementing different materials and processes and therefore there can be no standard comparisons of failure modes, for instance. This highlights the lack of empirical research in the area, and the need for testing to create practical insights. Therefore, to further understand the specific OPV material available for this research project and how it should be integrated into the textile, a number of tests were conducted to investigate both electrical failure and mechanical failure.

For these reasons, despite the design intent for the surrounding textile to carry the tensile forces as much as possible, the solar film was tested in a tensile testing machine (Figure 12). The apparatus was similar to that of the tensile fabric tests already described in Section 3.1, except a strong light source was added and the electrical performance of the solar film was also logged (using an Arduino system), while the tension was applied (Figure 11). In this way, the tensile load at which both electrical failure and mechanical failure occurred was identified.



FIG. 11 OPV strip test set-up, illuminated by bright light source.



FIG. 12 Mark 10 Instron Machine used in the testing.

3.2.1 Results of OPV Tensile Testing

The results were encouraging, showing the solar films were electrically functional up to around 500-600N tension, and 15mm extension. Mechanically, the films mostly showed a plastic mode of failure with viscous deformation of the PET encapsulant material at the yield point (at 560-680N) followed by progressive elongation and a gradual increase in tensile force. These preliminary results support the continued development of the textile, and inform the design choices. Further testing (for example, to understand the OPV behaviour when integrated into the textile, and the textile is tensioned) will be required. Finally, it should be noted that within industry, a secondary encapsulation can be added to an OPV film (in addition to the primary encapsulation present in all OPV film, including samples used in these tests) to increase the resilience of the modules to mechanical stress or environmental factors.

Integration into the textile also has an optical effect on the solar film, as certain warp yarns 'float' over the film in order to keep it in place. Preliminary tests were conducted to investigate the effect of different 'float' design strategies (varying in material and density) on the performance of the solar energy generation. These results were also encouraging, indicating that the peak performance is only reduced by approximately 10-15% with the chosen 'float' design. No optical modelling has been completed to further explain what is occurring, but it can be speculated that multiple optical phenomena are at play, not only shading (negatively affecting the irradiance on the solar film), but also reflection and scattering (positively affecting the irradiance). Further testing and analysis will inform the final design.

3.3 DESIGN CASE STUDY TO ANALYSE COMPARATIVE IMPACT OF SUNTEX

A preliminary overview of the quantitative and qualitative impact of installing a Suntex façade (compared to a traditional textile façade without integrated solar PV on the same building) is presented. A façade presents itself as a suitable first use case due to the rectilinear “panels” of textile required (as opposed to complicated or organic shapes) and the relatively lower loading compared to freeform tensile architecture structures as current practice is showing. Generally type I architectural textiles are used in these applications, the strength requirements for which appear to be in reach for a Suntex textile (based on the tensile strength results for the Suntex V2 samples as presented in Section 3.1.1, and calculations to predict the strength of Suntex V3).

The building in question is the Westraven Rijkswaterstaat building in Utrecht (The Netherlands), which was constructed in the 1970s and renovated to include a glass façade with a textile second skin in 2007 (the textile material was subsequently replaced in 2020). The light-weight addition of this Teflon-coated and open-weave fibre-glass textile improved the thermal management (and therefore the working environment) in the building in two ways: first, it acted as a wind baffle and allowed the employees to open their windows and thus control their own localised climate; secondly, it also functioned as a sun-shade without impeding the views, further reducing the energy required to cool the building (Hendriks, 2010). In this way, the Westraven renovation already highlights the tremendous potential of retrofitting with a second-skin textile façade to improve the sustainable credentials of existing buildings. Thus, this study will focus on the additional benefits uniquely offered by Suntex; namely the untapped potential of solar energy generation and the new aesthetic possibilities Suntex enables, and take the benefit of solar-shading as a given in this context.

The speculative design case and underlying analysis reveal some important considerations when designing a façade with Suntex, and the opportunities and challenges of applying the Suntex material as the chosen second skin façade textile. Finally, the analysis points to future improvements to make Suntex more impactful and/or attractive to the field of textile architecture.

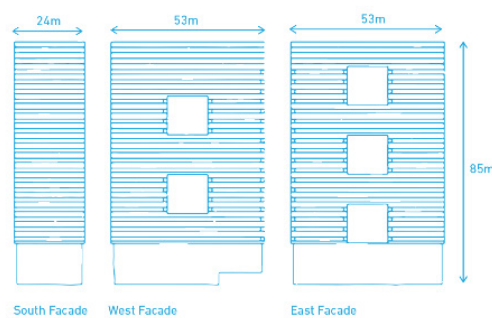


FIG. 13 Schematics of the façade surfaces in question.



FIG. 14 Aerial view of the Westraven building, showing aspect.

3.3.1 Quantitative Benefits: Energy Generation

The first parameters when assessing the potential of any photovoltaic application are available surface area and solar irradiance as indicated by the location and orientation of a site (and the presence or lack thereof of obstacles causing shading). In the existing renovation, the north façade of the Westraven building has an additional glass layer for sound insulation from the nearby motorway, whereas the sunnier south, west, and east façades have the textile second-skin which provides solar-shading (Figure 14). The available surface area on these three sunny façades is approximately 11 152m² (Figure 13), and the current textile covers 10 000m² to allow some fully open sections (Buitink, 2020) and therefore not increase the artificial lighting requirements inside the building. In theory, Suntex would cover this same area; the façades which require shading from the sun of course have the most solar irradiance and therefore excellent potential for photovoltaic energy generation.

The aim for the Suntex material was to achieve 50% coverage of active OPV area (though it must be noted that current iteration Suntex V3 in April 2022 achieved approximately 25% coverage of active OPV area), which in this case would result in 5 000 m² of OPV. The output of commercially available OPV film is currently approximately 20-50W_p/m² depending on the chosen colour (ASCA® Datasheet, 2021), and taking the peak output of the samples available for this project (approximately 40W_p/m²) indicates that this application would be a 200kW system (whereas in the near future when OPV will achieve 70 W_p/m² in production, a 350kW system will be possible with this same surface area). In practical terms, assuming 1602 hours of sunshine in Utrecht each year according to meteorological data (Current Results, 2010; KMNI, 2020) and noting that the Westraven building is the tallest in the locality and thus receives unobstructed sunshine (and making the simplified assumption that this sunshine falls equally on these three façades), this 200kW system could produce 320.4MWh each year. Contextually, this could provide 4% of the building's total energy consumption (or approximately 1 floor), or provide lighting to the entire building, which is generally 2.5% of a non-residential building's energy usage (EU Buildings Factsheet, 2013).

For reference, the rooftop surface of the Westraven building is approximately 1 272 m², roughly 11% of the surface area available on the three 'sunny' façades. Covering this rooftop area in traditional silicon solar panels could only make a system of approximately 160kW capacity (assuming 1 000 m² area available, and polycrystalline solar panels with a power conversion efficiency of 16% are utilised (Clean Energy Review, 2022)) thus emphasising the untapped potential of façade solar particularly in tall buildings such as this one. This example also points to the potential of third generation solar technologies such as OPV, which compensate for their lower efficiencies by being more versatile than traditional silicon solar technology.

It must be noted that this analysis simplifies the irradiance scenario and the methods used here are approximate, in order to quickly understand the magnitude of the impact. Detailed modelling of the irradiance, using software such as BIMsolar, would be required to optimise the positioning of Suntex solar textile in a true application. Additionally, any increased artificial lighting load would need to be quantified against the energy benefits. Nonetheless, the quantitative energy-generating potential of implementing Suntex solar textile as a second-skin façade material is clear, in addition to the solar-shading benefit it shares with many existing façade textiles.

4 FUTURE OUTLOOK

The societal value and commercial potential of Suntex does not rely merely on mechanical and electrical performance. In order to evaluate the impact of Suntex, besides the scientific results, it is relevant to include some more speculative reflections regarding the qualitative benefits and design considerations to be made in the process.

4.1 QUALITATIVE BENEFITS: AESTHETIC AND SOCIAL IMPACT

In a more qualitative sense, Suntex also presents new aesthetic possibilities for architects to explore and implement, by broadening the appearance of thin-film solar technology and the possibilities for aesthetic integration in building façades. In this way, although specific aesthetic styles are subjective and contextual, the potential for Suntex to manifest in different appearances creates opportunities for new visual perspectives on solar technology, which is a necessary step in the adoption of technologies into our everyday environment (Dongen, 2019; Sánchez-Pantoja, 2018).

In the context of the Westraven building, the appearance of the textile façade dominates the visual impact of the entire structure. The two iterations of the textile façade so far have been very dark in colour; first black PTFE-coated glass fabric in 2007 and now brown PVC-coated polyester fabric since 2020. If Suntex is created by designers with the architect's perspective in mind, more interesting colourways and gradients can be woven, with a more striking impact. Custom rolls of textile can be created to either camouflage or highlight the solar strips depending on the architect's vision. By their nature, textiles enable design freedom. The selection of yarn colour and type, and of weave pattern, can determine the colour and transparency of a textile and therefore open possibilities for new aesthetic qualities and indoor/outdoor ambiances.

Very often solar panels are out of sight on roofs or solar farms, which can make it difficult for people to engage and accept them as a necessary element of energy transition and modern energy harvesting (Reinders et al., 2020). The highly visible location of the Westraven building (conspicuous from both the A19 motorway and the busy Amsterdam-Rijn Canal) creates the perfect showcase platform for a new solar textile, with potential to not only increase awareness and acceptance of new solar technologies, but also to inspire further applications and other implementations of renewable technologies in our immediate built environment. In this way, retrofitting iconic buildings with a new solar textile could have a social impact and help accelerate the energy transition.

4.2 DESIGN CONSIDERATIONS FOR DEVELOPING AND IMPLEMENTING SUNTEX

Naturally, every innovation presents challenges, and this can be especially true in the construction industry. Creating a smart textile to meet the requirements described in Section 2.1 is difficult, and alterations to weaving machinery are required in order to accommodate efficiently weaving the solar film. The process of making robust electrical connections throughout this textile must be developed with industry; the integrated circuit must be robust and protected against the elements.

Further, the logistics of applying the finished textile, either to an existing building or to create a new structure, will present other challenges. The solar panel circuit must also be designed to be modular,

so the textile could be used in different lengths with different numbers of solar panels, while minimising efficiency losses. The power outlet points and route to energy storage must be designed in tandem with the frame or tensioning system, to efficiently use minimal materials and create a multi-functional frame. Extensive ageing testing must be completed to ensure that the Suntext textile will have a useful lifetime equal to (or surpassing) that of existing architectural textiles. Finally, all materials should be separable and recyclable at end of life.

5 CONCLUSION

This paper outlined the textile design and development process for Suntext, followed by the preliminary results obtained through experimental testing of samples. These test results validated the feasibility of the textile and pointed towards façades as a potential use case. The potential impact of the textile was then evaluated through the development of a case study that explored applying Suntext as energy harvesting building skin to a pre-existing building.

The design case study presented supports the fact that façades are an untapped surface area; in tall buildings they commonly provide a surface area that is a magnitude greater than that of roofs. In many countries, like the Netherlands, there is already great competition for the usage of 'greenfield' or undeveloped land; agriculture, housing, etc; thus, space-consuming solar farms are not an optimal solution. In the Netherlands alone, there are some 1,600 square kilometres of façade surface available, which means that by 2050, at least a third of the renewable energy potential of the built environment could be on façades (TNO, n.d)

If Suntext can be developed into an industrial off-the shelf and customizable architectural textile, it can support large-scale use. However, for this to happen more research is needed to solve the challenges described in 4.2 Design Considerations for developing and implementing Suntext. Despite these challenges, the preliminary research, testing, and development process is promising and the potential impact for the Suntext solar textile is clear. Furthermore, the rapid development of organic photovoltaic technology (and other solar thin film technologies such as CIGS, which could also be integrated within the textile) suggests that the future will bring higher efficiencies at lower costs. Therefore, the iterative loops of the development process outlined in this paper will be continued until May 2023. To evaluate an industrial production of Suntext further, a dialogue with industry partners will be started with the clear aim to evolve Suntext into an industrially manufacturable type I architectural textile.

As Suntext develops into a robust industrialised product for two-dimensional surfaces like façade cladding, custom made and three-dimensional solutions for a range of applications can also be explored. By replacing traditional architecture textiles which are used to create tensile structures such as tents or canopies, Suntext can not only provide shelter and shade, but also generate energy. A particularly compelling use case for a rugged Suntext tent is in humanitarian crises, when there is an urgent need for a quickly deployable solution to provide this shelter, shade, and energy. Similarly, the potential for off-grid or self-powered tents for the events sector is clear.

The need to make the built environment more sustainable as part of the energy transition, in tandem with reducing reliance on imported energy, is high on the global agenda. The European Union Solar Energy Strategy recognises the potential of solar, and the new and novel BIPV in particular, to decarbonise our building stock. An obligation to gradually install solar energy equipment on all

new and existing public and commercial buildings above a certain size and on all new residential buildings between 2026 and 2029 will accelerate this transition (European Commission, 2022). However, in order to achieve awareness and subsequently also acceptance, both by private individuals and professionals in the construction industry, new and visually attractive materials must be developed that offer a variety of integration possibilities for all kinds of surfaces. Only in this way can solar technology become both a functional and aesthetic part of our living environment and contribute to a more sustainable society.

Acknowledgements

With thanks to; a MIT R&D subsidy provided by the Dutch Ministry of Economic Affairs and Climate, which funds this two-year project; Saxion University of Applied Sciences, Holst Centre, Solliance and CT-Stevin II Lab TU Delft for collaboration.

References

- Ahriz, A., Mesloub, A., Djeflal, L., Alsolami, B.M., Ghosh, A. & Abdelhafez, M.H.H. (2022). 14The Use of Double-Skin Façades to Improve the Energy Consumption of High-Rise Office Buildings in a Mediterranean Climate (Csa). *Sustainability*, 6004. Retrieved from <https://doi.org/10.3390/su14106004>
- Architecture 2030 (2022). Retrieved from <https://architecture2030.org/why-the-building-sector/>
- ASCA® (2021). *Material Datasheet*. Retrieved from https://www.asca.com/wp-content/uploads/2021/07/Generic_data_sheet_EN.pdf?_ga=2.93076637.1039473980.1650881177-712994063.1650881177&_gac=1.260318847.1650892409.CjwKCAjwJZmT-BhB4EiwAynRmD8r6dylg0HQShJX32ohvUv-IErD-wWEOM6f5YJqYG8lx8aMC3E_EQBoCBv8QAvD_BwE
- ASCA®, *Efficiency Increase* (2021). *Asca increases performance of Organic Solar cells by integrating new semiconductors* Retrieved from <https://en.asca.com/latest-news/asca-increases-performance-of-organic-solar-cells-by-integrating-new-semiconductors>
- ASCA®, *EPBT* (2021). *Focus on the Energy Payback Time of the Asca Film*. Retrieved from <https://en.asca.com/latest-news/focus-on-focus-of-the-energy-payback-time-of-the-asca-film>
- Barney, D., & Szeman, I. (2021). *Solarity, an edition of South Atlantic Quarterly*. Duke University Press.
- Buitink (2020). *Westraven Façade cladding*. Retrieved from <https://www.buitink-technology.com/uk/architecture/facade-coverings/westraven-facade-cladding>
- Clean Energy Review (2022). *Most efficient solar panels in 2022*. Retrieved from <https://www.cleanenergyreviews.info/blog/most-efficient-solar-panels>
- Current Results. (2010). Retrieved from <https://www.currentresults.com/Weather/Netherlands/sunshine-annual-average.php>
- Dolara, A., Leva, S., Manzolini, G., Simonetti, R. & Trattenero, I. (2022). Outdoor Performance of Organic Photovoltaics: Comparative Analysis. *Energies* 2022, 15, 1620. <https://doi.org/10.3390/en15051620>
- Dongen, P. (2019). *A Designer's Material-Aesthetics Reflections on Fashion and Technology*. Doctoral Thesis Eindhoven University of Technology. ArtEZ Press
- European Commission. 2022. *EU Solar Energy Strategy*. Retrieved from <https://eur-lex.europa.eu/legal-content/EN/TXT/HTML/?uri=COM:2022:221:FIN>
- European Union Buildings Factsheet. (2013). *Energy usage*. Retrieved from https://ec.europa.eu/energy/eu-buildings-factsheets_en
- Fan, Z., De Bastiani, M., Garbugli, M., Monticelli, C., Zanelli, A., & Caironi, M. (2013). *Experimental investigation of the mechanical robustness of a commercial module and membrane-printed functional layers for flexible organic solar cells*. Retrieved from <https://www.sciencedirect.com/science/article/abs/pii/S1359836816308216>
- Hendriks, J. (2010). *Greening Modernism, Westraven Tower*, Council on Tall Buildings and Urban Habitat Research Papers. Retrieved from <https://global.ctbuh.org/resources/papers/download/325-greening-modernism-westraven-tower.pdf>
- Horn, S., Bagda, E., Brandau, K., & Welter, B. (2018). *Einfluss der Bauwerkintegrierten Photovoltaik in Fassaden bei der energetischen Bilanzierung von Gebäuden* (Teil 1). Bauphysik. [Influence of building-integrated photovoltaics in facades on the energy balance of buildings (Part 1). building physics] 40, 68–73. doi:10.1002/bapi.201810007. Retrieved from <https://onlinelibrary.wiley.com/doi/abs/10.1002/bapi.201810007>
- Hurenkamp, A. (2020). *TexEnergie: solar cells and textiles as a match made in heaven*. Retrieved from: <https://www.saxion.nl/nieuws/2020/12/texenergie-zonnecellen-en-textiel-als-een-match-made-in-heaven>
- Klem, J.R.D. (2006). Glass: a deadly conservation issue for birds. *Bird Observer* 34(2), 73-81

- KNMI Klimatologie, Koninklijk Nederlands Meteorologisch Instituut. (2020). Retrieved from: https://www.knmi.nl/klimaat-viewer/kaarten/zon/gemiddelde-zonneschijnduur/september/Periode_1991-2020
- IEA (2020). World Energy Outlook 2020, IEA, Paris. Retrieved from: <https://www.iea.org/reports/world-energy-outlook-2020>
- Kuhlmann, J.C., de Moor, H.H.C., Driesser, M.H.B., Bottenberg, E., Spee, C.I.M.A. & Brinks, G.J. (2018). Development of a Universal Solar Energy Harvesting System Suited for Textile Integration Including Flexible Energy Storage. *Journal of Fashion Technology & Textile Engineering* S4:012. doi: 10.4172/2329-9568.S4-012
- Mather, R. R. & Wilson, J. I. B. (2017). Fabrication of Photovoltaic Textiles. *Coatings* 7(5):63 doi:10.3390/coatings7050063 Methodspace (2021). *Case Study Methodology*. Retrieved from <https://www.methodspace.com/blog/case-study-methodology>
- Middelhaue, L., Girardin, L., Baldi, F. & Maréchal, F. (2021). Potential of Photovoltaic Panels on Building Envelopes for Decentralized District Energy Systems. *Frontiers in Energy Research*, 15 October 2021. <https://doi.org/10.3389/fenrg.2021.689781>
- Nathanson, A. (2021). *A History of Solar Power Art and Design. Part III 5. Textiles and Wearables*. Routledge
- Reinders, A. H. M. E., Lavrijssen, S., Folkerts, W., van Mierlo, B., Franco Garcia, L., Loonen, R. C. G. M., Cornelissen, H., Stremke, S., Alarcon Llado, E., Polman, A., & Weeber, A. W. (2020). *Integration of solar energy systems for increased societal support*. In Proceedings of 37th European Photovoltaic Solar Energy Conference and Exhibition (EU PVSEC) (pp. 1911-1914) Retrieved from: https://pure.tue.nl/ws/portalfiles/portal/168282829/20_eupvsec_reinders.pdf
- Sánchez-Pantoja, N., Vidal, R., & Pastor, M. (2018). Aesthetic impact of solar energy systems. *Renewable and Sustainable Energy Reviews*. 98. 227-238. 10.1016/j.rser.2018.09.021.
- Satharasinghe, A.S., Hughes-Riley, T., & Dias, T. (2020) A Review of Solar Energy Harvesting Electronic Textiles. *Sensors* 20(20):5938 DOI:10.3390/s20205938 Retrieved from https://www.researchgate.net/publication/328043412_Aesthetic_impact_of_solar_energy_systems
- Scheer, H. (2005). *A Solar Manifesto*. Routledge.
- Shareef Al-Azzawi, Rana & Al-Alwan, Hoda. (2021). *Sustainable Textile Architecture: History and Prospects*. IOP Conference Series Materials Science and Engineering. 1067. 10.1088/1757-899X/1067/1/012046.
- Smelik, A., Toussaint, L., & Van Dongen, P. (2016). Solar fashion: An embodied approach to wearable technology. *International Journal of Fashion Studies*, Vol 3, Nr 2, 1 October 2016
- Steim, R., Ameri, T., Schilinsky, P., Waldauf, C., Dennler, G., Scharber, M., & Brabec, C.J. (2011). Organic photovoltaics for low light applications. *Solar Energy Materials and Solar Cells* 95. 3256-3261. 10.1016/j.solmat.2011.07.011. Retrieved from: https://www.researchgate.net/publication/251618851_Organic_photovoltaics_for_low_light_applications
- System concepts (n.d). *Design Thinking Introduction*. Retrieved from <https://www.system-concepts.com/insights/design-thinking-introduction/>
- TNO (n.d). *Roadmap Renewable Electricity: Solar Panels in Façades*. Retrieved from <https://www.tno.nl/en/focus-areas/energy-transition/roadmaps/renewable-electricity/solar-energy/solar-energy-potential/solar-panels-facades/>
- UN Environment and International Energy Agency (2017). *Towards a zero-emission, efficient, and resilient buildings and construction sector. Global Status Report 2017*. Retrieved from https://www.worldgbc.org/sites/default/files/UNEP%20188_GABC_en%20%28web%29.pdf
- USA Department of Energy (2022). *Organic Photovoltaics Research*. Retrieved from: <https://www.energy.gov/eere/solar/organic-photovoltaics-research>
- Van Hinte, E., & Beukers, A. (2020). *Designing Lightness. Structures for Saving Energy*. Nai010 Publishers
- World Economic Forum, in collaboration with Accenture (2022). *Fostering Effective Energy Transition*. Retrieved from https://www3.weforum.org/docs/WEF_Energy_Transition_Index_2022.pdf



JOURNAL OF FACADE DESIGN & ENGINEERING

VOLUME 10 / NUMBER 2 / 2022

- V **Editorial**
Ulrich Knaack
- 001 **Active, Passive and Cyber-Physical Adaptive Façade Strategies: a Comparative Analysis Through Case Studies**
Jens Böke, Paul-Rouven Denz, Natchai Suwannapruk, Puttakhun Vongsingha
- 019 **Influence of Automated Façades on Occupants: A Review**
Pedro de la Barra, Alessandra Luna-Navarro, Alejandro Prieto, Claudio Vásquez, Ulrick Knaack
- 039 **CoolSkin**
Andreas Greiner, Olaf Böckmann, Simon Weber, Martin Ostermann, Micha Schaefer
- 057 **Renovating Modern Heritage – The Upgraded Façade of Commerzbank Düsseldorf**
Rouven S. Grom, Andreas W. Putz
- 071 **Timber-based Façades with Different Connections and Claddings: Assessing Materials' Reusability, Water Use and Global Warming Potential**
Miren Juaristi Gutierrez, Ilaria Sebastiani, Stefano Avesani
- 087 **The Potential of Static and Thermo-chromic Window Films for Energy Efficient Building Renovations**
A.J.J. Kragt, E.R. van den Ham, H. Sentjens, A.P.H.J. Schenning, T. Klein
- 105 **Additively Manufactured Urban Multispecies Façades for Building Renovation**
Iuliia Larikova, Julia Fleckenstein, Ata Chokhachian, Thomas Auer, Wolfgang Weisser, Kathrin Dörfler
- 127 **Retrofitting Potential of Building envelopes Based on Semantic Surface Models Derived From Point Clouds**
Edina Selimović, Florian Noichl, Kasimir Forth, André Borrmann
- 141 **Suntex: Weaving Solar Energy Into Building Skin**
Pauline van Dongen, Ellen Britton, Anna Wetzel, Rogier Houtman, Ahmed Mohamed Ahmed, Stephanie Ramos

TU DELFT
ISSN PRINT 2213-302X
ISSN ONLINE 2213-3038

